

**REMOTE SENSING OF FIRE EFFECTS ON TAMARISK
EVAPOTRANSPIRATION AND REGENERATION**

By

Nicole Alkov

**Submitted in Partial Fulfillment
of the Requirements for the
Masters in Science in Hydrology**

**New Mexico Institute of Mining and Technology
Department of Earth and Environmental Science
Socorro, New Mexico**

December, 2008

ABSTRACT

Millions of dollars have been spent in New Mexico to remove tamarisk from riparian lands along the Rio Grande and restore previously monotypic tamarisk areas with native species such as cottonwood and willow. Elevated evapotranspiration (ET) rates of tamarisk are a main factor in motivating the invasive species' control. One of the tamarisk removal techniques is through the use of controlled burning. In this study, Landsat and MODIS satellite imagery was used in conjunction with the Surface Energy Balance Algorithm for Land (SEBAL) computer model to compare ET and Normalized Differenced Vegetation Index (NDVI) of tamarisk covered riparian areas before and after three recent fires: 1. Mitchell Fire of April 9-16, 2005, which burned 414 hectares; 2. Marcial Fire of May 3-10, 2006, which burned 2,250 hectares; and 3. Bosquecito Fire of June 6-9, 2006, which burned 260 hectares. By comparing the remote sensing results to field point measurements, groundwater and soil data, we evaluate the spatial and temporal ET and NDVI as a proxy for vegetation recovery after fires. Our results demonstrate: 1. Tamarisk ET rebounds much faster after fire than previously thought; tamarisk ET is established as early as one month after fire, and one year after fire tamarisk density and ET returns to pre-fire conditions; 2. The use of herbicide-burn followed by flooding is highly effective in long-term tamarisk eradication; 3. MODIS NDVI data products are able to detect the signal of fire when the fire occurs in the middle of the growing season rather than in the beginning. Concerning environmental factors such as soil regimes and ground

water levels on post-fire ET, the presence of a thick clay layer, versus a shallow lense, appeared to induce capillary rise of soil moisture to reach the soil surface within an area of elevated ET at the Marcial Fire site, and there appears to be a link between elevated groundwater levels and elevated SEBAL-generated values for instantaneous and daily ET and Crop Coefficient data.

This thesis project will ultimately inform hydrological and ecological managers around the globe on tamarisk regenerative behavior and changes in ET post-fire, and will evaluate the effectiveness of the use of fire in river restoration projects. In addition, this thesis project illustrates the power of remote sensing of vegetation regeneration as a sophisticated, cost-effective and accurate alternative to the costly, conventional vegetation monitoring method of point source data collection in the field by individuals.

ACKNOWLEDGEMENTS

I would first like to thank my research advisor Jan Hendrickx for his continued dedication and perseverance towards this project during my residence at New Mexico Tech and while out of state pursuing a professional career in Arizona. Without his perseverance this project would have reached a standstill after my transition into the working world. I would also like to thank my committee members Rob Bowman and Enrique Vivoni for providing feedback, support and patience. I would also like to thank my field partner, Jerry Hess, who taught me the ropes of FIREMON sampling and served as an invaluable role model as a skilled outdoorsman, jubilant neighbor and generous friend. Without being “broken” in the field during this project, I would not be able to withstand the pressing conditions of fieldwork as a professional hydrogeologist in Arizona in the heat of summer.

I would also like to thank Nyleen Troxle-Stowe of the Socorro Soil Water Conservation District, Gina Dello Russo of the Bosque del Apache NWR and Salim Bawazir of NMSU for providing advisory and informational assistance. Thank you to Bruce Harrison and his Soils Class for providing soil analysis and hard labor. I would also like to thank the US Department of Agriculture, NM Experimental Program to Stimulate Competitive Research (NM EPSCoR) and The Energetic Materials Research and Testing Center (EMRTC) for providing funding for my research.

I would like to thank students in my research group for providing support and encouragement: Kathy Fleming, Sung-ho Hong and Jesus Gomez. I would

also like to thank Lewis Gillard for his cheerful willingness to provide ArcGIS support, officemate H ernan Moreno for his kind reassurance, Kate Richards for being a great resource during my first year and Felicia Navarro for her guidance.

This would not have been possible without steadfast support of my parents, Michael and Melanie, who taught me never to quit and are staunch supporters of the importance of lifelong learning and commitment to the community and environment.

TABLE OF CONTENTS

	Page
ABSTRACT	
ACKNOWLEDGEMENTS.....	ii
TABLE OF CONTENTS.....	iv
LIST OF FIGURES.....	v
LIST OF TABLES.....	xii
CHAPTER 1. INTRODUCTION.....	1
1.1 Motivation.....	1
1.2 Tamarisk ET.....	2
1.3 Tamarisk-Fire Control.....	5
1.4 Objectives.....	7
CHAPTER 2. TAMARISK LITERATURE REVIEW.....	8
2.1 Tamarisk Ecology.....	8
2.2 Tamarisk Control Methods.....	10
2.3 Tamarisk-Fire Ecology.....	14
2.4 Socorro County Fire History.....	19
CHAPTER 3. METHODS AND MATERIALS.....	23
3.1 Description of the 3 Fires Investigated.....	23
3.2 Field Sampling Methods.....	40
3.2.1 Vegetation Monitoring and Sampling.....	40
3.2.2 Soil Hydrology Observations.....	51
3.3 Surface Energy Balance Algorithm For Land (SEBAL).....	51
3.4 Satellite Imagery.....	59
3.4.1 LANDSAT Imagery.....	59
3.4.2 MODIS Imagery.....	61
3.5 ArcGIS – 9 Pixel Analysis.....	67
CHAPTER 4. RESULTS AND DISCUSSION.....	72
4.1 Dynamics of Albedo, NDVI, ET and Surface Temperature.....	72
4.2 9-Pixel Bar Graphs.....	93
4.3 Crop Coefficient Over Time.....	111
4.4 MODIS NDVI 16-Day Composite Plots.....	116
4.5 Field Observations.....	122
4.5.1 Summer 2006 Field Sampling Results.....	122
4.5.2 Soils.....	136
4.6 Groundwater Data from the Interstate Stream Commission (ISC).....	147
CHAPTER 5. CONCLUSIONS AND FUTURE RESEARCH.....	157
5.1 Conclusions.....	157
5.2 Future Research.....	165
CHAPTER 6. REFERENCES.....	166
APPENDIX A. 9-PIXEL PLOTS.....	181
APPENDIX B. SUMMER 2006 FIELD SAMPLING DATA.....	194
APPENDIX C. SUMMER 2006 FIELD SAMPLING MAPS.....	217

LIST OF FIGURES

	Page
Figure 1.1. Mean depletions for the Socorro Reach of the Rio Grande River (NM OSE, 2006).....	2
Figure 1.2. Tamarisk extensive root system (UNM, 2006).....	4
Figure 2.1. Tamarisk distribution (in purple) throughout New Mexico (USDA, 2006).....	9
Figure 2.2. Examples of tamarisk control techniques (left to right): herbicide spraying via helicopter, cut-stump biomass clearing, and mechanical removal via bulldozer (SSWCD, 2007).....	12
Figure 2.3. Image of a prescribed fire in a Tamarisk-infested area at the Bosque del Apache NWR (BDA NWR, 2004).....	18
Figure 2.4. Map of New Mexico within the United States. In addition, map of the counties within New Mexico with Socorro County within the red square.....	20
Figure 2.5. Number of fires per year for Socorro County (1987-2006). Courtesy of Doug Boykin, NM State Forestry.....	21
Figure 2.6. Average hectares per fire per year for Socorro County (1987-2006).....	21
Figure 3.1. Mitchell, Marcial and Bosquecito Fire locations within the state of New Mexico.....	23
Figure 3.2. Mitchell Fire site field sampling transects and macroplot locations.....	25
Figure 3.3. Herbicide spraying in the Mandeville track in September of 2003 (SSWCD, 2007).....	27
Figure 3.4. Top row: Images taken during the Mitchell Fire, on April 11, 2005. Bottom row. 1 st image: Sprayed (light brown soil, left) versus non-sprayed (dark brown soil, right); 2 nd image: Non-sprayed (left, dark brown soil) versus sprayed (right, light soil) (SSWCD, 2008).....	28
Figure 3.5. Top row: Images taken 1 month after the Mitchell Fire (SSWCD, 2008).....	29
Figure 3.6. Top row: Images taken two month after the Mitchell Fire of tamarisk resprouts. Bottom row: Tamarisk resprouts with cottonwood grove two months after the fire (SSWCD, 2008).....	30
Figure 3.7. Marcial Fire site with field sampling transects and macroplot locations.....	32
Figure 3.8. Images taken during the Marcial Fire. Top 2 rows from May 4, 2006, last row from May 10, 2006 (SSWCD, 2008).....	34
Figure 3.9. Images taken on June 16, 2006, 1 month after the Marcial Fire (SSWCD, 2008).....	35
Figure 3.10. Bosquecito Fire site field sampling transects and macroplot locations.....	37
Figure 3.11. Herbicide spraying in the Rhodes track in September of 2003 (SSWCD, 2007).....	38

Figure 3.12. Images taken during the Bosquecito Fire, on June 16, 2006 (SSWCD, 2008).....	39
Figure 3.13. Marcial Fire site, Summer 2006 Field Campaign, Nicole (left) and Jerry Hess (right).....	40
Figure 3.14. Illustration of field sampling using the Line Transect method and Macroplots.....	43
Figure 3.15. Cottonwood (left) and willow (right) resprouts.....	48
Figure 3.16. FIREMON Codes for field sampling form (NBII, 2004).....	49
Figure 3.17. FIREMON Codes and percentages for field sampling form (NBII, 2004).....	50
Figure 3.18. FIREMON percentages for field sampling form (NBII, 2004).....	50
Figure 3.19. The Surface Energy Balance.....	58
Figure 3.20. Four LANDSAT 5 TM Images from 2006 and 2007.....	60
Figure 3.21. Image size comparison of a LANDSAT Image and MODIS image with the state of New Mexico outlined in red.....	62
Figure 3.22. Subset of a LANDSAT Image from May 21, 2007 with the 3 fire Sites to illustrate 30-meter pixel resolution.....	65
Figure 3.23. Subset of a 16-Day Composited MODIS Image from May 10-25, 2007 with the 3 fire sites to illustrate 250 meter pixel resolution.....	66
Figure 3.24. 9-Pixel Plots at the Mitchell Fire Site.....	69
Figure 3.25. 9-Pixel Plots at the Marcial Fire Site.....	70
Figure 3.26. 9-Pixel Plots at the Marcial Fire Site.....	71
Figure 4.1. Albedo maps for before and after the Mitchell Fire derived from the SEBAL model applied to Landsat satellite image.....	77
Figure 4.2. Normalized Difference Vegetation Index (NDVI) maps for before and after the Mitchell Fire derived from the SEBAL model applied to Landsat satellite imagery.....	78
Figure 4.3. Instantaneous Evapotranspiration maps for before and after the Mitchell Fire derived from the SEBAL model applied to Landsat satellite imagery.....	79
Figure 4.4. Daily Evapotranspiration maps for before and after the Mitchell Fire derived from the SEBAL model applied to Landsat satellite imagery.....	80
Figure 4.5. Albedo maps for before and after the Marcial Fire derived from the SEBAL model applied to Landsat satellite imagery.....	83
Figure 4.6. Normalized Difference Vegetation Index (NDVI) maps for before and after the Marcial Fire derived from the SEBAL model applied to Landsat satellite imagery.....	84
Figure 4.7. Instantaneous Evapotranspiration maps for before and after the Marcial Fire derived from the SEBAL model applied to Landsat satellite imagery.....	85
Figure 4.8. Daily Evapotranspiration maps for before and after the Marcial Fire derived from the SEBAL model applied to Landsat satellite imagery.....	86
Figure 4.9. Albedo maps for before and after the Bosquecito Fire derived from the SEBAL model applied to Landsat satellite imagery.....	89
Figure 4.10. Normalized Difference Vegetation Index (NDVI) maps for before and after the Bosquecito Fire derived from the SEBAL model applied to	

Landsat satellite imagery.....	90
Figure 4.11. Instantaneous Evapotranspiration maps for before and after the Bosquecito Fire derived from the SEBAL model applied to Landsat satellite imagery.....	91
Figure 4.12. Daily Evapotranspiration maps for before and after the Bosquecito Fire derived from the SEBAL model applied to Landsat satellite Imagery.....	92
Figure 4.13. Plots of Albedo and Ground Heat Flux derived from the SEBAL model and the stated image dates. Each 9-Pixel represents a macroplot sampling location from the Summer 2006 Field Campaign.....	96
Figure 4.14. Plots of Surface Temperature and NDVI derived from the SEBAL model and the stated image dates. Each 9-Pixel represents a macroplot sampling location from the Summer 2006 Field Campaign.....	97
Figure 4.15. Plots of LAI and Instantaneous Evapotranspiration derived from the SEBAL model and the stated image dates. Each 9-Pixel represents a macroplot sampling location from the Summer 2006 Field Campaign.....	98
Figure 4.16. Plots of Daily Evapotranspiration and the Crop Coefficient derived from the SEBAL model and the stated image dates. Each 9-Pixel represents a macroplot sampling location from the Summer 2006 Field Campaign.....	99
Figure 4.17. Plots of Albedo and Ground Heat Flux derived from the SEBAL model and the stated image dates. Each 9-Pixel represents a macroplot sampling location from the Summer 2006 Field Campaign.....	101
Figure 4.18. Plots of Surface Temperature and NDVI derived from the SEBAL model and the stated image dates. Each 9-Pixel represents a macroplot sampling location from the Summer 2006 Field Campaign.....	102
Figure 4.19. Plots of Leaf Area Index and Instantaneous Evapotranspiration derived from the SEBAL model and the stated image dates. Each 9-Pixel represents a macroplot sampling location from the Summer 2006 Field Campaign.....	103
Figure 4.20. Plots of Daily Evapotranspiration and Crop Coefficient derived from the SEBAL model and the stated image dates. Each 9-Pixel represents a macroplot sampling location from the Summer 2006 Field Campaign...	104
Figure 4.21. Plot of Socorro County monthly precipitation for 2000-2007 (DRI, 2007).....	105
Figure 4.22. Plots of Albedo and Ground Heat Flux derived from the SEBAL model and the stated image dates. Each 9-Pixel represents a macroplot sampling location from the Summer 2006 Field Campaign.....	107
Figure 4.23. Plots of Surface Temperature and NDVI derived from the SEBAL model and the stated image dates. Each 9-Pixel represents a macroplot sampling location from the Summer 2006 Field Campaign.....	108
Figure 4.24. Plots of Leaf Area Index and Instantaneous ET derived from the SEBAL model and the stated image dates. Each 9-Pixel represents a macroplot sampling location from the Summer 2006 Field Campaign...	109
Figure 4.25. Plots of Daily Evapotranspiration and the Crop Coefficient derived	

from the SEBAL model and the stated image dates. Each 9-Pixel represents a macroplot sampling location from the Summer 2006 Field Campaign.....	110
Figure 4.26. Kc over time for the 9-Pixel Plots, including Control Site data....	112
Figure 4.27. Kc over time for the 9-Pixel Plots, including Control Site data....	114
Figure 4.28. Representative groundwater well in proximity to the Marcial Fire. Total well depth is 19.5 feet. The blue circles represent elevated groundwater table levels in May of each year (ISC, 2007).....	114
Figure 4.29. Kc over time for the 9-Pixel Plots, including Control Site data....	116
Figure 4.30. MODIS-derived Average NDVI seasonal profile with standard deviation bars for the Mitchell Fire Site. The red circle indicates the composite dates that were immediately impacted by the fire.....	119
Figure 4.31. MODIS-derived Average NDVI seasonal profile with standard deviation bars for the Marcial Fire Site. The red circle indicates the composite dates that were immediately impacted by the fire.....	120
Figure 4.32. MODIS-derived Average NDVI seasonal profile for the Bosquecito Fire Site. The red circle indicates the composite dates that were immediately impacted by the fire.....	121
Figure 4.33. MODIS-derived Average NDVI seasonal profiles for the 3 fire Sites.....	121
Figure 4.34. Ocular measurements of tamarisk cover from the Summer 2006 Field Campaign. Additional figures can be found in Appendix C.....	125
Figure 4.35. Ocular measurements of dominant vegetation (tamarisk) stand height from the Summer 2006 Field Campaign. Additional figures can be found in Appendix C.....	126
Figure 4.36. Ocular measurements of vegetation and environmental parameters from the Summer 2006 Field Campaign.....	129
Figure 4.37. Ocular measurements of vegetation and environmental parameters from The Summer 2006 Field Campaign.....	130
Figure 4.38. Ocular measurements of vegetation and environmental parameters from the Summer 2006 Field Campaign.....	134
Figure 4.39. Ocular measurements of vegetation and environmental parameters from the Summer 2006 Field Campaign.....	135
Figure 4.40. Surficial Geology map courtesy of the NM Bureau of Geology. The circled macroplot represents a 9-Pixel Plot with anomalously low Daily and Instantaneous ET values over time, independent of the fire.....	138
Figure 4.41. Cross section created from soil sampling performed in February 2008.....	139
Figure 4.42. Surficial Geology map courtesy of the NM Bureau of Geology. The circled macroplot is 9-Pixel Plot number 42/SM1, a macroplot with anomalously low Daily and Instantaneous ET values over time, independent of the fire.....	141
Figure 4.43. Cross section created from soil sampling performed in February 2008.....	142
Figure 4.44. Surficial Geology map courtesy of the NM Bureau of Geology. 9-Pixel Plot 43/BQC 1 is located within the black square and represents a 9-	

Pixel Plot with anomalously high Daily and Instantaneous ET values over time, independent of the fire.....	145
Figure 4.45. Cross section created from soil sampling performed in February 2008.....	146
Figure 4.46. Groundwater wells near the Mitchell Fire (ISC, 2007).....	149
Figure 4.47. Groundwater wells at the HWY Transect, near the Mitchell Fire (ISC, 2007).....	150
Figure 4.48. Representative groundwater well in proximity to the Mitchell Fire. Total well depth is 18.7 feet (ISC, 2007).....	150
Figure 4.49. Groundwater wells near the Marcial Fire (ISC, 2007).....	151
Figure 4.50. Groundwater wells near the Mitchell Fire, focusing on the wells near the Northwest portion of the fire (ISC, 2007).....	152
Figure 4.51. Groundwater wells at the SMC Transect, near the Marcial Fire (ISC, 2007).....	153
Figure 4.52. Representative groundwater well in proximity to the Marcial Fire. Total well depth is 19.5 feet. The blue circles represent elevated groundwater table levels in May of each year (ISC, 2007).....	153
Figure 4.53. Groundwater wells near the Bosquecito Fire (ISC, 2007).....	154
Figure 4.54. Groundwater wells at the BRN Transect, near the Marcial Fire (ISC, 2007).....	155
Figure 4.55. Representative groundwater well in proximity to the Bosquecito Fire. Total well depth is 16.7 feet (ISC, 2007).....	155
Figure 4.56. MODIS-derived Average NDVI seasonal profiles for the 3 fire sites.....	156
Figure A.1. Plots of Albedo and Ground Heat Flux derived from the SEBAL model and the stated image dates. Each 9-Pixel represents a macroplot sampling location from the Summer 2006 Field Campaign.....	182
Figure A.2. Plots of Surface Temperature and NDVI derived from the SEBAL model and the stated image dates. Each 9-Pixel represents a macroplot sampling location from the Summer 2006 Field Campaign.....	183
Figure A.3. Plots of LAI and Instantaneous Evapotranspiration derived from the SEBAL model and the stated image dates. Each 9-Pixel represents a macroplot sampling location from the Summer 2006 Field Campaign...	184
Figure A.4. Plots of Daily Evapotranspiration and the Crop Coefficient derived from the SEBAL model and the stated image dates. Each 9-Pixel represents a macroplot sampling location from the Summer 2006 Field Campaign.....	185
Figure A.5. Plots of Albedo and Ground Heat Flux derived from the SEBAL model and the stated image dates. Each 9-Pixel represents a macroplot sampling location from the Summer 2006 Field Campaign.....	186
Figure A.6. Plots of Surface Temperature and NDVI derived from the SEBAL model and the stated image dates. Each 9-Pixel represents a macroplot sampling location from the Summer 2006 Field Campaign.....	187
Figure A.7. Plots of Leaf Area Index and Instantaneous Evapotranspiration derived from the SEBAL model and the stated image dates. Each 9-Pixel	

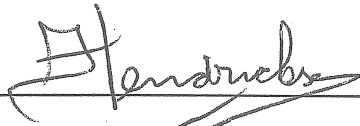
represents a macroplot sampling location from the Summer 2006 Field Campaign.....	188
Figure A.8. Plots of Daily Evapotranspiration and Crop Coefficient derived from the SEBAL model and the stated image dates. Each 9-Pixel represents a macroplot sampling location from the Summer 2006 Field Campaign....	189
Figure A.9. Plots of Albedo and Ground Heat Flux derived from the SEBAL model and the stated image dates. Each 9-Pixel represents a macroplot sampling location from the Summer 2006 Field Campaign.....	190
Figure A.10. Plots of Surface Temperature and NDVI derived from the SEBAL model and the stated image dates. Each 9-Pixel represents a macroplot sampling location from the Summer 2006 Field Campaign.....	191
Figure A.11. Plots of LAI and Instantaneous Evapotranspiration derived from the SEBAL model and the stated image dates. Each 9-Pixel represents a macroplot sampling location from the Summer 2006 Field Campaign....	192
Figure A.12. Plots of Daily Evapotranspiration and the Crop Coefficient derived from the SEBAL model and the stated image dates. Each 9-Pixel represents a macroplot sampling location from the Summer 2006 Field Campaign.....	193
Figure C.1. Ocular measurements of vegetation and environmental parameters from the Summer 2006 Field Campaign.....	218
Figure C.2. Ocular measurements of vegetation and environmental parameters from the Summer 2006 Field Campaign.....	219
Figure C.3. Ocular measurements of vegetation and environmental parameters from the Summer 2006 Field Campaign.....	220
Figure C.4. Ocular measurements of vegetation and environmental parameters from the Summer 2006 Field Campaign.....	221
Figure C.5. Ocular measurements of vegetation and environmental parameters from the Summer 2006 Field Campaign.....	222
Figure C.6. Ocular measurements of vegetation and environmental parameters from the Summer 2006 Field Campaign.....	223
Figure C.7. Ocular measurements of vegetation and environmental parameters from the Summer 2006 Field Campaign.....	224
Figure C.8. Ocular measurements of vegetation and environmental parameters from the Summer 2006 Field Campaign.....	225
Figure C.9. Ocular measurements of vegetation and environmental parameters from the Summer 2006 Field Campaign.....	226
Figure C.10. Ocular measurements of vegetation and environmental parameters from the Summer 2006 Field Campaign.....	227
Figure C.11. Ocular measurements of vegetation and environmental parameters from the Summer 2006 Field Campaign.....	228
Figure C.12. Ocular measurements of vegetation and environmental parameters from the Summer 2006 Field Campaign.....	229
Figure C.13. Ocular measurements of vegetation and environmental parameters from the Summer 2006 Field Campaign.....	230
Figure C.14. Ocular measurements of vegetation and environmental parameters from the Summer 2006 Field Campaign.....	231

Figure C.15. Ocular measurements of vegetation and environmental parameters from the Summer 2006 Field Campaign.....	232
Figure C.16. Ocular measurements of vegetation and environmental parameters from the Summer 2006 Field Campaign.....	233
Figure C.17. Ocular measurements of vegetation and environmental parameters from the Summer 2006 Field Campaign.....	234
Figure C.18. Ocular measurements of vegetation and environmental parameters from the Summer 2006 Field Campaign.....	235
Figure C.19. Ocular measurements of vegetation and environmental parameters from the Summer 2006 Field Campaign.....	236
Figure C.20. Ocular measurements of vegetation and environmental parameters from the Summer 2006 Field Campaign.....	237
Figure C.21. Ocular measurements of vegetation and environmental parameters from the Summer 2006 Field Campaign.....	238
Figure C.22. Ocular measurements of vegetation and environmental parameters from the Summer 2006 Field Campaign.....	239

LIST OF TABLES

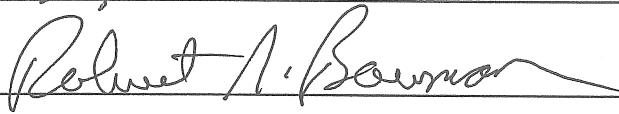
	Page
Table 1.1. Published data sources, management method, spatial scale, and ET measure for <i>Tamarisk ramosissima</i> (Cleverly et al., 2002).....	5
Table 2.1. Count of WUI Communities and Average Hazard Rating (NM State Forestry, 2006).....	22
Table 3.1. MODIS Image dates, every 16 days, used for NDVI analysis.....	63
Table B.1. Summary of ocular data collected at the Mitchell Fire Site in October of 2006, 18 months after the fire.....	188
Table B.2. Summary of data collected at the Marcial Fire Site in August of 2006.....	192
Table B.3. Summary of data collected in September of 2006.....	202

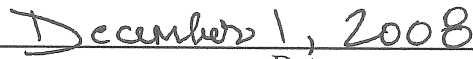
This thesis is accepted on behalf of the
Faculty of the Institute by the following committee:



Advisor





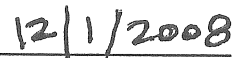


Date

I release this document to the New Mexico Institute of Mining and Technology.



Student's Signature



Date

1. INTRODUCTION

1.1 Motivation

Evapotranspiration (ET) is defined as the total amount of water that is transferred from the earth's surface to the atmosphere by evaporation from soil and water surfaces and transpiration from growing vegetation. ET is a major component in the hydrologic cycle of semi-arid regions with scarce water supplies, such as New Mexico and the Southwestern USA. In arid and semi-arid basins, water loss to the atmosphere from riparian corridors generally dominates the components of a basin's water budget. For example, in the Middle Rio Grande basin well over 90% of surface water depletions are due to open water evaporation, soil evaporation, riparian and agricultural ET (Cleverly et al., 2002; Dahm et al., 2002). ET from riparian vegetation has been estimated to represent 30% of the total depletions in the Middle Rio Grande water budget (Cleverly et al., 2006).

Within the study region, the Socorro Reach of the Middle Rio Grande, there are various water demands including agricultural, riparian, wildlife, and municipal needs (Figure 1.1). This reach of the Rio Grande historically runs dry in the summer, which may strain agricultural and environmental needs. Low river flows may result in New Mexico defaulting on obligations legislated in the Rio Grande Compact of 1938 (Middle Rio Grande Regional Water Plan, 2004).

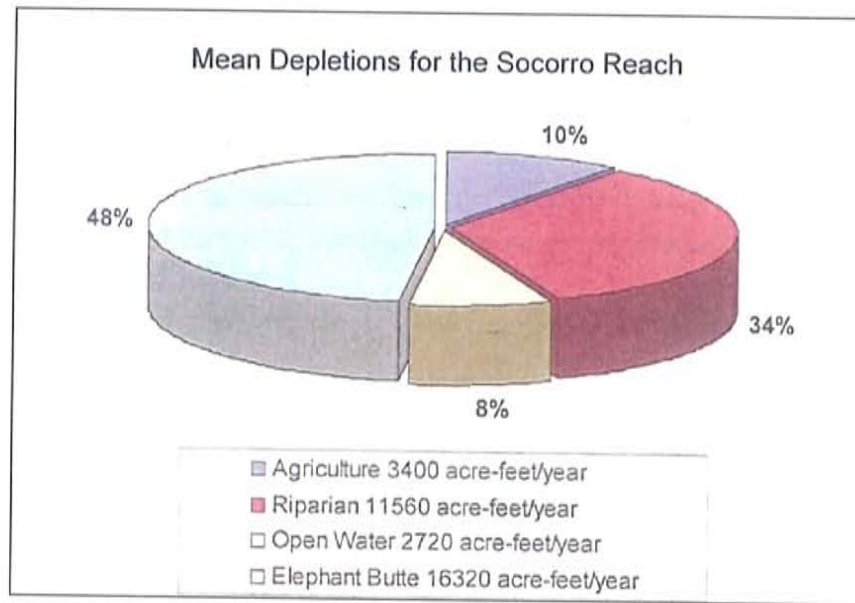


Figure 1.1 Mean depletions for the Socorro Reach of the Rio Grande River (NM OSE, 2006).

1.2 Tamarisk ET

The vegetation species in focus within this thesis which is of great concern to the citizens of New Mexico, and produces immense evaporative losses in the Middle Rio Grande Basin, is the tamarisk (*Tamarix ramosissima*), otherwise known as the salt cedar. ET rates of tamarisk are amongst the highest of southwestern phreatophytes (Brotherson et al., 1984), deep-rooted plants often found in arid environments that obtain water a permanent ground supply or from the water table. Tamarisk water consumption has the ability to drain pools and dry up perennial springs (Brotherson et al., 1984). On an individual basis, tamarisk stands have transpiration rates similar to native riparian plants such as cottonwood and willow (Anderson, 1982); however, tamarisk tends to grow at higher densities than native riparian vegetation and as a result uses more water

per unit area (Sala et al., 1996). The longer a community has been invaded by tamarisk, the greater the capacity to decrease groundwater levels and decrease water resource availability.

The growth of tamarisk infestation depends on the water table depth and the hydrologic history of an area. Tamarisk's deeply penetrating roots portrayed in Figure 1.2 are observed at depths as great as 30 meters (Robinson 1958) and gives it the ability to access more available water than plants with shallow root systems (Everitt, 1980). When the water table is high, tamarisk develop a taproot and secondary roots that occupy all zones of the soil profile above the water table (Robinson, 1958). As water table depth increases, tamarisk must send its roots down further to reach the capillary fringe; thus water use decreases with increasing water table depth. Water tables can fluctuate considerably due to seasonal and annual changes in inflows as well as fluvial processes (Shafroth et al. 2000) and transpiration by riparian vegetation. Horton et al. (2001) found that a water table decline of 1.1 m from the previous year level of 2.0 m resulted in 92-100% mortality of cottonwood and willow saplings, whereas, only 0-13% of tamarisk stems died.

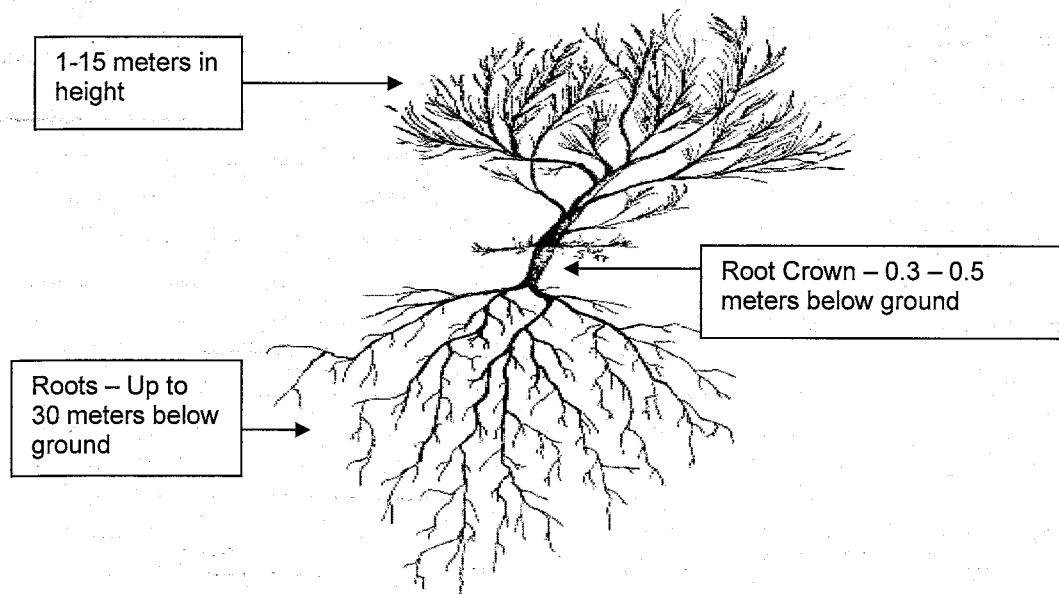


Figure 1.2. Tamarisk extensive root system (UNM, 2006).

Evapotranspiration is very site specific due to differences in water table depth, salinity, and hydraulic conductivity of the soil, as well as due to differences in vegetation characteristics, atmospheric conditions, time of day, and method used to calculate water use (White et al., 2003). At the Bosque del Apache National Wildlife Refuge National Wildlife Refuge (BDA NWR), ET rates from a dense stand of tamarisk was 1.2 m/yr during the growing season of April 5 to November 21 (Bawazir, 2000). In comparison, a sparse stand of cottonwood used 0.8 m/yr during the same growing season. Also at the BDA, average ET rates at flooded tamarisk sites from December to March were 5.4 ± 0.2 mm/day, with a maximum of 9.8 mm/day in the growing season (Cleverly et al., 2002). James Cleverly of the University of New Mexico compiled a comprehensive table on published *Tamarisk ramosissima* ET figures “that is first of its kind” and

provided below in Table 1.1. The table states the various methods and ranges in the determination of tamarisk ET.

Study	Method	ET range
<i>Leaf-level</i>		
Anderson, 1982	<i>In situ</i>	2.2–2.5 mmol m ⁻² s ⁻¹
Busch & Smith, 1995	<i>In situ</i>	3–8 mmol m ⁻² s ⁻¹
<i>Canopy-level</i>		
Gay & Fritschen, 1979	Lysimeter	6.2–9.4 mm day ⁻¹
Sala <i>et al.</i> , 1996	Sap flux	0.3–0.6 kg (m ² leaf area) ⁻¹ h ⁻¹
Cleverly <i>et al.</i> , 1997	Sap flux	600–1000 kg (m ² sapwood area) ⁻¹ h ⁻¹
Devitt <i>et al.</i> , 1997a	Sap flux	0–2.1 kg (m ² leaf area) ⁻¹ h ⁻¹
Devitt <i>et al.</i> , 1997a	Sap flux	0–21 kg (m ² leaf area) ⁻¹ h ⁻¹
Devitt <i>et al.</i> , 1997b	Sap flux	200–2,000 kg (m ² sapwood area) ⁻¹ h ⁻¹
Glenn <i>et al.</i> , 1998	Lysimeter	12.9 ± 0.67 g (g fresh weight) ⁻¹ day ⁻¹
Xu <i>et al.</i> , 1998	Lysimeter	3.1–3.8 mm day ⁻¹
<i>Stand-level</i>		
Culler <i>et al.</i> , 1976	Near-IR	1.3–3.1 mm day ⁻¹
Gay & Fritschen, 1979	Bowen Ratio	7.2–9.5 mm day ⁻¹
Davenport <i>et al.</i> , 1982	Lysimeter*	2.2–15.8 mm day ⁻¹
Sala <i>et al.</i> , 1996	Sap flux*	5.4–20.2 mm day ⁻¹
Sala <i>et al.</i> , 1996	Penman–Monteith	3.1–8.2 mm day ⁻¹
Devitt <i>et al.</i> , 1997a	Penman–Monteith	3.5–8.0 mm day ⁻¹
Hansen & Gorbach, 1997	Blaney–Criddle	2.0–2.7 mm day ⁻¹
Devitt <i>et al.</i> , 1998	Bowen Ratio	0–12.5 mm day ⁻¹

Leaf-level data were collected using a leaf chamber on intact plants in the field (*in situ*).

*Scaled up from the canopy level.

Table 1.1 Published data sources, management method, spatial scale, and ET measure for *Tamarisk ramosissima* (Cleverly *et al.*, 2002).

1.3 Tamarisk-Fire Control

In recent years, fire has been used as a natural and cost effective mechanism in the control of tamarisk infestation at the local Bosque Del Apache National Wildlife Refuge (BDA NWR) and within riparian corridors of the Southwest. Tamarisk is a fire adapted species—it regrows early after fire—but little is known about the timing of tamarisk regrowth after wildfires. Even less is

known about regrowth during the crucial first few weeks to 2 months after a fire, the critical time when the process of tamarisk succession begins. A canopy fire at Lees Ferry, Arizona, killed 10% of mature tamarisk plants, and surviving plants produced shoots that exceeded 1.8 m (6 feet) in height within 5 months (Stevens, 1989). Regrowth of surviving tamarisk plants after a July wildfire at Lake Meredith National Recreation Area, Texas, exceeded 1.8 m (6 feet) at the end of that growing season (Fox et al, 2001). Tamarisk recovery has been studied in the time frame of 6-months and years, but this thesis is the first to quantitatively examine post-fire recovery in a time series fashion of weeks to 2 years after fire, using ET as a proxy for vegetation regeneration.

Monitoring post-fire tamarisk ET and vegetation recovery is important to establish post-fire tamarisk management, such as spraying the tamarisk with herbicide after a burn, an integrative technique that has been proven to be up to 93% effective (McDaniel and Taylor, 2003) in tamarisk eradication. The Bosque del Apache NWR has implemented highly effective integrated tamarisk management approaches including combinations of herbicide, burning and mechanical control treatment. The final goal is to replant previously tamarisk infested areas with native vegetation species such as cottonwood and willow, vegetation with comparatively lower ET rates in sparsely populated communities. The revegetation with native species will serve to improve habitat for several species of birds, small mammals, reptiles, and amphibians in the Bosque del Apache National Wildlife Refuge. This thesis will demonstrate that the use of fire alone to control tamarisk is generally ineffective, and will provide additional

information pertinent to the timing of regrowth after wild fires, an area of study where much is unknown.

Junming Wang of the New Mexico State University was the “first, and only” researcher to use SEBAL to estimate and contrast ET at burned and non-burned areas to infer the spatial-temporal vegetation recovery after fires (Wang et al., 2005). His work revealed ET maps from before and after the Los Alamos Fire of May 2000 and found 47% recovery of the piñon-juniper woodland biota 3 years after the fire (Wang et al., 2005). His paper was the sole source formally relating SEBAL, ET and vegetation recovery.

1.4 Objectives

The overall goal of this thesis is to quantify how wild fires affect the ET and vegetation regeneration of tamarisk in the Middle Rio Grande Valley. The specific objectives are the following:

1. Quantify changes in ET and vegetation cover due to wild fires using Landsat and MODIS satellite imagery.
2. Use observations on ET and vegetation cover changes before and after wild fires to determine the optimal timing for the elimination of Tamarisk re-sprouts using herbicides and mechanical removal.

2. TAMARISK LITERATURE REVIEW

2.1 Tamarisk Ecology

Among the most well known non-native invasive plant species in the southwestern United States are trees of the family Tamaricaceae (Genus *Tamarix*), also referred to as tamarisk or salt cedar. Tamarisk is native to southern Europe and Asia, where it occurs from the Near East to the Caspian Sea and across Asia to China and Korea. An estimated eight to twelve *Tamarix* species were introduced into North America in the 1800's as means of flood and stream bank erosion control, as protective barriers against wind, and in some cases, as ornamental shrubbery (USDA-NRCS, 2006). These introduced species have long since become naturalized and hybridized into species that are now considered to be highly invasive throughout the U.S., particularly in the Southwest. Tamarisk species currently line many rivers, streams, and lakes in the Southwest and are common along the shores of Texas, extending to Southern North Carolina and down into the Gulf of Mexico (USDA-NRCS, 2006), and some species may be capable of invading colder climates in the U.S. (Sexton et al., 2002).

Four species of Tamarisk are reportedly found in New Mexico: *Tamarix ramosissima* (*ramosissima* meaning "most densely branched") or tamarisk, *Tamarix chinensis* or five stamen tamarisk, *Tamarix parviflora* or small flower tamarisk, and *Tamarix gallica* or French tamarisk. Together, these four species

cover 20 counties of New Mexico, the distribution of which is shown in purple in Figure 2.1 (USDA, 2006). Tamarisk is currently considered a Class C Noxious Weed in New Mexico by the United States Department of Agriculture (USDA, 2006). This listing implies that tamarisk is considered a widespread invasive plant, and that laws are currently being considered or implemented to gain control over its spread and environmental consequences.

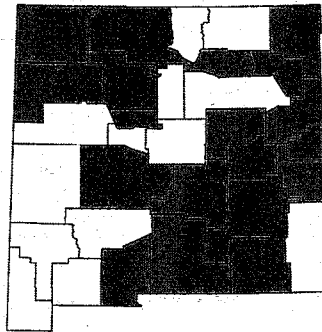


Figure 2.1. Tamarisk distribution (in purple) throughout New Mexico (USDA, 2006).

Long term measures have been executed by local government agencies, such as The Socorro Soil Water Conservation District (SSWCD), the Fish and Wildlife Service (FWS), United States Department of Agriculture (USDA), and United States Forest Service (USFS) to eradicate tamarisk on public and private lands and revegetate previously-tamarisk areas with local riparian vegetation species such native Rio Grande cottonwood (*Populus deltoids* var. *wislenzii* and Godding's willow (*Salix gooddingii*), as well as vegetation that fosters habitat to the federally endangered Southwestern willow flycatcher (WIFL) (*Empidonax traillii extimus*). The measures serve for restoration and legislative purposes.

The Supreme Court Decree of 1988 set conditions that New Mexico must meet compact obligations with delivery of water to Texas. The Soil and Water

Conservation Districts, through the New Mexico Association of Conservation Districts, have worked with the New Mexico State Legislature on opportunities to enhance flows on the Rio Grande. The Legislature approved funding during the 2002, 2003, 2004, and 2005 legislative sessions. The Lower Rio Grande Salt Cedar Control Project (SSWCD) has used this funding to treat tamarisk, aid in restoration and monitor treatments in Socorro, Sierra, Caballo and La Union Soil and Water Conservation Districts in Socorro, Sierra, and Dona Ana counties (SSWCD, 2007).

The USDA, USFS, and FWS have joined together to create \$64.4 million dollar Integrated Vegetation Management (IVM) 10-year program to prevent the spread of non-natives such as the Tamarisk, Russian olive (*Elaeagnus angustifolia*) and Siberian elm (*Ulmus pumila*), to control existing infestations, maintain the health of native plant communities, and restore native plant communities throughout the five major river systems in New Mexico (Parker et al., 2005). The agencies believe that the dense stands of exotic species have limited recreational value, increase the chance of wildfire, decrease water availability, and degrade biological diversity. The IVM proposes the use of chemical, biological, mechanical and fire management techniques in order to control present non-native infestations (Parker et. al 2005).

2.2 Tamarisk Control Methods

Techniques used to control tamarisk have included various combinations of herbicide application, mechanical control, burning and biological control.

Photos of aerial herbicide treatment, cut-stump biomass clearing, and mechanical removal via bulldozer are provided in Figure 2.2 to explore the range in spatial scale in herbicide treatment, from large application via herbicide to cutting stump-by-stump. Treatments have proven satisfactory primarily due to the flexibility in employing one or several of these techniques if and when required. Arsenal herbicide (American Cyanamid, 1994) has been used in both ground and aerial applications. Controlled burning may be used to decrease tamarisk biomass and in preparation for revegetation following aerial spraying. Mechanical control involves root plowing and raking using heavy equipment. Bulldozers pull large plows about 45 cm below the ground surface, sheering root crowns from the remainder of the root mass. The root crown is the underground portion of the plant from which resprouts arise. Root crowns are then pulled from the ground using large rakes and then stacked for burning with front-end loaders equipped with brush rakes. The operation leaves an even surface which facilitates flooding or planting. Combinations of mechanical and chemical control have also been used (FWS, 2004). Decisions for the type of control can depend on soil type, equipment availability, time constraints, fire danger, environmental sensitivity, and the degree of infestation. Costs for tamarisk control range from less than \$125/acre for herbicide-plus-burn control to \$395/acre for mechanical control (FWS, 2004). Regardless of the control measure employed, monitoring should occur to assess control and cost effectiveness.

One of the tamarisk removal techniques is through the use of controlled burning. Tamarisk is early successional after fire, but little is known about

succession rates to full maturity. Knowledge of succession rates will provide ecological managers with a timetable for the implementation of combined control techniques, such as burning followed by herbicide treatment, that have been proven to maximize tamarisk clearing of up to 93% (McDaniel and Taylor 2003). In addition, the project aims to provide a time table for the implementation of combined burn-herbicide control techniques, as an alternative to costly tamarisk removal methods such as mechanical removal or cut-stump herbicide application.



Figure 2.2. Examples of tamarisk control techniques (left to right): herbicide spraying via helicopter, cut-stump biomass clearing, and mechanical removal via bulldozer (SSWCD, 2007).

Fire as a Management Tool

In some areas, prescribed fire can be used to manage tamarisk by eliminating the closed canopy, slowing the rate of invasion, and allowing desirable vegetation to respond, thereby increasing diversity in monotypic tamarisk stands. Burning these communities under controlled conditions can also reduce the potential for costly wildfires that must be suppressed to avoid property loss (Rascher et al. 2001).

Fire in Conjunction with Herbicide

Use of fire alone to control tamarisk is generally ineffective. Prescribed fire can be used to thin dense tamarisk infestations prior to follow up application of herbicide (Lovich 2000) as a dual-control method. Experiments at the Ouray National Wildlife Refuge in Randlett, Utah, indicate that prescribed burning coupled with herbicide application in the spring, fall and winter are ineffective at controlling tamarisk, while prescribed burning coupled with herbicide application in July can be effective. Burning in late July prevented 64% of tamarisk plants from resprouting the following year, while spraying resprouts with the herbicide 2,4-Dichlorophenoxyacetic acid (2,4-D) one month after the July burn prevented 99% of the plants from resprouting. Burning and spraying with 2,4-D in September and October resulted in 12% and 5% tamarisk plant mortality, respectively. Using Triclopyr-ester as a stump treatment or as a basal bark spray also prevented resprouts by 99%, while Triclopyr-amine provided poor control (Howard et al., 1983). Basal applications of imazapyr did not effectively control burned, resprouting tamarisk one growing season after treatment at Lake Meredith National Recreation Area, Texas (Fox, 2000).

Fire in Conjunction with Herbicide and Mechanical Control

A summer wildfire at Lake Meredith National Recreation Area, Texas, provided an opportunity to investigate tamarisk response to wildfire and to

mechanical and chemical control following fire. Many tamarisks were completely consumed by the wildfire. Regrowth of surviving plants exceeded 1.8 m at the end of that growing season. About 20.2 hectares (50 acres) of the burned tamarisk were roller-chopped the following June. Triclopyr was applied in February and again in March as individual plant basal treatments to 100 fire generated resprouts each month. Treatment efficacy was evaluated 12 months after treatment. Tamarisk mortality was 60%. The combined effect of summer wildfire and roller chopping was 85% mortality. Herbicide applications resulted in 90% and 95% mortality from February and March treatments, respectively. Preliminary results indicate that dormant season individual plant treatment with 25% Triclopyr following burning is an effective method for managing tamarisk infestations (Fox, 2001).

2.3 Tamarisk-Fire Ecology

Fire Importance

Fire has a powerful influence on ecosystem dynamics and function across a large variety of biomes. Fire-induced changes in ecosystem functioning and in plant and animal species composition mostly occur as a consequence of biomass loss and alterations of soil properties (Seastedt et al., 1991). These changes imply increasing light arriving to the soil surface, loss of carbon and other nutrients from the overall ecosystem, and an effect on the fertilization of soils (Seastedt et al., 1991). In recent years, the fundamental role of fire in maintaining ecosystem function has been recognized, which has led to subsequent concern about the consequences of human impacts in altering the

natural cycles of wildfire disturbances. Monitoring postfire regeneration is important to establish postfire resource management and to design revegetation programs.

Fires also have profound effects on land use, production, local economies, global trace gas emissions and health. Fire potential depends on the amount of dead and live vegetation, the moisture in the live vegetation, and the moisture in the dead vegetation. Uncontrolled wildfires can have an immense impact on the human population and the environment, as was witnessed in the wildfires in Utah and South Tahoe, California during July of 2007, and the Southern California wildfires of October of 2007. A fire analysis cycle can be defined that moves from mapping the potential for a fire start if there is ignition, to detecting the start of a fire, through monitoring the progression of a fire, to mapping the extent of the fire scars and the progression of vegetation regeneration. Such information is useful to managers, policy makers and scientists interested in mitigating and evaluating the effects of wildfires.

Local firefighters quickly control most fires while they are still fairly small. However, a significant number of fires exceed the ability of the first fire suppression forces to contain them and spread to cause loss of life and substantial damage to natural resources and property. To minimize this threat of loss from wildfires, fire managers must be able to plan protection strategies that are appropriate for local areas. A prerequisite for this planning is the ability to assess and map, for large areas, the local potential for a major fire to occur. Using such geospatial information, managers can establish priorities for

prevention activities to reduce the risk of wildfire spread and for allocating suppression forces to improve the probability of quickly controlling fires in areas of high concern (Klaver et al., 2003).

Fires in semi-arid regions can result in complete consumption of vegetation cover, ground litter and fuels, in addition to the exposure and/or darkening and brightening of soil due to ash deposition (Rogan and Yool, 2001). Light or moderate fires can result in the partial consumption of vegetation cover, litter, and fuels with little soil exposure or ash deposition. The post-fire appearance of burned sites may be used to estimate the severity of a burn.

Tamarisk Fire-Adaptation

Tamarisk is a fire-adapted species with more efficient fire recovery mechanisms than nearly all native riparian species (Anderson et al., 1982). Tamarisk can form new plants by sprouting from the root crown and stem segments (Brotherson et al., 1987). Following fire, tamarisk is better able to utilize available soil moisture, higher soil concentrations of mineral elements, and increased soil pH than native woody riparian species (Anderson et al., 1982). The ability of tamarisk to tolerate high levels of soil salinity may also favor it in the post-fire environment, as soil salinity tends to increase after fire (Anderson et al., 1982). The adaptations have likely been a significant factor promoting its rapid colonization of waterways. In native riparian plant communities dominated by cottonwood, willows, or mesquite, wildfires are infrequent (Busch and Smith, 1993). In contrast, intervals between fires are considerably shorter in tamarisk-

infested areas. It has been hypothesized that tamarisk, like other plant species that readily resprout, might have developed adaptive characteristics that enhance flammability of plant communities where they grow (Busch and Smith, 1993). This can lead to replacement of cottonwood and willow that are not adapted to fire. In support of this, Anderson et al. (1982) demonstrated that 21 of 25 tamarisk stands along the lower Colorado River burned within a 15-yr period. Fires burned 35% of tamarisk-dominated vegetation on the lower Colorado River floodplain between 1981 and 1992, compared to only 2% of communities of honey mesquite or screw bean mesquite during the same time period (Busch, 1995). Increased incidence of fire in tamarisk stands has been attributed to substantial accumulation of leaf litter, as well as dead and senesced woody material. Fuel buildup by tamarisk promotes fire every 10 to 20 yr in North American desert riparian settings (Lovich et al., 1994).

Fire Effects

Tamarisk is usually top-killed by fire, and severe fire may also kill the root crown (Ellis et al., 2006). Tamarisk seeds withstand a dry heat of 212 °F (100 °C) for 20 minutes; higher temperatures kill seeds within a few minutes (Horton et al., 1960). A photo example of the fierce nature of tamarisk fire charring above ground biomass is provided in Figure 2.3, as shot locally at the Bosque del Apache National Wildlife Refuge. The immediate effect of fire on tamarisk depends on fire severity, which is largely a function of the quantity and quality of fuels present. Tamarisk leaves are not highly flammable due to high moisture content, even though they contain volatile oils. Tamarisk flammability increases

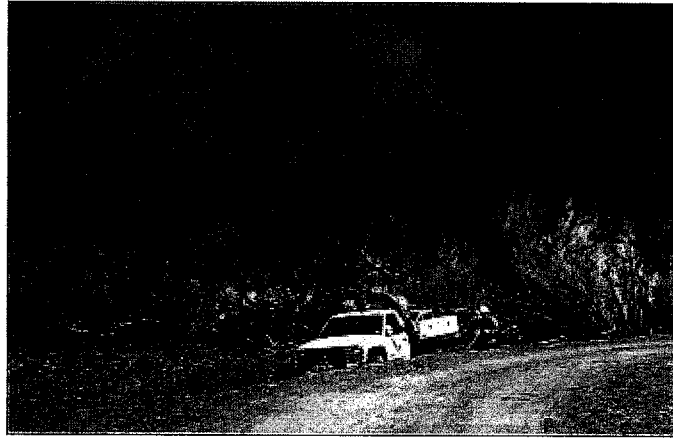


Figure 2.3. Image of a prescribed fire in a Tamarisk-infested area at the Bosque del Apache NWR (BDA NWR, 2004).

with the build-up of dead and senescent woody material within the plant (Busch, 1995). When plants burn under high fuel loads, fire tends to be more severe--top-killing many plants and increasing the likelihood of killing the root crown of some individuals (Ellis et al., 2006).

Timing of fire can affect tamarisk response due to its effects on fire severity, subsequent climate conditions, or phenological stage. Under stressed conditions, as many as half of the shrubs may not survive burning (Horton, 1977). Ongoing research in eastern New Mexico is being conducted to determine the best phenological stage to burn and reburn tamarisk to reduce density, canopy, and hazardous fuel load. Phenological stages at which treatments have been applied include: dormancy, leaf elongation, first bloom, full canopy, and leaf senescence (Holdt et al., 2002). A review by Grace (2001) suggests that burning during the peak of summer has the strongest adverse effect on tamarisk, presumably due to subsequent water stress. Ellis et al.

(2001) suggested that tamarisk stands are highly susceptible to fires due to accumulation of organic debris in the absence of flooding.

Short-term responses of riparian vegetation to a wildfire were monitored at two study sites at the BDA NWR. Fire severity reflected the amount of organic debris present before the fire, which reflected flooding history at the two sites. Fire severity was lower at the site with a more extensive flooding history and less debris. Resprouting was prevalent among cottonwoods at both burn sites including basal stem sprouts, root crown sprouts, and root suckering. However, of the native Rio Grande cottonwoods in the area, only those located in an area that experienced lower fire severity (the area had been regularly flooded) retained viable aboveground tissue two years after the fire. Considering the fuel accumulations along the Middle Rio Grande Valley it is likely that fire severity will continue to be high and the loss of mature cottonwoods may be extensive. Reducing current fuel load, either by restoring flooding or by mechanical removal, is needed to lessen the impact of fires on riparian forests along the Rio Grande (Ellis et al., 2006).

2.4 Socorro County Fire History

To provide a generalized assessment of fire occurrence in the vicinity, a review was conducted of a Socorro Fire database from 1987 to 2006 made available by Doug Boykin of New Mexico State Forestry. For reference, a map of the counties within the state of New Mexico is found in Figure 2.4. Exclusive of the 2005 Mitchell Fire and 2006 Marcial and Bosquecito Fires, there have been

744 fires during the 20 year period. The 20-year average within Socorro County was approximately 35.4 fires per year; a histogram of number of fires per year for a 20 year period in Socorro County is provided in Figure 2.5. Average annual acreage-burned was approximately 39.2 hectares (96.8 acres); a histogram of average hectares burned for a 20 year period in Socorro County is provided in Figure 2.6.



Figure 2.4. Map of New Mexico within the United States. In addition, map of the counties within New Mexico with Socorro County within the red square.

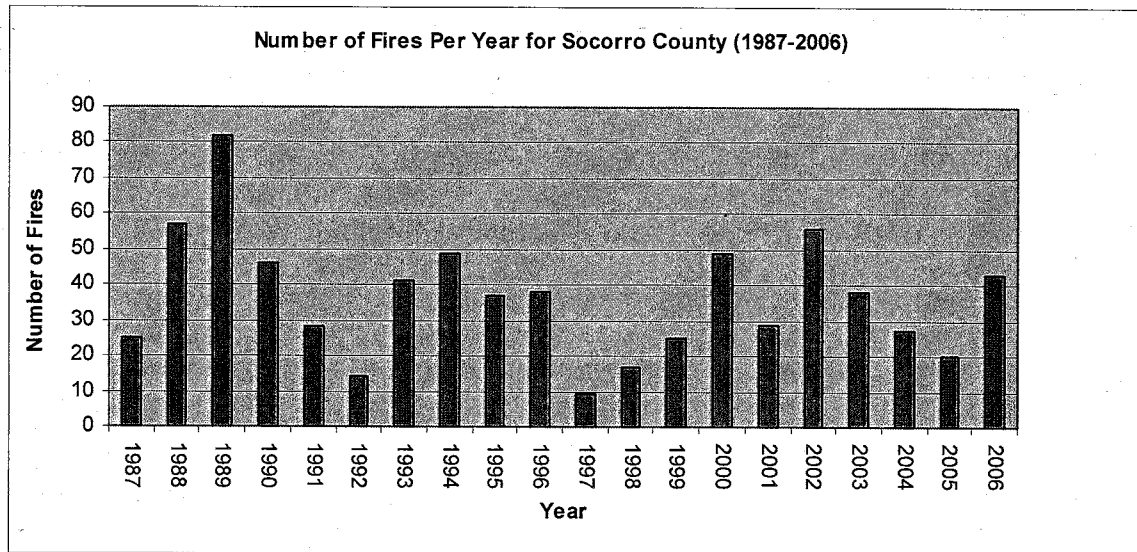


Figure 2.5. Number of fires per year for Socorro County (1987-2006). Courtesy of Doug Boykin, NM State Forestry.

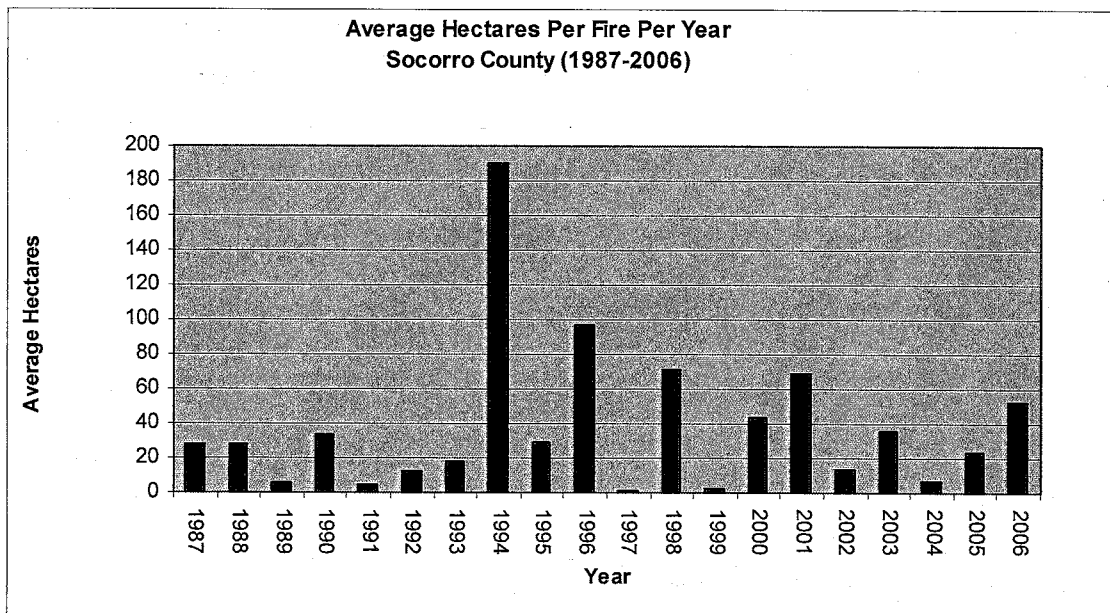


Figure 2.6. Average hectares per fire per year for Socorro County (1987-2006)

Wildland Urban Interface (WUI) Areas

Socorro County receives an abnormally high number of lightning storms and ground strikes, due mainly to the topographical change from desert to

mountains; and receives only 25 cm (10 inches) of rainfall, annually in lower elevations, to 76 cm (30 inches) in the higher elevations above 3,048 m (10,000 feet), annually (NM State Forestry, 2006). With increased residential growth in or near the forest boundary and the bosque areas (Wildland Urban Interface or WUI), risk from catastrophic wildfire has increased. Private holdings are being developed with multiple structures and limited access. This growth has also increased the traffic on our roadways, resulting in safety concerns both for emergency response and urban interface fire evacuations (NM State Forestry, 2006).

The Socorro County Rural Fire District compiles information on rural communities located within the Wildland Urban Interface (WUI) acres, construction materials, roads, bridges, driveways, roads, turnarounds, water availability, and closest Interface, gathering data on vegetation fuels, terrain, slope, aspect, number of lots, estimated human density, total fire department. The data was analyzed and an Average Hazard Rating is determined for each community. Table 2.1 identifies the number of communities in each hazard rating, with acreage (NM State Forestry, 2006).

Number of WUI Areas	Average Hazard	Acreage
9	Low	95,650
11	Medium	151,140
14	High	126,960
Total Acres		373,750

Table 2.1. Count of WUI Communities and Average Hazard Rating (NM State Forestry, 2006)

3. METHODS AND MATERIALS

3.1 Description of the 3 Fires Investigated

Three recent fires were chosen for this study due to their proximity to New Mexico Tech, high proportion of tamarisk infestation and their relatively large size: 1. Mitchell Fire of April 9-16, 2005, which burned 414 hectares; 2. Marcial Fire of May 3-10, 2006, which burned 2,250 hectares; and 3. Bosquecito Fire of June 6-9, 2006, which burned 260 hectares. The three fires can be seen below in Figure 3.1.

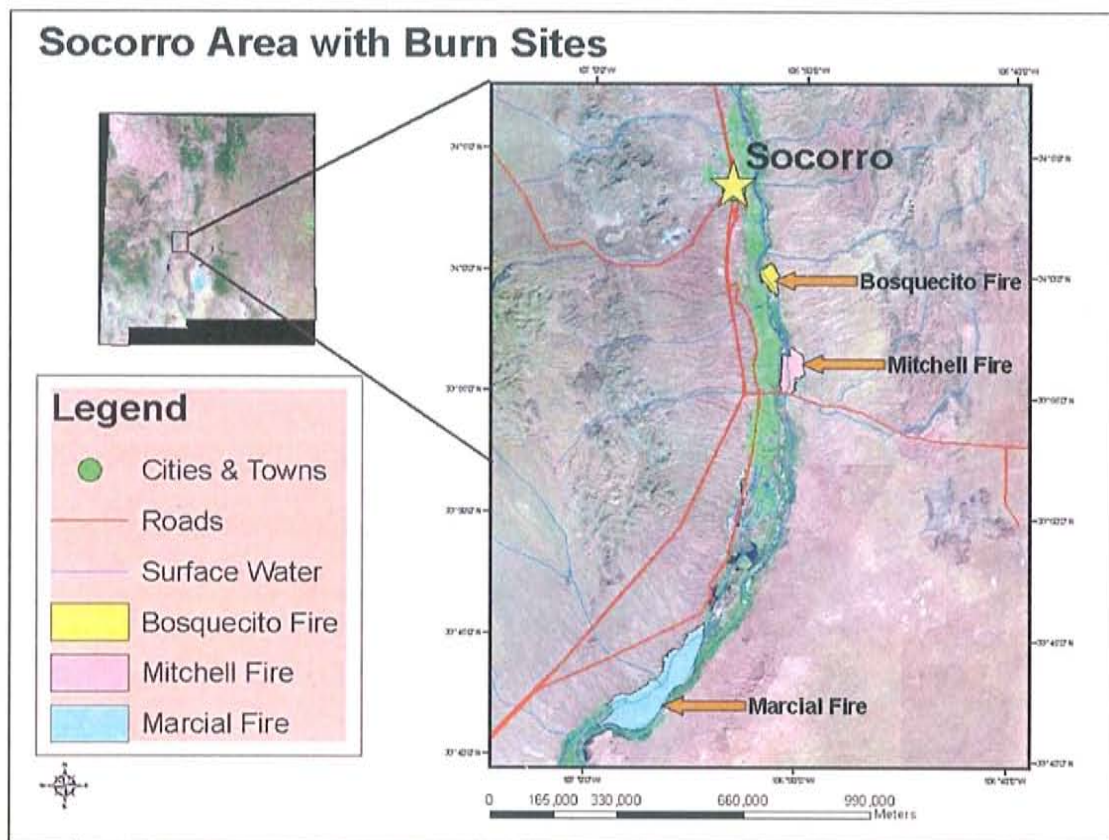


Figure 3.1. Mitchell, Marcial and Bosquecito Fire locations within the state of New Mexico.

1. Mitchell Fire

The Mitchell Fire ignited on April 9, 2005 in the riparian corridor along the Middle Rio Grande in San Antonio New Mexico, due north of Highway 380 (Figure 3.2). The blaze started when a private landowner operating a grinder sent sparks into some grass, resulting in a fire of 414 hectares (1,024 acres). Properties in danger included homes, residential storage, agricultural cultivation and livestock. The fire burned a mixture of non-native and native floodplain bosque vegetation. Overstory vegetation at the burn site was dominated by non-native tamarisk (*Tamarix ramossissima*) with large patches of native Rio Grande cottonwood (*Populus deltoids* var. *wislenzii*), and Godding's willow (*Salix gooddingii*). Understory vegetation was dominated by native willows (*Salix exigua*), honey mesquite (*Prosopis glandulosa*), and other native and non-native shrubs, forbs, and grasses. Fire suppression consisted of burnout and holding with fire engine crews on established roads and fire-line construction with bulldozers. The fire was 70% contained on April 11 and controlled on April 16, 2005; between 60 and 70 firefighters were involved in battling the fire (Associated Press, 2005).

**Mitchell Fire (April 9 - 16, 2005)
Field Sampling Locations
Sampling Performed in October of 2006**



Figure 3.2. Mitchell Fire site field sampling transects and macroplot locations.

Herbicide Treatment

Aerial herbicide treatments occurred on the Mandeville Track (Figure 3.3) in September of 2003 as funded by the SSWCD. Spraying is always done in the fall to prevent from the herbicide interacting with the nesting season of the endangered Southwest Willow Flycatcher (WIFL). According to the herbicide manufacturers, the land was to remain intact for 3 years before being followed up by additional control methods such as root plowing, cut-stump or burning. The herbicide killed all the above-ground tamarisk biomass but did not sufficiently kill the root crown nor below ground root matter prior to the Mitchell Fire. After the Mitchell Fire, in May of 2006, the SSCWD followed up with root plowing within the Mandeville track and finished in May of 2007 (Troxel-Stowe, Nyleen. Personal Interview. 7 March 2008). In February of 2008 replanting and seeding with native vegetation was performed within the plot.

Mitchell Fire
Aerial Herbicide Spraying in September of 2003
Mandeville Property

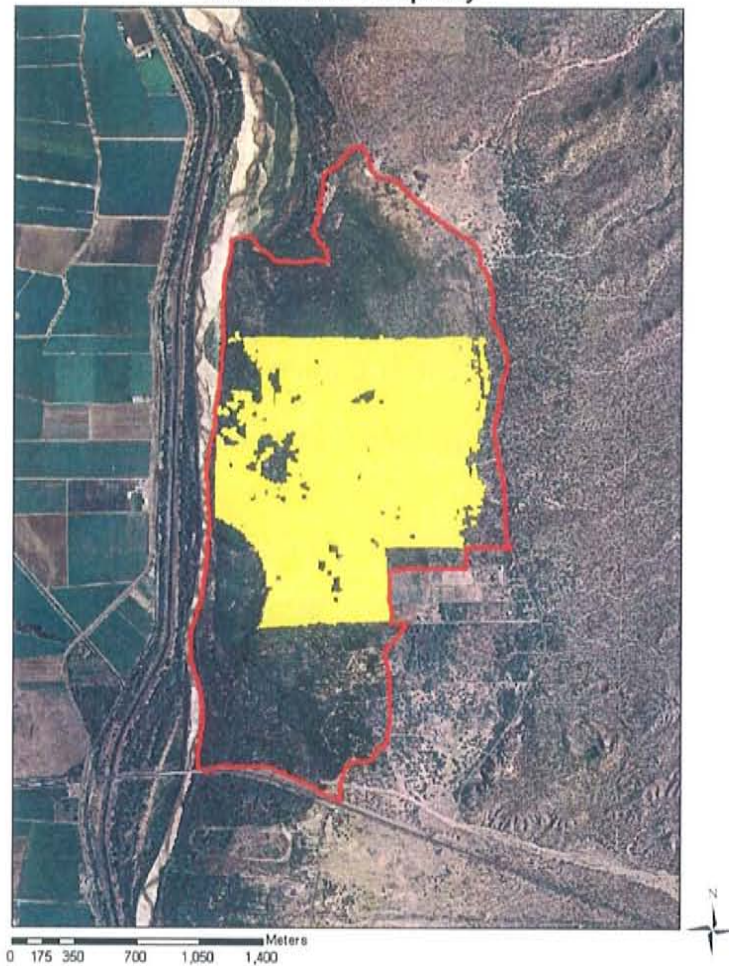


Figure 3.3. Herbicide spraying in the Mandeville track in September of 2003 (SSWCD, 2007).

Mitchell Fire Photos

Photos of the Mitchell Fire were obtained from the Socorro Soil Water Conservation District (Figures 3.4-3.6). The fire charred the basal bark portion of the tamarisk and the leaves were incinerated (Figure 3.4, top row). If the fire was of higher intensity it would have incinerated all the above-ground basal biomass and would likely kill the root crown below. The bottom photos in Figure 3.4 portray the charring to ash that occurred in the herbicide-treated portion of the Mandeville track. The dark brown portions are likely tamarisk-blackened and charred remnants from the fire.

1. During fire, April 11, 2005

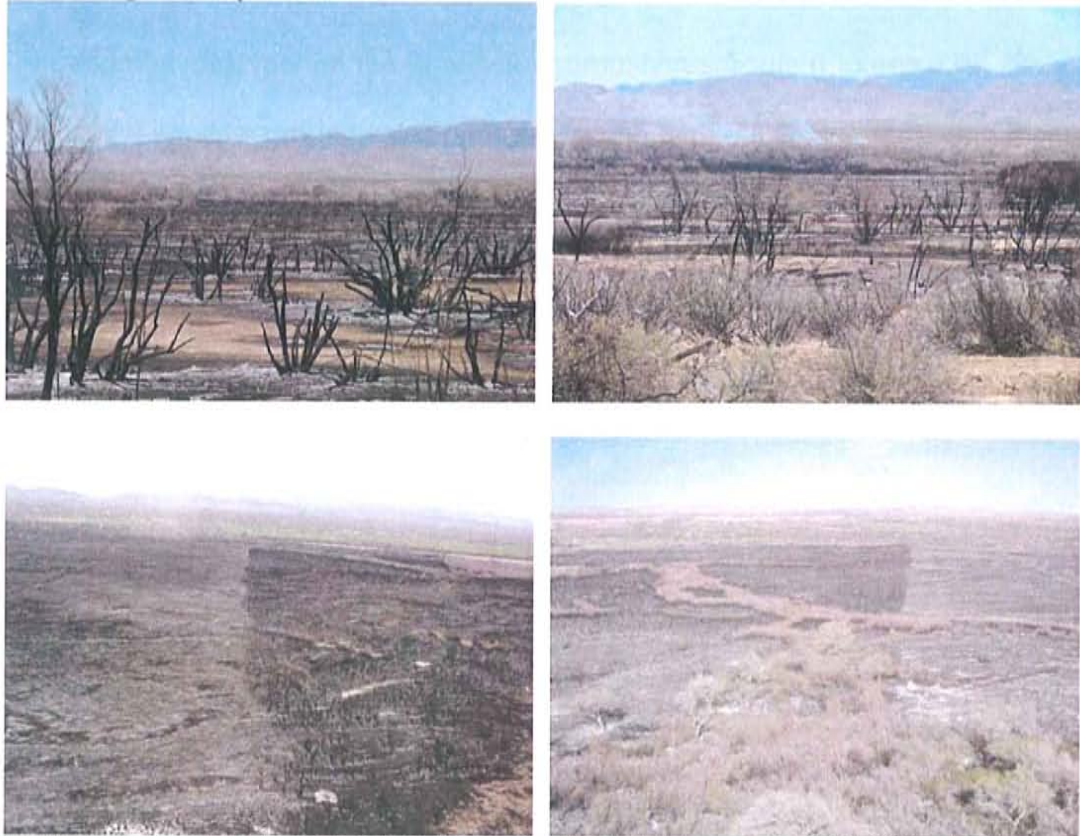


Figure 3.4. Top row: Images taken during the Mitchell Fire, on April 11, 2005. Bottom row. 1st image: Sprayed (light brown soil, left) versus non-sprayed (dark brown soil, right); 2nd image: Non-sprayed (left, dark brown soil) versus sprayed (right, light soil) (SSWCD, 2008).

One month after the fire, tamarisk resprouts appear at the Mitchell Fire site (Figure 3.5), growing from the root crown which was not impacted by the fire.

2. One Month after the fire, May 16, 2005



Figure 3.5. Top row: Images taken 1 month after the Mitchell Fire (SSWCD, 2008).

Two months after the fire the tamarisk rigorously resprouts (Figures 3.6), likely due to the shallow groundwater table, soils with high capillary forces, and the nature of fire as serving as a catalyst in “furious” regeneration.

3. Two Months after the Mitchell fire, June 29, 2005



Figure 3.6. Top row: Images taken two month after the Mitchell Fire of tamarisk resprouts. Bottom row: Tamarisk resprouts with cottonwood grove two months after the fire (SSWCD, 2008).

2. Marcial Fire

The Marcial Fire ignited on May 3, 2006 near the historic town of San Marcial, Socorro County, New Mexico, and Fort Craig (Figure 3.7). Properties in danger included 4 structures, a Bureau of Reclamation storage yard, a railroad trellis, 2 railroad bridges, and critical habitat for the endangered species the Southwestern Willow Flycatcher (WIFL) (Parametrix, 2006). The fire burned a mixture of non-native and native floodplain bosque vegetation. Overstory vegetation at the burn site was dominated by non-native tamarisk with large patches of native Rio Grande cottonwood and Godding's willow. Understory

vegetation was dominated by native willows, honey mesquite, and other native and non-native shrubs, forbs, and grasses (Parametrix, 2006). Fire suppression consisted of burnout and holding with fire engine crews on established roads and indirect fire-line construction with bulldozers. Containment was difficult due to limited access, heavy fuel loading, and extreme fire behavior including fire heights greater than 60 m (200 feet) (Parametrix, 2006). The fire was contained on May 6 and controlled on May 10, 2006. More than 60 firefighters from the FWS, San Antonio (NM) Volunteer Fire Department, New Mexico State Forestry Division, Bureau of Land Management, U.S. Forest Service and contractors were involved in fighting the fire. The fire burned 1,966 hectares (4,857 acres) with an estimated suppression cost of \$265,000 (Parametrix, 2006).

Marcial Fire History

The Marcial Fire was not the first fire to have occurred in the area (Parametrix, 2006). In March of 1994, a fire above San Marcial and Road 178 consumed approximately 120 hectares (300 acres) of mixed vegetation (mostly tamarisk). In 1997, approximately 809 hectares (2,000 acres) of tamarisk and other vegetation burned in the northern portion of the Armendaris Ranch, owned by Ted Turner. This fire was similar to the Marcial Fire, although it did not burn 100% "clean" and there was considerable dead standing vegetation remaining. In 2005, a fire north of the Low Flow Conveyance Channel (LFCC) channel near Tiffany burned approximately 8 hectares (20 acres) (Parametrix 2006).

Marcial Fire (May 3 - 10, 2006)
Field Sampling Locations
Sampling Performed in August 2006

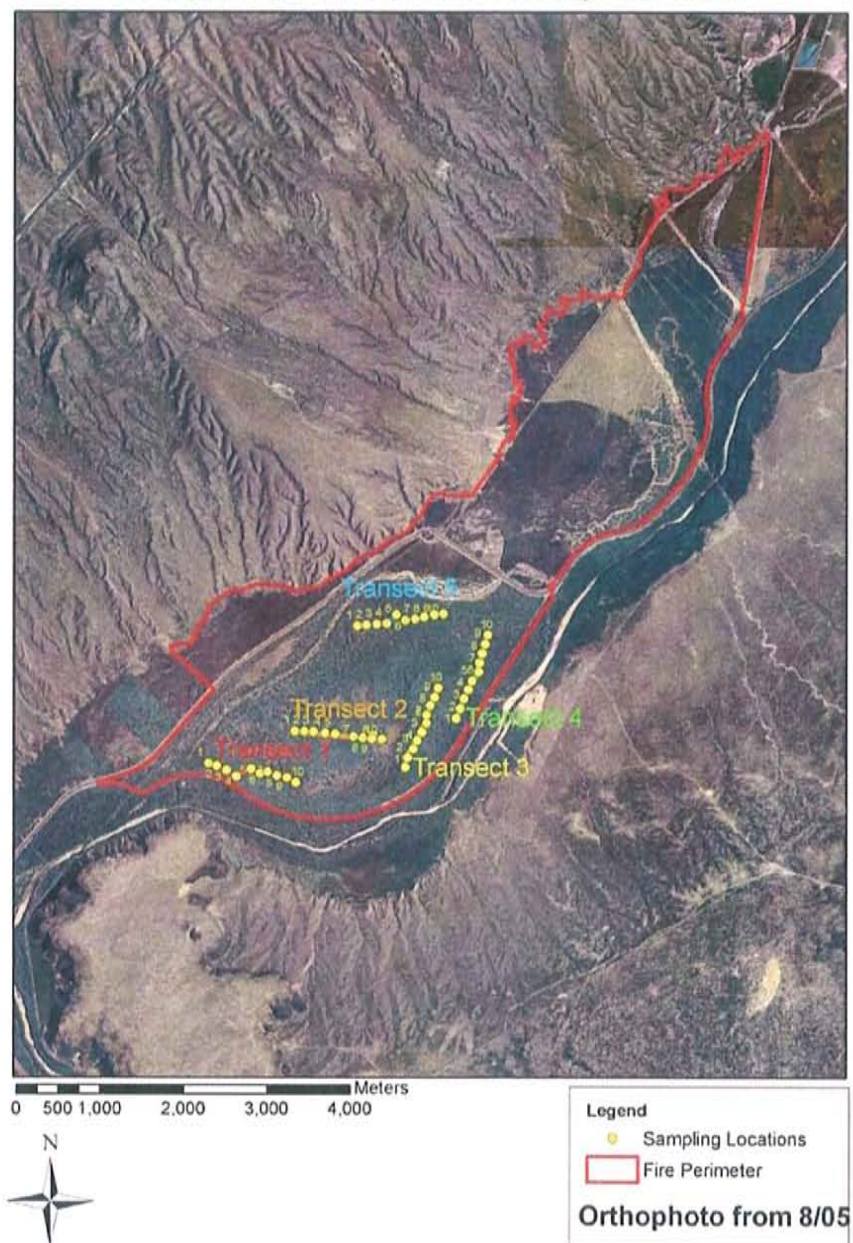


Figure 3.7. Marcial Fire site with field sampling transects and macroplot locations.

Marcial Fire Photos

The first 4 photos are taken west of the fire, near the entrance to Armadaris Ranch. Photos immediately following the fire display charred basal bark and tamarisk basal bark that has been incinerated due to the higher intensity burn in that area. Note the cottonwood grove that was spared.

1. During fire, May 4 and May 10, 2006



Figure 3.8. Images taken during the Marcial Fire. Top 2 rows from May 4, 2006, last row from May 10, 2006, immediately following the fire (SSWCD, 2008).

Photos below, taken 1 month after the Marcial Fire, show rigorous tamarisk regeneration, with resprout heights that appear to be less than 30 cm.

2. Photos from 1 Month after the Fire, June 16, 2006



Figure 3.9. Images taken on June 16, 2006, 1 month after the Marcial Fire (SSWCD, 2008).

3. Bosquecito Fire

The Bosquecito Fire ignited on June 6, 2006 along the riparian corridor of the Rio Grande, approximately six miles south of Socorro, New Mexico, as a result of lightening (Figure 3.10). The fire was estimated to be 260 hectares (640 acres), burning on the east and west sides of the river. The fuels that were consumed include predominantly tamarisk, grass and cottonwood. An evacuation was in effect for twelve homes on the north side of Bosquecito as a precaution, but there were no homes in immediate danger. State Forestry, U.S. Fish and Wildlife, San Antonio, Abeytas and The Middle Rio Grande

Conservancy District all had crews on the fire. There were 45 firefighters were assigned, supported by fire engines and a bulldozer. A Type 1 helicopter was at the fire to make water drops. Governor Bill Richardson was scheduled to be in Socorro on June 7, 2006 for a news conference where he was to sign executive orders to authorize the release of \$3 million for firefighting, fire prevention and post-fire cleanup. The fire was controlled on June 9, 2006 (Albuquerque Journal, 2006).

Herbicide Treatment

In September of 2003 the Rhodes tract (Figure 3.11) received aerial herbicide treatments; the cottonwood groves were excluded. The above-ground tamarisk biomass was killed by the herbicide. Unfortunately, the root crown and below ground root matter were not impacted. The SSWCD was advised by the herbicide manufacturers to wait three years before extracting the roots and mulching the residual biomass.

Bosquecito Fire (June 6 - 9, 2006)
Field Sampling Locations
Sampling Performed in September of 2006

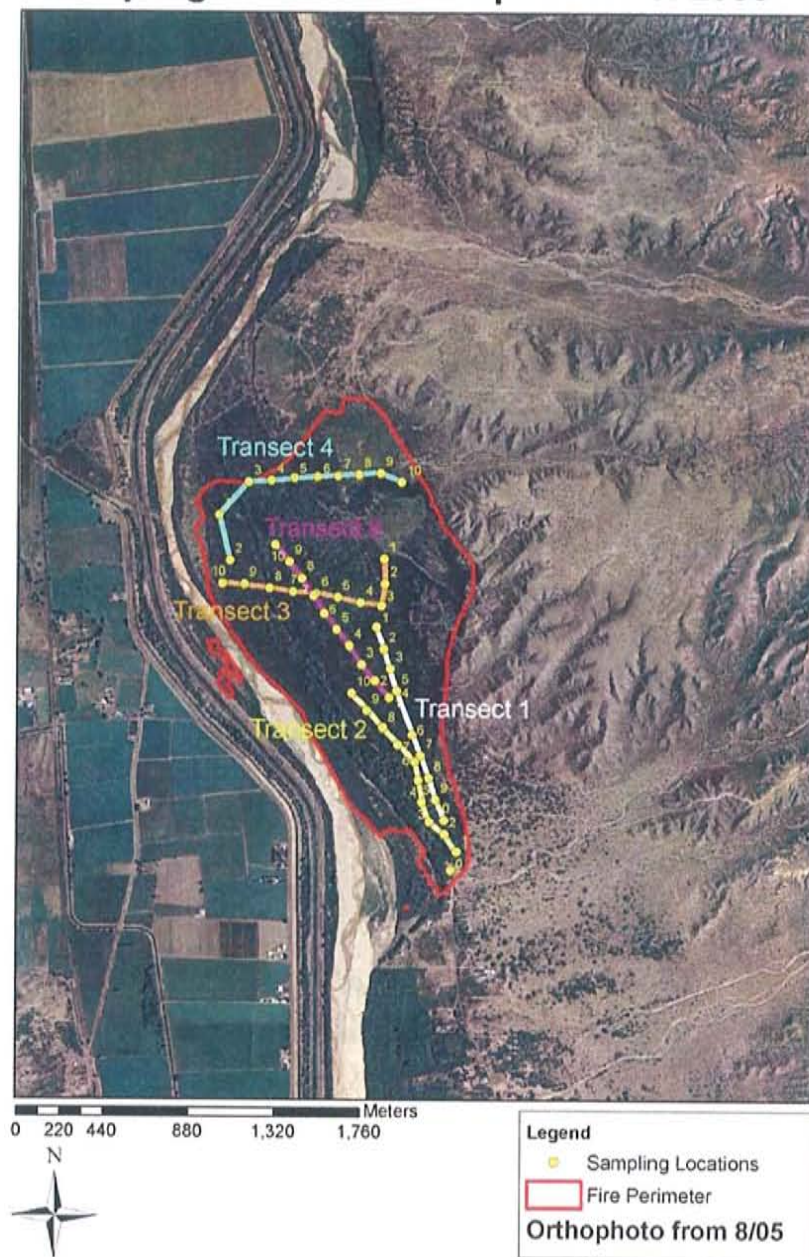


Figure 3.10. Bosquecito Fire site field sampling transects and macroplot locations.

Bosquecito Fire
Aerial Herbicide Spraying in September of 2003
Rhodes Property

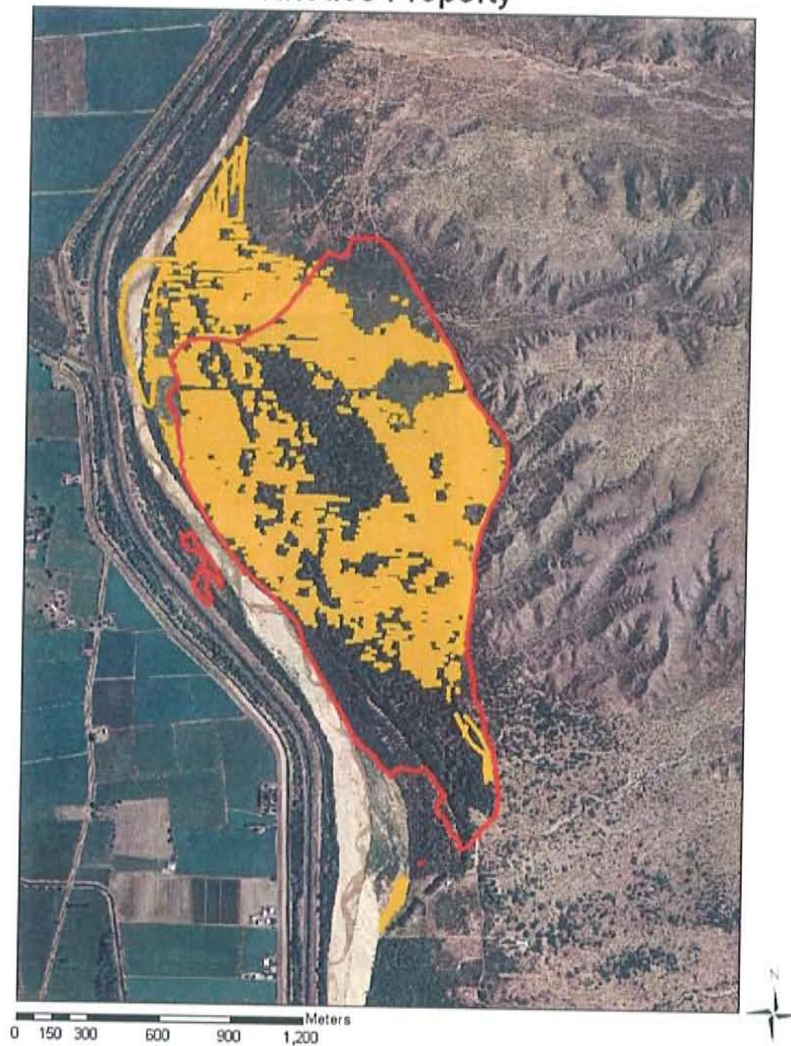


Figure 3.11. Herbicide sprayed areas (in orange) in the Rhodes tract of the Bosquecito Fire (outlined in red) during September of 2003 (SSWCD, 2007).

Bosquecito Fire Photos

The SSWCD only had photos during the fire on file. This fire was the only natural, lightning-caused fire and burned the hottest. Note the white ash in the top-right photo and how eradicated is most of the above ground biomass in the bottom photo, except for large tamarisk stands (Figure 3.12).

1. During fire, June 7, 2006



Figure 3.12. Images taken during the Bosquecito Fire, on June 16, 2006 (SSWCD, 2008).

3.2 Field Sampling Methods

3.2.1 Vegetation Monitoring and Sampling

The purpose of the sampling was to obtain quantitative estimates of vegetation recovery in the Tamarisk bosque woodland habitat 3 months after the Bosquecito and Marcial Fires, and 18 months after the Mitchell Fire. Five transects, with 10 macroplots along each transect were selected for intensive sampling within each of the 3 burn sites. The sampling was performed under the guidance of Mr. Jerry Hess and FIREMON Protocol from August to October of 2006.



Figure 3.13. Marcial Fire site, Summer 2006 Field Campaign, Nicole (left) and Jerry Hess (right).

Fire Effects Monitoring and Inventory System (FIREMON)

FIREMON is a Joint Fire Sciences Project that provides fire managers and scientists from all agencies with a comprehensive set of fire effects monitoring

and inventory protocols. It was developed by USFS Rocky Mountain Research Station, Missoula Fire Sciences Laboratory, the USGS Northern Rocky Mountain Science Center, and Systems for Environmental Management. It is designed to help the fire manager determine how plots should be placed on the landscape and what sampling methods should be used at each plot location based on the project funding and objectives. FIREMON's biggest asset is that it is highly flexible with only four required fields. Fire managers can select a simple sampling scheme – for instance, taking only photographs at every plot, at one point in time – to an intensive, statistical scheme requiring detailed sampling over multiple visits. FIREMON has been extensively reviewed in the field – across a number of ecosystems – and by station statisticians to ensure a useful, tested product (Lutes et al., 2003).

FIREMON consists of four main components. First, the Integrated Sampling Strategy leads the fire manager through text, guides and keys to suggest the appropriate sampling approach (relevé or statistical), sampling intensity (detailed, alternative or simple) and sampling methods based on project funding and objectives. Second, FIREMON includes a number of sampling methods allowing the fire manager to assess many ecosystem attributes. The sampling methods provide data for the following components: plot description, trees, fire severity, fire behavior and vegetation cover. Third, data is stored in the Microsoft Access or Excel database. Data entry forms are field forms that are filled out in short-hand notation that is queried according to designated percentage classes (Figure 3.14). Last, the data can be imported into ArcGIS or

the FIREMON Analysis Toolbox for statistical comparison and analysis (Lutes et al., 2003).

Site Selection

The sites where the Mitchell, Bosquecito and San Marcial Fires occurred were considered for sampling. Five transects, each of 1 km in length, were chosen and evenly spaced within each fire site (Figures 3.1, 3.7 and 3.10). 10 macroplots, with 110-m separation distance, were positioned along each transect. The azimuth of each starting macroplot location was measured and recorded, along with its location in UTM.

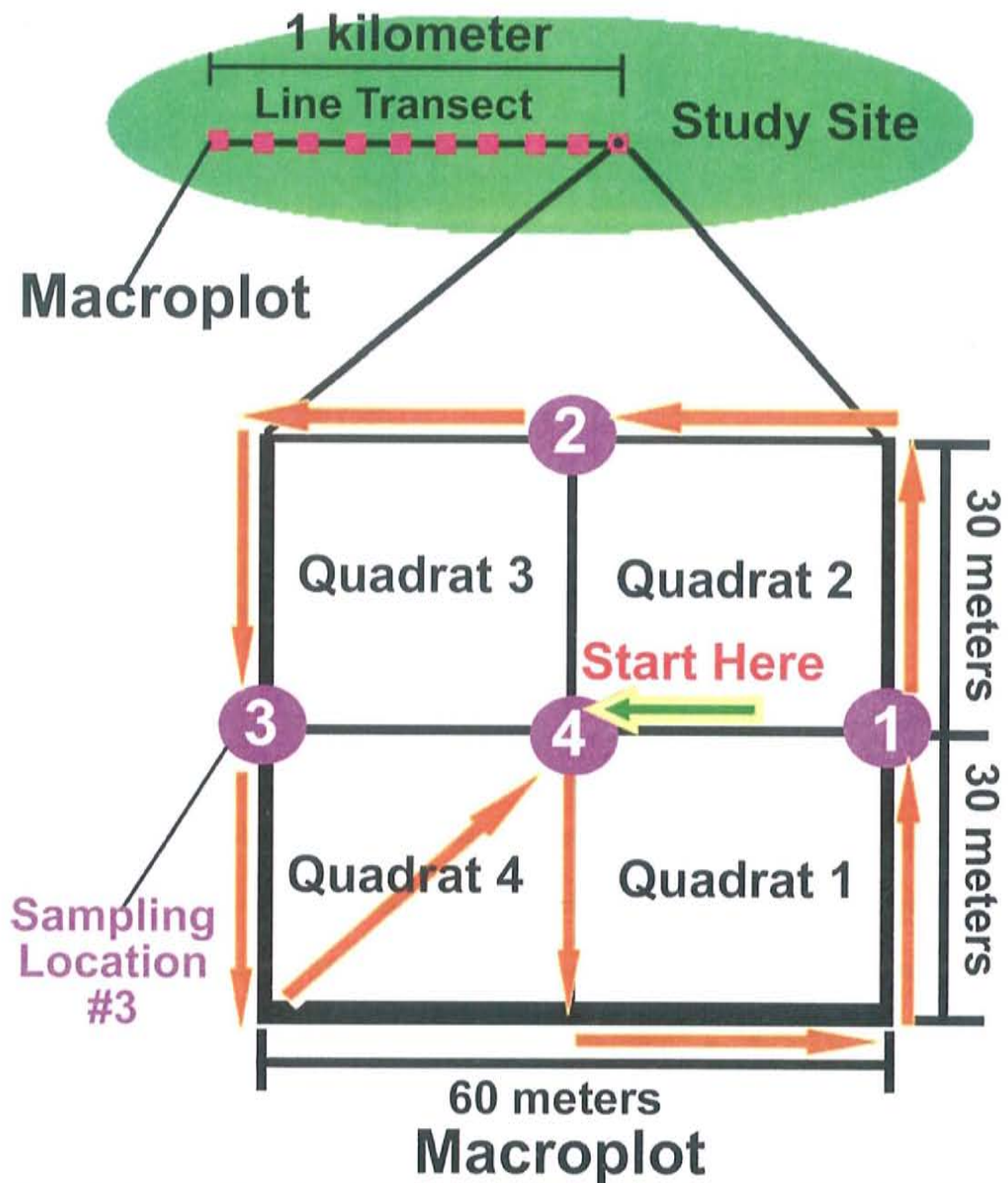


Figure 3.14. Illustration of field sampling using the Line Transect method and Macroplots.

Required Materials

- Compass
- GPS
- 2-meter measuring rod
- Field sampling form
- Writing utensils

Field Procedures

Macroplot 1, Transect 1 of each of the 3 fire sites was traveled to by means of GPS. Upon arrival to the center point of the first macroplot of the first transect, the following site data was collected:

- Transect Number
- Macroplot Number
- GPS Waypoint Number
- GPS Location (UTM)
- GPS Elevation
- Soil Texture
- Erosion Type
- Erosion Severity
- Crust Description

Macroplot Layout

The macroplot is 60 x 60 meters (Figure 3.14), four times the area of a Landsat pixel of 30 x 30 meters. Within each macroplot are 4 quadrats, each of 30 x 30 meter dimensions. Starting from the center point of the first macroplot, the four quadrats were transversed using the following directions: 1. Head south 30 meters, east 30 meters and north 30 meters, reaching Sampling Location 1; 2. North 30 meters and west 30 meters, reaching Sampling Location 2; 3. West 30 meters and south 30 meters, reaching Stop 3; 4. South 30 meters and northeast 42 meters, reaching Stop 4, the center point of the macroplot. The distances transversed while walking were measured and monitored using a 2-meter measuring rod.

At each sampling location, the following environmental data was collected on a field sampling form:

1. Tamarisk Maturity
 - Seedling Cover (tree height below 4.5 feet)
 - Sapling Cover (tree height greater than 4.5 feet)
 - Tamarisk Seasonal Stage
2. Dominant Species
 - Species Classification
 - Stand Height
3. Vegetation Cover Percentages
 - Tamarisk
 - Cottonwood
 - Grass
 - Forb
 - Graminoid
4. Soil
 - Bare Soil Cover
 - Soil Texture
 - Crust Discription
5. Erosion
 - Erosion Type
 - Erosion Severity
6. Fire
 - Fire Severity

Data for each parameter was averaged over the four quadrats, resulting in one value per macroplot and can be found in tabular form in Appendix B.

Cover (%)

Cover means vegetation cover and is expressed as the percentage of the surface area over which a plant exerts its influence upon other components of the ecosystem. Cover values presented for each species are average amongst

the quadrats within each macroplot. Total vegetation cover is a separate variable representing observations of gross cover of the vegetation in its entirety.

Line Transects

In the culmination of data collection at one macroplot, the azimuth of the line transect was determined and measured with a compass. The line transect (Figures 3.1, 3.7 and 3.10) was transversed along the selected azimuth for 110 meters to the center point of macroplot number 2 using a compass, 2-meter measuring stick and a USGS 7.5' map. Data collection for each of the four quadrats within the macroplot was repeated for each macroplot, until reaching the 10th macroplot along each transect.

At the culmination of one transect, the following transect was traveled to via GPS navigation. The macroplot data collection was then repeated for the further macroplots along the 5 transects, for each of the 3 fire site locations. Data was transferred into Excel databases, and linked to macroplot locations in ArcGIS.

Control Site

In order to minimize the effect of the remaining scene-dependent factors (atmospheric, topographic, and climatic effects and changes in detector gain or offset), vegetated control areas, "reference areas" were chosen. The areas were selected from the non-burnt bosque tamarisk woodland because it was spatially near the burns and because its general characteristics (soil, humidity, topography

and type of vegetation) were representative of pre-burnt areas. Satellite data can be acquired over the test and reference area; thus the existing differences between the burnt and un-burnt forests may be obtained. In this way, the scene-dependent effects will not affect the results because they could be considered to be the same for both areas.

Map Creation

Maps for the burn sites were prepared with the use of ArcGIS, USGS Topographic Quadrangles and maps from the NM Bureau of Geology.

Treatment of Data

During vegetation sampling, raw data for each quadrat were recorded on printed field sheets and subsequently transferred to an Excel database. Each database record consisted of one sampling event for one macroplot (containing 4 quadrats). Data in each record included Transect Number, Macroplot Number, GPS, Waypoint Number, GPS Location (UTM), GPS Elevation, Soil Texture, Erosion Type, Erosion Severity, Crust Description, Seedling Cover (tree height below 4.5 feet), Sapling Cover (tree height greater than 4.5 feet), Tamarisk Seasonal Stage, Dominant Species, stand height of the dominant species, tree cover, grass cover, forb cover, graminoid cover, and bare soil cover and type. An example of types of vegetation encountered other than tamarisk, cottonwood and willow (Figure 3.15).



Figure 3.15. Cottonwood (left) and willow (right) resprouts.

Firemon Codes for Field Sampling

Short hand notation was used in the field to denote soil type, erosion type and erosion severity, following the guidelines of FIREMON protocol (Figures 3.16 and 3.17). When estimating cover, percentages were estimated occularly and recorded as pertinent to the FIREMON guidelines for Cover Classes. For example, a quadrat with approximately 80% of tamarisk would be recorded as 80% because it falls within the range of 75-85% (Figure 3.18).

Soil Types			
Code	Description	Code	Description
C	Clay	S	Sand
CL	Clay loam	SC	Sandy clay
COS	Coarse sand	SCL	Sandy clay loam
COSL	Coarse sandy loam	SI	Silt
FS	Fine sand	SIC	Silty clay
FSL	Fine sandy loam	SICL	Silty clay loam
L	Loam	SIL	Silt loam
LCOS	Loamy coarse sand	SL	Sandy loam
LFS	Loamy fine sand	VFS	Very fine sand
LS	Loamy sand	VFSL	Very fine sandy loam
LVFS	Loamy very fine sand	X	Did not assess

Erosion Type Types	
Code	Erosion type
S	Stable, no erosion evident
R	Water erosion, rill
H	Water erosion, sheet
G	Water erosion, gully
T	Water erosion, tunnel
W	Wind erosion
O	Other type of erosion
X	Did not assess

Figure 3.16. FIREMON Codes for field sampling form (NBII, 2004).

Erosion Severity Codes

Code	Erosion severity
0	Stable, no erosion is evident.
1	Low erosion severity; small amounts of material are lost from the plot. On average less than 25 percent of the upper 8 in. (20 cm) of soil surface have been lost across the macroplot. Throughout most of the area the thickness of the soil surface layer is within the normal range of variability of the uneroded soil.
2	Moderate erosion severity; moderate amounts of material are lost from the plot. On average between 25 and 75 percent of the upper 8 in. (20 cm) of soil surface have been lost across the macroplot. Erosion patterns may range from small, uneroded areas to small areas of severely eroded sites.
3	High erosion severity; Large amounts of material are lost from the plot. On average 75 percent or more of the upper 8 in. (20 cm) of soil surface have been lost across the macroplot. Material from deeper horizons in the soil profile is visible.
4	Very high erosion severity; Very large amounts of material are lost from the plot. All of the upper 8 in. (20 cm) of soil surface have been lost across the macroplot. Erosion has removed material from deeper horizons of the soil profile throughout most of the area.
-1	Unable to assess

Figure 3.17. FIREMON Codes and percentages for field sampling form (NBII, 2004).

Cover Classes

Code	Canopy cover
0	Zero percent canopy cover
0.5	>0-1 percent of canopy cover
3	>1-5 percent canopy cover
10	>5-15 percent canopy cover
20	>15-25 percent canopy cover
30	>25-35 percent canopy cover
40	>35-45 percent canopy cover
50	>45-55 percent canopy cover
60	>55-65 percent canopy cover
70	>65-75 percent canopy cover
80	>75-85 percent canopy cover
90	>85-95 percent canopy cover
98	>95-100 percent canopy cover

Figure 3.18. FIREMON percentages for field sampling form (NBII, 2004).

Erosion Severity Codes

Code	Erosion severity
0	Stable, no erosion is evident.
1	Low erosion severity; small amounts of material are lost from the plot. On average less than 25 percent of the upper 8 in. (20 cm) of soil surface have been lost across the macroplot. Throughout most of the area the thickness of the soil surface layer is within the normal range of variability of the uneroded soil.
2	Moderate erosion severity; moderate amounts of material are lost from the plot. On average between 25 and 75 percent of the upper 8 in. (20 cm) of soil surface have been lost across the macroplot. Erosion patterns may range from small, uneroded areas to small areas of severely eroded sites.
3	High erosion severity; Large amounts of material are lost from the plot. On average 75 percent or more of the upper 8 in. (20 cm) of soil surface have been lost across the macroplot. Material from deeper horizons in the soil profile is visible.
4	Very high erosion severity; Very large amounts of material are lost from the plot. All of the upper 8 in. (20 cm) of soil surface have been lost across the macroplot. Erosion has removed material from deeper horizons of the soil profile throughout most of the area.
-1	Unable to assess

Figure 3.17. FIREMON Codes and percentages for field sampling form (NBII, 2004).

Cover Classes

Code	Canopy cover
0	Zero percent canopy cover
0.5	>0-1 percent of canopy cover
3	>1-5 percent canopy cover
10	>5-15 percent canopy cover
20	>15-25 percent canopy cover
30	>25-35 percent canopy cover
40	>35-45 percent canopy cover
50	>45-55 percent canopy cover
60	>55-65 percent canopy cover
70	>65-75 percent canopy cover
80	>75-85 percent canopy cover
90	>85-95 percent canopy cover
98	>95-100 percent canopy cover

Figure 3.18. FIREMON percentages for field sampling form (NBII, 2004).

3.2.2 Soil Hydrology Observations

Professor Bruce Harrison and Nicole Alkov traveled to specific areas within the Mitchell, Marcial and Bosquecito Fires which had consistently low Instantaneous and Daily ET values, before and after the fire—independent of the fire. Soil sampling and characterization was performed to the groundwater table at one location within the Mitchell Fire with characteristically low Instantaneously and Daily ET rates. For the Marcial Fire, two locations were sampled, one inside and one outside of the low Instantaneous and Daily ET areas. Concerning the Bosquecito Fire, sampling was conducted during a field trip including Bruce Harrison's Soils Class, and occurred along a North-South transect encompassing areas with high and low Instantaneous and Daily ET rates. They used a hand auger to determine soil types and stratigraphy as well as to find a depth to the ground water table. Findings from the field trips can be found in Section 4.5.3.

3.3 Surface Energy Balance Algorithm For Land (SEBAL)

SEBAL is a remote sensing flux algorithm that solves the instantaneous surface energy balance for every pixel of a satellite image (Bastiaanssen et al., 1998, 2005) such as Landsat or MODIS (Moderate Resolution Imaging Spectroradiometer). The software ERDAS IMAGINE (Leica Geosystems) is used to process every pixel of the satellite image through the SEBAL algorithm via the ERDAS IMAGINE Model Maker tool. ERDAS IMAGINE is a raster graphics editor and remote sensing application that allows the user to display, enhance and model digital images. It is a toolbox allowing the user to

perform numerous operations on an image and answer geographical questions.

The SEBAL method is based on the computation of surface albedo, surface temperature and vegetation index from multi-spectral satellite data. The surface albedo is used to calculate net short wave radiation, and surface temperature for the calculation of net long wave radiation, soil heat flux and sensible heat flux. The vegetation index governs the soil heat flux by incorporating light interception by canopies, and is used to express the aerodynamic roughness of the landscape. The latent heat flux is computed as the residual of the surface energy balance. Air humidity measurements are not needed because evaporation is computed from the latent heat flux. SEBAL has been applied for water balance estimations, irrigation performance assessment studies (Roerink et al., 1997), and for weather prediction studies (Van de Hurk et al., 1997).

The components of the energy balance are:

$$R_n - G - H = \lambda E \quad (1)$$

where R_n is the net incoming radiation flux (W m^{-2}), G is the ground heat flux (W m^{-2}), H is the sensible heat flux (W m^{-2}), and λE is the latent heat flux (W m^{-2}), which is the evapotranspiration rate. The parameter λ is the latent heat of vaporization of water (J kg^{-1}) and E is the vapor flux ($\text{kg m}^{-2} \text{s}^{-1}$). Evapotranspiration E includes both bare soil evaporation and vegetation transpiration.

The net radiation R_n is estimated from the remotely sensed surface albedo, surface temperature, and solar radiation calculated from meteorological formulas (Iqbal, 1983). The ground heat flux G is determined through semi-empirical relationships with R_n , surface albedo, surface temperature, and vegetation index (Bastiaanssen et al., 1998, 2005). The sensible heat H is calculated from the following formula:

$$H = \rho_a C_p \frac{T_{aero} - T_a}{r_{ah}} \quad (2)$$

where ρ_a is the density of air (kg m^{-3}), C_p is the specific heat of air ($\text{J kg}^{-1} \text{K}^{-1}$), r_{ah} is the aerodynamic resistance to heat transfer (s m^{-1}), T_{aero} is the surface aerodynamic temperature, and T_a is the air temperature either measured at a standard screen height or the potential temperature in the mixed layer (Brutsaert et al., 1993). The aerodynamic resistance to heat transfer is affected by windspeed, atmospheric stability and surface roughness (Brutsaert, 1982). The apparent simplicity of Eq. (2) is deceptive since T_{aero} cannot be measured by remote sensing. Remote sensing techniques measure the radiometric surface temperature T_{rad} which is not the same as the aerodynamic temperature.

The two temperatures usually differ by 1–5 °C. SEBAL is a practical method that overcomes the problem of inferring the aerodynamic temperature from the radiometric temperature and the need for near-surface air temperature measurements by directly estimating the temperature difference between T_1 and T_2 taken at two arbitrary elevations z_1 and z_2 without explicitly solving for the

absolute temperature at a given height. The temperature difference for a dry surface without evaporation is obtained from the inversion of the sensible heat transfer equation setting latent heat flux $\lambda E = 0$, so that $H = R_n - G$ (Bastiaanssen et al., 1998, 2005).

$$T_1 - T_2 = \Delta T_a = \frac{H r_{ah}}{\rho_a c_p} \quad (3)$$

For a wet surface all available energy ($R_n - G$) is used for evaporation λE so that $H = 0$ and $\Delta T_a = 0$.

Field measurements (Bastiaanssen et al., 1998) have shown that the relationship between T_{rad} and ΔT_a is approximately linear

$$\Delta T_a = c_1 T_{rad} - c_2 \quad (4)$$

where c_1 and c_2 are the linear regression coefficients valid for one particular moment (the time and date the image is taken) and landscape. By using the minimum and maximum values of ΔT_a as calculated for the coldest and warmest pixel, the extremes of H are used to find the regression coefficient c_1 and c_2 which will prevent outliers of H -fluxes. Thus, the empirical Eq. (4) relies on spatial differences in the radiometric surface temperature rather than absolute surface temperatures to minimize the influence of atmospheric corrections and surface emissivity uncertainties (Compaoré et al., 2007).

Eq. (3) has two unknowns: ΔT_a and the aerodynamic resistance to heat transfer r_{ah} , which is affected by wind speed, atmospheric stability, and surface roughness. To find a wind speed representative over a heterogeneous landscape, first wind speed at a height 200 m above the ground surface is considered and assumed to be spatially constant. The wind speed at 200 m can be obtained by an upward extrapolation of a wind speed measurement at 2 or 10 m assuming a logarithmic wind profile or from mesoscale atmospheric model simulations (Compaoré et al., 2007). The wind speed at each pixel is obtained by a downward extrapolation using the surface roughness, which is determined for each pixel using an empirical relationship between surface momentum roughness z_{om} and the Normalized Difference Vegetation Index (NDVI) (Huette, 1988). The end result of these calculations is the determination of final values for r_{ah} and ΔT_a for each pixel using an iterative approach that takes into account the stability of the atmosphere. After replacing $T_{aero} - T_a$ in Eq. (2) by ΔT_a the sensible heat flux H is calculated for each pixel. Then, the latent heat flux λE or evaporation rate is derived for each pixel using Eq. (1).

The correct selection of the temperatures of the cold and hot pixel for the derivation of parameters c_1 and c_2 in Eq. (4) is the most critical step in the entire SEBAL process. An error of a few degrees will cause serious distortion of the distribution of the sensible and latent heat fluxes over an image. The ranking of the heat fluxes from smallest to largest will still be correct but their absolute values can be considerably flawed. The cold pixel is selected in areas with well-watered healthy crops with full soil cover or in shallow water bodies

(Bastiaanssen et al., 2005). The cold pixel is chosen as the coldest pixel within this area. Over the cold pixel it is assumed $\Delta T_a = 0$, which implies that

$H = 0$ and $\lambda E = R_n - G$. The hot pixel is selected from a dry bare agricultural field with negligible E . There are hotter pixels in the scene (e.g. a parking lot or sparsely-vegetated desert), but the E over the cooler dry bare agricultural field is already expected to be zero. Thus, for any pixel cooler than the hot pixel, $E > 0$, and for any pixel warmer than the hot pixel, $E = 0$.

SEBAL yields an estimate of the instantaneous evaporation E at the time of the Landsat overpass around 10:30 a.m. This instantaneous evaporation rate must then be extrapolated to obtain the daily evaporation. The extrapolation is done using the evaporative fraction EF (i.e., the ratio of latent heat over the sum of latent and sensible heat) which has been shown to be approximately constant during the day (Brutsaert and Sugita, 1992; Shuttleworth et al., 1989).

$$EF_{inst} = \frac{R_n - G - H}{R_n - G} = \frac{\lambda E_{inst}}{\lambda E_{inst} - H_{inst}} \approx EF_{24} \quad (5)$$

Therefore, multiplication of the instantaneous EF_{inst} determined from SEBAL with the total daily available energy yields the daily evaporation rate λE_{24} (Bastiaanssen et al., 1998a).

$$\lambda E_{24} = EF_{inst} \cdot (R_{n24} - G_{24}) \quad (6)$$

and

$$E_{24} = \frac{EFinst \cdot (R_{n24} - G_{24})}{\lambda} \quad (7)$$

where λE_{24} is daily latent heat flux ($\text{MJ m}^{-2} \text{ day}^{-1}$), E_{24} is daily evaporation (mm d^{-1}), G_{24} is daily soil heat flux ($\text{MJ m}^{-2} \text{ day}^{-1}$). The daily net radiation R_{n24} ($\text{MJ m}^{-2} \text{ day}^{-1}$) for a clear day is obtained by a semi-empirical expression (de Bruin, 1987):

$$R_{n24} = 0.0864 \cdot [(1 - \alpha) \cdot R_{a24} \cdot \tau_{sw} - 110 \tau_{sw}] \quad (8)$$

$$R_{a24} = (0.5 / 24) \cdot G_{sc} \cdot d_r \cdot \sum_{i=1}^{48} \cos(\theta) i \quad (9)$$

$$\tau_{sw} = 0.75 + 2 \cdot 10^{-5} \cdot z \quad (10)$$

where 0.0864 is the conversion parameter from W m^{-2} to $\text{MJ m}^{-2} \text{ day}^{-1}$, R_{a24} is the daily-averaged extraterrestrial shortwave radiation (W m^{-2}) which is daily-averaged incoming solar radiation unadjusted for atmospheric transmittance τ_{sw} (-), G_{sc} is the solar constant (1367 W m^{-2}), θ is solar incident angle (degree), d_r is the inverse squared relative earth-sun distance (-), and z is the elevation above sea level (m) (Tasumi and Allen, 2000).

Energy Balance for ET

ET is calculated as a “residual” of the energy balance

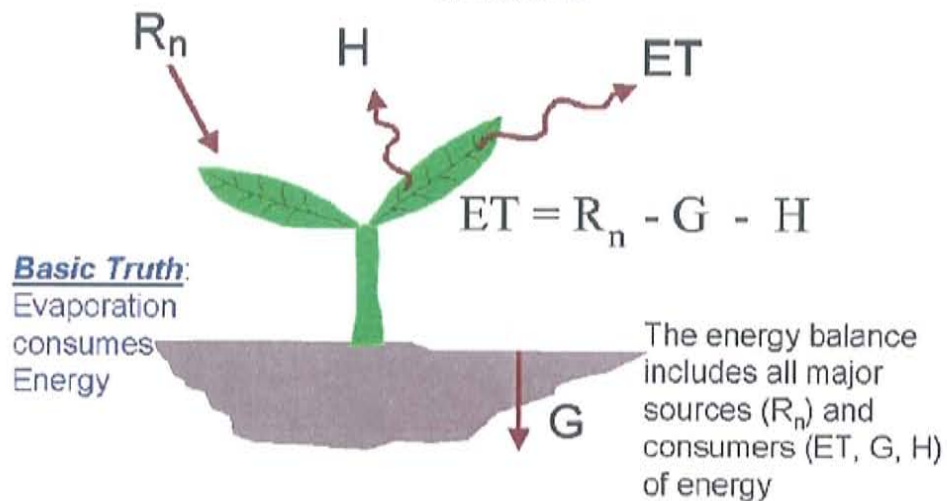


Figure 3.19. The Surface Energy Balance.

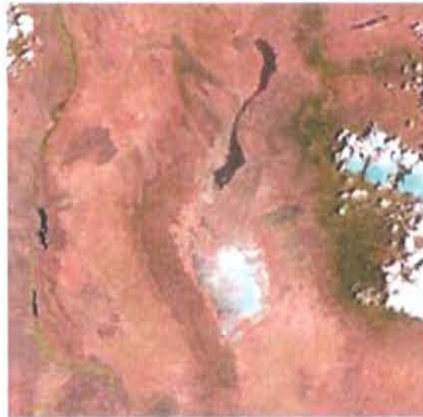
3.4 Satellite Imagery

3.4.1 LANDSAT Imagery

Post-fire regeneration was monitored by means of 15 images from Landsat 5 TM (Thematic Mapper) with spatial resolution of 30 m x 30 m covering the period of May 2002 - July 2007, before and after the three fires. The data was subsetting to include the fire areas and control areas outside the fire. The images had low amounts of cloud cover and were of high quality (Figure 3.20). The data was professionally georectified or georectified to a previously accredited georectified image with 30 m x 30 m resolution. The TM image dates for the fire analyses are the following:

1. May 31, 2002
2. May 12, 2004
3. May 28, 2004
4. June 13, 2004
5. July 6, 2004
6. July 31, 2004
7. September 17, 2004
8. May 22, 2005
9. July 2, 2005
10. August 3, 2005
11. July 21, 2006
12. May 18, 2006
13. June 19, 2006
14. May 21, 2007
15. July 8, 2007

**4 LANDSAT 5 TM Images
Row/Path 33/37
from 2006 and 2007**



May 18, 2006



June 19, 2006



May 21, 2007



July 8, 2007

Figure 3.20. Four LANDSAT 5 TM Images from 2006 and 2007.

Free Landsat Imagery

Under a transition toward a National Land Imaging Program sponsored by the Secretary of the Interior, the USGS is pursuing an aggressive schedule to provide users with electronic access to any Landsat scene held in the USGS managed national archive of global scenes dating back to Landsat 1 launched in 1972. By February 2009, any archive scene selected by a user will be processed automatically to a standard product recipe and available for electronic retrieval, at

no cost. All Landsat data purchasing options from the USGS will be discontinued by February 2009, once the entire Landsat archive can be accessed at no charge. Landsat scenes can be previewed and downloaded using the USGS online Global Visualization Viewer (USGS, 2008).

3.4.2 MODIS Imagery

The MODIS multi-temporal images used in this research were acquired from the NASA Terra Moderate Resolution Imaging Spectroradiometer (MODIS) satellite sensor. The relative size of a MODIS image compared to the size of a LANDSAT image and the state of New Mexico is portrayed in Figure 3.21. The MODIS 250 m NDVI product (MOD13Q1) provided the needed pre- and post-fire vegetation data. The spatial resolution of 250 meters is coarser than the Landsat resolution of 30 meters (Figures 3.22 and 3.23), but Hong (2008) proved high correlation between the two products when upscaling/downscaling between the data sets. The MOD13Q1 product represents spatial aggregates of the MODIS/Terra Vegetation Indices 16-day global 250 m sinusoidal-projection grid. The product contains two vegetation indices, the NDVI and Enhanced Vegetation Index (EVI). MODIS NDVI scenes were acquired for calendar years 2003 through mid-August 2007 ($n = 46$, 2003-2004; $n = 56$, 2005-August, 2007) from the NASA Earth Observing System (EOS) online data gateway (Table 3.1). Details documenting the MODIS NDVI compositing process and Quality Assessment Science Data Sets (QASDS) can be found at NASA's MODIS web site (MODIS, 1999).

LANDSAT Image Superimposed on a MODIS NDVI 16-Day Composite Image

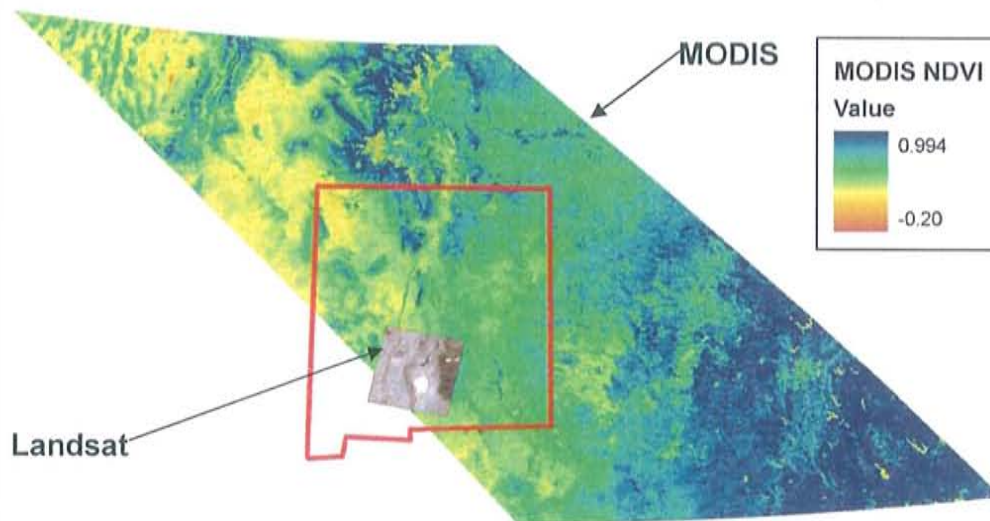


Figure 3.21. Image size comparison of a LANDSAT Image and MODIS image with the state of New Mexico outlined in red.

MODIS Image Dates				
2003	2004	2005	2006	2007
1/1/03	1/1/04	1/1/05	1/1/06	1/1/07
1/17/03	1/17/04	1/17/05	1/17/06	1/17/07
2/2/03	2/2/04	2/2/05	2/2/06	2/2/07
2/18/03	2/18/04	2/18/05	2/18/06	2/18/07
3/6/03	3/5/04	3/6/05	3/6/06	3/6/07
3/22/03	3/21/04	3/22/05	3/22/06	3/22/07
4/7/03	4/6/04	4/7/05	4/7/06	4/7/07
4/23/03	4/22/04	4/23/05	4/23/06	4/23/07
5/9/03	5/8/04	5/9/05	5/9/06	5/9/07
5/25/03	5/24/04	5/25/05	5/25/06	5/25/07
6/10/03	6/9/04	6/10/05	6/10/06	6/10/07
6/26/03	6/25/04	6/26/05	6/26/06	6/26/07
7/12/03	7/11/04	7/12/05	7/12/06	7/12/07
7/28/03	7/27/04	7/28/05	7/28/06	
8/13/03	8/12/04	8/13/05	8/13/06	
8/29/03	8/28/04	8/29/05	8/29/06	
9/14/03	9/13/04	9/14/05	9/14/06	
9/30/03	9/29/04	9/30/05	9/30/06	
10/16/03	10/15/04	10/16/05	10/16/06	
11/1/03	10/31/04	11/1/05	11/1/06	
11/17/03	11/16/04	11/17/05	11/17/06	
12/3/03	12/2/04	12/3/05	12/3/06	
12/19/03	12/18/04	12/19/05	12/19/06	

Table 3.1. MODIS Image dates, every 16 days, used for NDVI analysis.

The MODIS NDVI algorithm operates on a per-pixel basis and relies on multiple observations over a 16-day period to generate a composite image. The vegetation index compositing objective is to combine multiple images into a single cloud-free NDVI map, taking into account the variable atmosphere conditions, residual clouds, and a wide range of sensor view and sun angle conditions. The original images (dimensions 1200 km x 1200 km) were resampled using a nearest neighbor operator from their native Sinusoidal projection to the World Geodetic System 1984 (WGS 84). The individual scenes were subset to the Bosquecito, Mitchell and Marcial Fire sites. The subsets were

then run through the Zonal Statistics tool using a 250 m x 250 m grid cell in the Spatial Analyst application in ArcGIS. The Zonal Statistics tool was able to extract statistical information such as the mean, minimum, maximum and standard deviation of the NDVI amongst the 250 m x 250 m pixels comprised in each fire site from the time span of 2003 to August of 2007. Once the statistics were acquired, time series plots of the mean and standard deviation of NDVI over time were created for each of the three fire sites.

Post-fire regeneration was monitored by means of 102 MODIS NDVI 16-day Composite images with spatial resolution of 250 m x 250 m covering the period of January 1, 2003 to July 12, 2007, before and after the three fires. The data was subset to include the fire areas and data on the mean and standard deviation of NDVI was extracted for each date for each fire site using the Zonal Statistics tool in ArcGIS. The data was professionally georectified by NASA with 250 m x 250 m pixel resolution.

**LANDSAT 5 TM Image
May 21, 2007
30 Meter Resolution**



Figure 3.22. Subset of a LANDSAT Image from May 21, 2007 with the 3 fire sites to illustrate 30-meter pixel resolution.

MODIS NDVI 16-Day Composite Image
May 10-25, 2007
250 Meter Resolution

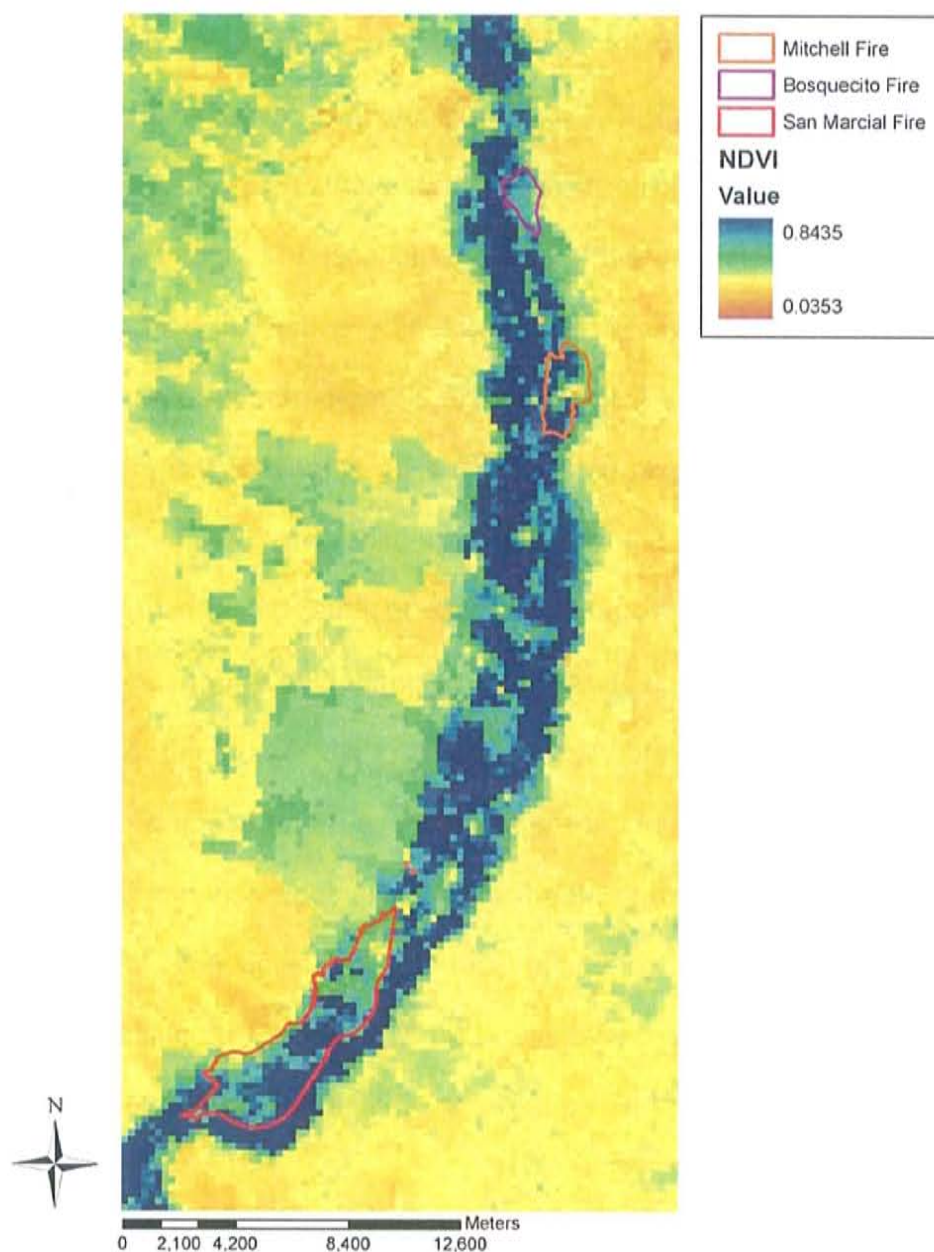


Figure 3.23. Subset of a 16-Day Composited MODIS Image from May 10-25, 2007 with the 3 fire sites to illustrate 250 meter pixel resolution.

3.5 ArcGIS – 9 Pixel Analysis

Spectral response data was obtained from 15 Landsat TM images. The purpose of the imagery analysis was to track changes in albedo (α), daily and instantaneous ET, ground heat flux (G), Leaf Area Index (LAI), NDVI, and surface temperature (T_s) after fire at the 3 fire locations. This was done by extracting data on the above parameters from 3x3 "9-Pixel Plots" Landsat TM super-pixel groupings from SEBAL output which is calculated for each 30x30 meter pixel in a TM image. The location and size of the 9-Pixel Plots for each of the 3 fires is portrayed in Figures 3.24-3.26. Specifically, the data (mean and standard deviation of the parameters) is extracted using the Zonal Statistics tool in ArcGIS. The target coordinates for each of these pixel groups representing the center points of the 126 macroplot study sites on the ground. This analysis was also useful in comparing Landsat data on the above stated parameters to ground data collected in the field campaign from August – October, 2006. The areal dimensions of the study sites in relation to the corresponding target pixels and super-pixels are based on an assessment of map location accuracy as well as the character of tamarisk woodland and its variability over space. Associating ground points and pixel data can introduce geometric error; however, many authors suggest using 3x3 or 5x5 TM pixel window as a way of reducing the chance variability due to the location of the target pixel (Ahern et al., 1998, White et al., 1996).

In general, there is a trade off to be made when seeking an acceptable location accuracy while, at the same time, trying to obtain an accurate

assessment of tamarisk character for a specific study site. By increasing the size of the areas on the TM image that correspond to the coordinates of the target sites on the ground, the likelihood of overlap is increased, but the potential for collecting extraneous spectral data for each of the sites is also increased. If the processes under investigation are taking place at smaller spatial scales, then inclusion of this extraneous data may dilute or generalize the spectral signatures to an acceptable degree (Pratt, 2001).

The character of tamarisk woodland, however, appears to change quite gradually over space with the more abrupt changes being associated with topographic features or amongst clumps of cottonwood communities. The changes associated with topography are usually evident even on the TM imagery and therefore are avoidable. Fortunately most--except Transect 1 of the Mitchell Fire, which was excluded from 9-Pixel analysis--of the 9-Pixel Plots are unaffected by edge effects caused by topography, roads, construction and human intervention.

Mitchell Fire 9-Pixel Plot Locations for SEBAL Analysis

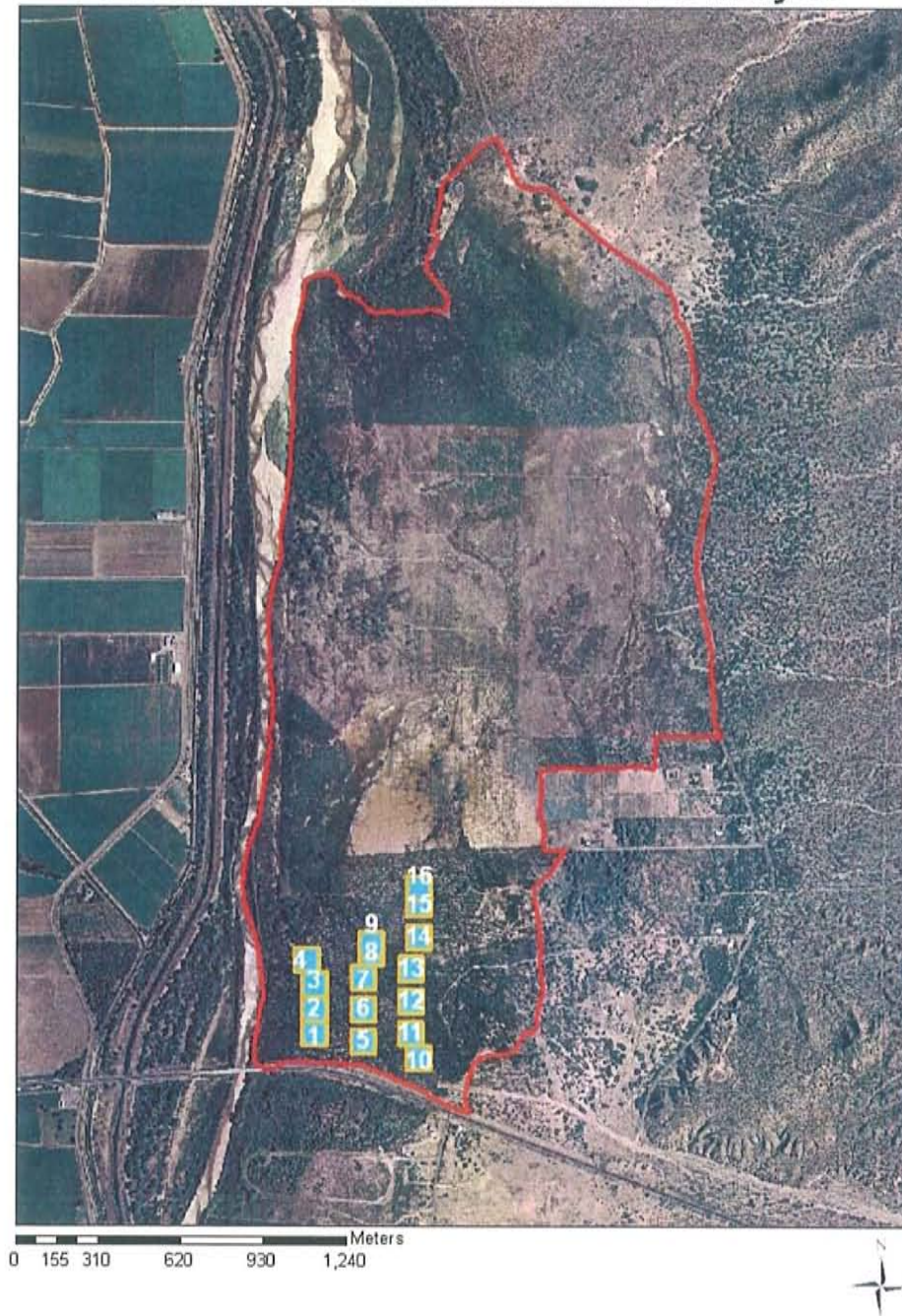


Figure 3.24. 9-Pixel Plots at the Mitchell Fire Site.

Marcial Fire Map 9-Pixel Plot Locations

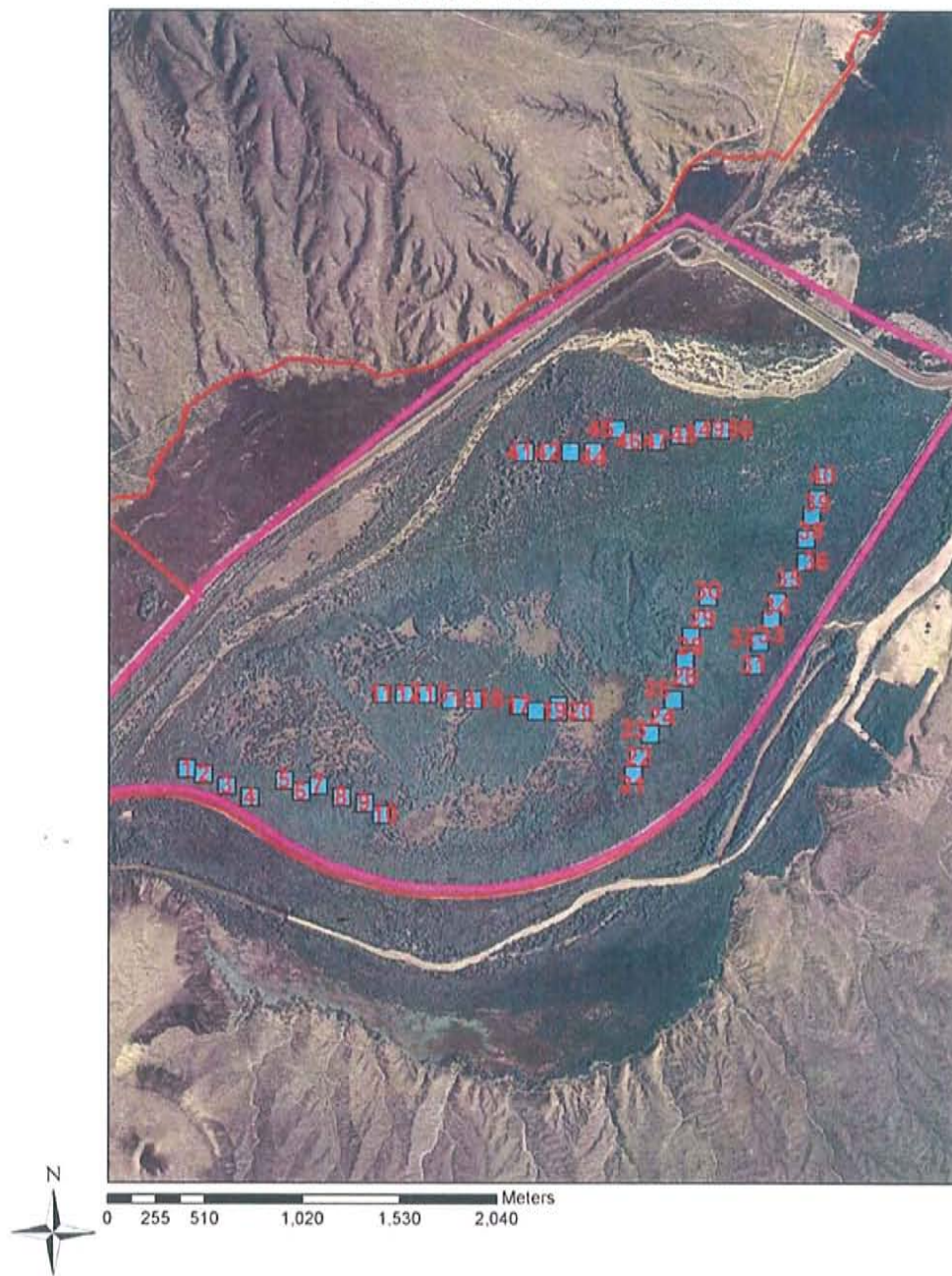


Figure 3.25. 9-Pixel Plots at the Marcial Fire Site.

Bosquecito Fire Map 9-Pixel Plot Locations

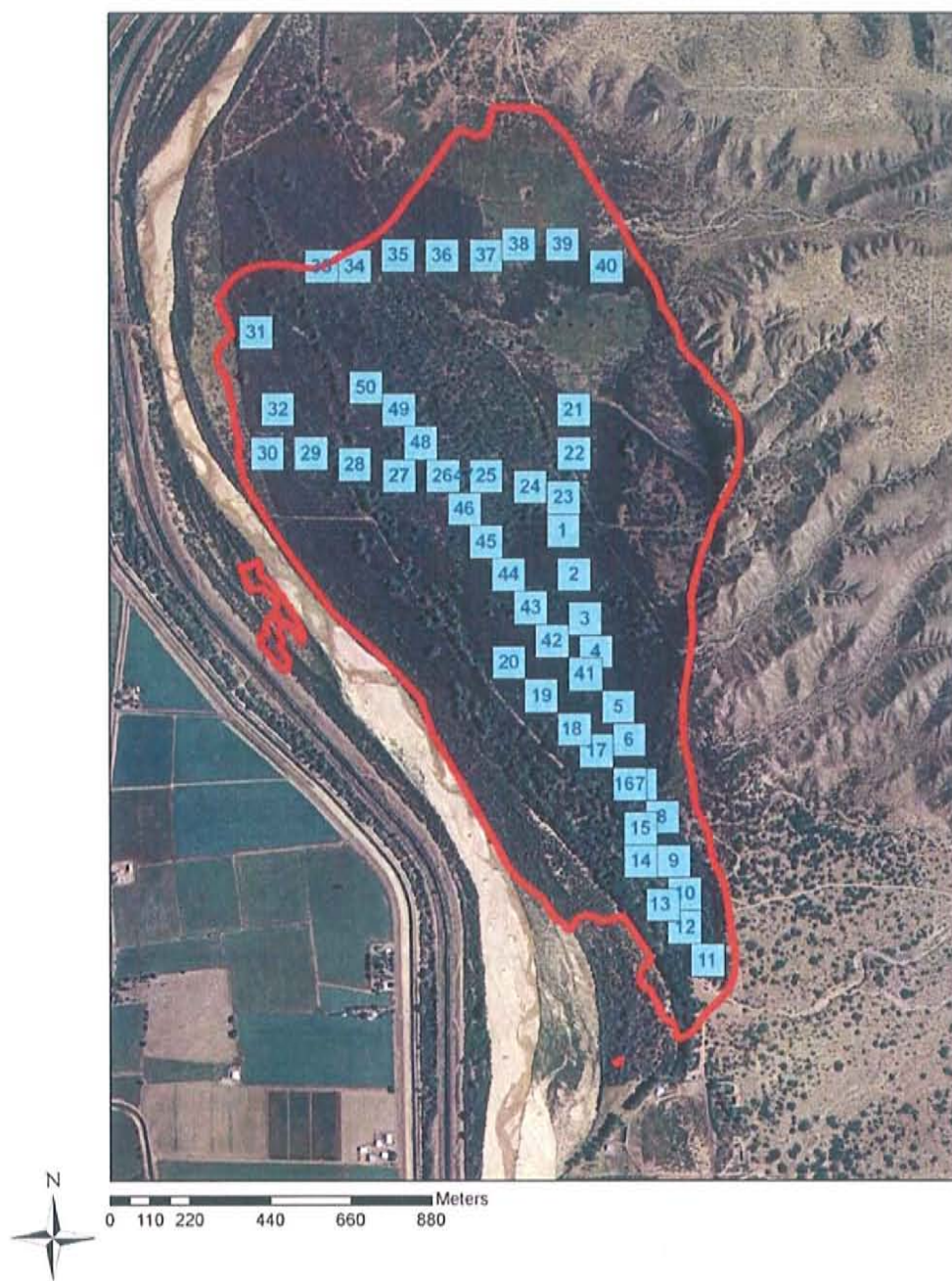


Figure 3.26. 9-Pixel Plots at the Marcial Fire Site.

4. RESULTS AND DISCUSSION

4.1 Dynamics of Albedo, NDVI, ET and Surface temperature

The following figures portray spatial and temporal changes in four key hydrological parameters—albedo, NDVI, Instantaneous and Daily ET—in order to assess changes in tamarisk water use before and after the Mitchell, Marcial and Bosquecito Fire. The maps presented below were generated via the SEBAL algorithm using weather data, satellite data and ERDAS IMAGINE. Albedo and NDVI give us a specific viewpoint of physical conditions on the ground: albedo is related to the reflectivity of the ground surface, which has characteristic values for particular materials, for example 0.17 for bare soil (Markvart, 2003) and 0.25 for green grass (Markvart, 2003). NDVI is related to the “greenness” or density of vegetation within the three sites. The NDVI of an area containing a light to dense vegetation canopy will tend to have values ranging from 0.3 to 0.8 while bare soils tend to generate rather small NDVI values of 0.1 to 0.2 (Gates, 1980).

The parameters of instantaneous and daily ET portray the nature of evapotranspiration, water consumption, and plant biomass growth for the vegetation located within the three sites. In addition, the ET parameters are used as a proxy for vegetation regeneration and recovery. Used together—albedo, NDVI, instantaneous and daily ET—one is able to deduce a time series of the recovery of tamarisk after fire.

The Mitchell Fire

Figures 4.1-4.4 in the following pages present the albedo, NDVI, instantaneous and daily ET before and after the Mitchell Fire. The figures presented allow us to assess ground conditions at the Mitchell Site and present snapshots on the return to pre-fire conditions due to vigorous tamarisk regeneration and environmental conditions. The dramatic impact of the Mitchell fire is evident by the comparison of the instantaneous ET (ET_{Inst}), daily Evapotranspiration (ET_{24}) and NDVI plots (Figures 4.1-4.3) before the fire and one month after the fire. The instantaneous and daily ET maps look similar but in fact they are different; the total daily available energy at every pixel within a Landsat image is taken into consideration when outputting data towards the daily ET map (Bastiaanssen et al., 1998a). The Instantaneous ET maps only account for ET at the exact moment of the satellite overpass time.

ET (Figures 4.1 and 4.2) is an excellent indicator of post-fire conditions, it mimics dramatic environmental changes better than NDVI, seen in Figure 4.3. One month after the fire, the ET maps indicate that there is zero ET—soil evaporation and transpiration—for the majority of the site. We assume there is little to negligible transpiration from the small tamarisk resprouts evident in photographs one month after the fire (Figure 3.4). We also assume that there is negligible soil evaporation soon after fire due to fire-induced hydrophobicity, or water repellency. Water repellent surfaces can reduce evaporation by disrupting the forces of capillary rise (DeBano, 1981) of moisture from the shallow ground water table up through the soil column. Researchers claim that coarse textured

sandy soils are more likely to become repellent as they have a relatively low surface area compared to finer materials. However, certain clay soils have been found to become repellent as the coatings have formed on aggregates of fine material. The NDVI maps in 4.3 do not portray the hydrophobic nature of post-fire clayey soils. In addition, the dramatic progression of tamarisk growth and regeneration from immediately after to two years after fire is not as pronounced as in the ET maps, photographs and field observations incorporated into this report.

Concerning changes in albedo post-fire, the grayish-black charring of the soil surface directly after fire is evident in the reduced-albedo portions of the site located within the Northern and Southern portions (Figure 4.4). One would expect more reduced-albedo conditions due to the blackening and charring of the soil as perceived during the Summer 2006 Field Campaign. However, some of the albedo decrease remained within the same albedo class (0.12-0.08) and, therefore, doesn't reveal itself on the map. For example, an albedo decrease of 0.12 to 0.09 would not be visualized by a color change in Figure 4.4. Another reason may be that immediately after the fire, in May 2005, the ash contained more white-gray materials (leading to an albedo increase) than was observed one year later in the field.

The middle portion of the site, the Mandeville Plot, was the most highly affected within the first few months after the fire because it was previously treated with herbicide in September of 2003—any remaining above-ground vegetation activity was eradicated by the fire. From the examination of

photographs from the SSWCD, it is apparent that tamarisk regeneration started occurring one month after the fire (Figure 3.4) from the root crown below ground surface. The fire was not intense enough to sear and destruct the root crown below, thereby allowing regeneration to occur. Regenerative activity two months after the fire is portrayed in Figures 3.5 and 3.6. One year later, May 18, 2006, there has been significant regeneration along the western and southern portion of the fire area (Figure 4.2). Two years later, July 8, 2007, the site looks similar to the conditions before the fire, except that the Mandeville Plot exhibits little to no daily ET (Figure 4.2) due to treatment with herbicide.

Following the fire, the Mandeville Plot was exposed to flooding during the record rainfall of the summer of 2006, and underwent mechanical removal of tamarisk root mass from the spring of 2006 to the spring of 2007. The exhibition of little to no daily and instantaneous ET as well as reduction in NDVI two years after the fire at the Mandeville Plot displays the efficacy of using the combination of herbicide, burn, flooding and mechanical removal in controlling tamarisk. Flooding from the torrential rains of the summer of 2006 suffocated the tamarisk by preventing exposure of oxygen from the atmosphere to leaf surfaces due to elevated surface water levels.

For the NDVI plots (Figure 4.2), there is an increase in NDVI 1 year and 2 years after the fire for the northern and southern portions of the Mitchell Fire site. Since the site is comprised of homogeneous tamarisk thickets—there are no other dominant vegetation types—the NDVI increase can be correlated to tamarisk regeneration because the tamarisk is the dominant vegetation type that

would produce the “greenness” signal. Tamarisk was the dominant species type during the Summer 2006 Field Campaign (Figure C.1). In addition, only two of the 16 9-Pixel Plots sampled during the field campaign displayed notable coverages of combined shrubs, graminoids and forbs, from 4 – 44% (Figure C.5).

Mitchell Fire

Fire Date: April 9-16, 2005

Parameter: Albedo

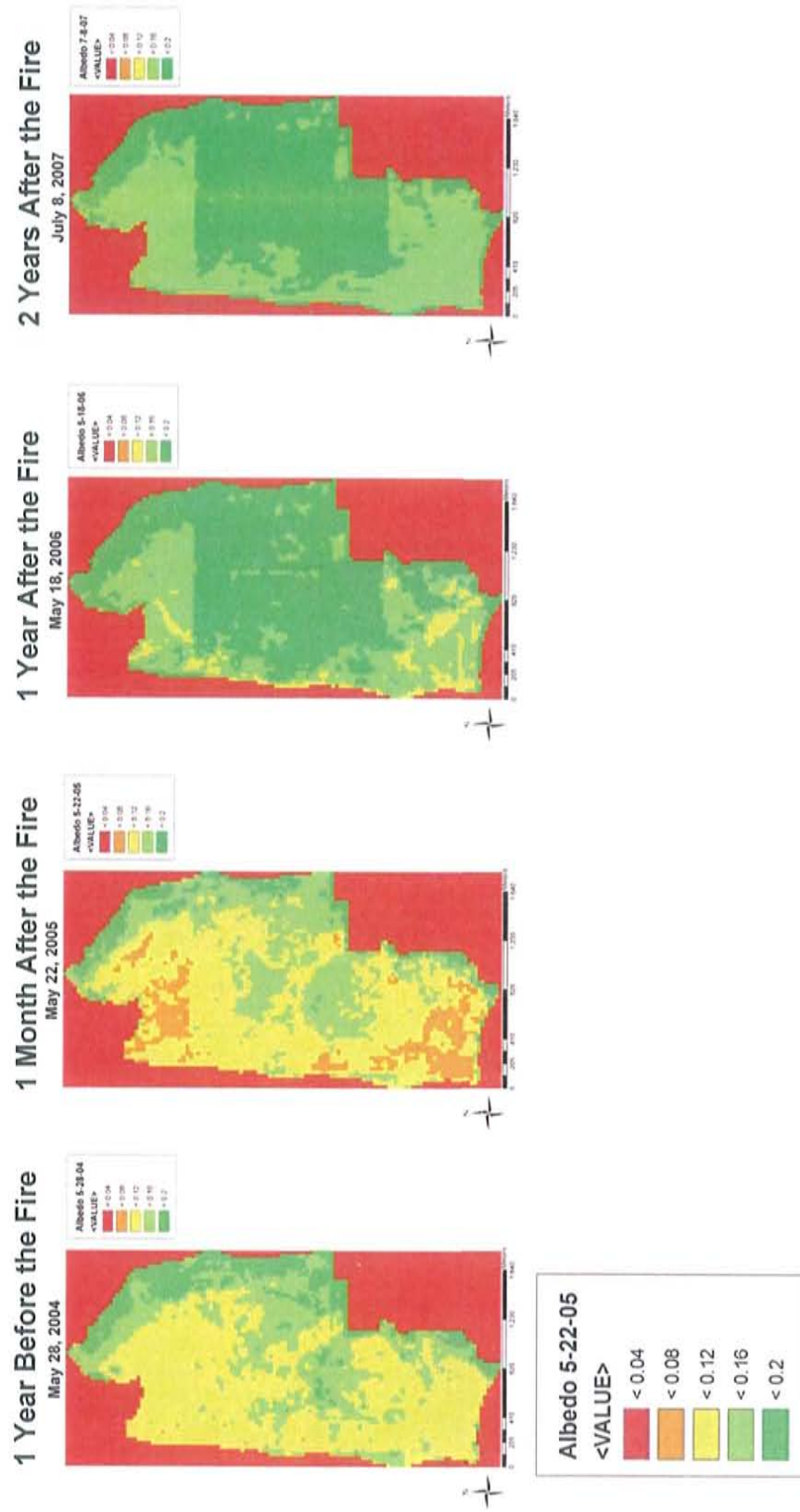


Figure 4.1. Albedo maps before and after the Mitchell Fire derived from the SEBAL model applied to Landsat satellite imagery.

Mitchell Fire
Fire Date: April 9-16, 2005
Parameter: NDVI

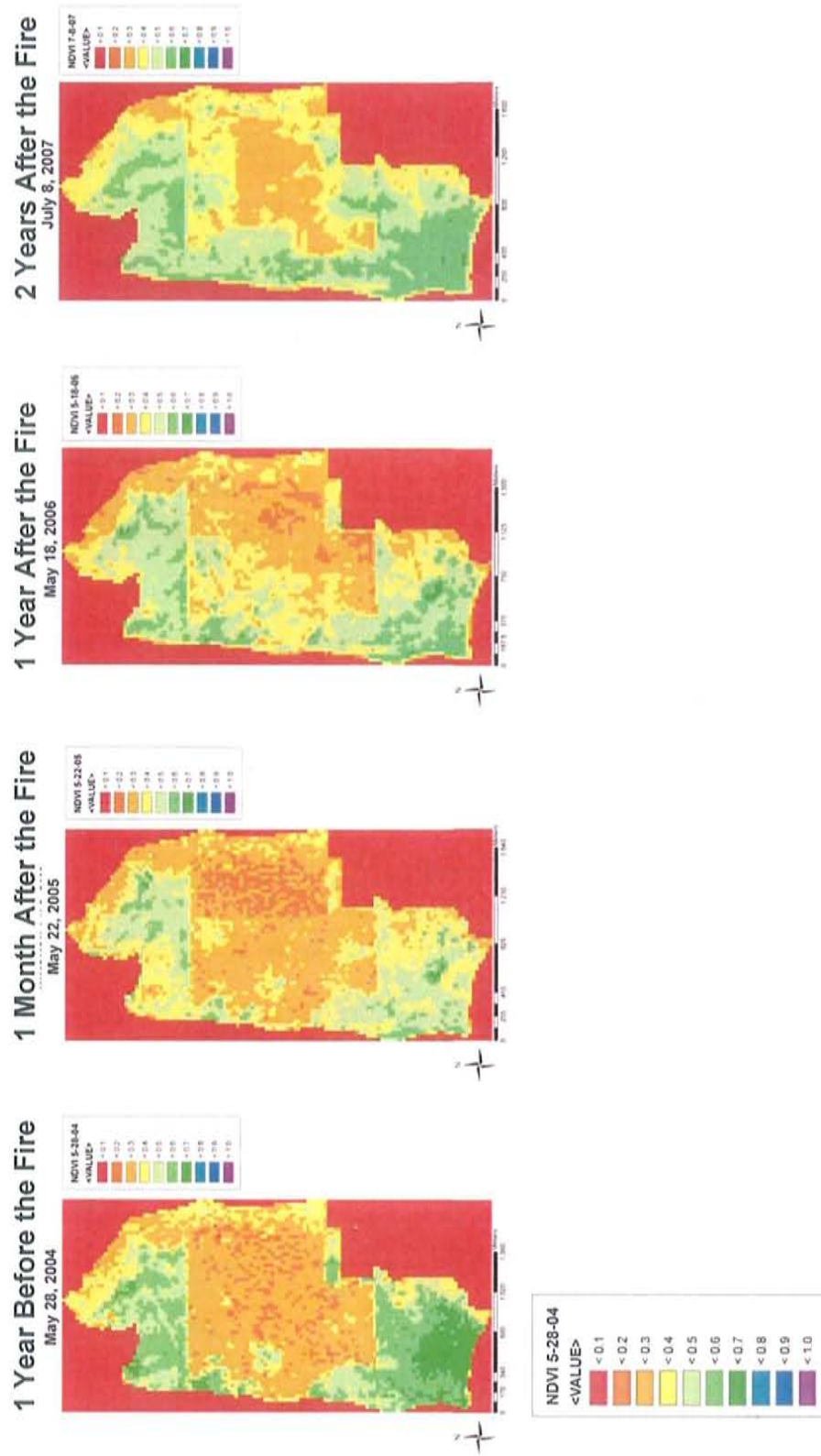


Figure 4.2. Normalized Difference Vegetation Index (NDVI) maps before and after the Mitchell Fire derived from the SEBAL model applied to Landsat satellite imagery.

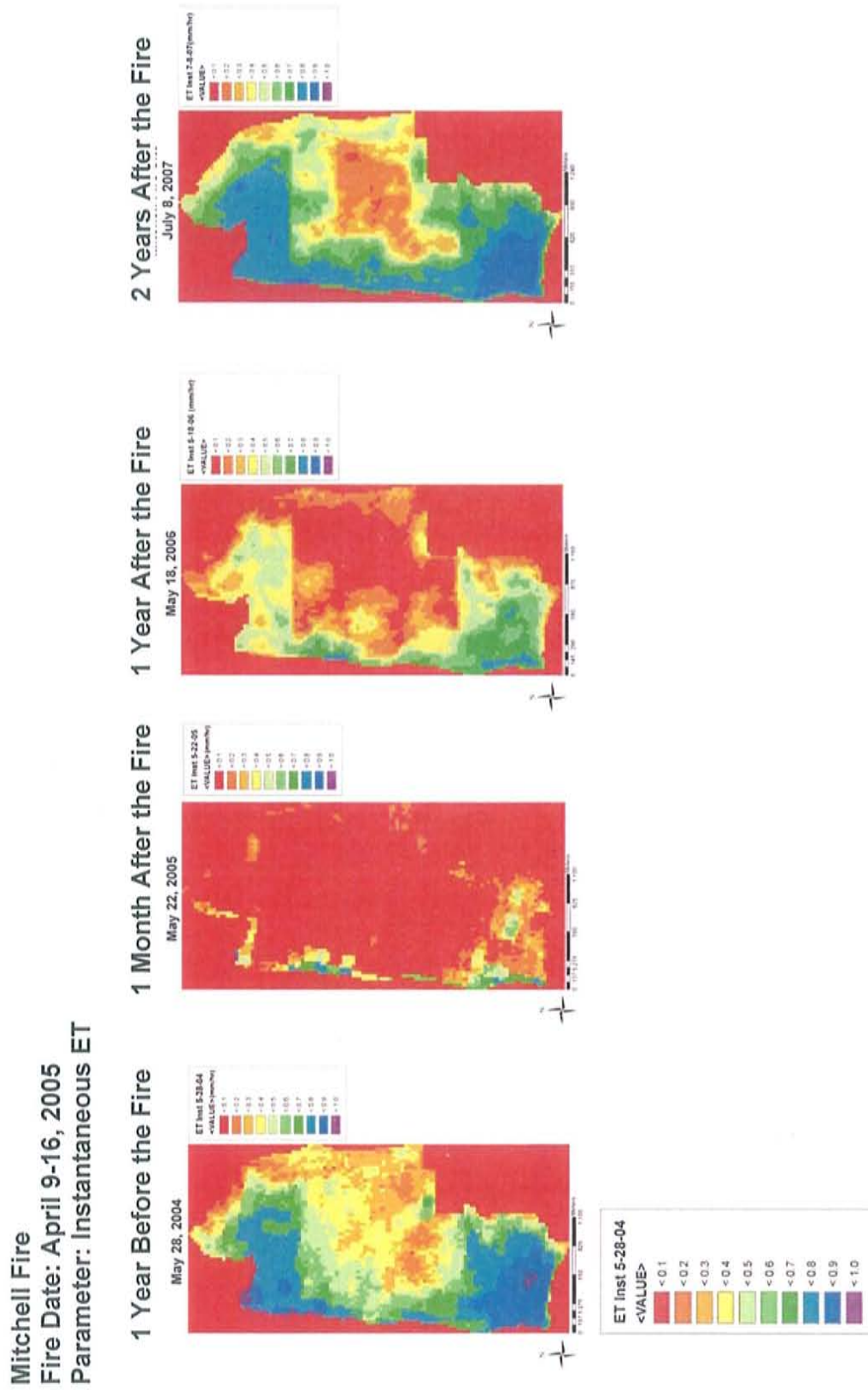


Figure 4.3. Instantaneous Evapotranspiration maps before and after the Mitchell Fire derived from the SEBAL model applied to Landsat satellite imagery.

Mitchell Fire
Fire Date: April 9-16, 2005
Parameter: Daily ET

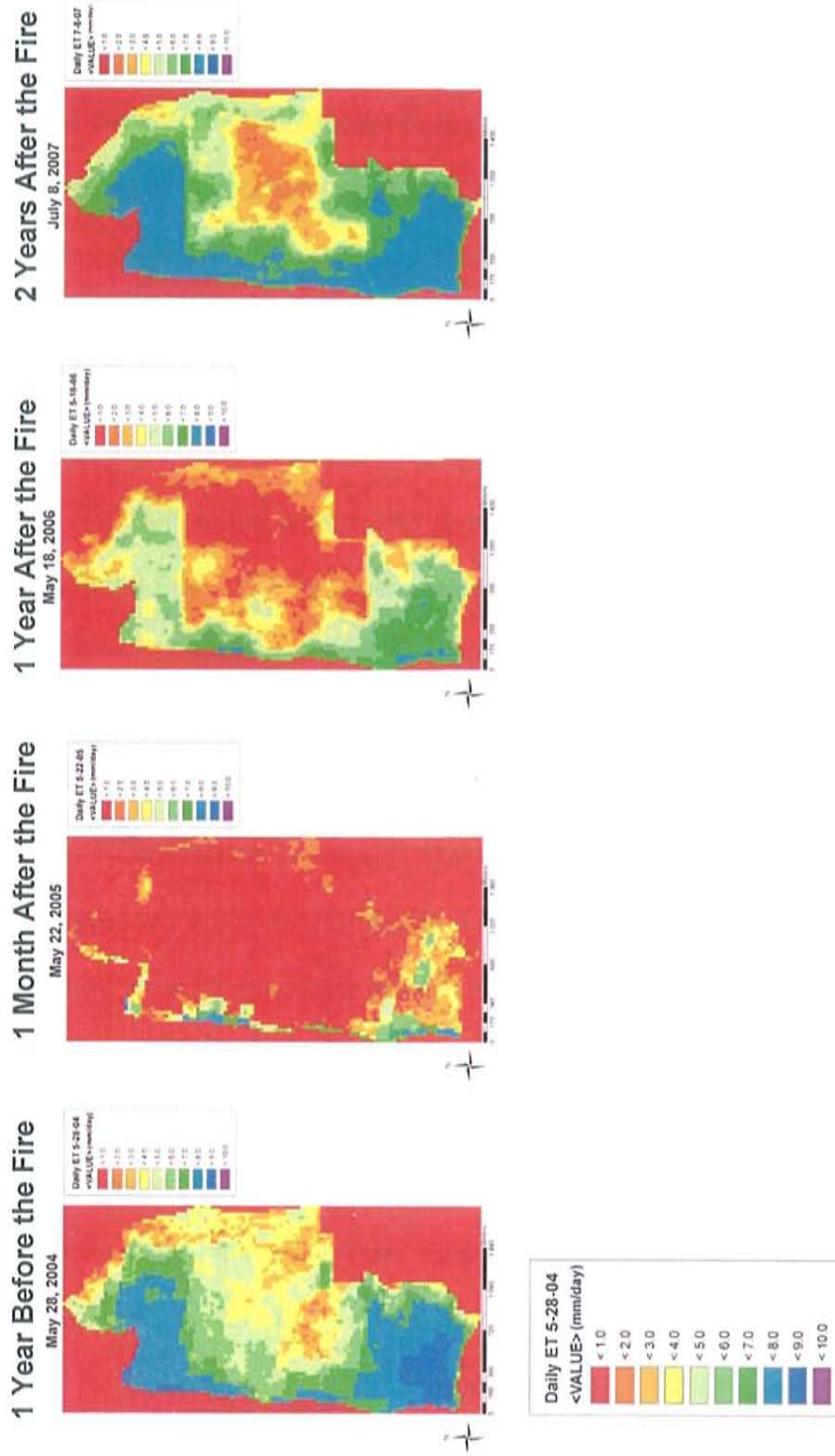


Figure 4.4. Daily Evapotranspiration maps before and after the Mitchell Fire derived from the SEBAL model applied to Landsat satellite imagery.

Marcial Fire

The Summer 2006 Field Campaign included the Tiffany Basin within the Marcial Fire site. Due to the site's location on the Armendaris Ranch and separation from the Bosque del Apache to the north, no site augmentation such as herbicide treatment, mechanical removal, or cottonwood pole plantings occurred before the fire (SSWCD, 2008). Before the fire, the site was in a natural state and populated by homogeneous tamarisk thickets with small clumps of cottonwood groves interspersed. Therefore, the discussion on Figures 4.5-4.8 portrays tamarisk regenerative behavior at a site that was previously undisturbed.

Figures 4.5-4.8 present the albedo, NDVI, instantaneous and daily ET before and after the Marcial Fire. The data generated eight days after the Marcial Fire displays a reduction in albedo within the Tiffany Basin study site area due to blackening and charring of the tamarisk bark and soil (Figure 4.5). Daily ET, instantaneous ET and NDVI have been dramatically reduced—ET rates are close to zero—for the entire portion of the site one month after the fire (Figures 4.6-4.8). These images were not able to detect the small amounts of ET produced from the very short tamarisk resprouts evident in photos from one month after the Marcial Fire (Figure 3.9).

Two months after the fire, July 21, 2006, albedo, NDVI, daily and instantaneous ET have all started to recover, but do not match pre-fire conditions (Figures 4.5-4.8). The findings from SEBAL data are concurrent with photographs taken at the Marcial Fire site one month after the fire (Figure 3.9). One year later, for dates May 21, 2007 and July 8, 2007, spatial instantaneous

and daily ET rates for the Tiffany Basin surpass the pre-fire ET images dated May 31, 2002 (Figure 4.8). The images for NDVI portray a decrease in NDVI for the images one and two months after the fire (Figure 4.6). For the image one year after the fire, NDVI has surpassed that of the image from four years before the fire, suggesting that the fire encouraged the tamarisk to regrow at a thicker, denser rate than pre-fire conditions.

Marcial Fire
Fire Date: May 3-10, 2006
Parameter: Albedo

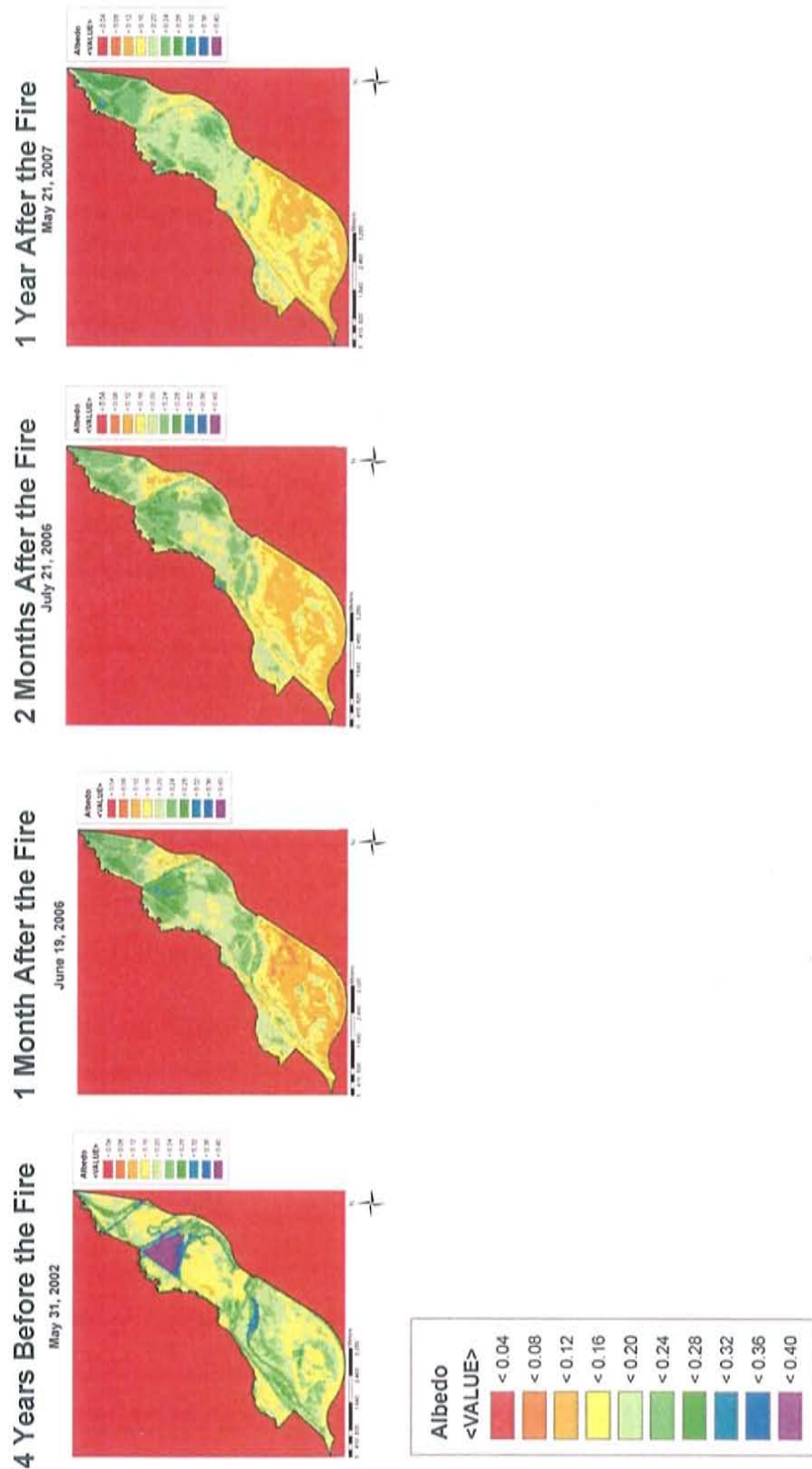


Figure 4.5. Albedo maps before and after the Marcial Fire derived from the SEBAL model applied to Landsat satellite imagery.

Marcial Fire
 Fire Date: May 3-10, 2006
 Parameter: NDVI

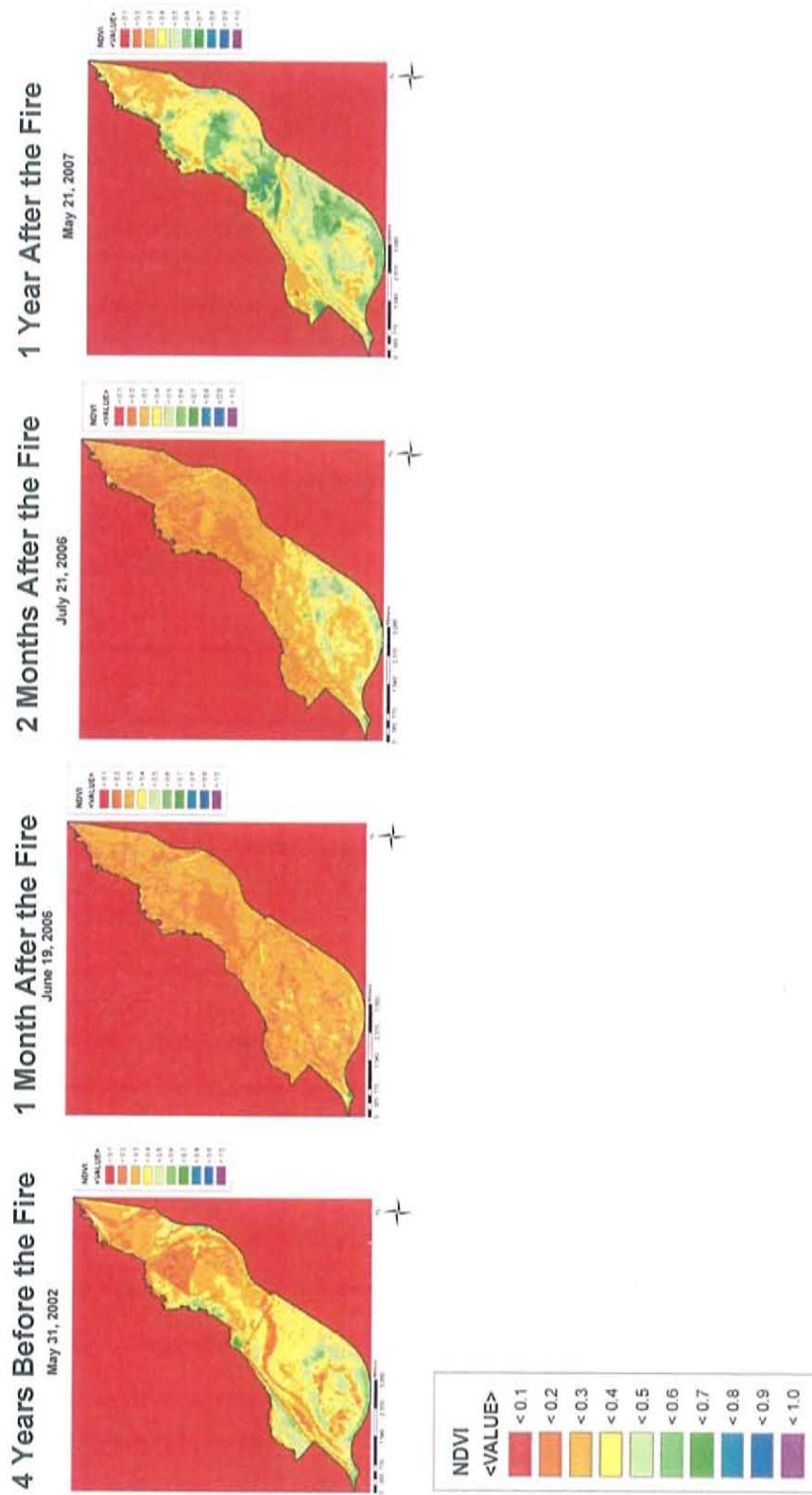


Figure 4.6. Normalized Difference Vegetation Index (NDVI) maps before and after the Marcial Fire derived from the SEBAL model applied to Landsat satellite imagery.

Marcial Fire
Fire Date: May 3-10, 2006
Parameter: Instantaneous ET

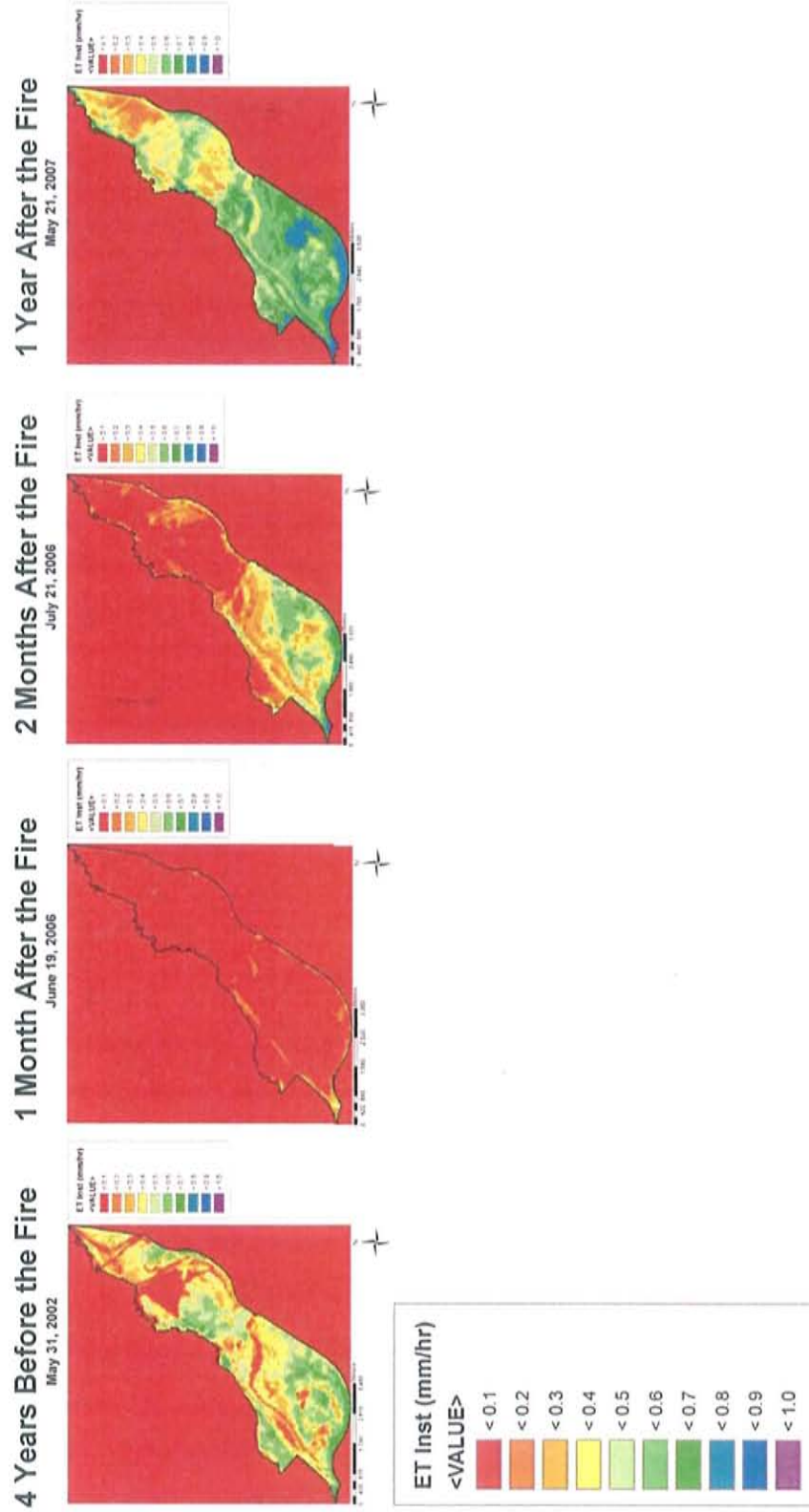


Figure 4.7. Instantaneous Evapotranspiration maps before and after the Marcial Fire derived from the SEBAL model applied to Landsat satellite imagery.

Marcial Fire
Fire Date: May 3-10, 2006
Parameter: Daily ET

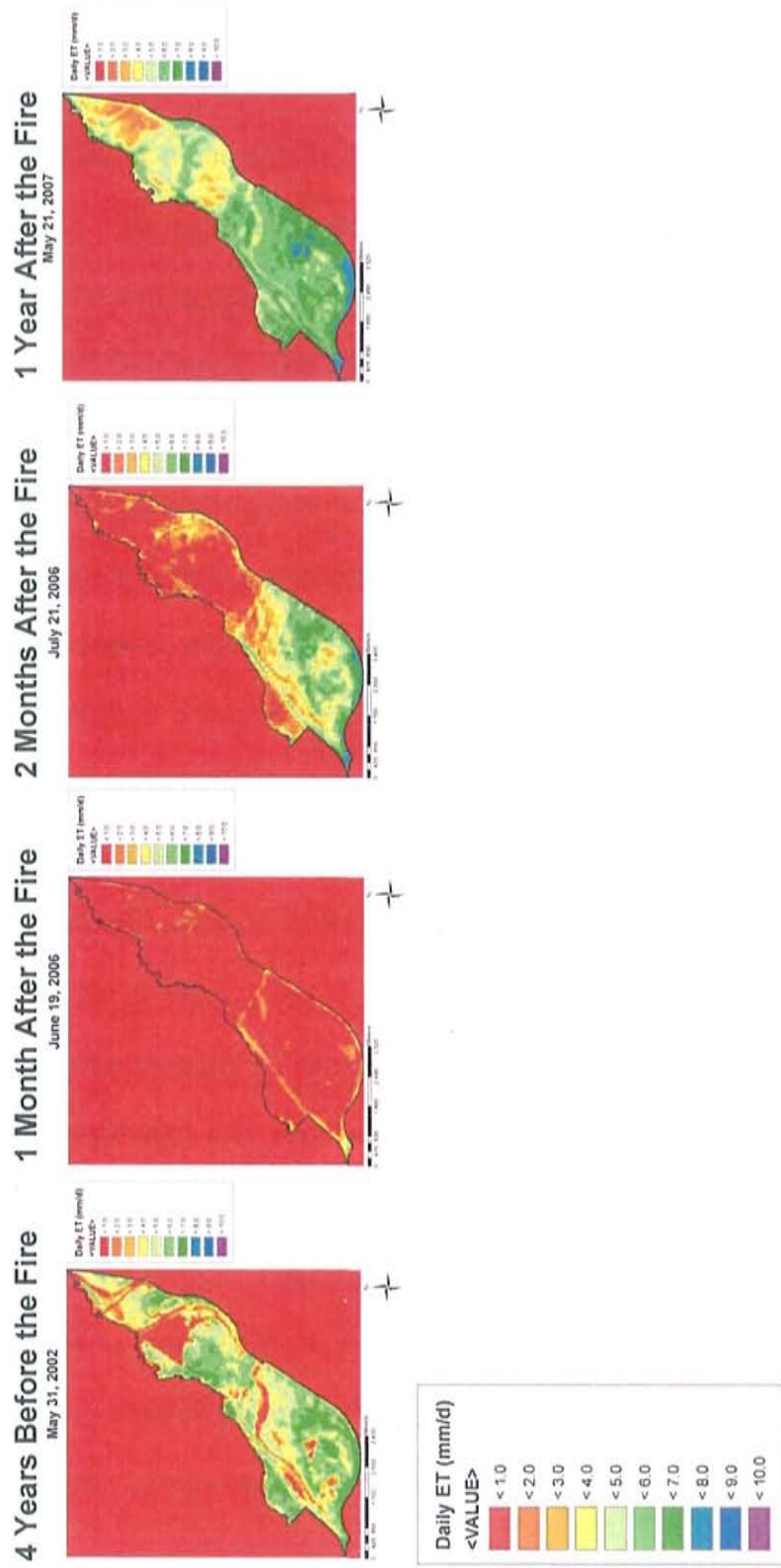


Figure 4.8. Daily Evapotranspiration maps before and after the Marcial Fire derived from the SEBAL model applied to Landsat satellite imagery.

Bosquecito Fire

Figures 4.9-4.12 present the albedo, NDVI, instantaneous and daily ET before and after the lightning-induced Bosquecito fire that burned the hottest of the three fires, fully consuming above-ground tamarisk biomass and bark in portions of the site. The fully-consumed portions of the site were left with a layer of light grey charred ash deposited on the ground surface, as evident during the Summer 2006 Field Campaign. The light grey deposit areas, which are patchy in nature and have a high reflectivity, are evident in the sporadic dark green portions of the image for albedo one month after the fire (Figure 4.9). 2008.

The increase in albedo perceived one year after the fire for the majority of the site (Figure 4.9) is most likely an overestimation in the model, as the vegetation regeneration occurred in patchy sections of the site, as perceived during the Summer 2006 Field Campaign and portrayed in the Bosquecito maps in upcoming Section 4.4.1. The data 10 days after the Bosquecito Fire displays the whole site strongly reduced in NDVI, daily and instantaneous ET (Figures 4.10-4.12). One month later, July 21, 2006, there remain great reductions in NDVI, daily and instantaneous ET throughout the site, with areas of regeneration occurring in the northwest and southwest boundaries of the fire (Figures 4.10-4.12). One year later, July 8, 2007, the central portion of the site is still greatly affected by the fire, as seen in reduced instantaneous and daily ET values in that section (Figures 4.11 and 4.12), due to the extremely high fire severity; high severity areas were observed during the field campaign of the summer of 2006. Regeneration predominantly occurs within the field-observed medium to low fire

severity areas in the Northern and Western boundaries of the fire (Figures 4.10-4.12). Fire severity greatly influenced the tamarisk's ability to re-sprout, degree of canopy degeneration and the biological environment for the tamarisk to re-establishment.

NDVI, a proxy for "greenness", displays the return to pre-fire conditions one year after the fire, with increased vegetation densities in the central portion of the site. The increased average NDVI of 0.4 in the central portion of the fire proposes the notion that the fire encouraged the tamarisk to regrow with a greater thickness and resilience than before the fire, when there was an average NDVI of 0.3 in that same region. The reduction in NDVI in the southwest portion of the site one year after the fire may be due to fire effects on different vegetation communities, such as cottonwood and willow, which may have been fully eradicated by the fire. The increase in NDVI in the northwest portion of the site may portray newfound tamarisk domination in secondary succession in areas which may have previously been occupied by cottonwood and willow. Due to tamarisk adaptation to fire, it is able to colonize areas previously occupied by native species that lack the fire adaptation, thus increasing NDVI due to the dense, thicket nature of tamarisk communities, compared to clumps of cottonwood and willow stands.

Bosquecito Fire
Fire Date: June 6-9, 2006
Parameter: Albedo

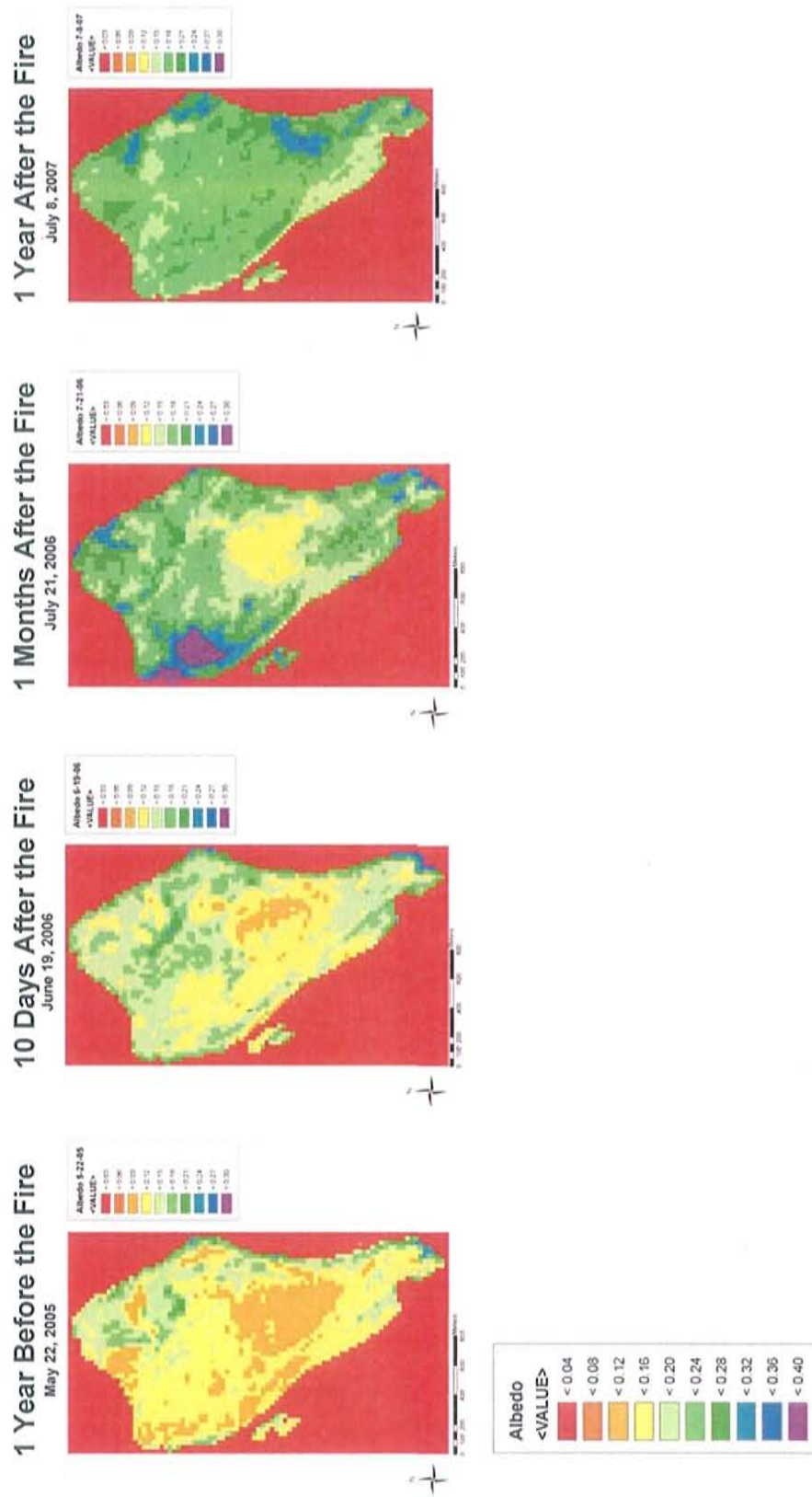


Figure 4.9. Albedo maps for before and after the Bosquecito Fire derived from the SEBAL model applied to Landsat satellite imagery.

Bosquesito Fire
Fire Date: June 6-9, 2006
Parameter: NDVI

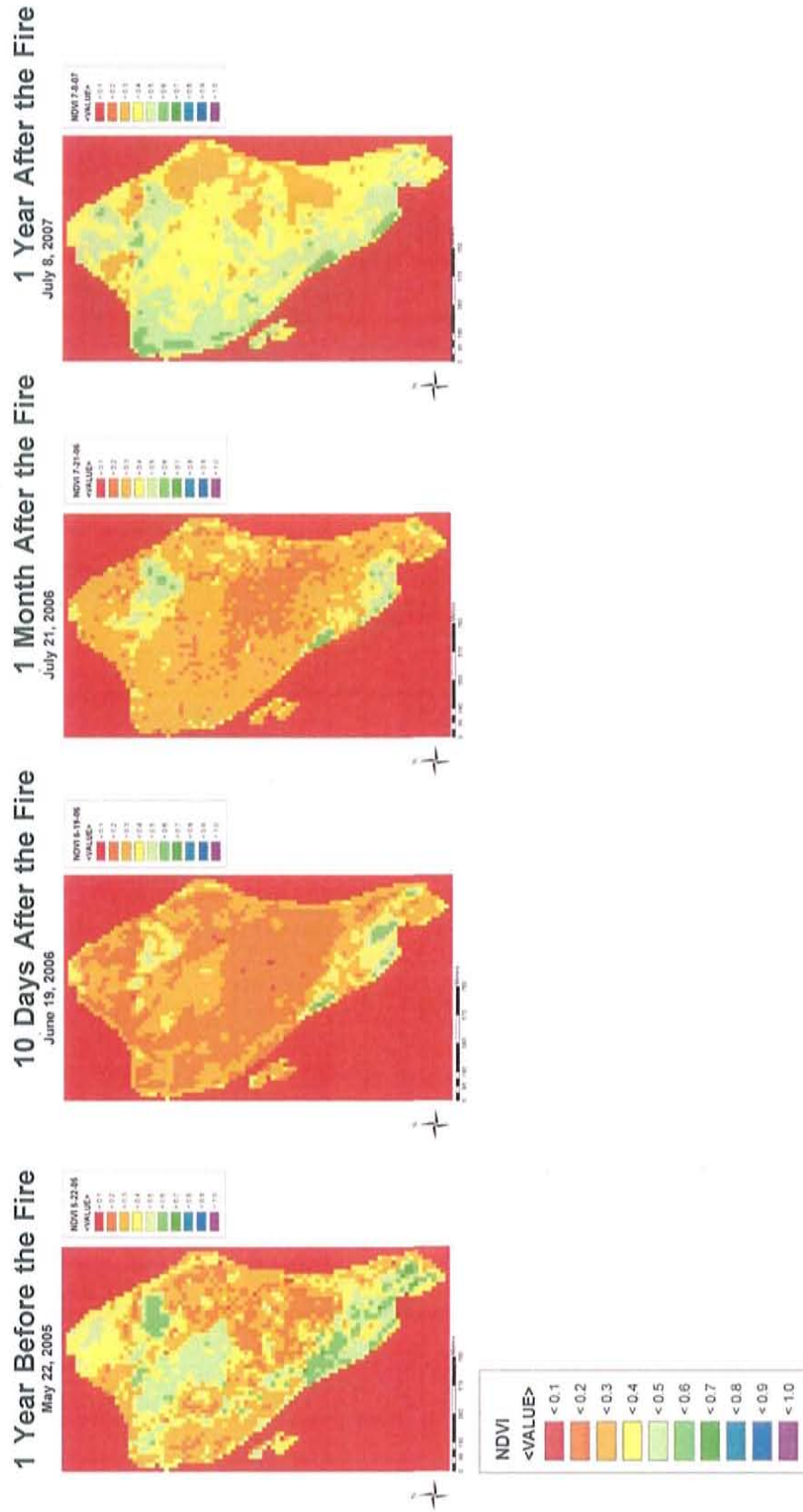


Figure 4.10. Normalized Difference Vegetation Index (NDVI) maps before and after the Bosquesito Fire derived from the SEBAL model applied to Landsat satellite imagery.

Bosquesito Fire

Fire Date: June 6-9, 2006

Parameter: Instantaneous ET

1 Year Before the Fire
May 22, 2005

10 Days After the Fire
June 19, 2006

1 Month After the Fire
July 21, 2006

1 Year After the Fire
July 8, 2007

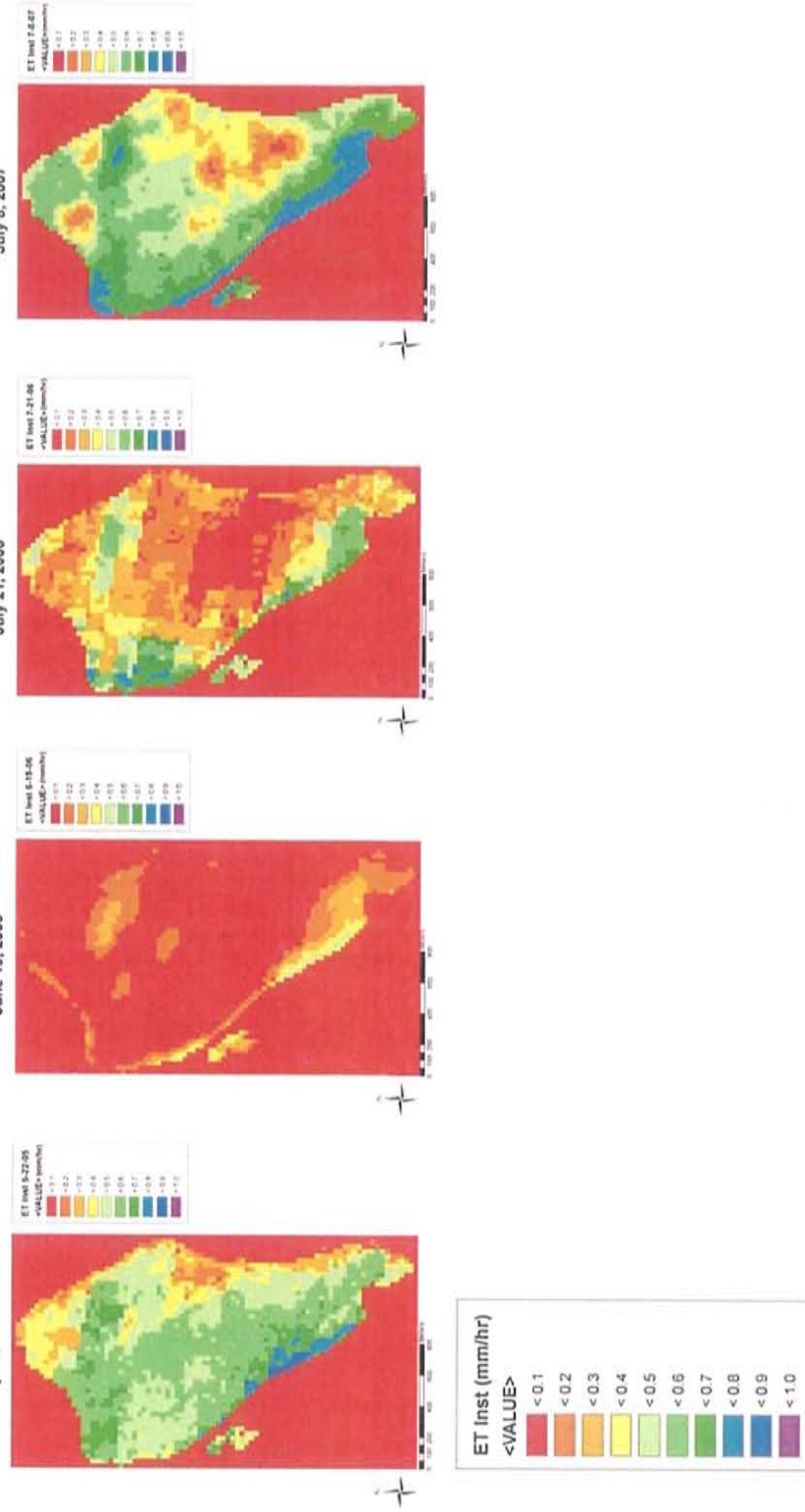


Figure 4.11. Instantaneous Evapotranspiration maps before and after the Bosquesito Fire derived from the SEBAL model applied to Landsat satellite imagery.

Bosquecito Fire
Fire Date: June 6-9, 2006
Parameter: Daily ET

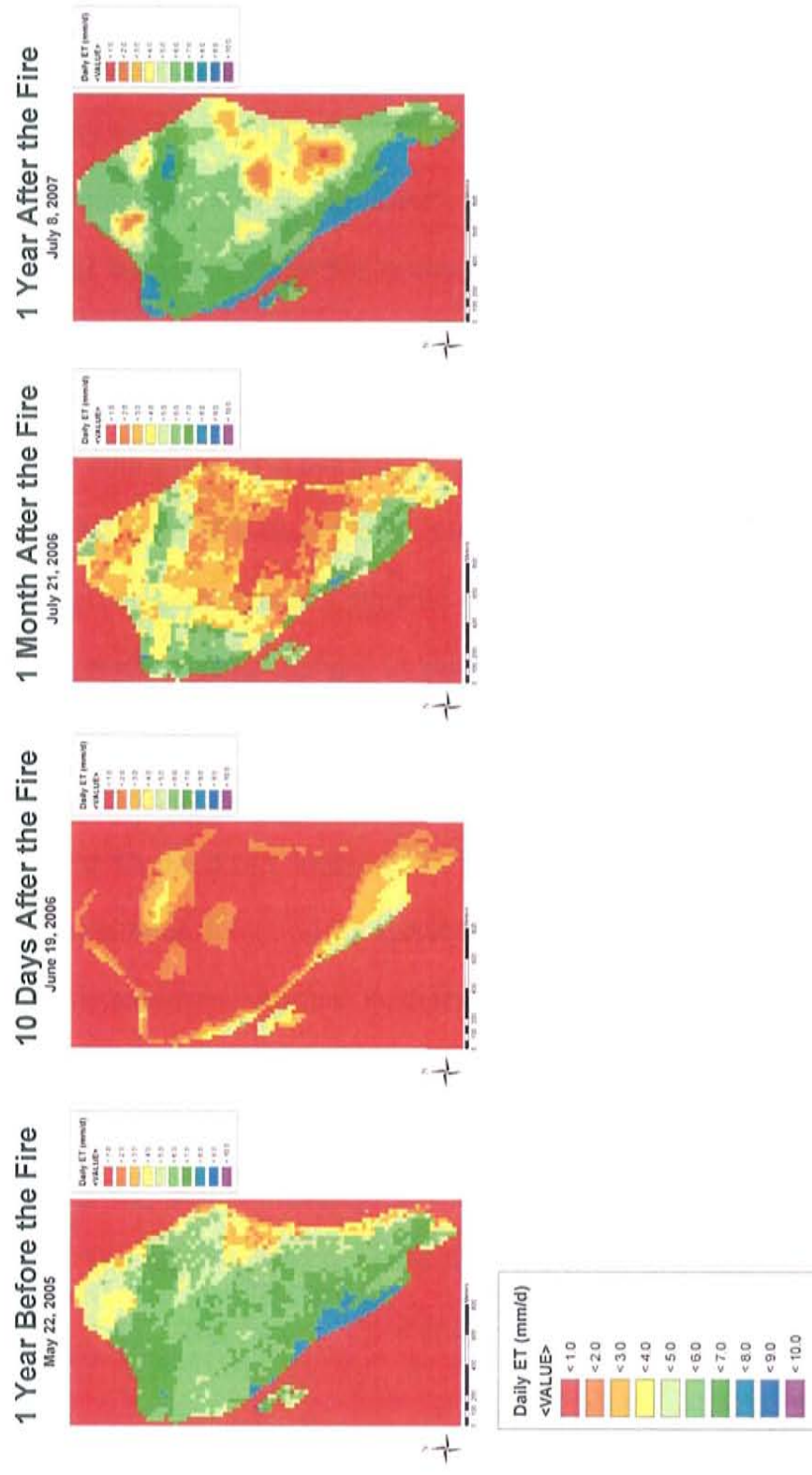


Figure 4.12. Daily Evapotranspiration maps before and after the Bosquecito Fire derived from the SEBAL model applied to Landsat satellite imagery.

4.2 9-Pixel Bar Graphs

9-Pixel Bar Graphs (Figures 4.13-4.16) were generated in order to do a comparison between the Summer 2006 Field Campaign data and the Landsat or MODIS maps discussed in Section 4.1. The 9-Pixel Bar Graphs provide a pinpointed, micro- perspective following select 9-pixels located within each fire over time, from one or two years before fire to one or two years after. The 9-Pixel Plot locations for each fire site are presented in Figures 3.24-3.26. The 4 or 5 dates in the bar graphs were selected from plots from 15 image dates in the available SEBAL/Landsat data explored in this project, and such data plots can be found in Appendix A in the form of 9-Pixel Plots. The image dates chosen for the bar graphs in this section best represent tamarisk regeneration post-fire.

The bar graphs portray changes in albedo, daily ET (ET_{24}), instantaneous ET (ET_{Inst}), ground heat flux (G), Leaf Area Index (LAI), Normalized Difference Vegetation Index ($NDVI$), and Surface temperature (T_s) and Crop Coefficient (K_c) at the 9-Pixel Plot for the 4 or 5 image dates per fire. Crop Coefficients (K_c) are used with the reference ET (ET_o) to estimate specific crop evapotranspiration rates. Reference evapotranspiration is defined as the ET from an extensive surface of clipped grass or alfalfa that is well-watered, and fully shades the ground (Allen, 2000). The Crop Coefficient is a dimensionless number (usually between 0.1 and 1.2) that is multiplied by the ET_o value to arrive at a crop ET (ET_c) estimate. The resulting ET_c is useful to hydrologists and can be used to help an irrigation manager schedule when

irrigation should occur and how much water should be put back into the soil (USDA, 2006).

On the 9-Pixel Bar Graphs each date is represented as a certain color. The 9-Pixel Plots correspond to field sampling locations, with the exact field sampling location corresponding to a location within the center pixel in each 9-Pixel Plot. Data was extracted for each 3x3 "9-Pixel Plot" from SEBAL output data using the Zonal Statistics tool in ArcGIS.

Mitchell Fire

Figures 4.13-4.16 present the changes of albedo, ground heat flux (G), surface temperature (T_s), Normalized Differenced Vegetation Index (NDVI), Leaf Area Index (LAI), instantaneous Evapotranspiration (ET_{inst}) and daily ET (ET_{24}), and Crop Coefficient (K_c) at the Mitchell fire. Pre-fire "baseline" conditions are represented by the date May 28, 2004 (in green). The fire has caused a large change in all the parameters as displayed by the first image after the fire, May 22, 2005 (in red) for all of the 9-Pixel Bar Graphs (Figures 4.13-4.16). The fire eradicated all above ground green basal vegetation; the pronounced change in the post-fire environment caused the most distinctive signal of change in the energy balance parameters. In addition, the tamarisk bark stumps left standing did not have potential for evapotranspiration. Strong indicators of the fire are the plots of ground heat flux (Figure 4.13) and surface temperature (Figure 4.14) that display elevated values due to the large proportion of exposed soil that was previously occupied by dense tamarisk thickets.

Four months after the fire, August 3, 2005 (in orange), all the parameters have started to move back to pre-fire conditions (Figures 4.13-4.16) as the tamarisk regenerates from the root crown below which was not destroyed by the fire. From photographs from the SSWCD, it is apparent that tamarisk regrowth started to appear as early as one month after the fire (Figure 3.4). Along with tamarisk, the Summer 2006 Field Campaign documented small populations of shrub, graminoid and forb species regrowing in the understory of the tamarisk, (Figure C.5), adding the response by the energy balance parameters. A year later, June 19, 2006 (in yellow) the energy balance parameters are still reduced compared to pre-fire conditions (Figures 4.13-4.16). A full return to pre-fire conditions is apparent two years later, July 8, 2007 (in blue), specifically in the ET_{Inst} , ET_{24} and K_c plots (Figures 4.15 and 4.16). This suggests that it took about two years after the Mitchell Fire for the tamarisk and small populations of shrub, graminoid and forb species to return to baseline, pre-fire conditions.

Mitchell Fire
Fire Date: April 9-16, 2005

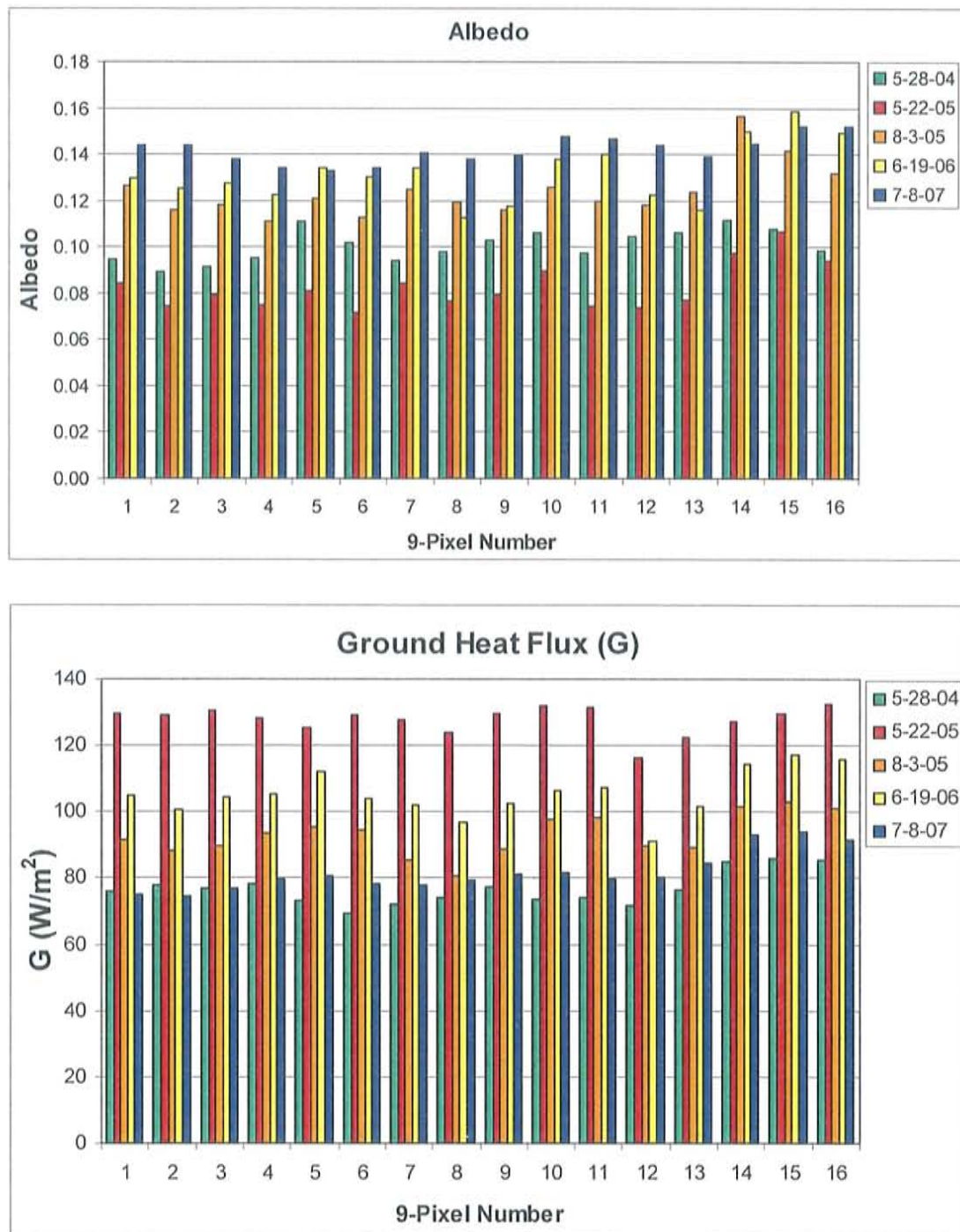


Figure 4.13. Plots of Albedo and Ground heat flux derived from the SEBAL model and the stated image dates. Each 9-Pixel represents a macroplot sampling location from the Summer 2006 Field Campaign.

Mitchell Fire

Fire Date: April 9-16, 2005

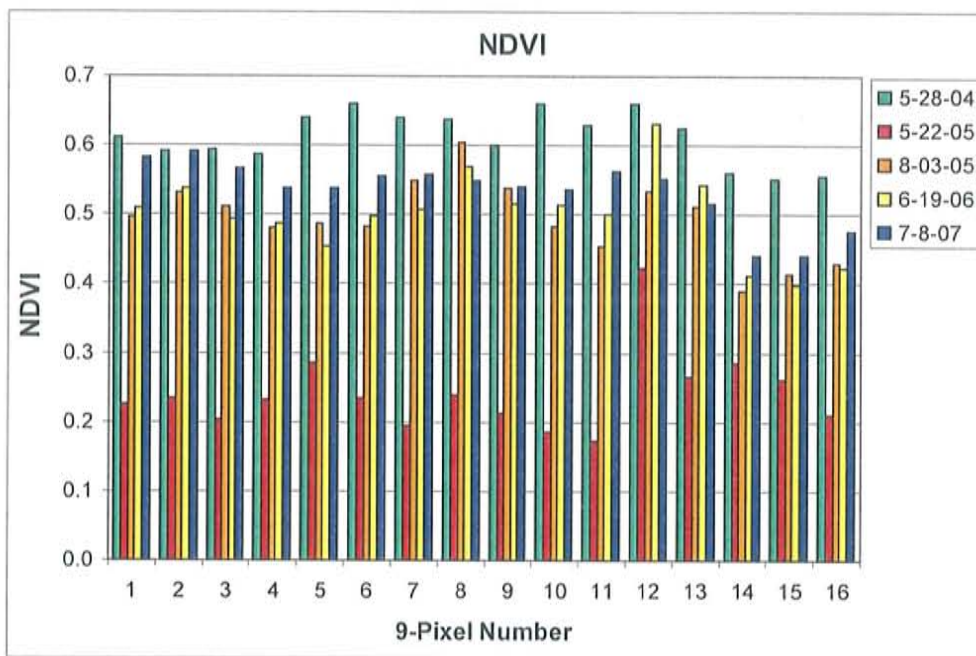
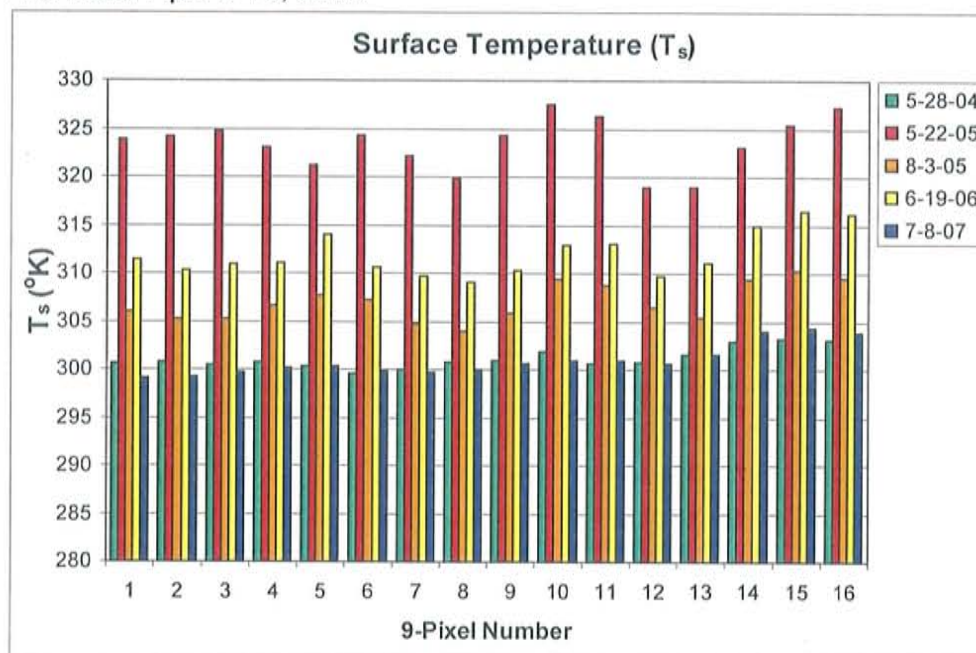


Figure 4.14. Plots of Surface temperature and NDVI derived from the SEBAL model and the stated image dates. Each 9-Pixel represents a macroplot sampling location from the Summer 2006 Field Campaign.

Mitchell Fire
Fire Date: April 9-16, 2005

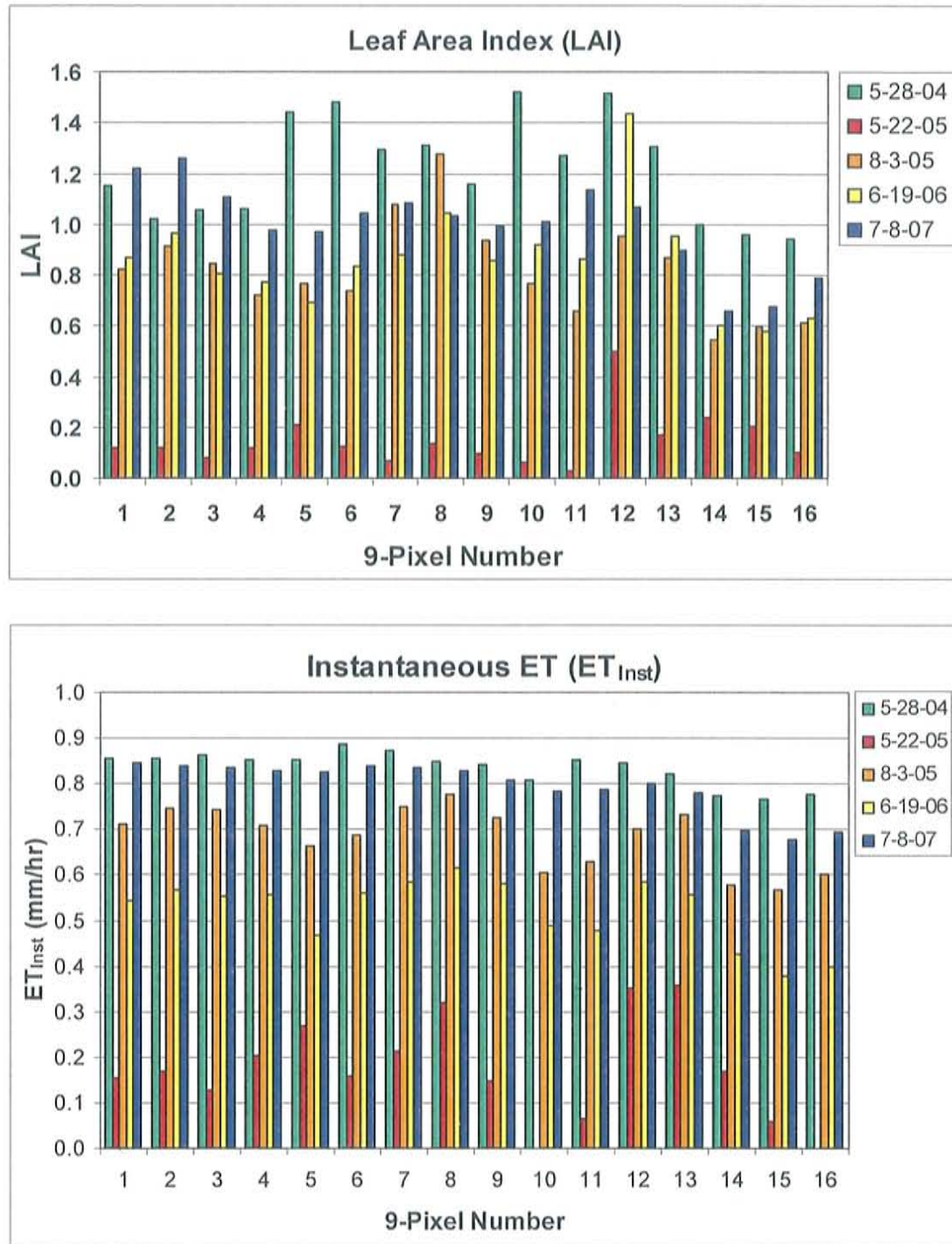


Figure 4.15. Plots of LAI and Instantaneous Evapotranspiration derived from the SEBAL model and the stated image dates. Each 9-Pixel represents a macroplot sampling location from the Summer 2006 Field Campaign.

Mitchell Fire
Fire Date: April 9-16, 2005

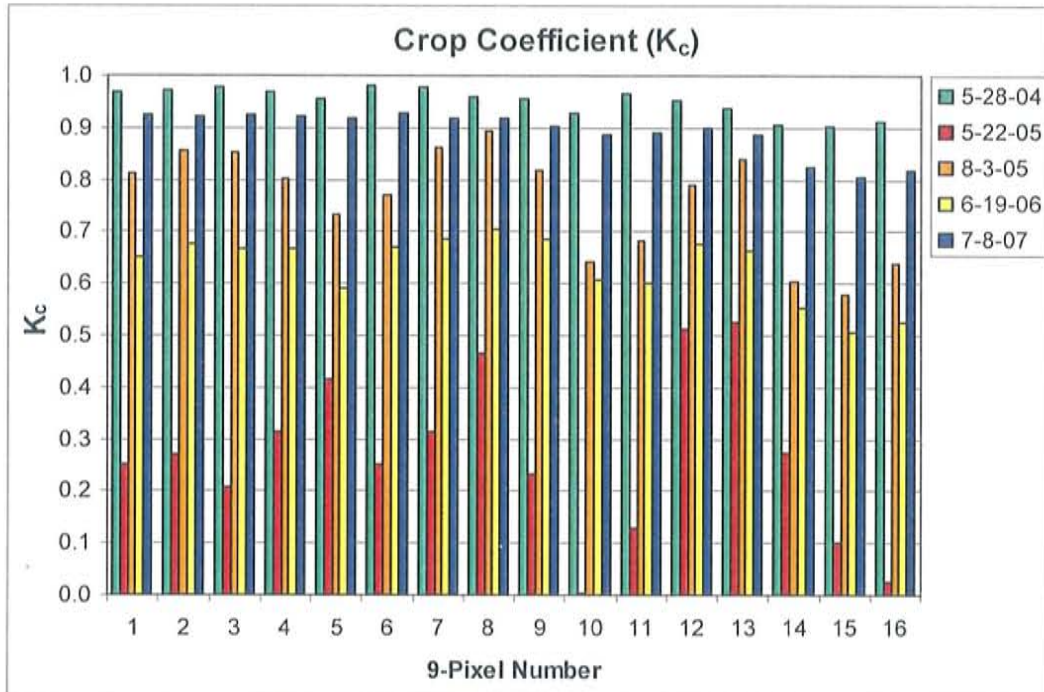
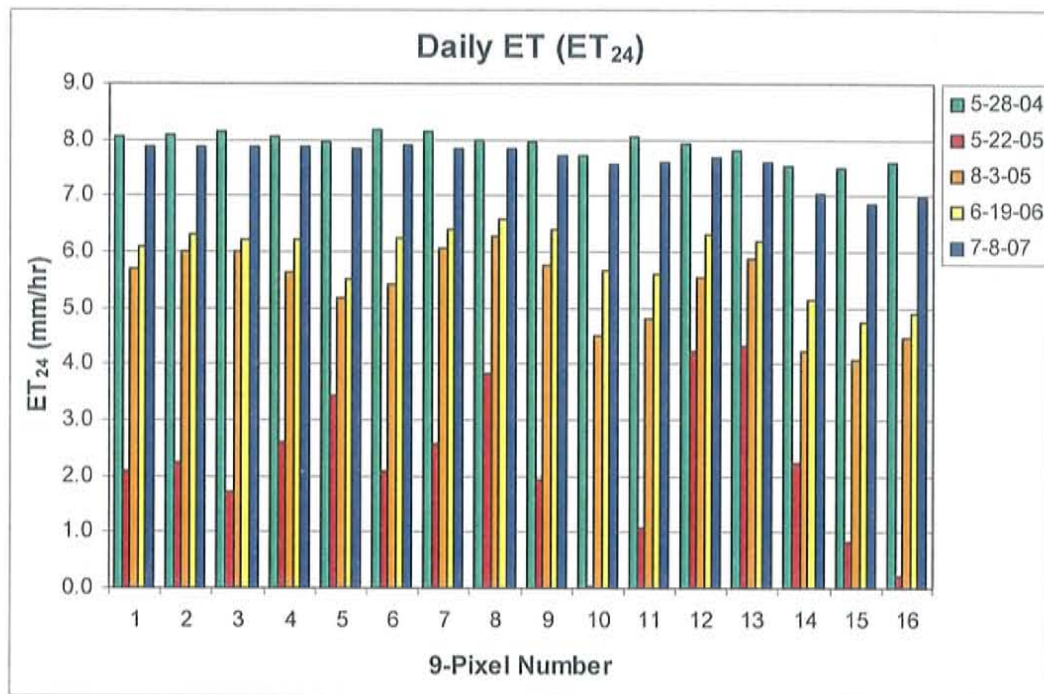


Figure 4.16. Plots of Daily Evapotranspiration and the Crop Coefficient derived from the SEBAL model and the stated image dates. Each 9-Pixel represents a macroplot sampling location from the Summer 2006 Field Campaign.

Marcial Fire

Figures 4.17-4.20 present bar graphs of albedo, ground heat flux (G), surface temperature (T_s), Normalized Differenced Vegetation Index (NDVI), Leaf Area Index (LAI), instantaneous ET (ET_{Inst}) and daily ET (ET_{24}) and Crop Coefficient (K_c) for the 9-Pixel Plots before and after the Marcial Fire. The SEBAL model failed to produce LAI output for May 31, 2002.

As with the Mitchell Fire, there is a large change in all energy balance parameters in the first and second image after the fire, May 18 and July 21, 2006 (in red and yellow, respectively) for all of the 9-Pixels (Figures 4.17-4.20). Eight days after the fire, May 18, 2006 (in red), there is a high proportion of zero values for the bar graphs of LAI, instantaneous and daily ET as well as the Crop Coefficient (Figures 4.19 and 4.20) which substantiates the eradication of all ET-producing above ground basal vegetation. The greater-than-zero peaks in the graphs for LAI, instantaneous and daily ET as well as the Crop Coefficient most likely are indicative of surficial soil evaporation.

Two months after the fire, July 21, 2006, the parameters have started to approach pre-fire background conditions (Figures 4.17-4.20). The background data image date is May 31, 2002, early on in the growing season and from a year with low precipitation which may explain why the plots for daily ET, instantaneous ET, and Crop Coefficient for that date are reduced compared to those from July 8, 2007 (Figure 4.21). One year later on all the plots, May 21 and July 8, 2007, the parameters approach the natural pre-fire conditions (Figures 4.17-4.20).

Marcial Fire

Fire Date: May 3-10, 2006

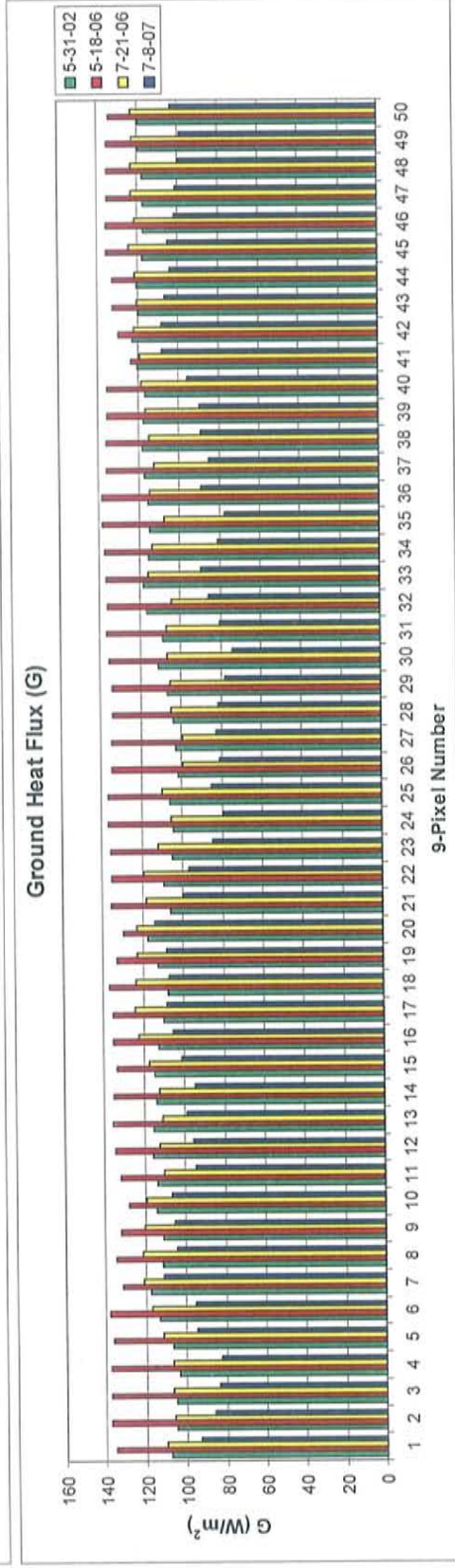
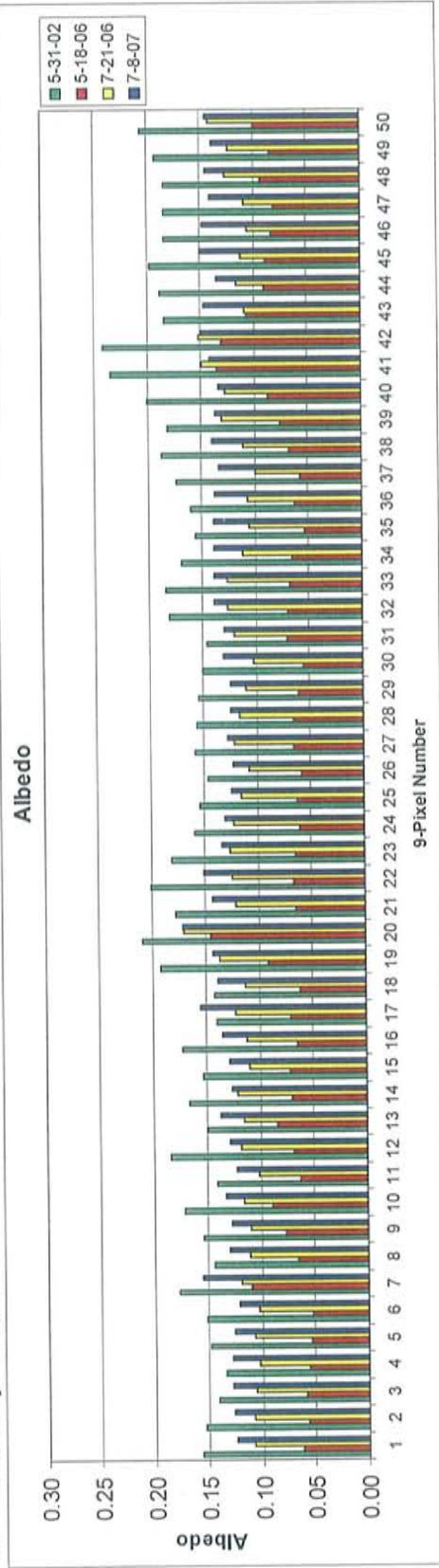


Figure 4.17. Plots of Albedo and Ground heat flux derived from the SEBAL model and the stated image dates. Each 9-Pixel represents a macroplot sampling location from the Summer 2006 Field Campaign.

Marcial Fire
Fire Date: May 3-10, 2006

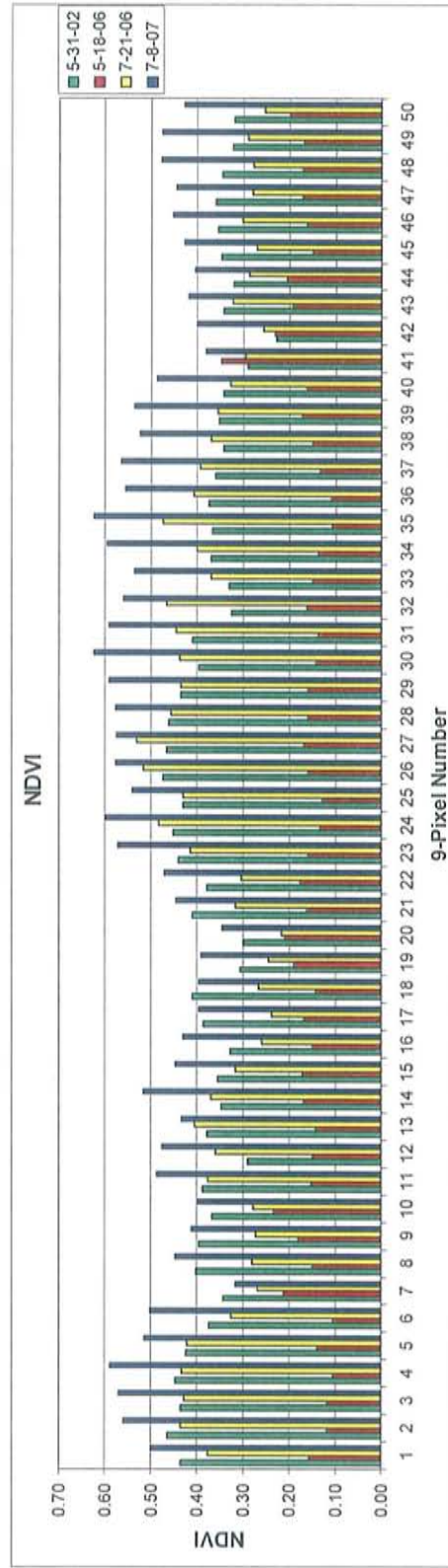
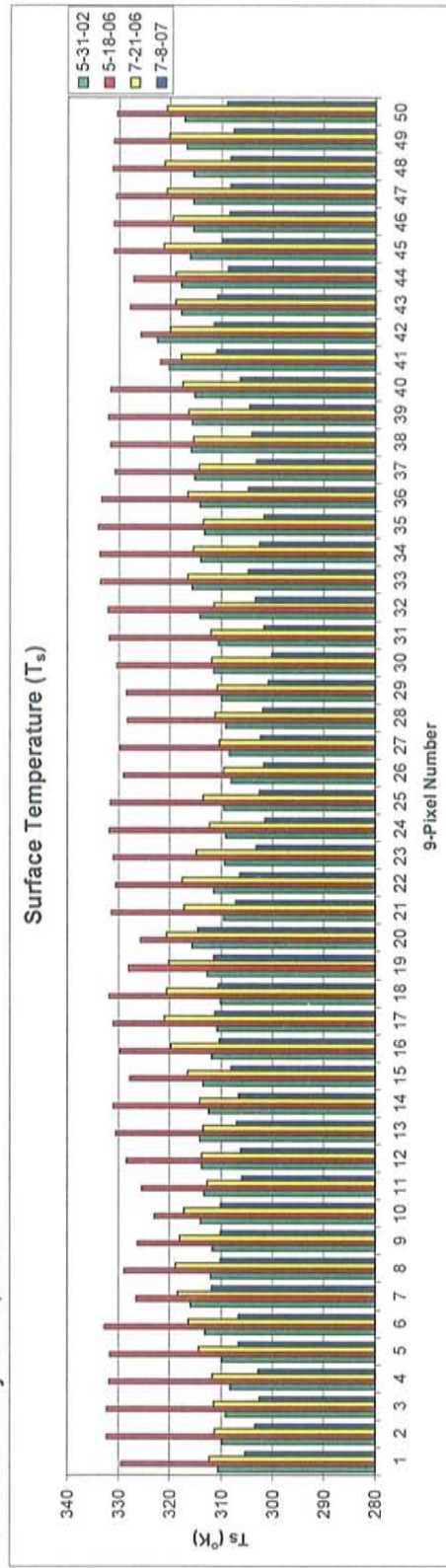


Figure 4.18. Plots of Surface temperature and NDVI derived from the SEBAL model and the stated image dates. Each 9-Pixel represents a macroplot sampling location from the Summer 2006 Field Campaign.

Marcial Fire
Fire Date: May 3-10, 2006

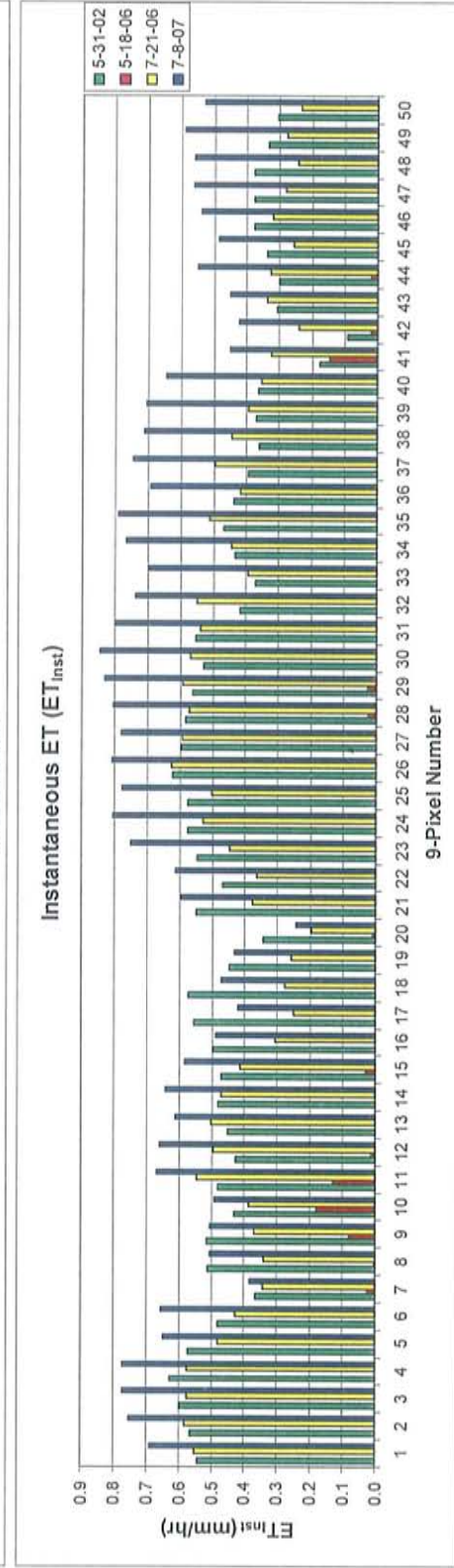
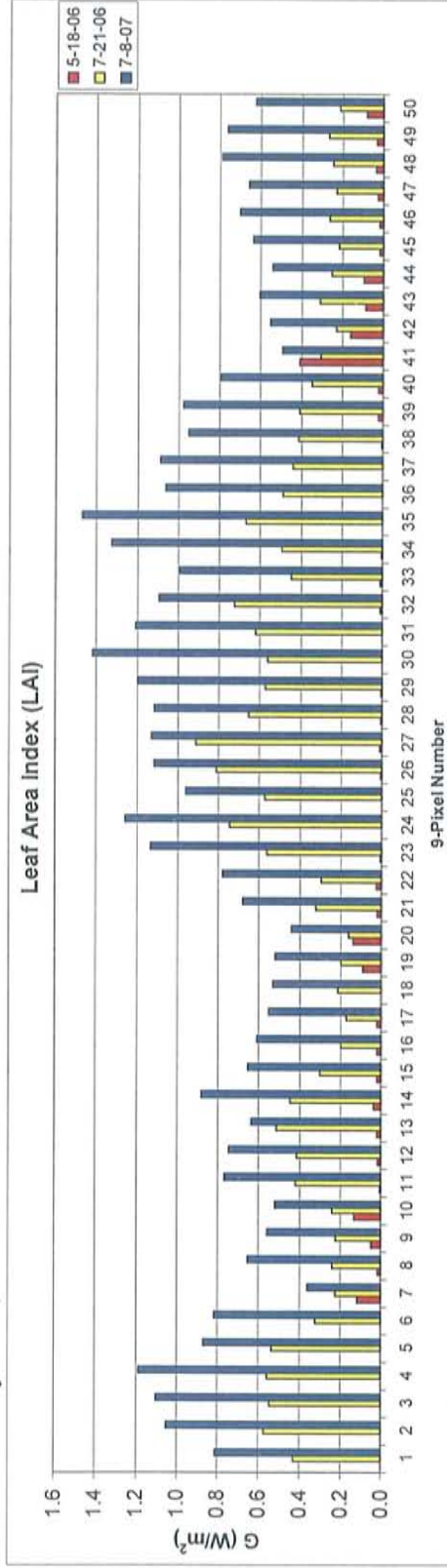


Figure 4.19. Plots of Leaf Area Index and Instantaneous Evapotranspiration derived from the SEBAL model and the stated image dates. Each 9-Pixel represents a macroplot sampling location from the Summer 2006 Field Campaign.

Marcial Fire
 Fire Date: May 3-10, 2006

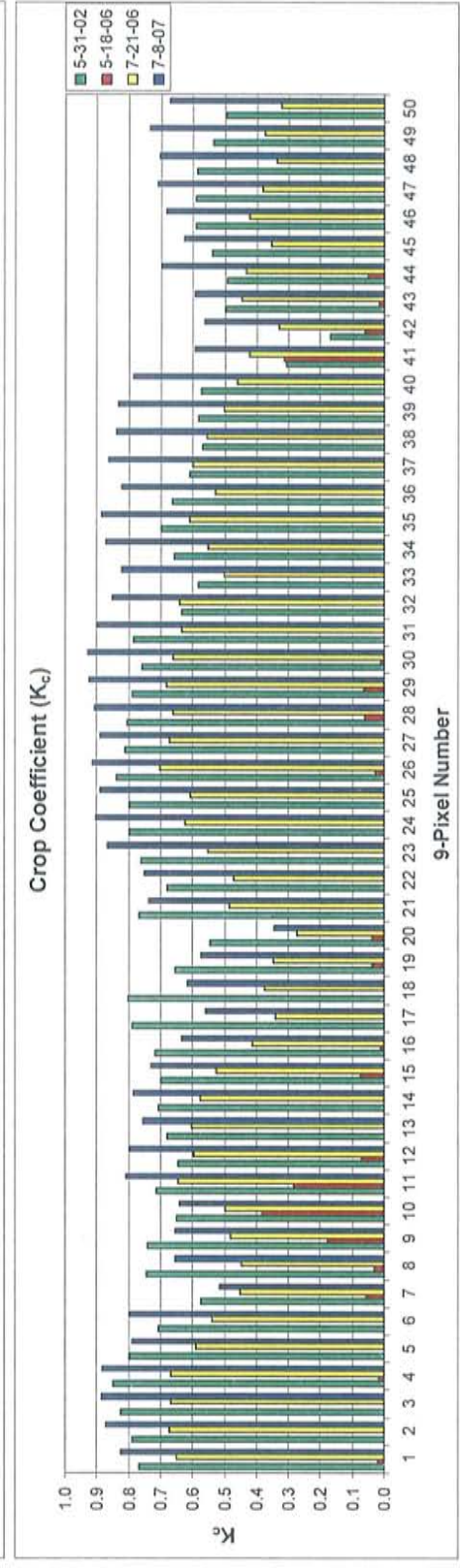
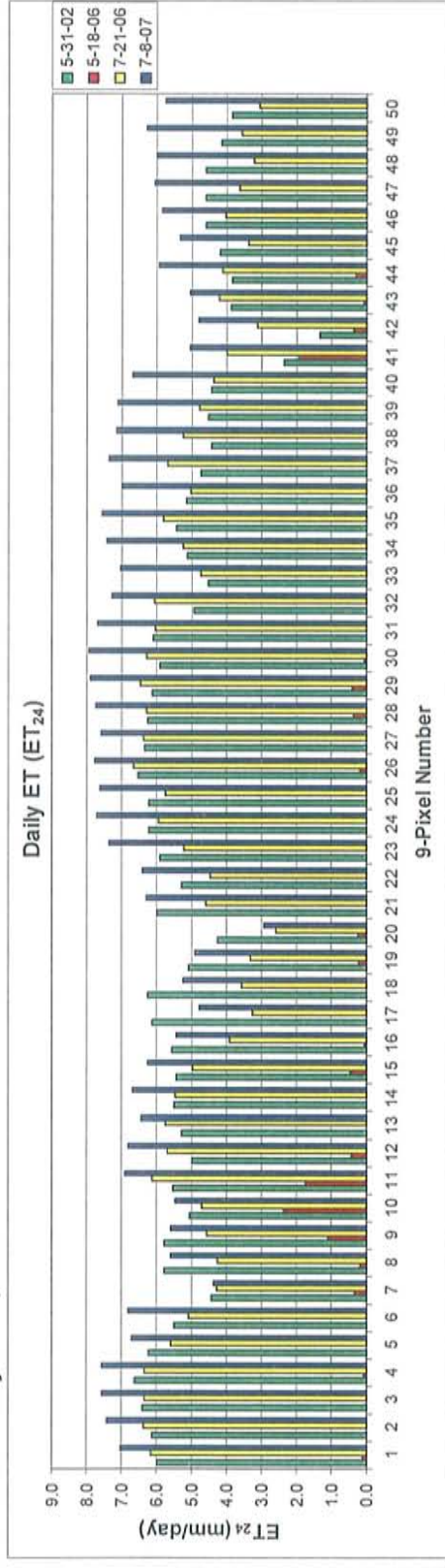


Figure 4.20. Plots of Daily Evapotranspiration and Crop Coefficient derived from the SEBAL model and the stated image dates. Each 9-Pixel represents a macroplot sampling location from the Summer 2006 Field Campaign.

Socorro County Monthly Precipitation

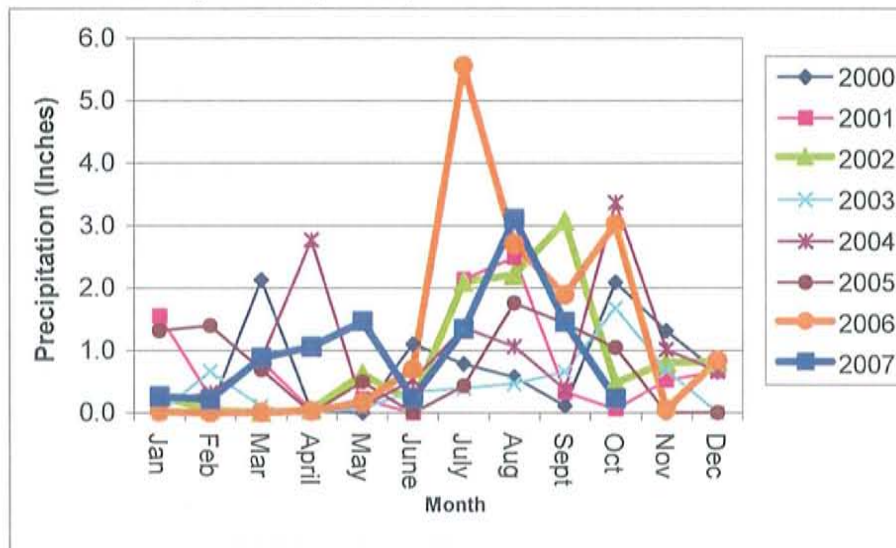


Figure 4.21. Plot of Socorro County monthly precipitation for 2000-2007 (DRI, 2007)

Bosquecito Fire

Figures 4.22-4.25 present albedo, ground heat flux (G), surface temperature (T_s), Normalized Differenced Vegetation Index (NDVI), Leaf Area Index (LAI), instantaneous Evapotranspiration (ET_{inst}) and daily ET (ET_{24}) and Crop Coefficient (K_c) for the 9-Pixel plots that were generated for 4 dates before and after the Bosquecito Fire.

There is a dramatic increase or decrease in the parameters in the first image (10 days) after the fire, June 19, 2006 (in red), for all of the 9-Pixel Plots (Figures 4.22-4.25). One month after the fire, July 21, 2006 (in yellow), the Crop Coefficient (K_c) starts to approach the pre-fire background conditions (Figure 4.25), postulating rapid tamarisk regeneration after only one month after fire, as well as populations of graminoids, forbs, shrubs and cottonwood groves were also encountered during the Summer 2006 Field Campaign, three months after

the fire (Figures C.14 and C.20). The data is an exaggeration of what was perceived during the field campaign three months after the fire: tamarisk coverages were low, from 0 to 0.5 % (Figure C.10), with the majority of the site occupied by bare soil (Figure C.12).

The disparity between the field and SEBAL data may be due to the complex nature of the post-fire vegetation communities within the site. The Bosquecito site has a greater distribution of dominant vegetation types such as cottonwood, forb, graminoids and shrubs (Figure C.14). The site also has less homogeneous tamarisk densities compared to the uniformly dense tamarisk thickets seen at the Mitchell and Marcial locations—the vegetation communities are gathered in clumps and are patchy with diverse soil and vegetation regimes and thus cause more variant profiles. The graph for Crop Coefficient (Figure 4.25) most likely best represents the post-fire regenerative behavior for the tamarisk within the site for the first few months after the fire. The Crop Coefficient standardizes the data for changes in daily weather conditions and is the best representative of evapotranspiration as a proxy for tamarisk regeneration.

Bosquecito Fire
Fire Date: June 6-9, 2006

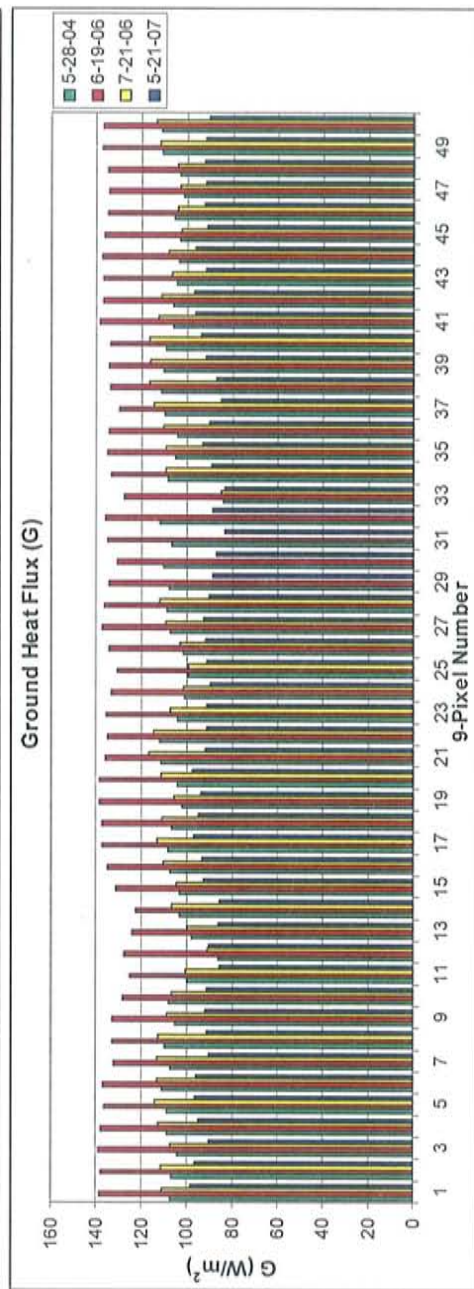
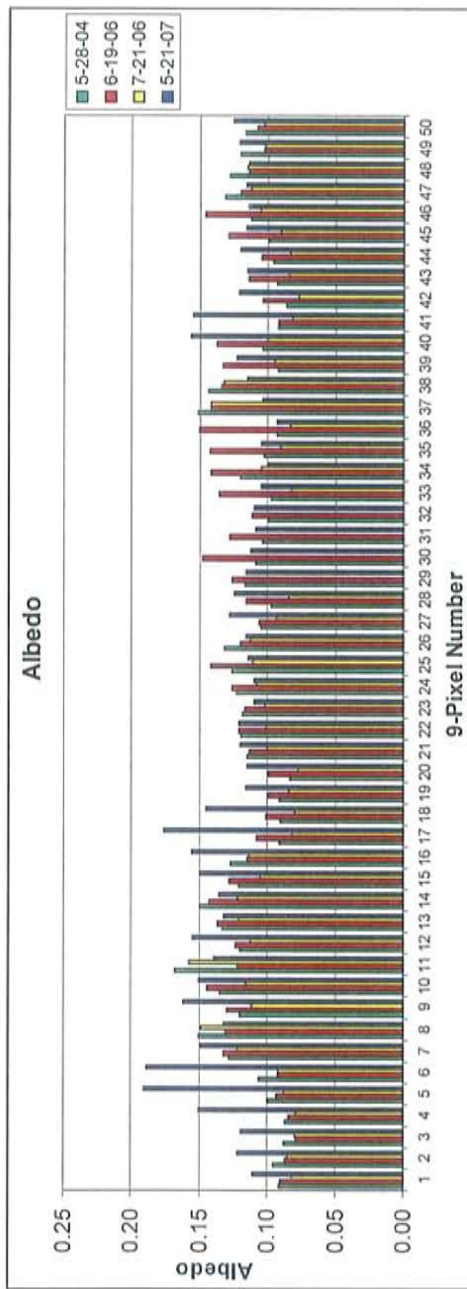


Figure 4.22. Plots of Albedo and Ground heat flux derived from the SEBAL model and the stated image dates. Each 9-Pixel represents a macroplot sampling location from the Summer 2006 Field Campaign.

Bosquecito Fire

Fire Date: June 6-9, 2006

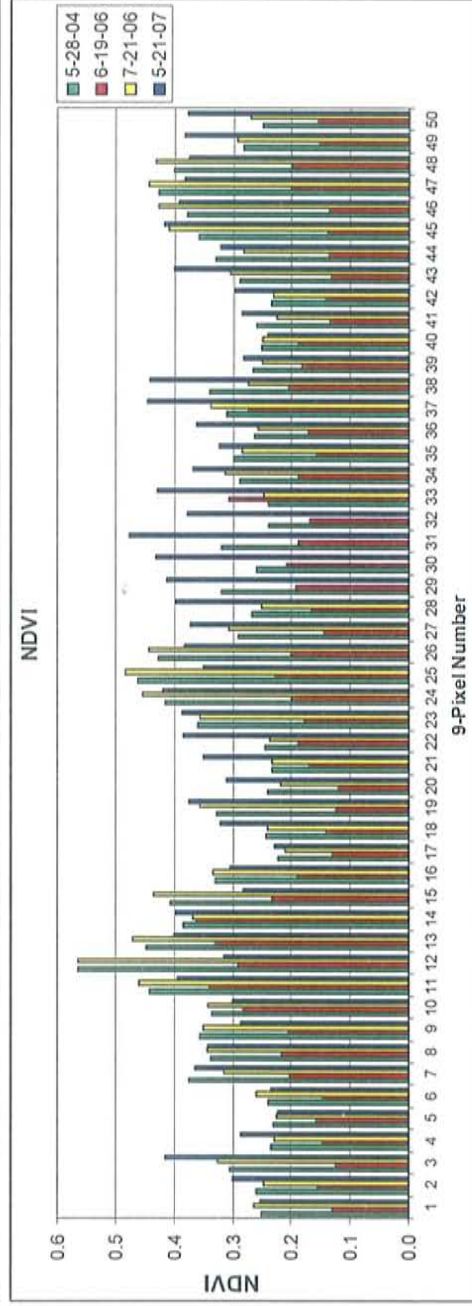
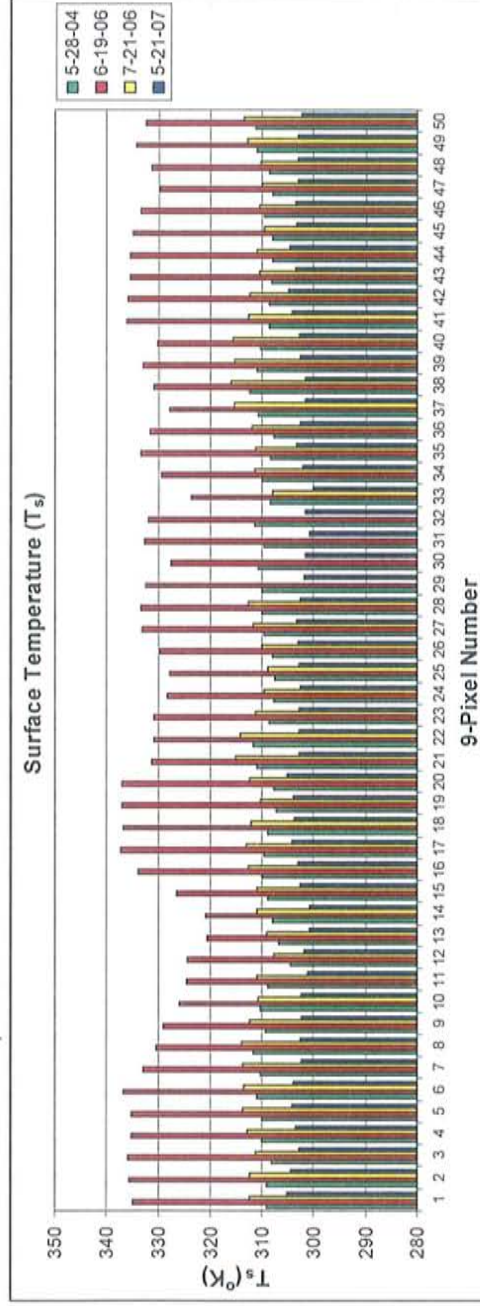


Figure 4.23. Plots of Surface temperature and NDVI derived from the SEBAL model and the stated image dates. Each 9-Pixel represents a macroplot sampling location from the Summer 2006 Field Campaign.

Bosquecito Fire
Fire Date: June 6-9, 2006

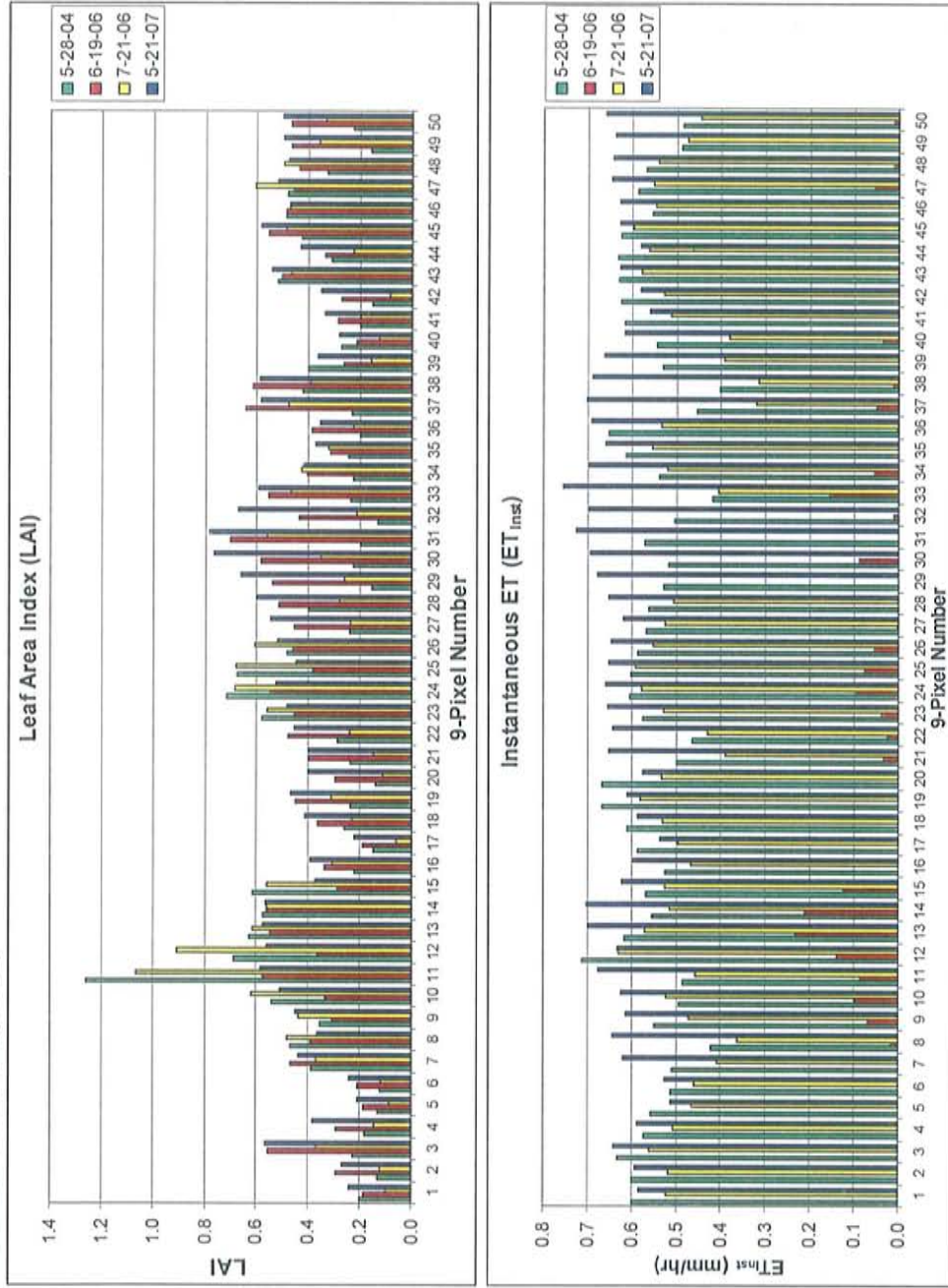


Figure 4.24. Plots of Leaf Area Index and Instantaneous ET derived from the SEBAL model and the stated image dates. Each 9-Pixel represents a macroplot sampling location from the Summer 2006 Field Campaign.

Bosquecito Fire
Fire Date: June 6-9, 2006

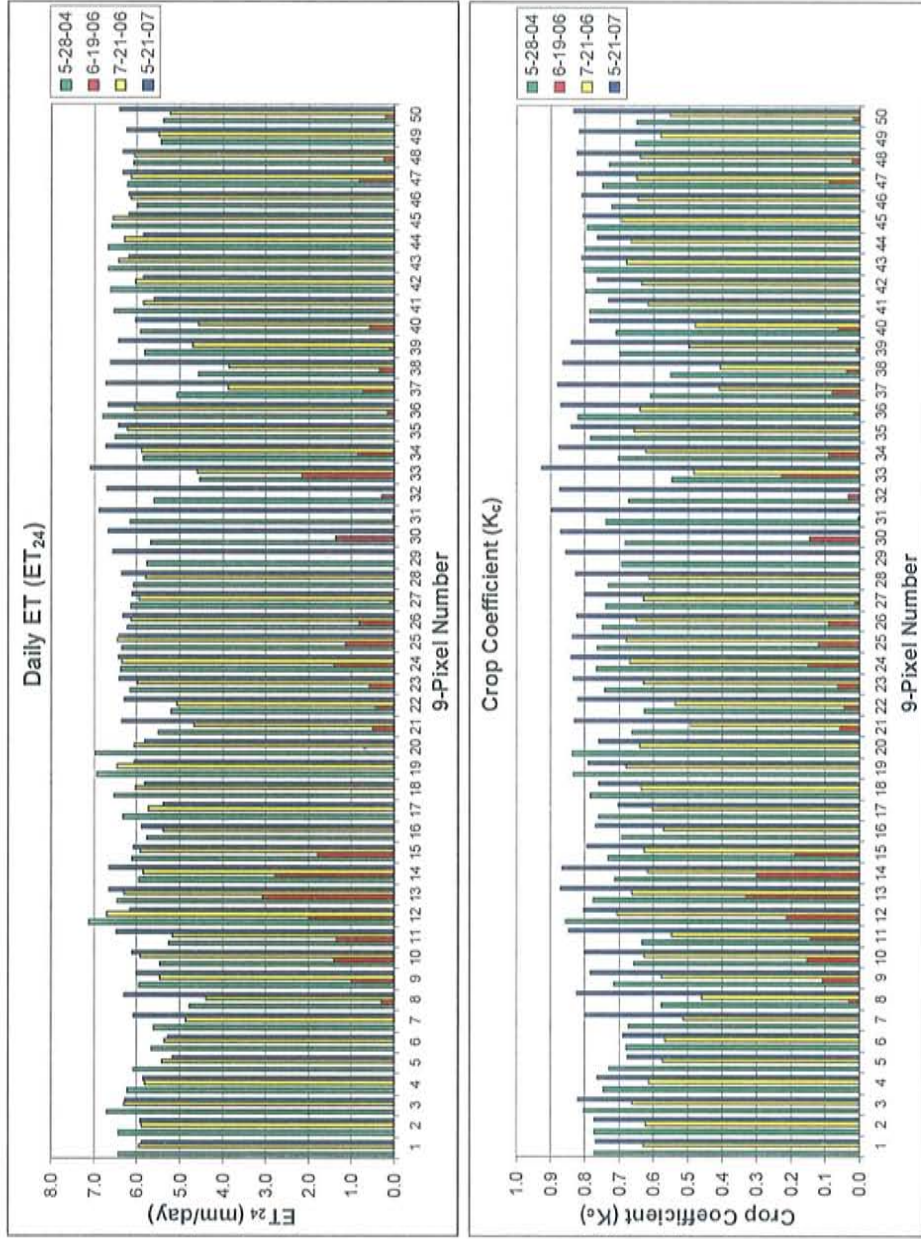


Figure 4.25. Plots of Daily Evapotranspiration and the Crop Coefficient derived from the SEBAL model and the stated image dates. Each 9-Pixel represents a macroplot sampling location from the Summer 2006 Field Campaign.

4.3 Crop Coefficient Over Time

Mitchell Fire

The Crop Coefficient (K_c) negates out the effects of daily weather differences and provides a more concrete estimate of ET for a crop and is a strong proxy for regeneration. Three control sites in close proximity to the Mitchell and Bosquecito Fires, containing similar soil and vegetation classes but unaffected by fire, were chosen for comparison to the data produced from the 9-Pixel Plots for all the SEBAL data/image dates on record (Figure 4.26). Crop Coefficient data was evaluated at three control sites, Control Sites 1, 2 and 3. Due to the consistency and strength of the data at Control Site 2, that site was chosen as the representative Control Site for comparison to Crop Coefficient data from the three fire sites.

From Figure 4.26, the 9-Pixel Plot Mitchell Fire data closely matches the Control Site data up until the data from the first image after the fire dated May 22, 2006. The 9-Pixel Plot data from the first image post-fire displays two 9-Pixel Plots with a Crop Coefficient of zero, meaning that there is no evapotranspiration occurring at those sites and the sites have been the most dramatically impacted by the fire. All of the 9-Pixel Plots are below the normal baseline K_c range of 0.6 to 1.2, but many 9-Pixel plots approach the K_c value of 0.6 meaning that regeneration is already beginning to occur 1 month after the fire. The 9-Pixels approach the ET behavior of the Control Site and become in synch on June 19, 2006, 14 months after the fire. Two years after the fire, May 21, 2007, the 9-

Pixel Plot K_c data has surpassed the Control Site data and K_c data for 1 year before the fire, May 12, 2004, postulating the notion that the tamarisk has regrown at a greater thickness and density that was present before the fire.

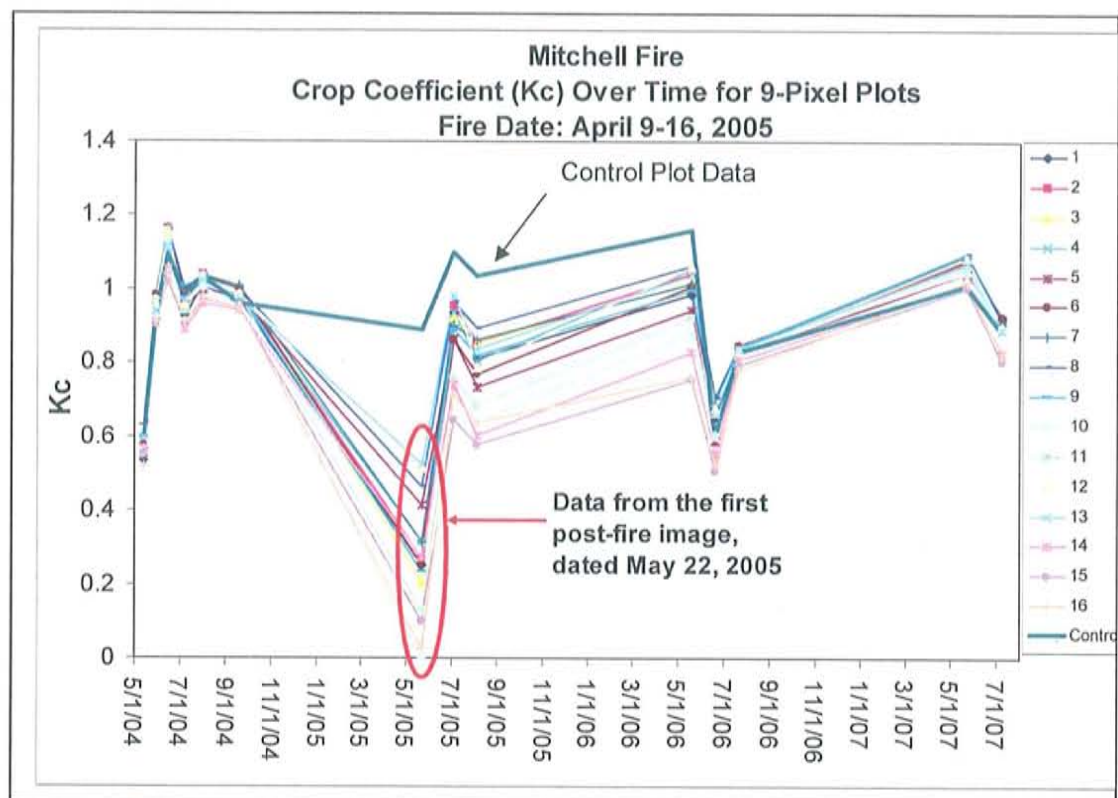


Figure 4.26. K_c over time for the 9-Pixel Plots, including Control Site data.

Marcial Fire

Figure 4.27 displays post-fire Crop Coefficient data for the Control Site and 9-Pixels within the Marcial site. Due to limited Landsat data for the Marcial Fire, the plot starts two years later than the plots for the Mitchell and Bosquecito Fires. The 9-Pixel data for the first image after fire, 8 days later, displays plots with Crop Coefficients greater than zero; such data can be related to elevated

ground water levels in May of 2006 (Figure 4.28). With an elevated groundwater table, water may have risen to the ground surface due to capillary forces and detected by the Landsat satellite. Crop Coefficient data for the 9-Pixel Plots on June 19, 2006 is zero and does not take into account evapotranspiration occurring from the small tamarisk resprouts that are evident in the photos taken by the SSWCD (Figure 3.9). The 9-Pixel Plot data for July 21, 2006, two months after the fire, displays rapid Crop Coefficient recovery towards the Control Plot data and is indicative of rapid tamarisk regrowth. One year after the fire, July 8, 2007, the tamarisk Crop Coefficient reaches levels similar to the Control Plot. An interesting facet of the plot is that the Crop Coefficient rebound has similar behavior for all the 50 9-Pixel Plots through time--the lines parallel each other and points are consistently high or low. This suggests a consistent tamarisk regenerative behavior for the site as a whole, reaching beyond the behavior of the individual 9-Pixel Plots.

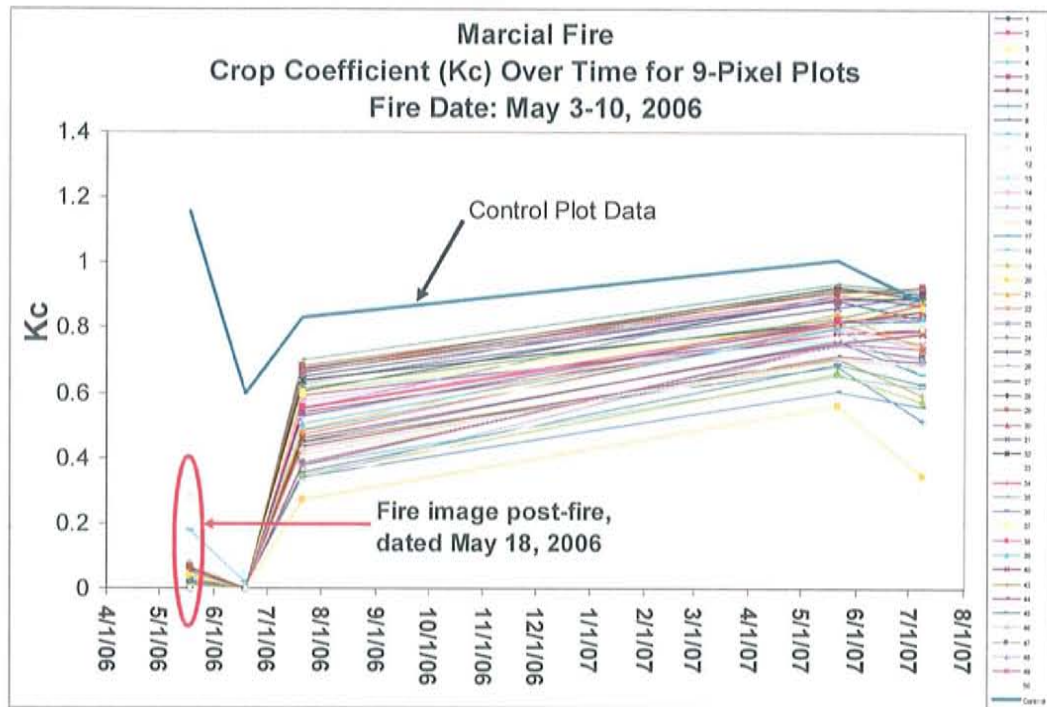


Figure 4.27. Kc over time for the 9-Pixel Plots, including Control Site data.

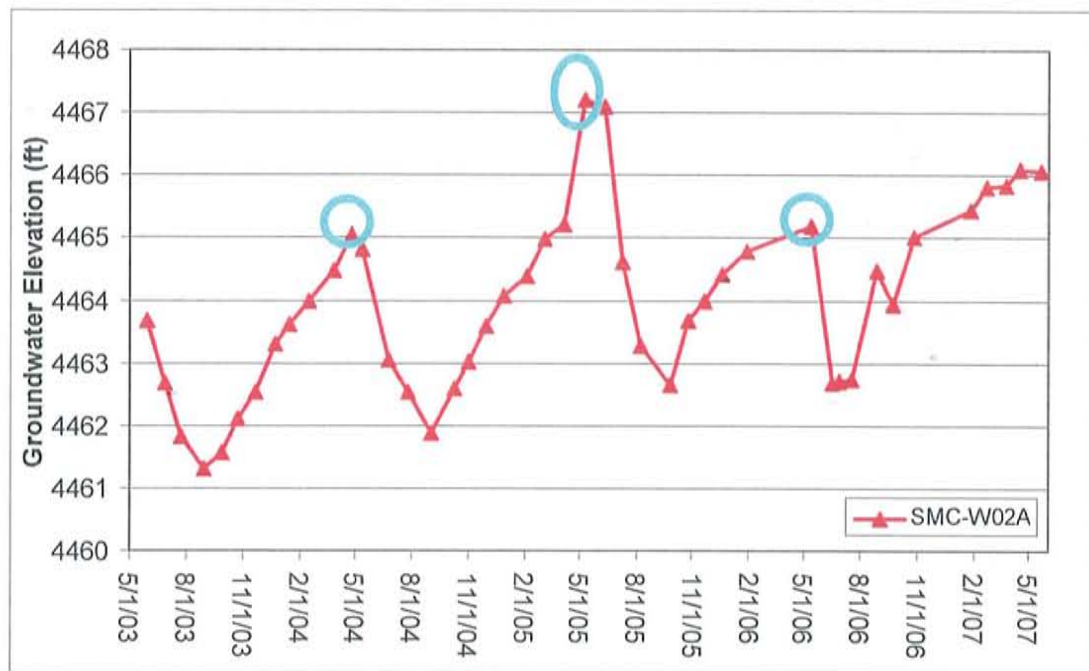


Figure 4.28. Representative groundwater well in proximity to the Marcial Fire. Total well depth is 19.5 feet. The blue circles represent elevated groundwater table levels in May of each year (ISC, 2007).

Bosquecito Fire

Figure 4.29 displays Crop Coefficient behavior for the Bosquecito site to be continually less than, and similar to, the data for the Control Plot up until the first image after fire. The first image after the fire, June 19, 2006, displays a decreased Crop Coefficient for all the 9-Pixel Plots. Although the tamarisk and vegetation appears to rebound post-fire, the Bosquecito Site experienced the most intense burn and the majority of the tamarisk at the site was eradicated, as evident during the Summer 2006 Field Campaign while sampling the site in September of 2006, three months after the fire. The rebound in the Crop Coefficient, and hence evapotranspiration, may be due to the Landsat sensor detecting soil evaporation at the exposed bare surface rather than plant transpiration with regrowth after fire.

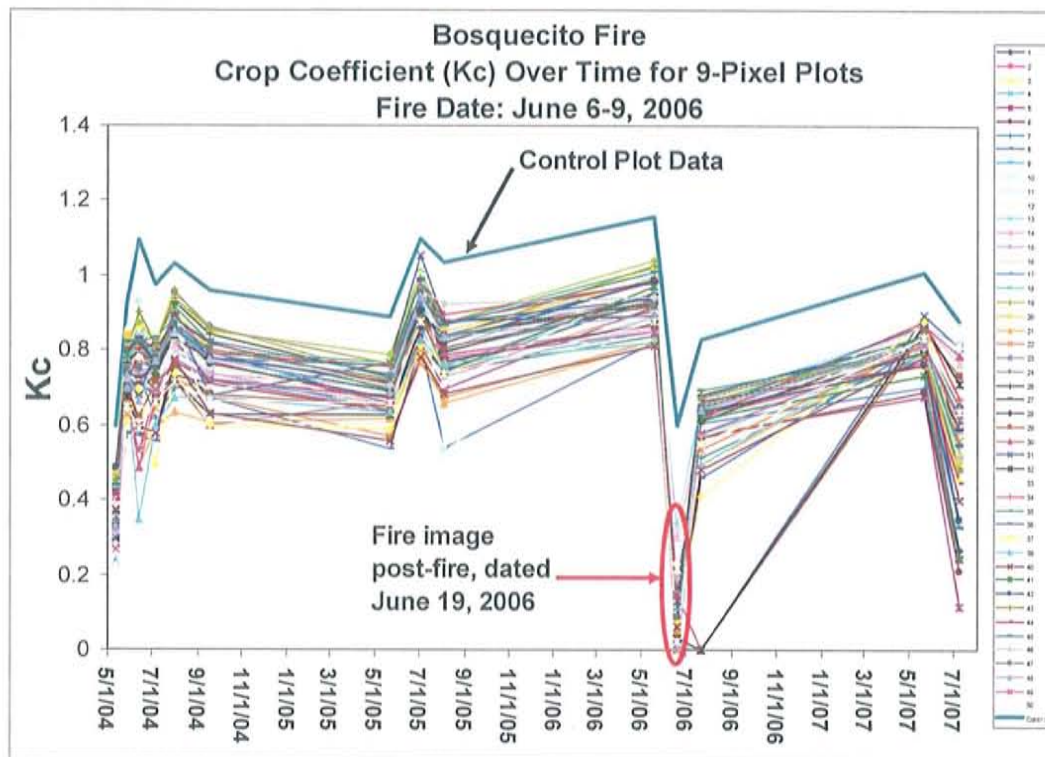


Figure 4.29. Kc over time for the 9-Pixel Plots, including Control Site data.

4.4 MODIS NDVI 16-Day Composite Plots

The original MODIS NDVI images (dimensions 1200 km x 1200 km) were subset to the Bosquecito, Mitchell and Marcial Fire sites and the Zonal Statistics tool in ArcGIS extracted the mean, minimum, maximum and standard deviation of the NDVI amongst the 250 m x 250 m pixels comprised in each fire site from the time span of 2003 to August of 2007. Once the statistics were acquired, time series plots of the mean and standard deviation of NDVI over time were created for each of the three fire sites to monitor vegetation regeneration after fire.

Multitemporal extracts of 16-day MODIS NDVI composites were made over 3 fire sites to assess MODIS capability to depict phenology and seasonal variations in vegetation activity after fire (Figures 4.30-4.33). The MODIS VI

composited products include four MODIS band reflectances (bands 1, 2, 3, and 6) and the sun and view angle geometry, corresponding to the selected pixel over the composite period. Missing composite periods, due to MODIS instrument and production related difficulties, are not displayed. The seasonality of the slender branched, scale-like leaves of the deciduous shrubs is depicted by the MODIS NDVIs as shown in Figures 4.30-4.33. The NDVI profiles show the growing season commencing in April and maximum green foliage over the months from June through September. There appeared to be less erratic variations in the NDVI data in the first half of the growing season compared to the second half. There is much less variation in the NDVI data during the dry down phase starting in October. The NDVI responds similarly to broad leaf and needle leaf forests with a gradual dry-down phase (Huete et al., 2002).

The NDVI indices depicted the important phenology events, such as onset of greenness (early May), peak greenness (August), and the dry down period (early October) (Figures 4.30-4.33). The dynamic range in NDVI for all the fire sites varied from 0.18 to 0.64 (Figure 4.33). The Marcial site produced the highest NDVI values, followed by the Mitchell site and the Bosquecito site, respectively (Figure 4.33). Maximum contrast among all the sites occurred during the summer growing season when all of the sites became separable, as based on their NDVI values. The Marcial site displayed the highest summer NDVI values because it is the site with the densest vegetation canopy with the least amount of soil visible from space. The highest NDVI values during the

summer were an expression of vegetation response during the summertime Southwestern North American Monsoon.

Soils generally exhibit a near-infrared spectral reflectance somewhat larger than the red, and thus tend to also generate rather small positive NDVI values (0.1 to 0.2) (Huete et. al, 2002), contributing to an overall decreased NDVI value for a site with a large soil regime. The Mitchell and Bosquecito profiles exhibit similar behavior since they are located in close proximity to each other and are within the same ecological environment and soils regime (Figure 4.33).

The NDVI seasonal curves appeared the most symmetrical at the Marcial site, but exhibit the closest down-sloping decrease in NDVI during the dry season of October to April (Figure 4.33). Vegetation assessment through MODIS data for the burned areas of the Mitchell, Marcial and Bosquecito fire sites showed both the important effect of seasonal variation and the strong impact of the fires on vegetation dynamics. Immediately following the fires there were signs of vegetation recovery (Figures 4.30-4.33). The Bosquecito Fire site displays a drastic drop in Average NDVI during the time of fire, followed by recovery within two months (Figure 4.32). This is most likely due to the timing of the fire, occurring in the middle of the growing season (June 6-9, 2006), during the time frame of rapid growth and rapidly increasing biomass. The Mitchell and Marcial Fires occurred in the beginning of the growing season, in April and May, respectively, during a period of slowly increasing biomass, and thus do not show evidence of much impact from the fire due to the lack of substantial green biomass. In addition, the regeneration recovery occurs in the timeframe of

weeks rather than months. The annual peak in NDVI around mid-August was reduced in the Marcial peak in the year following the fire.

Mitchell Fire

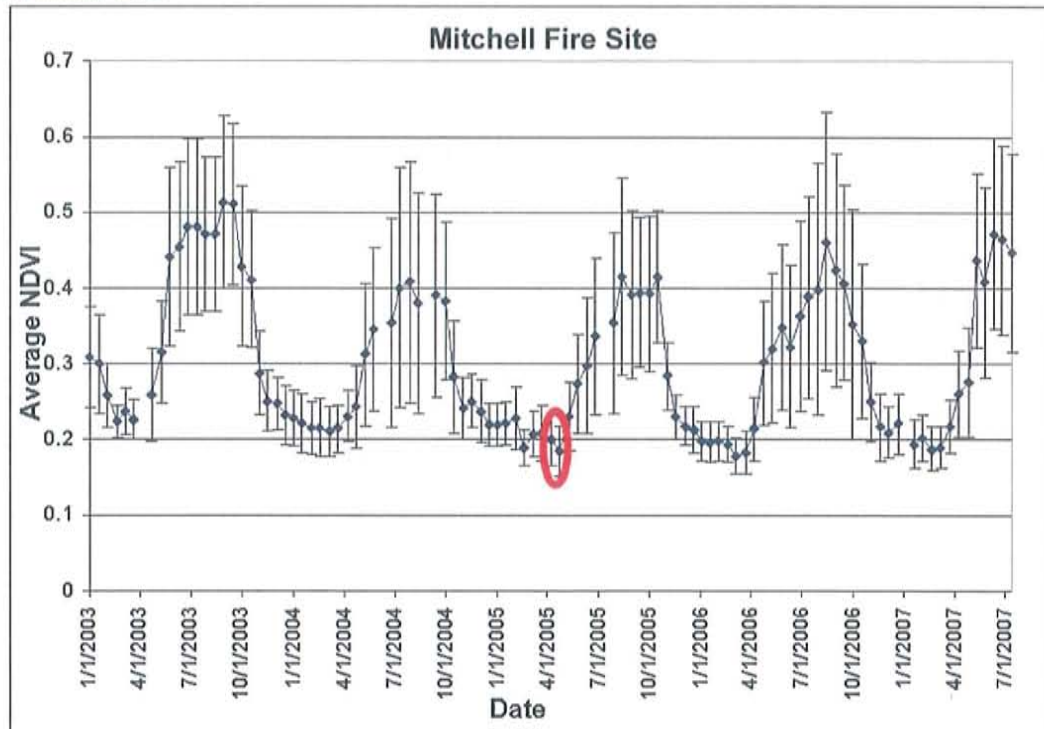


Figure 4.30. MODIS-derived Average NDVI seasonal profile with standard deviation bars for the Mitchell Fire Site. The red circle indicates the composite dates that were immediately impacted by the fire.

Marcial Fire

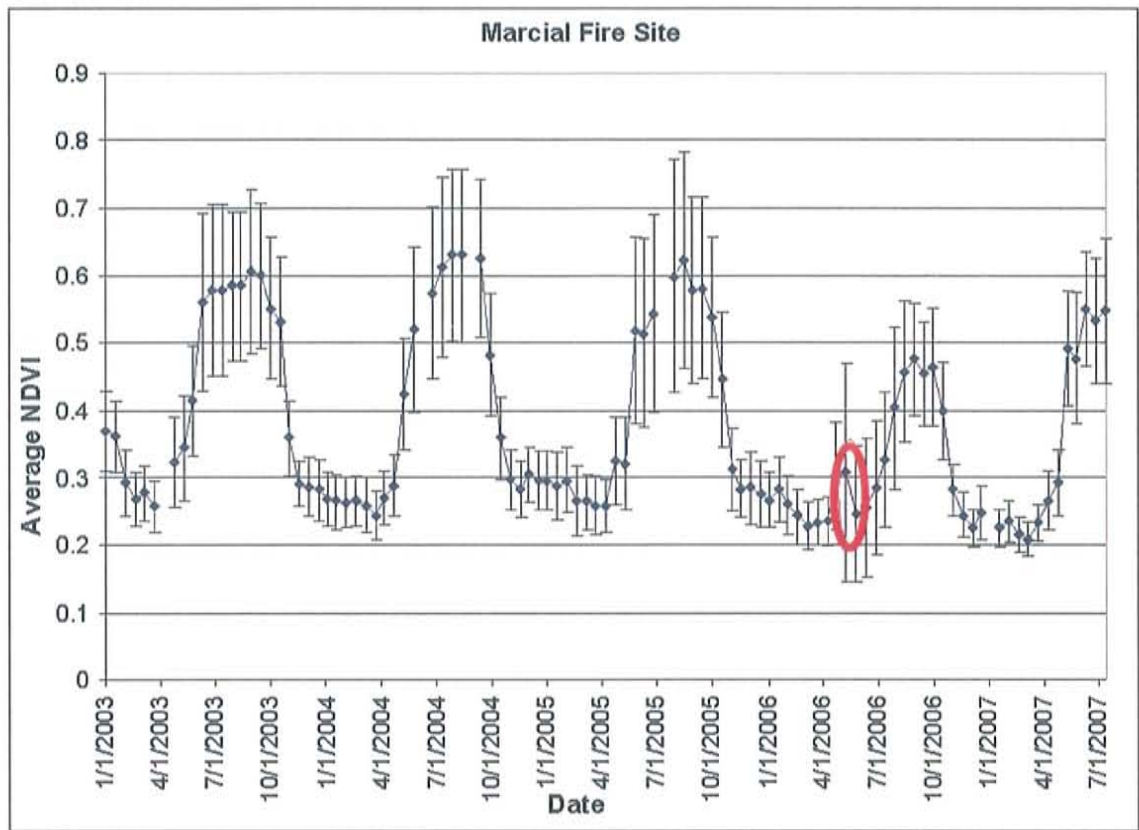


Figure 4.31. MODIS-derived Average NDVI seasonal profile with standard deviation bars for the Marcial Fire Site. The red circle indicates the composite dates that were immediately impacted by the fire.

Bosquecito Fire

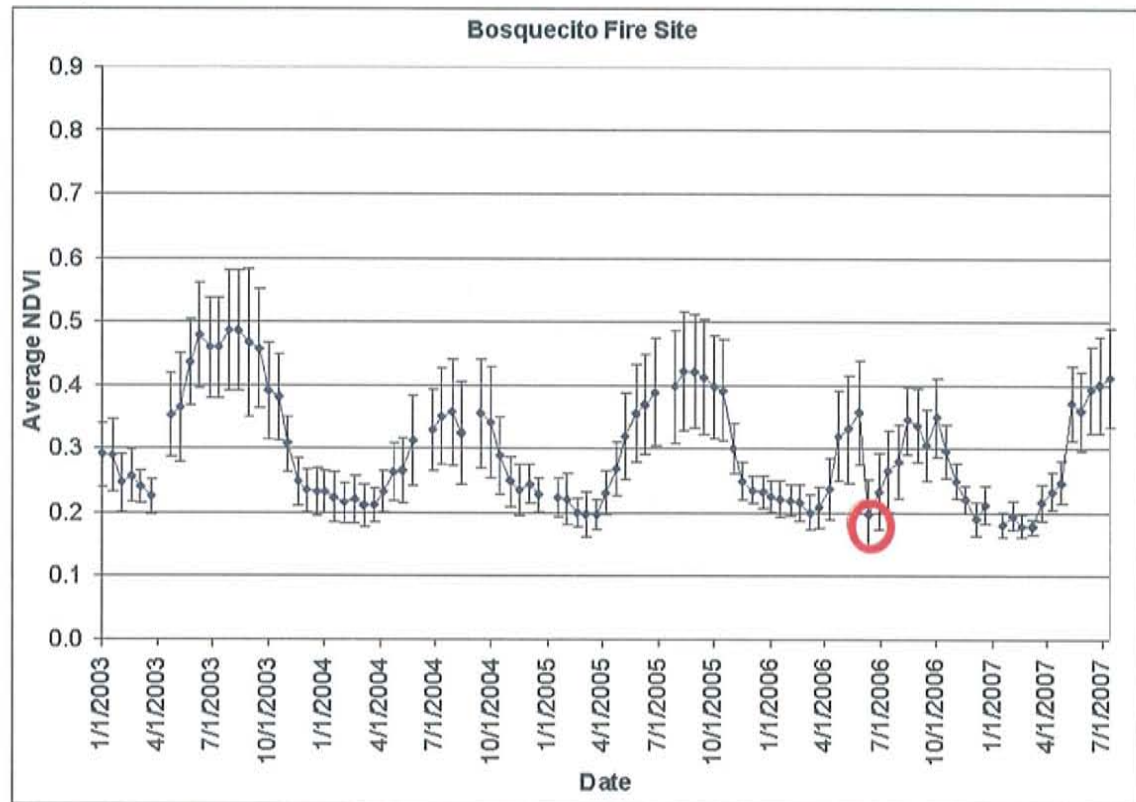


Figure 4.32. MODIS-derived Average NDVI seasonal profile for the Bosquecito Fire Site. The red circle indicates the composite dates that were immediately impacted by the fire.

All 3 Fire Sites.

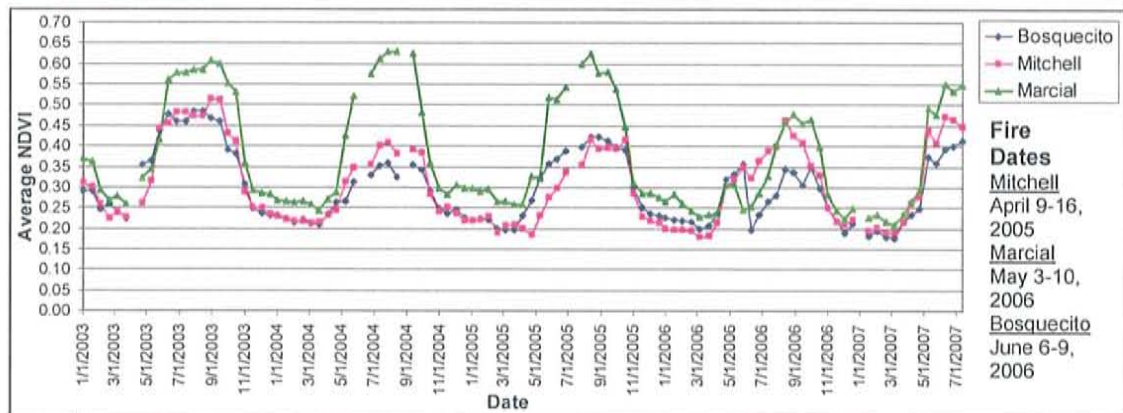


Figure 4.33. MODIS-derived Average NDVI seasonal profiles for the 3 fire sites.

4.5 Field Observations

4.5.1 Summer 2006 Field Sampling Results

The field data with location and ocular measurement data can be found in tabular form in Appendix B. Maps from the Summer 2006 Field Campaign were created to visually portray ocular measurements of various vegetation, soil and fire parameters data and can be found in Appendix C. The sampling followed the FIREMON protocol and was performed under the guidance of Mr. Jerry Hess. The sampling locations correspond to locations of the 9-Pixel Plots. The 9-Pixel Plot numbers have been labeled on the maps in the figures below in order to correlate with the 9-Pixel Bar Graphs presented in Section 4.2.

Field Sampling Summary

Tamarisk readily re-sprouted from its root crown after the three fires. During the Summer 2006 Field Campaign, average stand heights were observed to be 1.1 meters three months after the Bosquecito Fire, 2.1 meters 3 months after the Marcial Fire, and 3.7 meters 1 year and 4 months after the Mitchell Fire. Average Sapling Cover was observed to be 87% during the Mitchell field campaign, 52% during the Marcial field campaign and 4% during the Bosquecito field campaign. Average Bare Soil Cover was observed to be 10% during the Mitchell field campaign, 44% during the Marcial field campaign and 79% during the Bosquecito field campaign. Average tamarisk stage was observed to be senescent at the Mitchell site, growth/biomass production stage at the Marcial site and growth/biomass production at the Bosquecito Site. The fire intensity at

the Bosquecito Fire was much greater than at the other two fires, which produced an immediate effect on aerial vegetation; this was evident as observed total plant death within the majority of the site and partial destruction of the cottonwood communities.

Field Sampling Maps for each Site

Mitchell Fire

Site sampling occurred 1 year and 4 months after the Mitchell Fire along line transects. Maps that pictorially depict the sampling data are provided in Appendix C. The dominant species along Transect 2, 3 and 4 was tamarisk. Transect 1 will not be considered because it is along the edge of the road and thus experiences edge effects and is not occupied by representative tamarisk populations. There were high tamarisk densities, from 41-100% of each sampling macroplot, for the 3 transects. The map of tamarisk cover can be found in Figure 4.34 as well as in Appendix C. Half of the tamarisk along the three transects were approximately 3 meters in height and the other half were greater than 3 meters and up to 8 meters in height. The map of tamarisk height can be found in Figure 4.35 as well as in Appendix C. For bare soil in each macroplot, 20% of the plots had 0-3% bare soil, 60% of the plots had 4-10% and 20% of the plots had 11-20% bare soil. There were low populations of Comboveg (Combination of shrubs, forbs and graminoids (%)), around 0-3%. The tamarisk vegetation within all the plots was "4" or senescent. The top soil (0-0.1 meters

below ground surface) was clay, underlain by sand or silt. The fire was accidental, man-made, and the overall fire intensity was medium.

Comparison to SEBAL Fire Maps

Field sampling at the Mitchell Fire site occurred 1 year and 4 months after the fire, from October 11-25, 2006. The SEBAL Mitchell Fire maps dated May 18, 2006 (one year after the fire) have the closest date to the field sampling campaign (Figures 4.1-4.4). Instantaneous and daily ET maps dated May 18, 2006 display significant regeneration along the southern portion of the site where the Field Sampling Campaign took place (Figures 4.3-4.4). The NDVI plots (Figure 4.2) also display an increase in NDVI or "greenness" in the southern region, 1 year after the fire. Tamarisk was the dominant species type during the Summer 2006 Field Campaign (Figure C.1) and had grown to significant stand heights; even the shortest tamarisk macroplot had a significant height of 2.4 meters (Figure C.3).

Mitchell Fire Macroplot Sampling Tamarisk Cover (%) October 2006

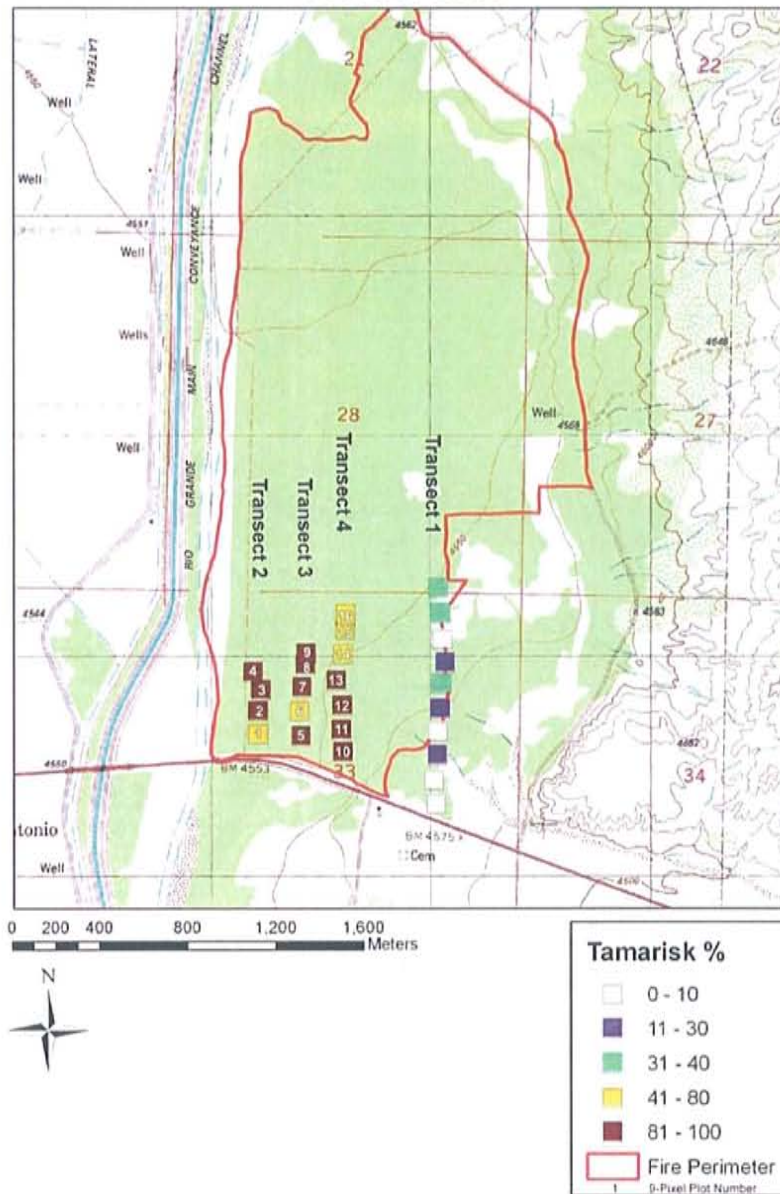


Figure 4.34. Ocular measurements of tamarisk cover from the Summer 2006 Field Campaign. Additional figures can be found in Appendix C.

Mitchell Fire Macroplot Sampling Dominant Vegetation Stand Height (meters) October 2006

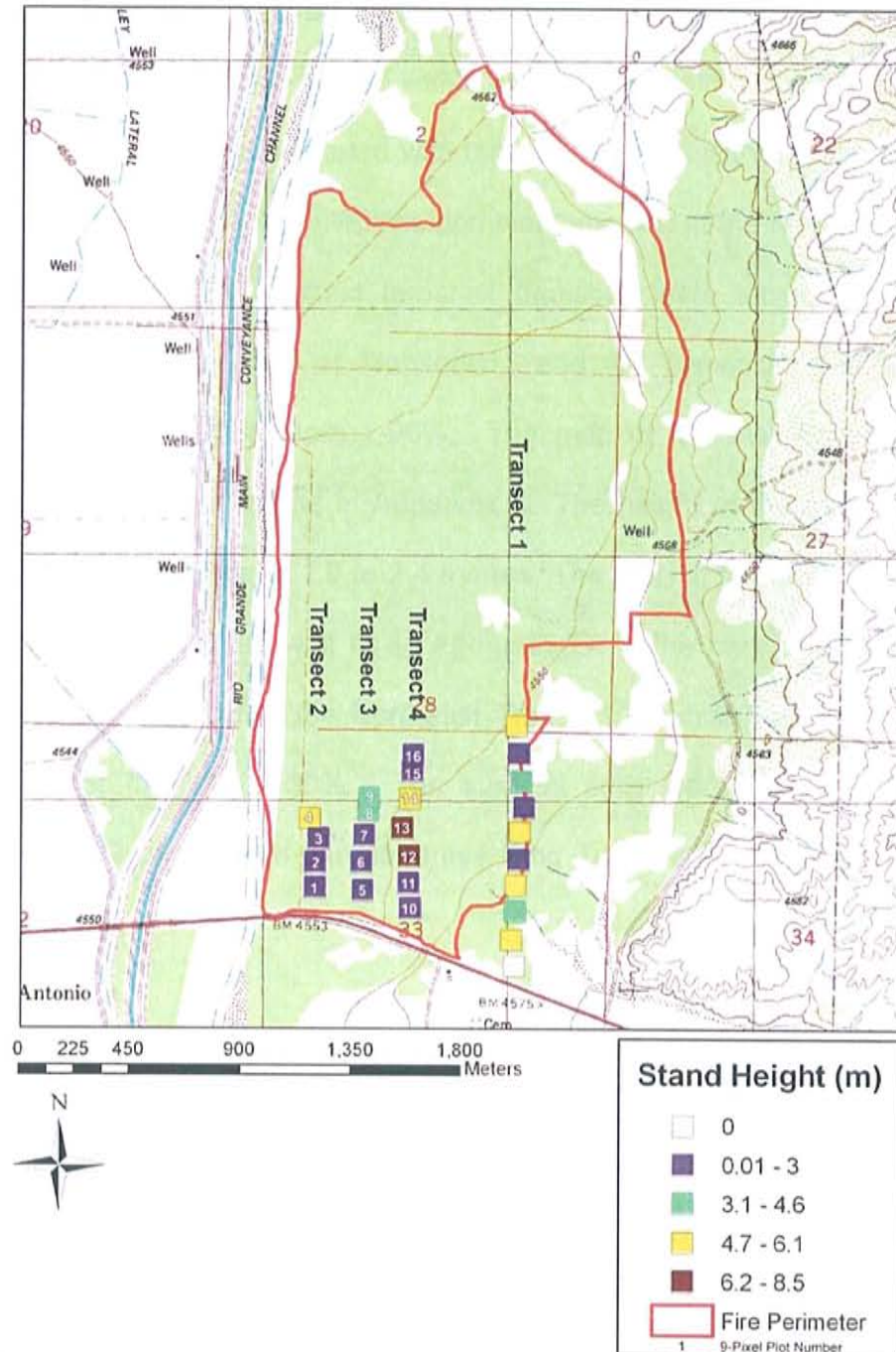


Figure 4.35. Ocular measurements of dominant vegetation (tamarisk) stand height from the Summer 2006 Field Campaign. Additional figures can be found in Appendix C.

Marcial Fire

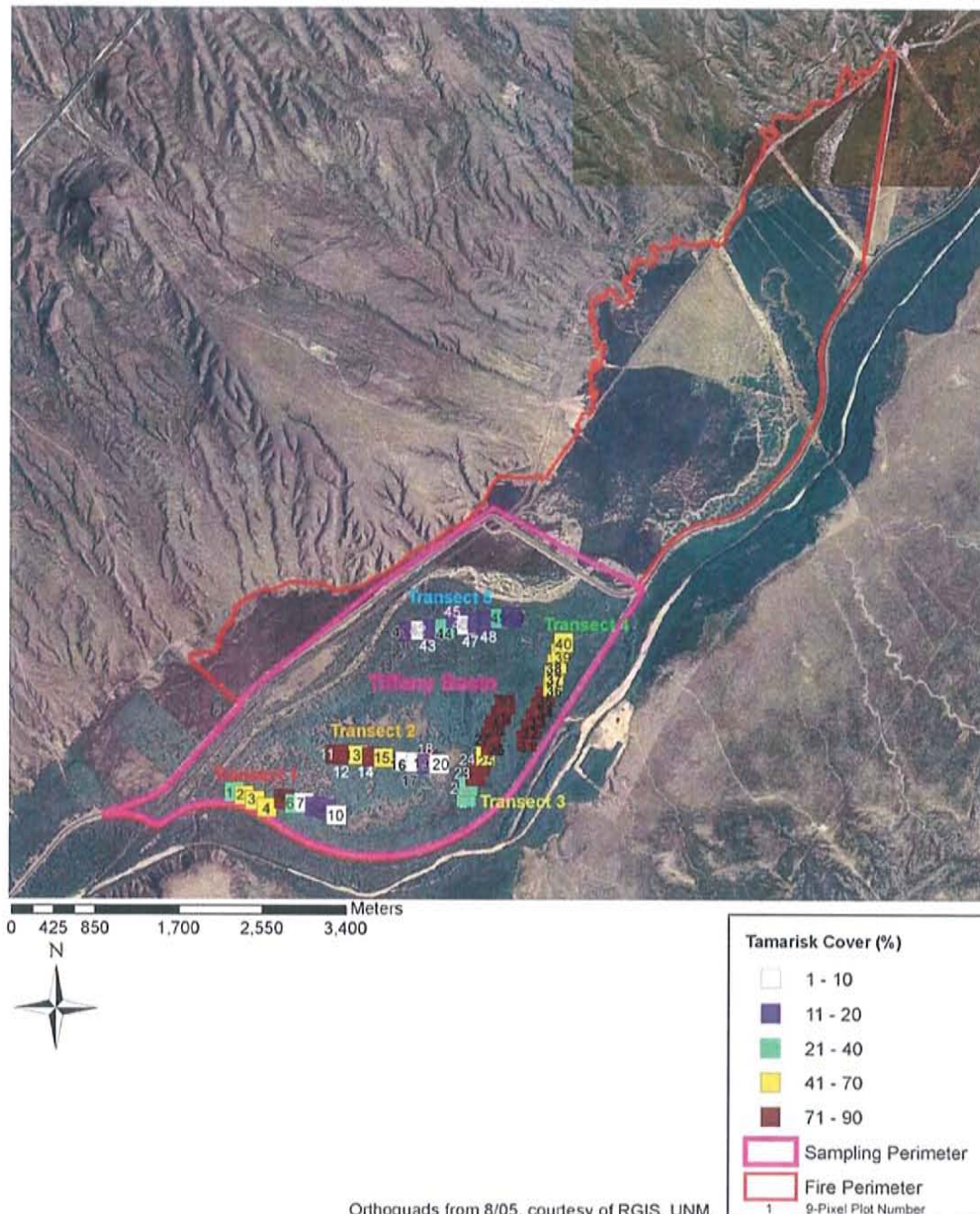
Site sampling occurred 3 months after the Marcial Fire along line transects. Maps that pictorially depict the sampling data are provided in Appendix C. Site sampling occurred within the Tiffany Basin of the Marical Fire. The area was consistently blanketed with tamarisk thickets with a low proportion of cottonwood groves with the site. The dominant species at the Marcial Fire site was also tamarisk. The highest tamarisk densities were located along the Eastern boundary at the fire, at Transects 3 and 4. Transects 1 and 2 had variable tamarisk densities, from 1-90%. The map of tamarisk cover can be found in Figure 4.36 as well as in Appendix C. The height of the tamarisk was predominantly in the range of 1.3 to 2.4 meters. The map of tamarisk height can be found in Figure 4.37 as well as in Appendix C. The bare soil cover was extremely variable except at the Northeast Transect 4, which had a consistent bare soil cover from 11 - 30%. The surficial soils were mainly silt along Transects 1, 2, 3 and 5, with fine sand overlying Transect 4. The fire intensity was also medium.

Comparison to SEBAL Fire Maps

Field sampling at the Marcial Fire site occurred three months after the fire, from August 7-23, 2006. The Landsat image/SEBAL data closest to that of the field sampling campaign date is from July 21, 2006, corresponding to Figures 4.5-4.8. From field sampling data, there was fairly thick and homogenous resprouting occurring, with some areas denser than others. The average

resprout height was 2.1 meters. Figure 4.5-4.8 display SEBAL data for July 21, 2006, the date closest to the field sampling campaign. Two months after the fire, July 21, 2006, albedo, NDVI, daily and instantaneous ET have all started to recover, but do not match pre-fire conditions (Figures 4.5-4.8), which matches the homogeneous tamarisk that was approaching heights of pre-fire conditions (Figure C.11). The findings from SEBAL data are concurrent with photographs taken at the Marcial Fire site one month after the fire (Figure 3.9) as well as Field Sampling Campaign data (Figures C.9-C.13).

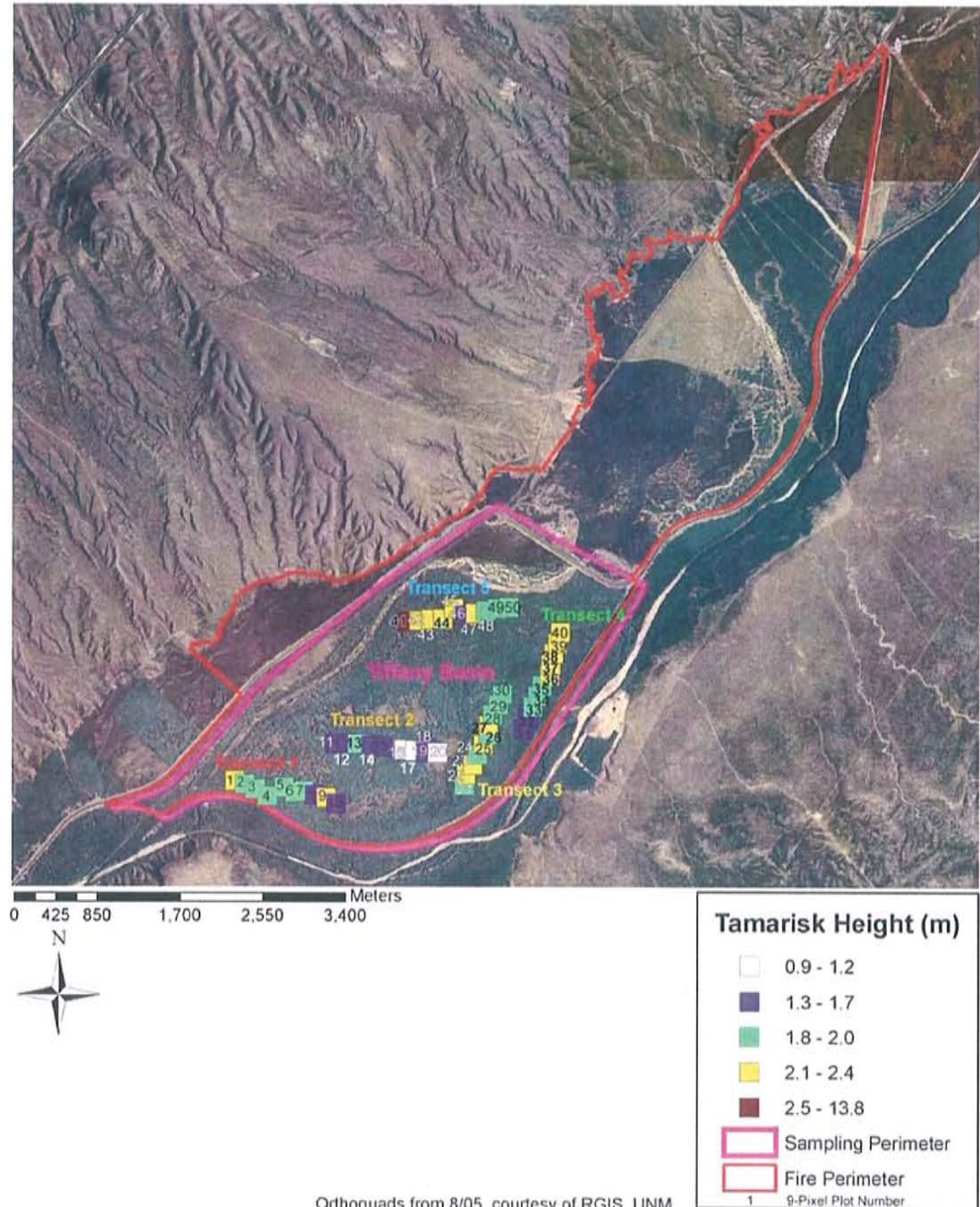
**Marcial Fire
Macroplot Sampling Map
Tamarisk Cover (%)
Sampling Performed in August of 2006**



Orthoquads from 8/05, courtesy of RGIS, UNM.

Figure 4.36. Ocular measurements of vegetation and environmental parameters from the Summer 2006 Field Campaign.

**Marcial Fire
Macroplot Sampling Map
Tamarisk Height (m)
Sampling Performed in August of 2006**



Orthoquads from 8/05, courtesy of RGIS, UNM.
Figure 4.37. Ocular measurements of vegetation and environmental parameters from The Summer 2006 Field Campaign.

Bosquecito Fire

Site sampling occurred 3 months after the Bosquecito Fire along line transects. Maps that pictorially depict the sampling data are provided in Appendix C. The dominant species at the Bosquecito Fire site is tamarisk, with cottonwood dominant in the southern portion of the site. Forbs were evident in 10% of the macroplots in the Northern portion of the site, around Transect 4. The fire burned extremely hot, consuming the above-ground tamarisk biomass of all the tamarisk populations and all that was left were short blackened stumps. The tamarisk populations that survived the fire (root crowns below intact) were located in the northwestern and southern portions. The map of tamarisk cover can be found in Figure 4.38 as well as in Appendix C. These populations were regenerating and reached a height up to 1.7 meters. The map of tamarisk height can be found in Figure 4.39 as well as in Appendix C. For the majority of the Bosquecito site, bare soil percentages were very high at 80-100%. There were low populations of Comboveg (Combination of shrubs, forbs and graminoids (%)); 20% of the macroplots had Comboveg cover around 4-20%; the rest of the site had very low Comboveg cover, around 0-3%. The tamarisk stands that survived and regenerated after the fire were in an early, young, growing stage. The site had variable soil types but predominantly silt, sandy clay and sand.

The field sampling campaign occurred between August and October of 2006, during a period of elevated precipitation throughout the state of New Mexico (Figure 4.21). For the year, 2006 New Mexico precipitation was above normal, with a January through November ranking of the 90th wettest year of 112 years.

The period January through May saw precipitation totals well below normal. However, the active monsoon season is evident in all climate divisions with July and August precipitation nearly double the normal across all but the northwest plateau. Statewide, summer precipitation ranked well above normal at 110th wettest of 112. The fall season, September through November, remained above normal (86th wettest of 112), even though November was exceptionally dry across the state (NOAA, 2006).

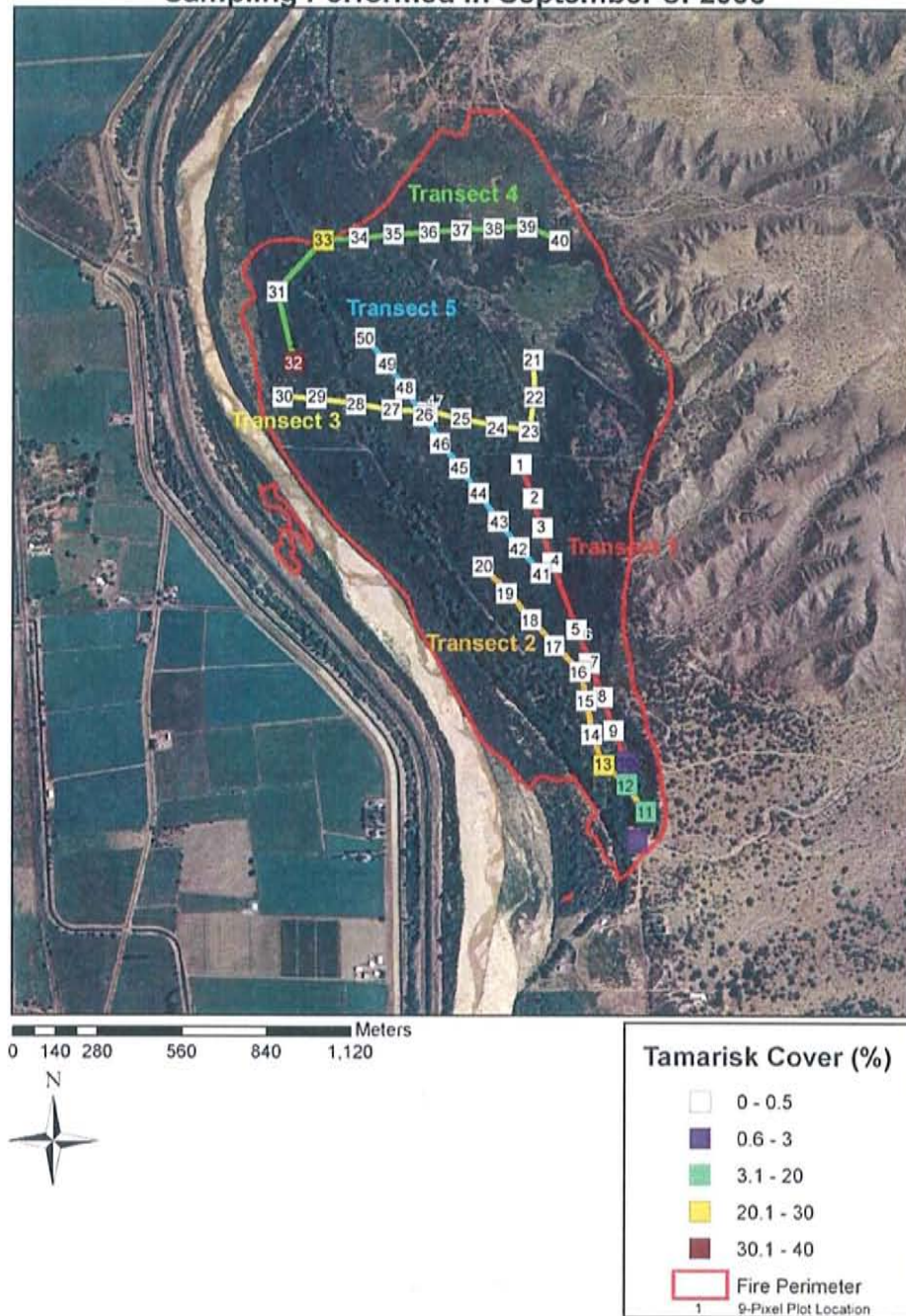
Elevated precipitation had two effects on tamarisk regeneration: 1. Encouraging succession in areas where flooding was not occurring and 2. Annihilating succession by drowning tamarisk in flooded areas where the ground water table was above the surface. The latter occurred at the Mandeville site where herbicide spraying occurred in September of 2003. The aboveground basal tamarisk was killed by the herbicide but the below ground root crowd remained intact until the flooding in the summer in 2006. The tamarisk drowned due to the flooding, and as of March 2008, wild spinach, sunflower and kochia have occupied the site that was previously dominated by tamarisk (Troxel Stowe, 2008).

Comparison to SEBAL Fire Maps

Field sampling at the Bosquecito Fire site occurred three months after the fire, from September 1-29, 2006. The Landsat image/SEBAL data closest to that of the field sampling campaign date is from July 21, 2006, one month after the fire, corresponding to Figures 4.9-4.12. The tamarisk resprouting after the fire

was spotty and there was mostly bare soil cover due to the high intensity of the fire. The Bosquecito Fire burned the hottest of the three and engulfed most basal tamarisk biomass. The high bare soil at field macroplots 1-10 and 39-41 (Figure C.19) is apparent in the NDVI map (Figure 4.10) and the central-portion of the instantaneous ET map (Figure 4.11). For the northern and southern portions of the ET maps (Figures 4.11-4.12), most of the ET occurring is most likely due to soil evaporation at the surface. Tamarisk cover was low in almost all the field macroplots except for numbers 10 to 14 (Figure C.15). The albedo map (Figure 4.9) with high albedo for the whole site, may be detecting the white-grey ash deposited on the surface.

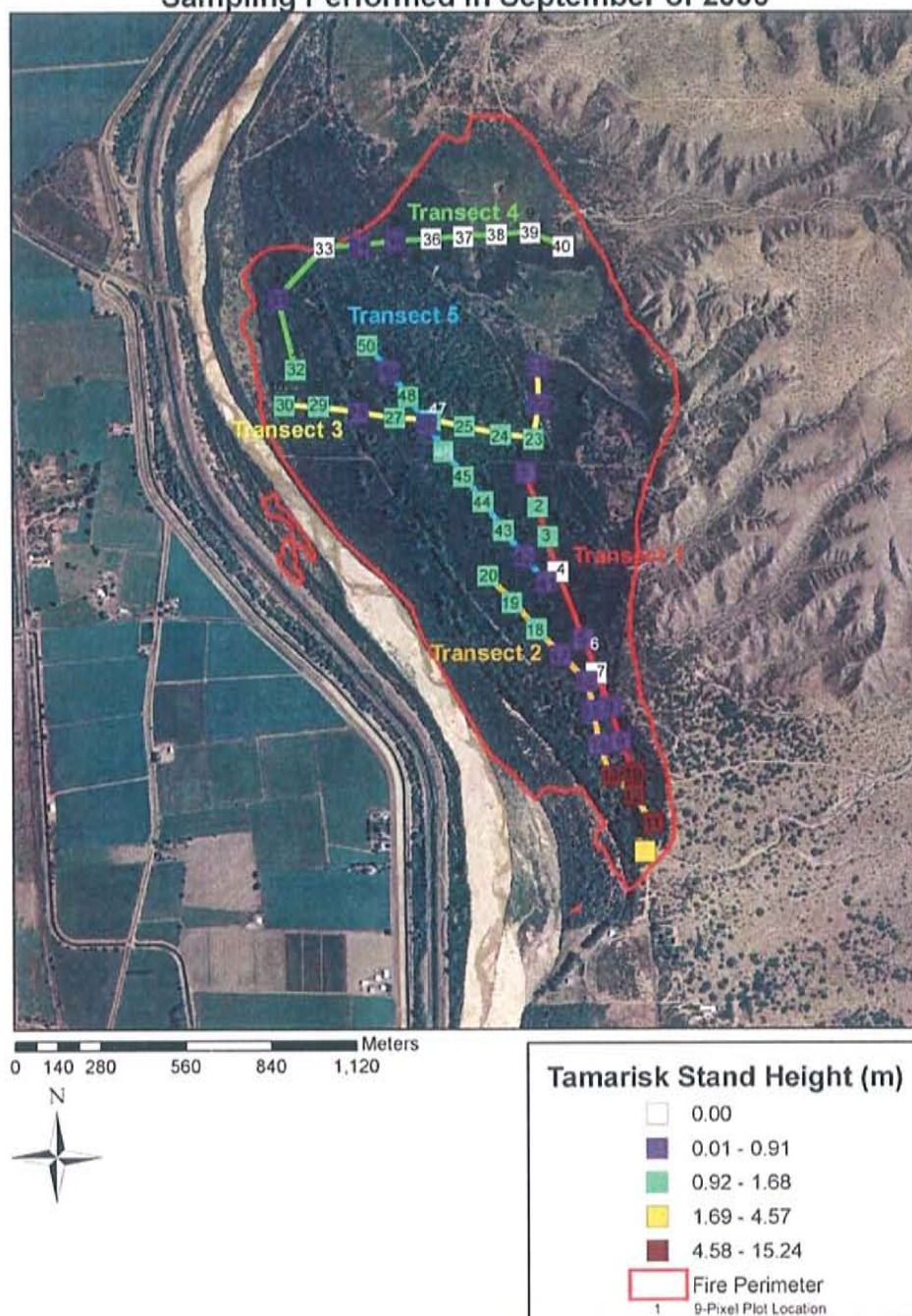
Bosquecito Fire
Macroplot Sampling Map
Tamarisk Cover (%)
Sampling Performed in September of 2006



Orthoquads from 8/05, courtesy of RGIS, UNM.

Figure 4.38. Ocular measurements of vegetation and environmental parameters from the Summer 2006 Field Campaign.

Bosquecito Fire
Macroplot Sampling Map
Tamarisk Stand Height (%)
Sampling Performed in September of 2006



Orthoquads from 8/05, courtesy of RGIS, UNM.

Figure 4.39. Ocular measurements of vegetation and environmental parameters from the Summer 2006 Field Campaign.

4.5.2 Soils

Professor Bruce Harrison and Nicole Alkov traveled to 9-Pixel Plots within the Mitchell, Marcial and Bosquecito Fires which had consistently high or low Instantaneous and Daily ET values, before and after the fire—independent of the fire. Soil sampling and characterization was performed to the groundwater table at the following locations: 1. Mitchell Fire site, 9-Pixel Number 10; Marcial Fire, 9-Pixel Number 42 and 312 meters west of 9-Pixel Number 42; and 3. Bosquecito Fire, at 9-Pixel Number 43, located within a cottonwood grove (Figures 4.40, 4.42 and 4.44). The following figures pictorially depict soil data accumulated from the NM Bureau of Geology (Figures 4.40, 4.42 and 4.44), as well as data collected in the field and composed into cross sections (Figures 4.41, 4.43 and 4.45).

Mitchell Fire Site

Hand augering was performed at the Mitchell Fire site, 9-Pixel Number 10, a pixel with consistently low ET before and after the fire. The augering spot was designated as MIT1 and occurred within the “Hch” area of Recent/Holocene channel deposits from the Rio Grande River (Figure 4.40). The lithology was comprised sand, silt and very fine silt; the cross section is provided in Figure 4.41. The absence of any clay layering may be the culprit for the consistently low ET at the site. Clay has a higher water storage capacity than silt and sand, as well as a higher matric potential. The lowered matric potentials due to silt and sand may not be able to induce capillary rise of moisture up to the ground surface, hence reflecting a lowered ET rate for that 9-Pixel. In addition, soil type is the main culprit since the ground water table behavior is normal, with respect

to the data from the well HWY E-3A, the "Representative Well" (Figures 4.47 and 4.48) that will be discussed in a future section. Another factor to consider is vegetation type and percent bare soil. The hand-augering (and hence 9-Pixel Number 10) occurred in an area with relatively high bare soil cover of approximately 30% with 70% tamarisk cover. The elevated percent of bare soil is also a factor in decreased ET. In addition, during the Summer 2006 Field Campaign, this 9-Pixel was one of the two to be overlain by very fine sand instead of a shallow layer of clay, decreasing surficial evaporative potential.

Geological map of the Hala Bala area, showing various geological units and their distribution. The map includes a legend on the right side with symbols for different geological units and a scale bar at the bottom.

Legend:

- Fire Perim
- Rch01
- Rsb01
- Rib01
- Rcb01
- Rcs01
- Rch35
- Rsb35
- Rcb35
- Rcs35
- Hch
- Hsb
- Hib
- Hcb
- Hcs
- Hal
- Hala
- Rat
- Hfy
- Hfo
- Pfa
- Pta
- QTu
- W01

Scale: 0 to 1,120 Meters

[illegible]

138

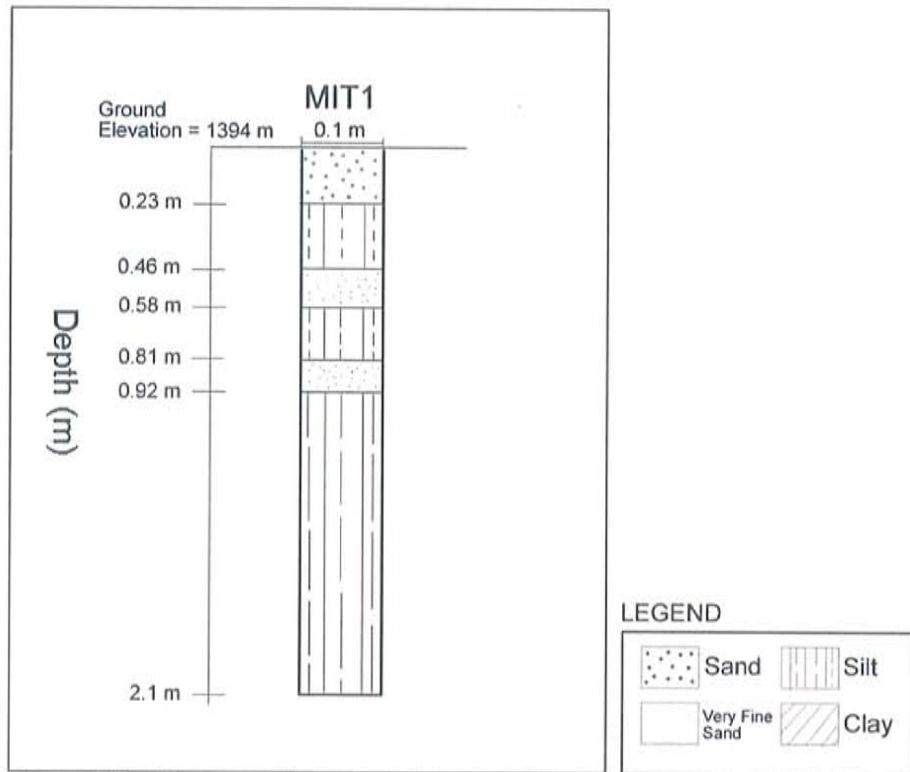


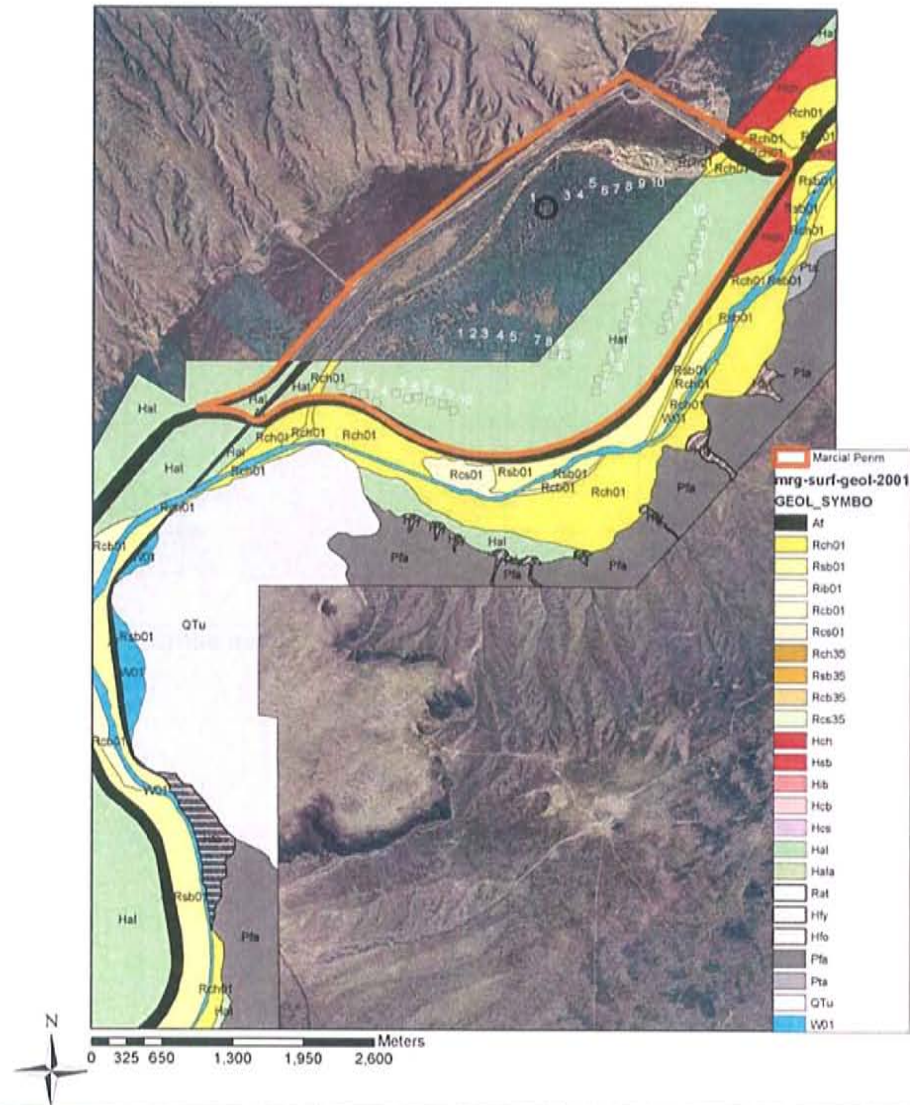
Figure 4.41. Cross section created from soil sampling performed in February 2008.

Marcial Fire Site

Hand augering was performed at the Mitchell Fire site, 9-Pixel Number 42, a pixel with consistently low ET before and after the fire (SM1), and at a site 312 meters west of SM1 with higher ET (SM2). Surficial soil mapping was not done exactly at the spot of 9-Pixel Number 42, but it is presumed that the site is overlain by "Hal", Recent/Holocene undifferentiated alluvial deposits that are in proximity to the 9-Pixel site (Figure 4.42). The lithology at SM1 and SM2 was comprised of silt, clay and sand and the cross sections are provided in Figure 4.43.

The 9-Pixel Plot 42 located at SM1 had much lower Instantaneous and Daily ET rates than that at SM2, located 312 meters west of SM1. SM2 has a much thicker clay layer (0.6 meters thick) at the groundwater table than SM1 which has two thin clay lenses 10 cm in depth (Figure 4.43). SM2's thick clay layer has a higher water storage capacity as well as matric potential, and may cause strong capillary rise up through the overlying silt layer, resulting in moisture reaching the surface which is detectable by the Landsat sensor and hence reflect elevated ET rate for that pixel. The hand-augering (and hence 9-Pixel Number 42) occurred in an area with relatively high bare soil cover of approximately 40% with 50% tamarisk and 10% cottonwood cover. The elevated percent of bare soil is also a factor in decreased ET. Unfortunately no ground water wells are located near 9-Pixel Number 42 for consideration.

Surficial Geology within the Marcial Fire



Unit Designations	Map Unit	pre 1935	1935	2000
Recent	Water		W25	W
Recent	Artificial fill	M	M	M
Recent/Holocene	Channel	Hch	Rch35	Rch01
Recent/Holocene	Channel Scour Bar	Hsb	Rsb35	Rsb01
Recent/Holocene	Channel Instream bar	Hb	Rb35	Rb01
Recent/Holocene	Channel Meander bend	Hcb	Rcb35	Rcb01
Recent/Holocene	Channel Overbank Spill	Hcs	Rcs35	Rcs01
Recent/Holocene	Alluvium - undifferentiated	Hal	Hal	Hal
Recent/Holocene	Alluvium - undifferentiated (agricultural)	Hala	Hala	Hala
Recent/Holocene	Tributary Channel Alluvium	Rat	Rat	Rat
Recent/Holocene	Tributary Fan Alluvium (coarser)	Hfy	Hfy	Hfy
Recent/Holocene	Tributary Fan Alluvium (finer)	Hfo	Hfo	Hfo
Pleistocene	Terrace Alluvium	Pta	Pta	Pta
Pleistocene	Tributary Fan Alluvium	Pfa	Pfa	Pfa
Pleistocene	Bedrock (sandstone, basalt, other)	QTu	QTu	QTu

Figure 4.42. Surficial Geology map courtesy of the NM Bureau of Geology. The circled macroplot is 9-Pixel Plot number 42/SM1, a macroplot with anomalously low daily and instantaneous ET values over time, independent of the fire.

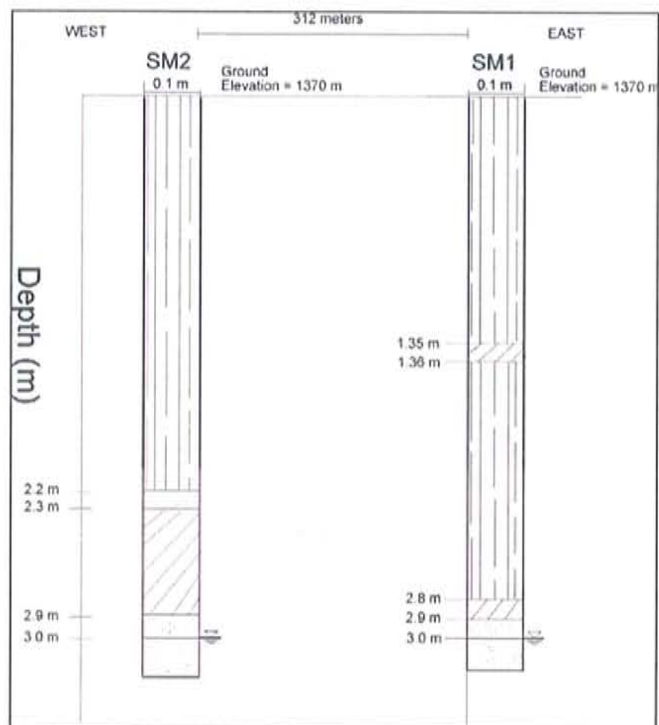


Figure 4.43. Cross section created from soil sampling performed in February 2008.

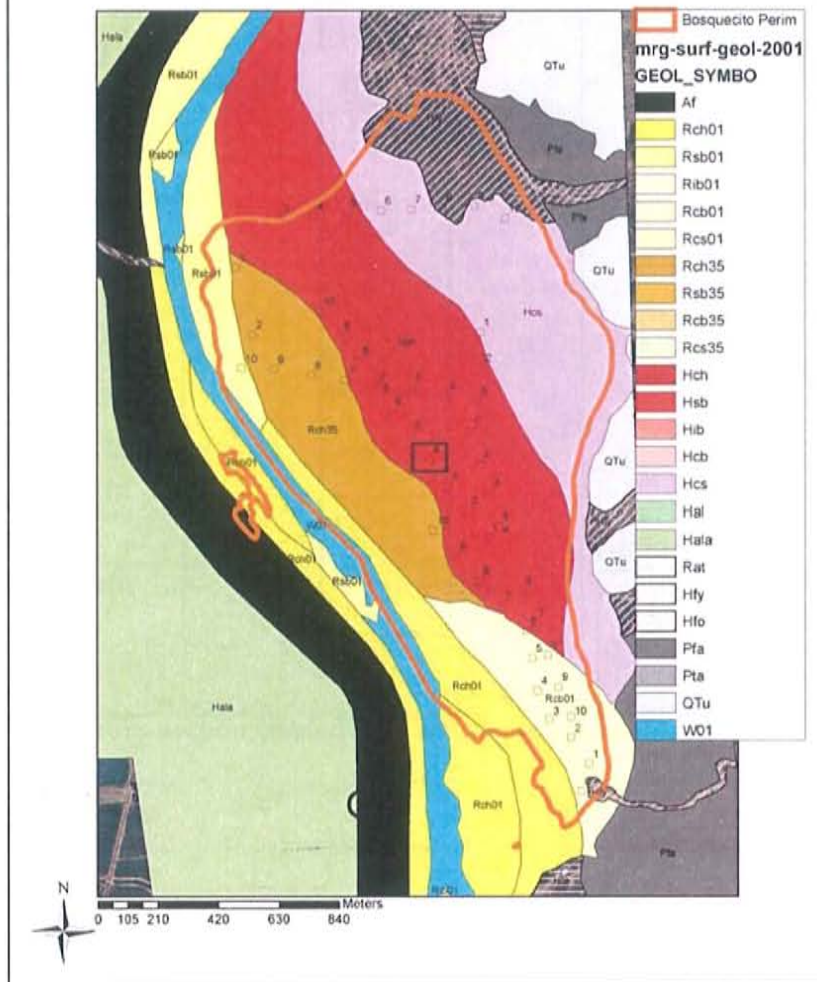
Bosquecito Fire Site

Hand augering was performed at the Bosquecito Fire site, 9-Pixel Number 43/BQC1, a pixel with consistently high ET before and after the fire. Hand augering was also performed at 9-Pixel Number 43/BQC1 and occurred within the "Hch" area of Recent/Holocene channel deposits from the Rio Grande River (Figure 4.44). The lithology at BQC1 was comprised of silt, clay and sand and the cross section is provided in Figure 4.45.

Hand augering was performed in a standing, live cottonwood grove at 9-Pixel Plot 43 within the Bosquecito Fire that has a high daily and instantaneous ET values for all image dates. The lithology was comprised of a 0.2 meter thick layer of silt at the surface. Below the silt was predominantly comprised of very fine sand with two layers of clay, one located from 0.23-0.69 meters of clay and a second thin clay layer located from 0.82-0.76 meters below ground surface. The thick clay layer from 0.23-0.69 meters has a higher water storage capacity as well as matric potential, and may cause strong capillary rise up through the overlying silt layer, resulting in moisture reaching the surface which is detectable by the Landsat sensor and hence reflect an elevated ET rate for that pixel. The hand-augering (and hence 9-Pixel Number 43) occurred in an area with relatively high bare soil cover of approximately 60% with 20% tamarisk and 20% cottonwood cover. In this case the elevated percent bare soil may have contributed towards the increase in ET, for there was more surface area for the moisture in the clay layer to percolate up to and become detected by the satellite. Ground water well BRN-E05A (Figure 4.54) is located near this 9-Pixel Plot and

has characteristically mid-level ground water levels that served a consistent supply of water to the layers above, which contributed towards percolating moisture up to the ground surface.

Surficial Geology within the Bosquecito Fire



Unit Designations				
Geologic Age	Map Unit	pre 1935	1935	2000
Recent	Water		W05	
Recent	Anthracite	At	At	At
Recent/Holocene	Channel	Hch	Rch35	Rch00
Recent/Holocene	Channel/Scrub Bar	Hsb	Rsb35	Rsb00
Recent/Holocene	Channel/Instream bar	Hib	Rib35	Rib00
Recent/Holocene	Channel/Meander bend	Hcb	Rcb35	Rcb00
Recent/Holocene	Channel/Coarse Splay	Hcs	Rcs35	Rcs00
Recent/Holocene	Alluvium - undifferentiated	Hal	Hal	Hal
Recent/Holocene	Alluvium - undifferentiated (agricultural)	Hala	Hala	Hala
Recent/Holocene	Tributary Channel Alluvium	Rat	Rat	Rat
Recent/Holocene	Tributary Fan Alluvium (younger)	Hfy	Hfy	Hfy
Recent/Holocene	Tributary Fan Alluvium (older)	Hfo	Hfo	Hfo
Pleistocene	Terrace Alluvium	Pta	Pta	Pta
Pleistocene	Tributary Fan Alluvium	Pfa	Pfa	Pfa
Neogene	Bedrock (sandstone, basalt, other)	QTu	QTu	QTu

Figure 4.44. Surficial Geology map courtesy of the NM Bureau of Geology. 9-Pixel Plot 43/BQC 1 is located within the black square and represents a 9-Pixel Plot with anomalously high daily and instantaneous ET values over time, independent of the fire.

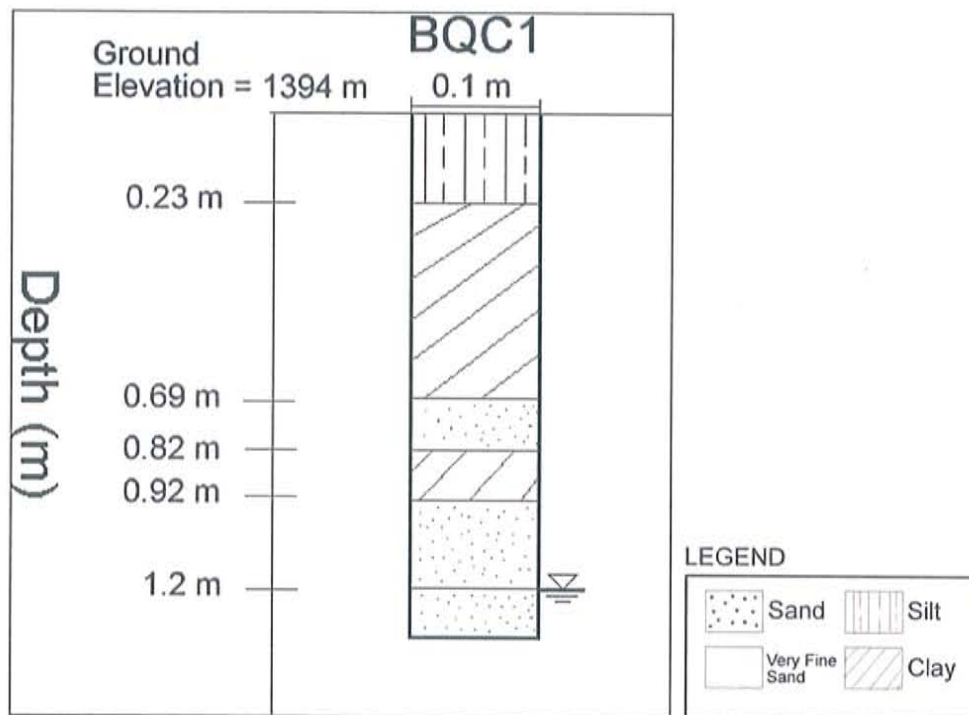


Figure 4.45. Cross section created from soil sampling performed in February 2008.

4.6 Groundwater Data from the Interstate Stream Commission (ISC)

Groundwater data was obtained from the NM Interstate Stream Commission (NM ISC) to determine the effect of groundwater table elevation on tamarisk post-fire regeneration. Well locations in proximity to the Mitchell, Marcial and Bosquecito Fire were mapped in ArcGIS (Figures 4.46, 4.49, 4.50, 4.53). Groundwater elevation data was plotted over time for the wells within the proximity of the fire sites to detect groundwater seasonal patterns, expose peaks due to the record rainfall during the summer of 2006 (Figures 4.47, 4.51, 4.54).

One "A" ground water observation well, screened at the ground water table (ISC, 2007) was determined to be the "Representative Well" for each fire site (Figures 4.48, 4.52, 4.55). Such wells are representative in that they display median groundwater elevation behavior with respect to the abundance of well data for each fire site. Sinusoidal behavior is evident for all three of the Representative Wells, with the peaks in the curves occurring during the peak of the tamarisk growing season, from May to July (Figures 4.48, 4.52, 4.55). Smooth, sinusoidal behavior is not as evident as the profile for the MODIS NDVI 16-Day Composite Plots for the 3 fire sites (Figure 4.56). The NDVI Composite plots portray and upward development of the curve from May to November with a peak in August, and low lying curve development from November to May. The cycles are continuous and consistent amongst the years (Figure 4.56). The groundwater elevation plots in Figures 4.48, 4.52 and 4.55 appear to have a "peak and crash" jagged behavior that is less sinusoidal in nature. Climatic

effects on groundwater table are drastic and definite while phonological and seasonal effects on the NDVI pattern are slower and more gradual. The NDVI-groundwater elevation plots appear to be linked during the peak of the tamarisk growing season, from May to July.

Mitchell Fire Site

Groundwater Monitoring Well Locations Mitchell Fire



Figure 4.46. Groundwater wells near the Mitchell Fire (ISC, 2007).

Groundwater Elevations for Wells at the HWY Transect

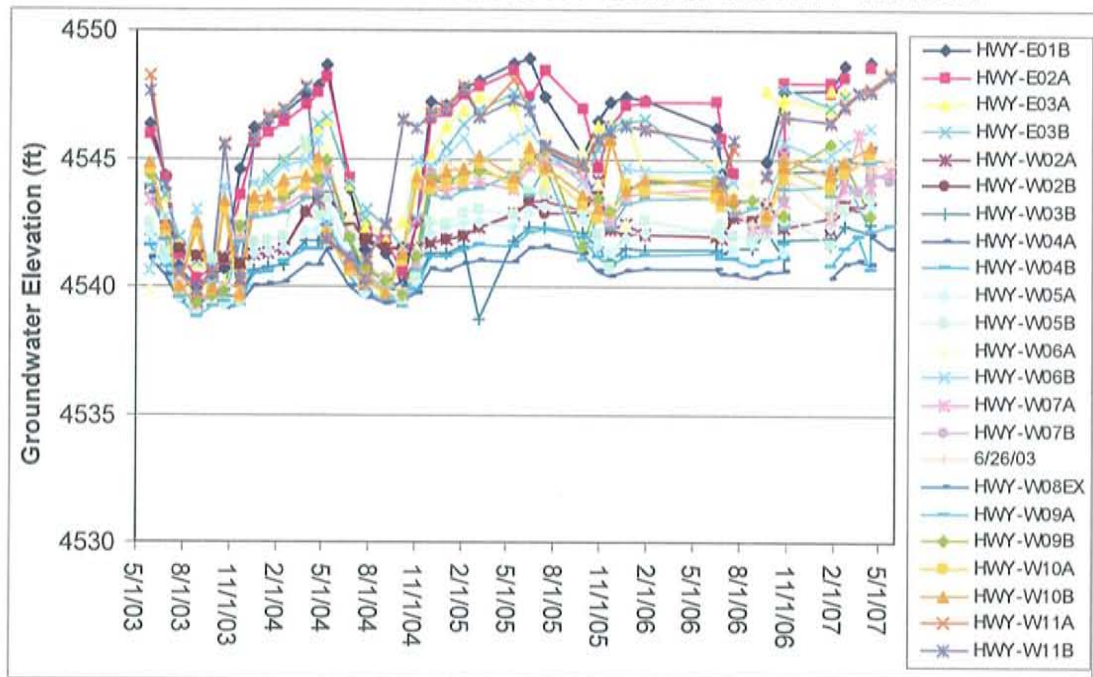


Figure 4.47. Groundwater wells at the HWY Transect, near the Mitchell Fire (ISC, 2007).

Representative Well at the Mitchell Fire Site

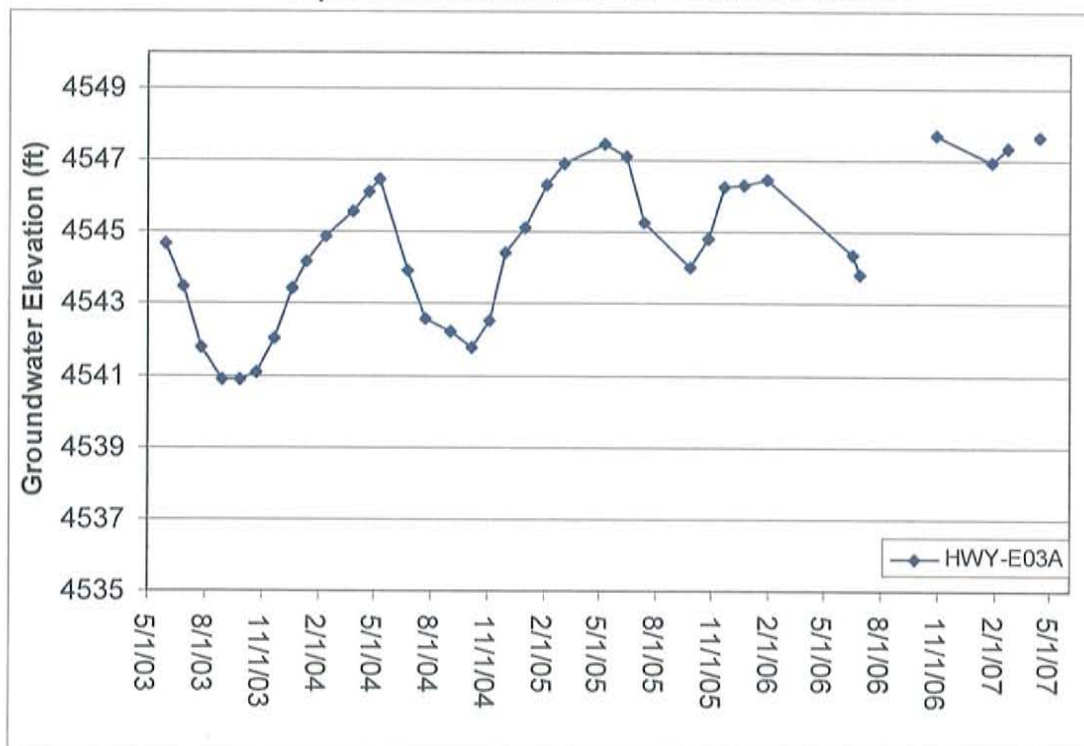


Figure 4.48. Representative groundwater well in proximity to the Mitchell Fire. Total well depth is 18.7 feet (ISC, 2007).

Marcial Fire Site

Groundwater Monitoring Well Locations Marcial Fire

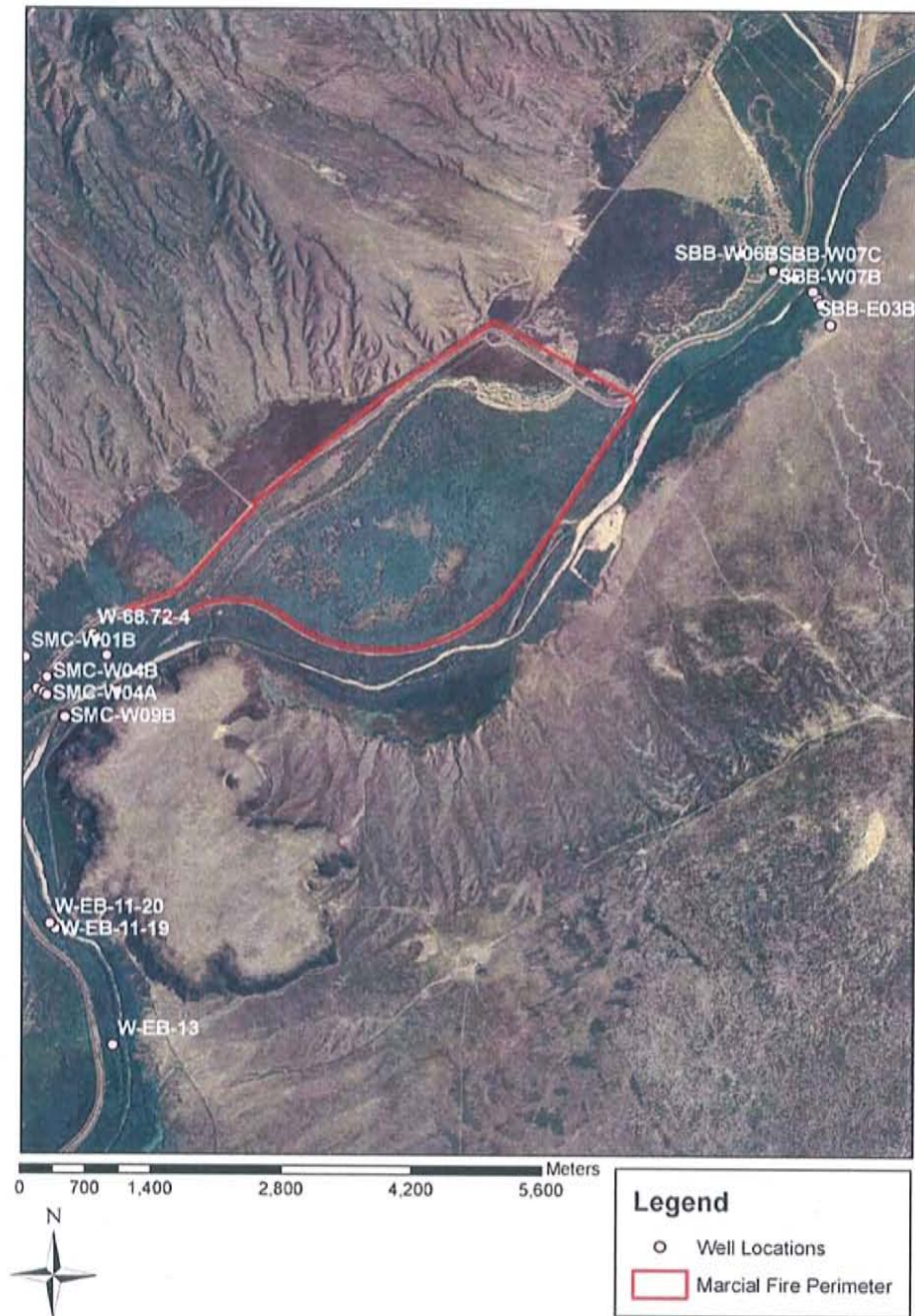


Figure 4.49. Groundwater wells near the Marcial Fire (ISC, 2007).

Groundwater Monitoring Well Locations Marcial Fire

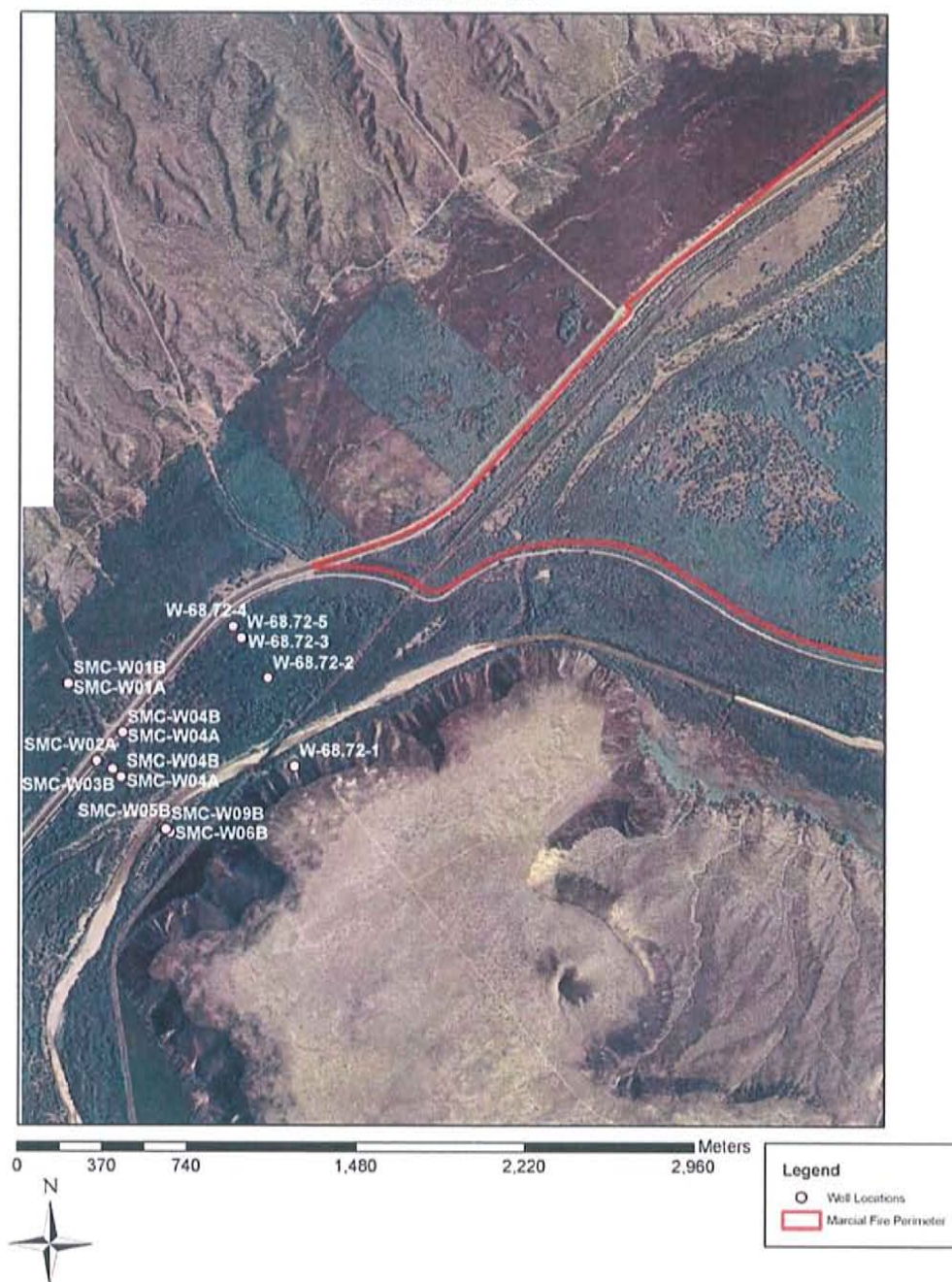


Figure 4.50. Groundwater wells near the Mitchell Fire, focusing on the wells near the Northwest portion of the fire (ISC, 2007).

Groundwater Elevations for Wells at the SMC Transect

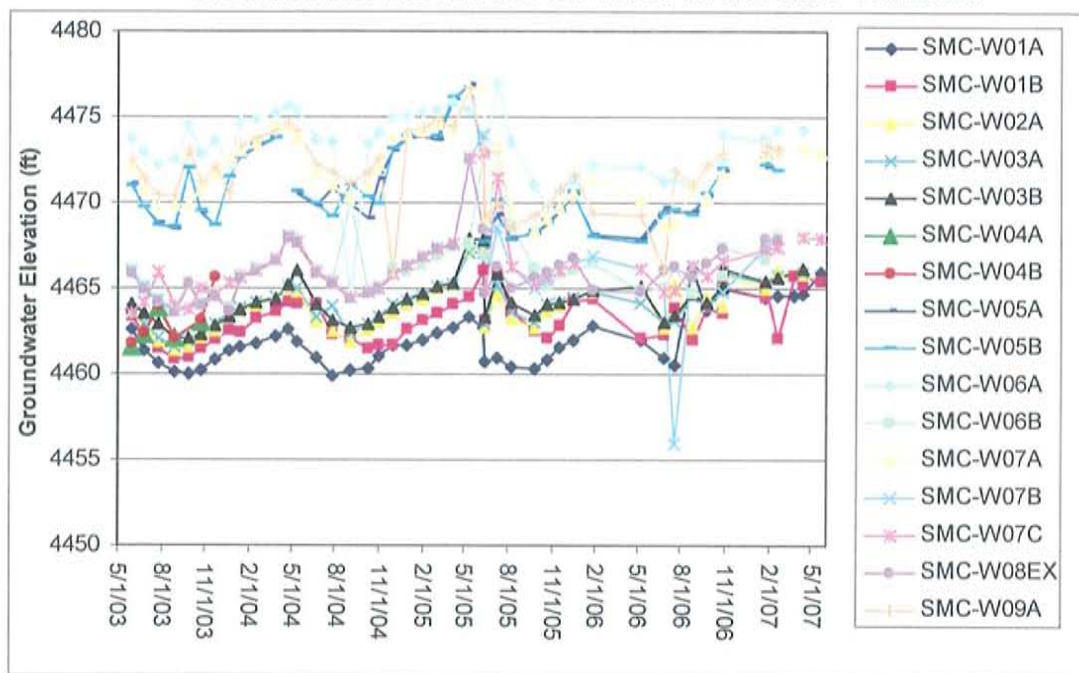


Figure 4.51. Groundwater wells at the SMC Transect, near the Marcial Fire (ISC, 2007).

Representative Well at the Marcial Fire Site

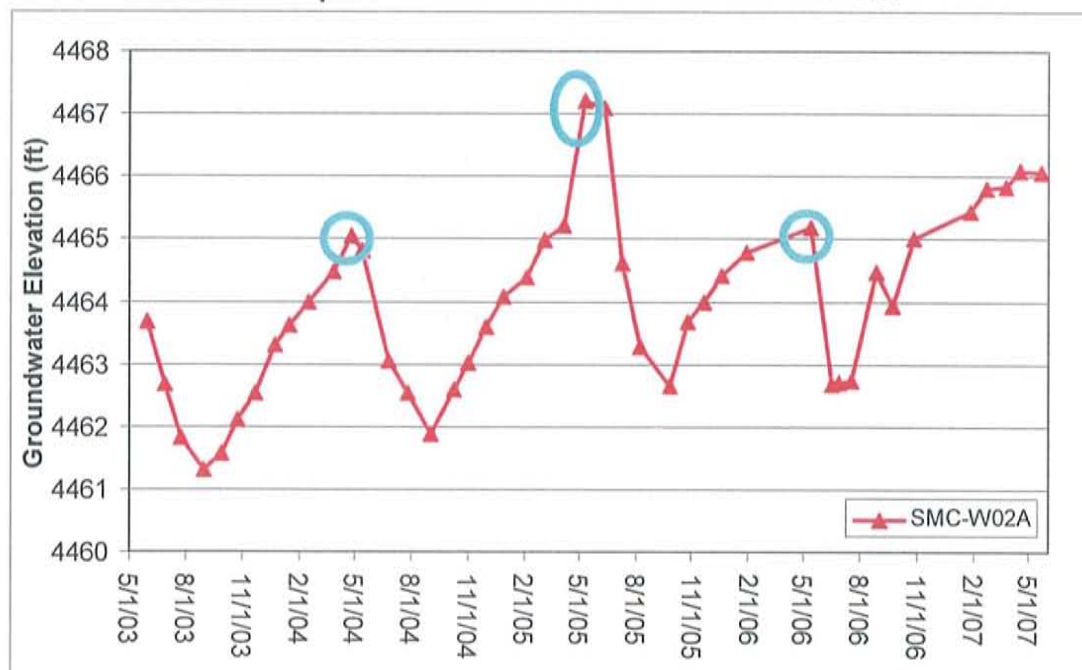


Figure 4.52. Representative groundwater well in proximity to the Marcial Fire. Total well depth is 19.5 feet. The blue circles represent elevated groundwater table levels in May of each year (ISC, 2007).

Bosquecito Fire Site

Groundwater Monitoring Well Locations Bosquecito Fire

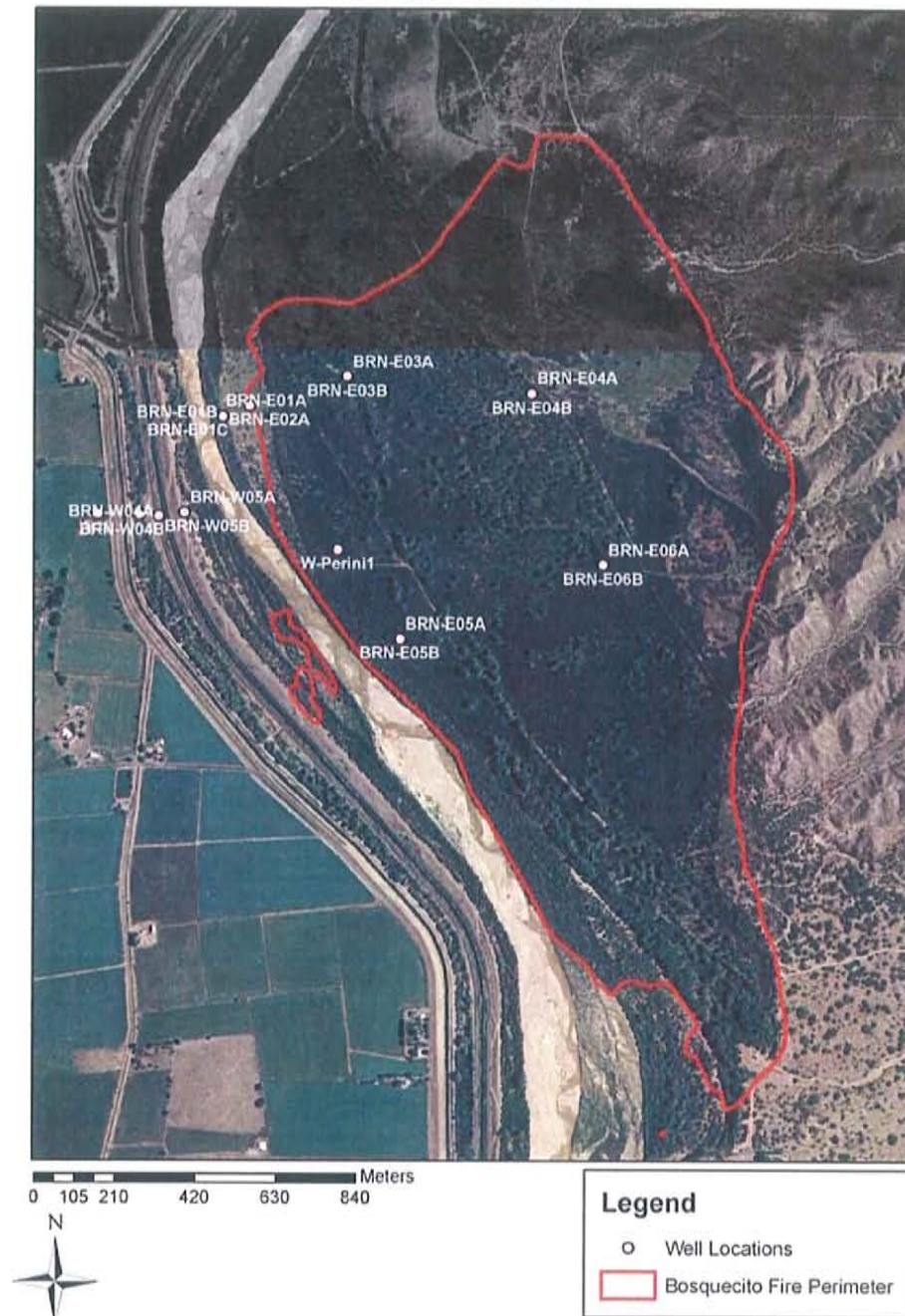


Figure 4.53. Groundwater wells near the Bosquecito Fire (ISC, 2007).

Groundwater Elevations for Wells at the BRN Transect

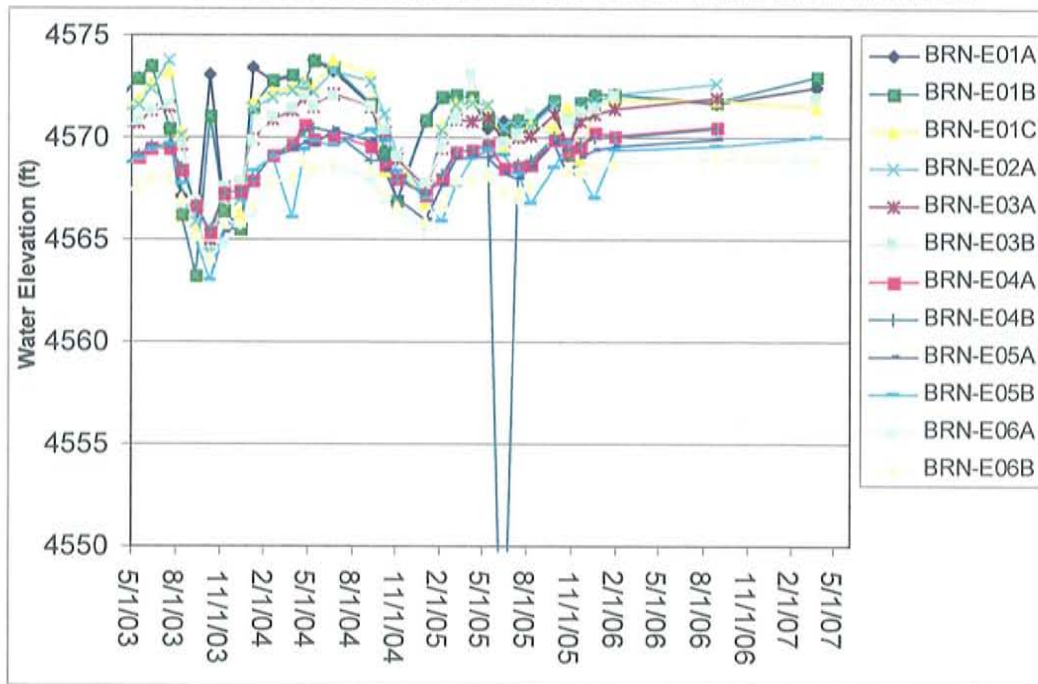


Figure 4.54. Groundwater wells at the BRN Transect, near the Marcial Fire (ISC, 2007).

Groundwater Elevation Data Representative Well at the Bosquecito Fire Site

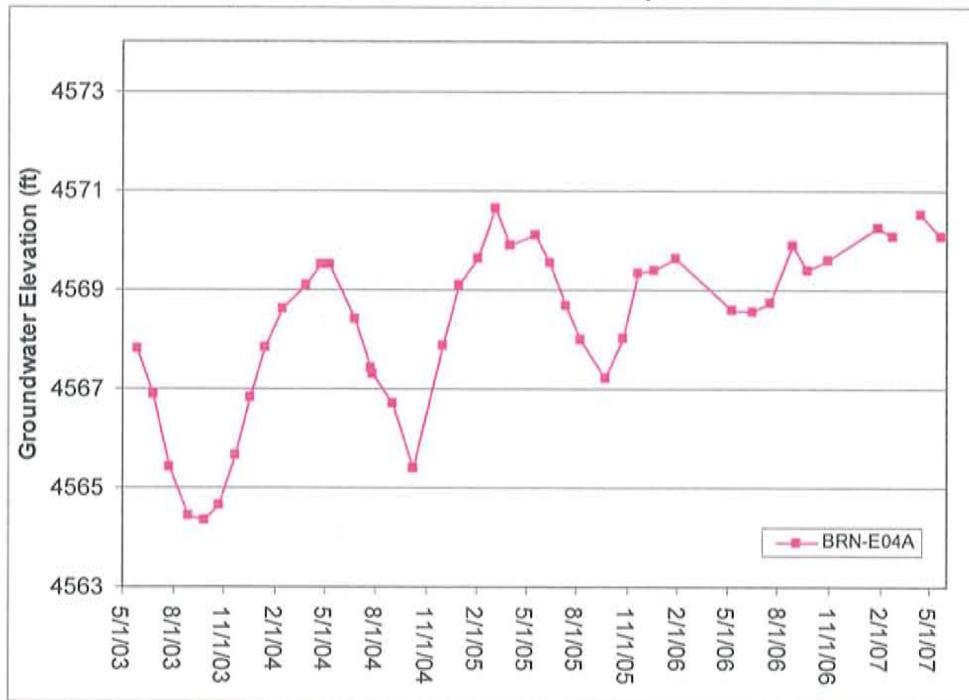


Figure 4.55. Representative groundwater well in proximity to the Bosquecito Fire. Total well depth is 16.7 feet (ISC, 2007).

MODIS NDVI 16-Day Composite Plots

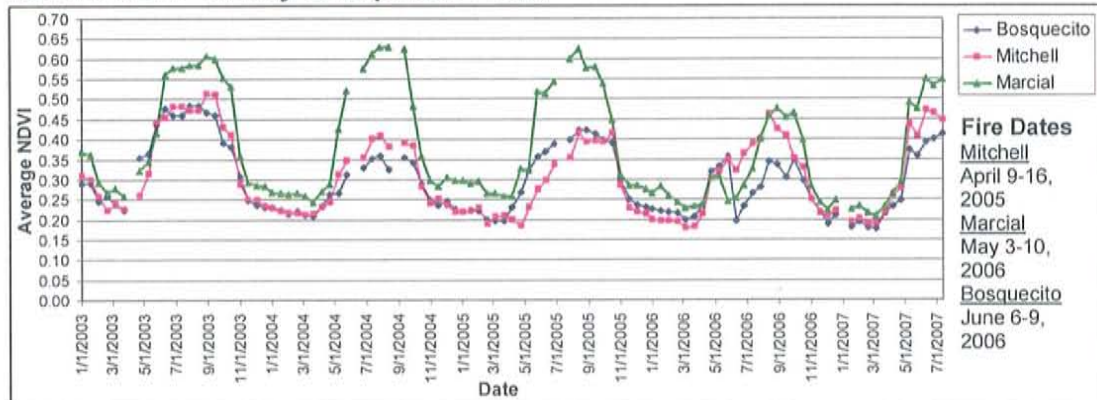


Figure 4.56. MODIS-derived Average NDVI seasonal profiles for the 3 fire sites.

5. CONCLUSIONS AND FUTURE RESEARCH

5.1 Conclusions

In recent years, fires have been used in the local Bosque Del Apache National Wildlife Refuge (BDA NWR) and the Southwest to remove invasive tamarisk vegetation which often has elevated evapotranspiration (ET) rates in dense homogenous communities that lack biodiversity. Such fire-based control methods have proven to be ineffective in tamarisk eradication—tamarisk is a fire adapted species—it regenerates early after fire as part of secondary ecological succession. Little is known about post-fire tamarisk regenerative behavior and less data is available on tamarisk post-fire regeneration rates to maturity.

In this project, tamarisk regeneration was studied by using tamarisk evapotranspiration (ET) as a proxy for post-fire tamarisk recovery. ET maps for three fires in study were created for before and after fire using Landsat imagery in association with the SEBAL computer algorithm in order to assess changes in post-fire ET post-fire as indicative of tamarisk recovery. Data from MODIS NDVI products, groundwater and soil sampling data also aided in explaining post-fire regenerative behavior at the three fire sites in study.

This project illustrated that tamarisk regenerates much faster than previously anticipated. Therefore, ecological managers would have to treat post-fire tamarisk sites within the span of a few months in order to obtain effective, permanent tamarisk management control before the tamarisk returns to pre-fire conditions as soon as one year after fire, as perceived at the three fire sites in

study. The final goal of tamarisk elimination is to replant previously tamarisk infested areas with vegetation that is native to New Mexico, such as the cottonwood and willow. From a hydrological standpoint, cottonwood and willow have comparatively lower ET rates than tamarisk in sparsely populated communities (Sala et al., 1996).

Satellite derived estimates of spatial ET computed using SEBAL computer model provide an accurate means for monitoring vegetation change and water consumption before and after fire. In this project, SEBAL was used to compare ET at the burned and unburned tamarisk covered areas of three recent fires: 1. Mitchell Fire of April 10-16, 2005, which burned 1,100 acres of private land, 2. Marcial Fire of May 3-6, 2006, which burned 4,819 acres of private land and 755 acres of the southern end of Bosque del Apache NWR, and 3. Bosquecito Fire of June 6-11, 2006, which burned 640 acres of private land. By comparing the SEBAL model results to field point measurements, the method evaluated its effectiveness of estimating spatial and temporal ET and vegetation recovery after fires. The following paragraphs will provide an overview from findings from the 3 fire sites.

Mitchell Fire

Concerning the Mitchell Fire which occurred in natural, non-disturbed homogeneous tamarisk thickets, it is apparent that regeneration may have started as early as one month after the fire; SEBAL data for the 9-Pixel Plots portrayed a rebound in NDVI, albedo and LAI for May 22, 2005, one month after

the fire, compared to pre-fire data from May 28, 2004. One year later there was significant regeneration, but overall the Crop Coefficient was reduced, with an average Crop Coefficient of 0.63 (June 19, 2006) rather than 0.95 one year before the fire (May 28, 2004). Two years later the average Crop Coefficient rebounded to pre-fire conditions, 0.89 for July 8, 2007, compared to 0.95 for May 28, 2004, one year before the fire. Hence, the natural, non-treated tamarisk areas within the Mitchell fire return to pre-fire conditions approximately two years after the fire.

Marcial Fire

For the Tiffany Basin within Marcial Fire, where field sampling occurred, two months after the fire, albedo, NDVI, LAI and the Crop Coefficient all started to recover at the 9-Pixel Plots but did not match the stated parameters' behavior for pre-fire conditions. The Marcial fire happened during the record rainfall year of 2006, encouraging succession in areas where flooding was not occurring. One year later, the average Crop Coefficient for the 9-Pixel Plots within the Marcial Fire, 0.80 for May 21, 2007, surpassed the pre-fire Crop Coefficient of 0.67 for the image dated May 31, 2002. The tamarisk may have regrown to a thicker population density with a greater evaporative potential than was evident before the fire.

Bosquecito Fire

For the Bosquecito Fire, the highest intensity burn, one month after the fire there appeared to be recovery in albedo, NDVI, LAI and the Crop Coefficient at the all of 9-Pixel Plots. This contradicts perceived field conditions of high soil/low tamarisk coverages recorded during the field campaign at the site three months after the high severity fire. High fire severity at the Bosquecito Fire greatly influenced the plant community's ability to resprout, degree of canopy degeneration, and biological environment for plant to establishment. The disparity between the field and SEBAL data may be due to the complex interplay of additional non-tamarisk communities of cottonwood, forb, graminoid and shrub species located within the site. Thus, SEBAL data presented may not be representative of tamarisk post-fire behavior, but representative of the behavior of the diversity of vegetation communities that occur on the periphery of the tamarisk communities. Low values for the tamarisk Crop Coefficient for 10 days after the fire most likely represent post-fire regenerative behavior for the tamarisk within the site for the first few months after the fire. One year later, the average Crop Coefficient for the 9-Pixel Plots within the Bosquecito Fire, 0.81 for May 21, 2007 surpassed the pre-fire Crop Coefficient of 0.72 for the image dated May 28, 2004. Tamarisk regeneration was evident during the soil sampling campaign of February of 2008, but the tamarisk had not regrown to heights and densities that were evident before the fire. Once again this may be due to the variable nature of

the vegetation communities at the site and postulates that SEBAL is a more-accurate model at sites with homogenous vegetation types before and after fire.

MODIS Data

In addition to studying Landsat imagery, MODIS NDVI image products were also utilized in this study, using NDVI as a proxy for vegetation recovery. Multitemporal extracts of 16-day MODIS NDVI composites were made over 3 fire sites to assess MODIS capability to depict phenology and seasonal variations in vegetation activity after fire. The NDVI indices depicted the important phenology events, such as onset of greenness (early May), peak greenness (August), and the dry down period (early October). Vegetation assessment through MODIS data for the burned areas of the Mitchell, Marcial and Bosquecito fire sites showed both the important effect of seasonal variation and the strong impact of the fires on vegetation dynamics. Immediately following the fires there were signs of vegetation recovery and these findings are consistent with the behavior of SEBAL ET results from Landsat imagery.

MODIS NDVI data for the Bosquecito Fire site displayed a drastic drop in Average NDVI during the time of fire, followed by recovery within two months. This is most likely due to the timing of the fire, occurring in the middle of the growing season (June 6-9, 2006), during the time frame of rapid growth and rapidly increasing biomass. The Mitchell and Marcial Fires occurred in the beginning of the growing season, in April and May respectively, during a period of slowly increasing biomass, and thus do not show evidence of much impact

from the fire due to the lack of substantial green biomass in the period early growing season.

Soil and Groundwater Data

In addition to NDVI, soil and groundwater data was gathered in order to assess the environmental hydro/geologic effect on evapotranspiration and vegetation regeneration. With respect to groundwater data we will focus on the data for the Marcial fire site. Groundwater elevations for the representative well for the Marcial site, SMW-W02A, were high around the date of the fire, with a measured ground water elevation on the day of the fire, May 10, 2006, of 4465.18 ft above sea level (asl). This elevation is 2.5 feet higher than the lower ground water elevation of 4462.67 ft-asl for June 14, 2006, one month after the fire. At the annual peak time of groundwater levels for the Marcial site--May of each year--the elevated groundwater levels may have induced moisture to reach the surface via capillary rise, resulting in unusual elevated SEBAL-generated values for the ET_{Inst} , ET_{24} and K_c data for the first image taken 8 days after the fire compared to the second image taken 1 month after the fire. With an elevated groundwater table, water may have risen to the ground surface due to capillary forces and thus detected by the Landsat satellite and SEBAL model.

As for lithology effects, the presence or absence of a thick clay layer had an effect on surficial soil moisture and thus satellite-detectable evapotranspiration at the ground surface exposed in the aftermath of fire. The presence of a thick clay layer, versus a shallow lense, appeared to induce capillary rise of soil moisture to

reach the soil surface within an area of elevated ET at the Marcial fire site. The surficial moisture was detectable by the Landsat satellite and was reflected in elevated ET values produced by the SEBAL algorithm. In contrast, a pixel in proximity to the high ET pixel, but underlain by two thin clay lenses, did not exhibit elevated ET values. The thin clay layers may not have produced enough of a matric potential gradient to induce capillary rise of moisture to the surface, thus less surficial moisture was detected by the Landsat sensor, leading to lowered ET rates for that pixel. This postulation was made by holding all other environmental parameters constant.

Overall, this project found tamarisk regeneration rates to be much faster than had previously been accepted for tamarisk post-fire succession. For example, a canopy fire at Lees Ferry, Arizona, killed 10% of mature tamarisk plants, and surviving plants produced shoots that exceeded 1.8 meters (6 feet) in height within 5 months (Stevens, 1989). In comparison, the Marcial Fire Site explored in this project exposed surviving tamarisk shoots that exceeded 2.1 meters (7 feet) in height within 3 months after the fire. The Bosquecito Fire Site explored in this project exposed surviving tamarisk shoots that exceeded 1.5 meters (5 feet) in height within 3 months after the fire and the Mitchell Fire Site exposed surviving tamarisk shoots that exceeded 6 meters (20 feet) in height within 18 months after the fire.

The above-stated regeneration rates suggest that following a tamarisk burn, ecological managers must *immediately* execute integrated control methods such as post-burn herbicide treatment, mechanical removal or flooding in order to

facilitate long term and widespread tamarisk eradication. The integrated control mechanism of herbicide-burn followed by flooding was 100% effective in tamarisk control within the Mandeville Plot of the Mitchell Fire, as the plot was exposed to herbicide treatment in 2003, burn in 2005, and extensive flooding in the summer of 2006--completely eradicating all tamarisk. As evidence to the success of herbicide-burn-flooding, in February of 2008 the SSWCD replanted portions of the Mandeville plot with cottonwood poles, and will begin seeding with native vegetation in the summer of 2008.

The final goal of this project is to stress the importance of attacking tamarisk resprouts after one or two months after fire after fire with an integrated control approach utilizing fire, herbicide, mechanical removal and flooding, in conjunction with analysis from remote sensing. The power of remote sensing of vegetation regeneration serves as a sophisticated, cost-effective and accurate alternative to the costly, conventional vegetation monitoring method of point source data collection in the field by individuals. With the assimilation of remote sensing into the everyday life—Google Maps, GPS, ArcGIS in the public and private sector, free Landsat imagery in 2009—remote sensing is the way of the future and must be integrated into tamarisk management programs within the local wildlife refuges, providing the link between local environmental managers and cutting-edge, innovative university-lead research. For innovation in science and technology ultimately is the only way to win the fight with invasive species, ensuring natural, pristine and sustainable ecosystems for generations to come.

5.2 Future Research

1. Install permanent macroplots from the 2006 Field Campaign in order to observe changes in vegetation, groundwater and soil properties from a long-term prospective.
2. Obtain additional Landsat images, before and after the Marcial fire, in order to compare to pre-fire conditions and fine tune the available data, as well as strengthen the data set. Consequently, Landsat images will be available at no cost in February 2009 as released by the USGS via the USGS Global Visualization Viewer or USGS Earth Explorer image viewers.
3. Explore the water savings, if any, in the burning of tamarisk. This is done by comparing Crop Coefficient figures from before and after the fire.
4. Extend the MODIS data set in order to have a comprehensive, up-to-date, data set on NDVI 16-day Composite Plots extending to the present.
5. Study fires that occurred 5 and 10 years ago in order to study long term effects of post-fire succession on tamarisk ET and water use.
6. Become involved with the Bosque Del Apache and SSWCD with current tamarisk-related control and revegetation projects.

6. REFERENCES

- Ahern, F., Janetos, A.C., Langham, E. (1998) Global Observation of Forest Cover: One component of CEOS' Integrated Global Observing Strategy. *Proceedings of the 27th International Symposium on Remote Sensing of Environment*. Tromso, Norway, June 8-12. In: Global and Regional Vegetation fire: Monitoring from Space: Planning a Coordinated International Effort. (ed) Ahern, F.J., Goldammer, J.G., Justice, C.O. 2001. SPB Academic Publishing.
- Albuquerque Journal (2006) Bosque Fire Forces Evacuations. [Online] Available at: http://www.abqjournal.com/abqnews/index.php?option=com_content&task=view&id=1028&Itemid=2 (accessed 24 June 2006) Albuquerque Journal News, Albuquerque, NM.
- Allen, R. G., Tasumi, M., Morse, A., and Trezza, R. (2005) Satellite-based Evapotranspiration by Energy Balance for Western States Water Management. *Proceedings of the ASCE/EWRI World Water and Environmental Resources Congress*, May 15-19, 2005.
- Anderholm, S.K. (1987) Hydrogeology of the Socorro and La Jencia Basins, Socorro County, New Mexico, U.S. Geological Survey Water-Resources Investigations Report 84-4342, 62 pp.
- Anderson, J.E. (1982) Factors controlling transpiration and photosynthesis in *Tamarix chinensis* Lour. *Ecology*, 63 (1) pp. 48-56.
- Associated Press (2005) Firefighters battle bosque fire near San Antonio, N.M. [Online] Available at: <http://www.freenewmexican.com/news/12538.html> (accessed 5 October 2005) AP, San Antonio, NM.
- Bastiaanssen et. al. (2005) SEBAL Model with Remotely Sensed Data to Improve Water-Resources Management under Actual Field Conditions. *Journal of Irrigation and Drainage Engineering*, 131, pp. 85-93.
- Bastiaanssen, W.G.M. (2000) SEBAL-based sensible and latent heat fluxes in the Irrigated Gediz Basin, Turkey. *J. Hydrol.*, 229, pp. 87-100.
- Bastiaanssen, W.G.M., Ahmad, M.D., Chemin, Y. (2002) Satellite surveillance of evaporative depletion across the Indus Basin. *Water Resour. Res.*, 38, pp. 1273 - 1281.
- Bastiaanssen, W.G.M., Bandara, K.M.P.S. (2001) Evaporative depletion assessments for irrigated watersheds in Sri Lanka. *Irrigat. Sci.*, 21, pp. 1-15.

Bastiaanssen, W.G.M., E.J.M. Noordman, H. Pelgrum, G. Davids, B.P. Thoreson, and R.G. Allen (2005) SEBAL model with remotely sensed data to improve water-resources management under actual field conditions. *Journal of Irrigation and Drainage Engineering*, 131, pp. 85-93.

Bastiaanssen, W.G.M., Menenti, M., Feddes, R.A., Holtslag, A.A.M. (1998) A remote sensing surface energy balance algorithm for land (SEBAL). Part 1: Formulation. *J. Hydrol.*, 212-213 (1), pp. 198-212.

Bastiaanssen, W.G.M., Noordman, E.J.M., Pelgrum, H., Davids, G., Thoreson, B.P., Allen, R.G. (2005) SEBAL model with remotely sensed data to improve water-resources management under actual field conditions. *J. Irrigat. Drain. Eng.*, 131, pp. 85-93.

Bastiaanssen, W.G.M., Pelgrum, H., Wang, J., Ma, Y., Moreno, J.F., Roerink, G.J., Roebeling, R.A., Wal, T.V.D. (1998a). A remote sensing surface energy balance algorithm for land (SEBAL). Part 2: Validation. *J. Hydrol.* 212-213 (1), pp. 213-229.

Bawazir, A.S. (2000) Saltcedar and cottonwood riparian evapotranspiration
Boyd, D.S., and F.M. Danson (2005) Satellite sensing of forest resources: three decades of research development. *Progress Physical Geography*, 29, pp.1-26.

Brotherson, Jack D. and Field, Dean (1987) Tamarix: impacts of a successful weed. *Rangelands*. 9(3) pp. 110-112.

Brutsaert, W., Hsu, A.Y., Schmugge, T.J. (1993) Parameterization of surface heat fluxes above a forest with satellite thermal sensing and boundary layer soundings. *J. Appl. Meteorol.*, 32, pp. 909-917.

Brutsaert, W., Sugita, M. (1992) Application of self-preservation in the diurnal evolution of the surface energy budget to determine daily evaporation. *J. Geophys. Res.*, 97, pp. 18377-18382.

Busch, D.E. (1995) Effects of fire on southwestern riparian plant community structure. *Southwestern Nat*, 40, pp. 259-276.

Busch, D.E. and S.D. Smith (1993) Effects of fire on water and salinity relationships of riparian woody taxa. *Oecologia*, 94, pp. 186-194.

Busch, David E. (1995) Effects of fire on southwestern riparian plant community structure. *The Southwestern Naturalist*. 40(3) pp. 259-267.

Busch, David E.; Smith, Stanley D. 1993. Effects of fire on water salinity relations of riparian woody taxa. *Oecologia*. 94, pp.186-194

C. Justice, E. Vermote, J. R. G. Townshend, R. Defries, D. P. Roy, D.K. Hall, V. V. Salomonson, J. Privette, G. Riggs, A. Strahler, W. Lucht, R. Myneni, Y. Knjazihhin, S. Running, R. Nemani, Z. Wan, A. Huete, W. van Leeuwen, R. Wolfe, L. Giglio, J-P. Muller, P. Lewis, and M. Barnsley (1998) The Moderate Resolution Imaging Spectroradiometer (MODIS): Land remote sensing for global change research," *IEEE Trans. Geosci. Remote Sens.*, 36, pp. 1228-1249.

Canadell, J., and López-Soria, L. (1998) Lignotuber reserves support regrowth following clipping of two Mediterranean shrubs. *Functional Ecology*, 12, pp. 31-38.

Cather, S. M., Chamberlin, R. M., Chapin, C. E., and McIntosh, W. C. (1994) Stratigraphic consequences of episodic extension in the Lemitar Mountains, central Rio Grande rift, *Basins of the Rio Grande rift—Structure, stratigraphy, and tectonic setting*, Geological Society of America, 291, pp. 157-170.

Chen PY, Fedosejevs G, Tiscareno-Lopez M, et al. (2006) Assessment of MODIS-EVI, MODIS-NDVI and vegetation-NDVI composite data using agricultural measurements: An example at corn fields in western Mexico, *Environmental Monitoring and Assessment*, 119 (1-3) pp. 69-82.

Choudhury, B. J. (1987) Relationship Between Vegetation Indices, Radiation Absorption, and Net Photosynthesis Evaluated By a Sensitivity Analysis. *Remote Sensing of Environment*, 22, pp. 209-233.

Chuvieco, E. & Congalton, R. G. (1988) Mapping and inventory of forest fires from digital processing of TM data. *Geocarto International*, 3, pp. 41-53.

Clark, L.K. (2000) *Pictures at a conflagration: Remote Sensing and GIS techniques for mapping and analysing prescribed fire in the Madrean Archipelago*. M.A Thesis, Department of Geography and Regional Development, University of Arizona, Tucson AZ. 234 pp.

Cleverly, J.R., Dahm, C.N., Thibault, J.R., Gilroy, D.J., and Allred Coonrod, J.E. (2002) Seasonal estimates of actual evapotranspiration from *Tamarix* spp. ramosissima stands using 3-dimensional eddy covariance. *J. of Arid Environ.* 52:181-197.

Cleverly, J.R., Dahm, C.N., and Thibault, J.R. (2004) State-of-the-art Technologies for Evaluating Water Use by Riparian Vegetation: UNM Hydrogeoecology & the Middle Rio Grande. *In* Identifying Technologies to Improve Regional Water Stewardship: North -Middle Rio Grande Corridor Symposium. Albuquerque, NM: The University of New Mexico. pp. 267-277.

Dahm, C.N., Cleverly, J.R., Coonrod, J.E.A., Thibault, J.R., McDonnell, D.E., and

Davenport, D.C., Martin, P.E., and Hagan, R.M. (1982) Evapotranspiration from riparian vegetation: Water relations and irrecoverable losses for saltcedar. *J. of Soil and Water Conservation*, pp. 233-236.

Dahm, C.N., Cleverly, J.R., Coonrod, J.E.A., Thibault, J.R., McDonnell, D.E., and Gilroy, D.J. (2002) Evapotranspiration at the land-water interface in a semi-arid drainage basin. *Freshwater Biology*, 47, pp.831-846.

de Bruin, H.A.R. (1987) In: Hooghart, J.C. (Ed.), From Penman to Makkink, . In: Evaporation and Weather. Proceedings and Information, vol. 39. TNO Committee on Hydrological Research, The Hague, pp. 5-31.

DeBano, L.F., Savage, S.M., and D.A. Hamilton. (1976) The transfer of heat and hydrophobic substances during burning. *Soil Sci. Soc. Am. Proc.*, 40, pp. 779-782.

Díaz-Delgado, R., Lloret, F., Pons, X. (2003) Influence of fire severity on plant regeneration by means of remote sensing imagery. *International Journal of Remote Sensing*, 24 (8) pp. 1751-1761.

Díaz-Delgado, R., Lloret, F., Pons, X. 2003. Influence of fire severity on plant regeneration by means of remote sensing imagery. *International Journal of Remote Sensing*. 24 (8) pp. 1751-1761.

Díaz-Delgado, R., Lloret, F., Pons, X. and Terradas, J. (2002) Satellite evidence of decreasing resilience in Mediterranean plant communities after recurrent wildfires, *Ecology*, 83 (8) pp. 2293-2303

Díaz-Delgado, R., X. Pons y F. Lloret (2001) Fire severity effects on vegetation recovery after fire. The Bigues i Riells wildfire case study, In: 3rd International Workshop on Remote sensing and GIS applications to Forest Fire Management. New methods and sensors, Paris, EARSeL, pp. 152-155.

Duncan, Celestine A. ; Jachetta, John J. ; Brown, Melissa L. ; Carrithers, Vanelle F. ; Clark, Janet K. ; DiTomaso, Joseph M. ; Lym, Rodney G. ; McDaniel, Kirk C. ; Renz, Mark J. ; Rice, Peter M. (2004) Assessing the economic, environmental, and societal losses from invasive plants on rangeland and wildlands. *Weed Technology*, 18 (5) pp. 1411-1416.

Duncan, J., Stow, D., Franklin, J., and Hope, A. S. (1993) Assessing the relationship between spectral vegetation indices and shrub cover in the Jornada Basin, New Mexico. *International Journal of Remote Sensing*, 14, pp. 3395-3416.

Eastwood, J., Plummer, S.E., Stocks, B.J. and Wyatt, B. (1998) The potential of SPOT-Vegetation data for fire scar detection in boreal forests. *International Journal of Remote Sensing*, 19, pp. 3681-3687.

Egan, Thomas B. (1999) Afton Canyon Riparian Restoration Project: Fourth year status report. *Proceedings of the California Weed Sciences Society*, 51, pp. 130-145.

Ellis, Lisa M (2006) Short-term response of woody plants to fire in a Rio Grande riparian forest, central New Mexico, USA. *Biological Conservation*, 97, pp. 159-170.

Ellis, Lisa M.; Crawford, Clifford S.; Molles, Manuel C., Jr. (1998) Comparison of litter dynamics in native and exotic riparian vegetation along the middle Rio Grande of central New Mexico, U.S.A. *Journal of Arid Environments*, 38 (2) pp. 283-296.

Elmore, Andrew J., Mustard, John F., Manning, Sara J., Lobell, David B. (2000) Quantifying Vegetation Change in Semi-Arid Environments: Precision and Accuracy of Spectral Mixture Analysis and the Normalized Difference Vegetation Index. *Remote Sensing of Environment*, 73, pp. 87-102.

EROS Data Center, U.S. Geological Survey. Global Forest Fire Watch: Wildfire Potential, Detection, Monitoring and Assessment, [Online]. Available at: <http://www.na.unep.net/globalfire/indofire/firepaper.html> (accessed 5 March, 2007). U.S. Geological Survey. Menlo Park, CA

Everitt, Benjamin L. (1980) Ecology of saltcedar—a plea for research. *En-* Everitt, James H.; Escobar, David E.; Alaniz, Mario A.; Davis, Michael R.; Richerson, James V. (1996) Using spatial information technologies to map Chinese tamarisk (*Tamarix chinensis*) infestations. *Weed Science*, 44 (1) pp. 194-201.

Fiorella, M. & Ripple, W. J. (1993) Analysis of conifer forest regeneration using Landsat Thematic Mapper data. *Photogrammetric Engineering and Remote Sensing*, 59, pp.1383-1388.

Fox, Russell B.; Mitchell, Robert B.; Davin, Michael (2000) Saltcedar management at Lake Meredith National Recreation Area. In: Zwank, Phillip J.; Smith, Loren M., eds. Research highlights - 2000: Range, wildlife, & fisheries management. Volume 31. Lubbock, TX: Texas Tech University, College of Agricultural Sciences and Natural Resources: 27-28.

Fox, Russell; Mitchell, Rob; Davin, Mike (2001) Managing saltcedar after a summer wildfire in the Texas rolling plains. In: McArthur, E. Durant; Fairbanks,

Daniel J., compilers. Shrubland ecosystem genetics and biodiversity: proceedings; 2000 June 13-15; Provo, UT. Proc. RMRS-P-21. Ogden, UT: U.S. Department of Agriculture, Forest Service, Rocky Mountain Research Station: 236-237.

Gamon, J. A., Field, C. B., Goulden, M. L., Griffin, K. L., Hartley, A. E., Joel, G., Peñuelas, J., and Valentini, R. (1995) Relationships between NDVI, canopy structure, and photosynthesis in three California vegetation types. *Ecological Applications*, 5, pp. 28-41.

García-Haro, F.J., Gilabert, M.A., Melía, J. (2001) Monitoring fire-affected areas using Thematic Mapper data. *International Journal Remote Sensing*, 22 (4) pp. 533-549.

Gary, Howard L. and Horton, Jerome S. (1965) Some sprouting characteristics of five-stamen tamarisk. *Research Note RM-39*. U.S. Department of Agriculture, Forest Service, Rocky Mountain Forest and Range Experiment Station. 7 pp.

Gatewood, J.S., Robinson, T.W., Colby, B.R., Hem, J.D., and Halpenny, L.C. (1950) Use of water by bottom-land vegetation in Lower Safford Valley, Arizona. *Geol. Survey Water-Supply Paper 1103*, 216 pp.

Grace, James B.; Smith, Melinda D.; Grace, Susan L.; [and others] (2001) Interactions between fire and invasive plants in temperate grasslands of North America. Proceedings of the invasive species workshop: The role of fire in the control and spread of invasive species. The first national congress on fire ecology, prevention, and management. San Diego, CA, 27 November - 1 December, 2001.

Hendrickx et al. (2005) Mapping sensible and latent heat fluxes in arid areas using optical imagery. *Proc. International Society for Optical Engineering (SPIE)*, 5811, pp. 138-146.

Hendrickx et al. (2006) Mapping energy balance fluxes and root zone soil moisture in the White Volta Basin using optical imagery. *Proc. International Society for Optical Engineering (SPIE)*, 6239, pp. 238-249.

Hendrickx, J.M.H., and S.-h. Hong (2005) Mapping sensible and latent heat fluxes in areid areas using optical imagery. *Proc. International Society for Optical Engineering (SPIE)*, 5811, pp.138-146.

Henry, M. C. and A. S. Hope (1998) Monitoring Post-Burn Recovery of Chaparral Vegetation in Southern California using Multi-Temporal Satellite Data. *International Journal of Remote Sensing*, 19, pp. 3097-3107.

Horton, J. S.; Mounts, F. C.; Kraft, J. M. (1960) Seed germination and seedling establishment of phreatophyte species. Station Paper No. 48. Fort Collins, CO: U.S. Department of Agriculture, Forest Service, Rocky Mountain Forest and Range Experiment Station, 26 pp.

Horton, J.L., Kolb, T.E., and Hart, S.C. (2001) Physiological responses to groundwater depth varies among species and with river flow regulation. *Ecol. Applications*, 11(4), pp. 1046-1059.

Horton, Jerome S. (1977) The development and perpetuation of the permanent tamarisk type in the phreatophyte zone of the Southwest. In: Johnson, R. Roy; Jones, Dale A., tech. coords. Importance, preservation and management of riparian habitat: a symposium: Proceedings; 1977 July 9; Tucson, AZ. General Technical Report RM-43. Fort Collins, CO: U.S. Department of Agriculture, Forest Service, Rocky Mountain Forest and Range Experiment Station: 124-127.

Howard, S. W.; Dirar, A. E.; Evens, J. O.; Provenza, R. D. (1983) The use of herbicides and/or fire to control saltcedar (*Tamarix*). *Western Society of Weed Science*, 36, pp. 65-72.

Huete, A. (1988) Soil-adjusted vegetation index (SAVI), *Remote Sens. Environ.*, 25, pp. 89-105.

Huete, A., Didan, K., Miura, T., and Rodriguez, E. (2002) Overview of the Radiometric and Biophysical Performance of the MODIS Vegetation Indices. *Remote Sensing of Environment*, 83, pp. 195-213.

Huete, A., Justice, C. and Liu, H. (1994) Development of vegetation and soil indices for MODIS-EOS, *Remote Sensing of Environment*, 49 (3) pp. 224-234.

Jakubauskas, M.E., Lulla, K.P., Mausel, P.W. (1990) Assessment of vegetation change in a fire altered forest landscape. *Photogrammetric Engineering and Remote Sensing*, 56, pp. 371-377.

Jakubauskas, M. E., Lulla, K. P. & Mausel, P. W. (1990) Assessment of vegetation changed in a fire altered forest landscape. *Photogrammetric Engineering and Remote Sensing*, 56, pp. 371-377.

Jakubauskas, M.E., Lulla, K.P., Mausel, P.W. (1990) Assessment of Vegetation change on a fire-altered landscape. *Photogrammetric Engineering and Remote Sensing*, 56, pp. 371-377.

Jin, S. and Sader, S. (2005) MODIS time-series imagery for forest disturbance detection and quantification of patch size effects, *Remote Sensing of Environment*, 99, pp. 462-470.

Jordan et. al. (2007). Remote-Sensing Based Methodology for Evaluation of Water Savings Associated with River Ecosystem Restoration Projects. In: Proposal to Provide Remote Sensing Based Evaluation of Water Savings RFP #FY07-SWQB RER Initiative, Albuquerque, NM.

Joshi, C., Leeuw, J. D., and van Duren, I. C. (2004) Remote sensing and GIS applications for mapping and spatial modeling of invasive species, *ISPRS*, 35 (B7-7) pp. 669-677.

Justice, D. H., Salomonson, V., Privette, J., Riggs, G., Strahler, A., Lucht, R., Myneni, R., Knjazihhin, Y., Running, S., Nemani, R., Vermote, E., Townshend, J., Defries, R., Roy, D., Wan, Z., Huete, A., van Leeuwen, R., Wolfe, R., Giglio, L., Muller, J.-P., Lewis, P., & Barnsley, M. (1998). The Moderate Resolution Imaging Spectroradiometer (MODIS): land remote sensing for global change research. *IEEE Transactions on Geoscience and Remote Sensing*, 36, pp.1228-1249.

Kerpez, T.A. and N.S. Smith (1987) Saltcedar control for wildlife habitat improvement in the southwestern United States. Washington, DC, U.S. Fish & Wildlife Serv. Resource Pub.169, 16 pp.

Klaver, J.W.; Klaver, R.W.; Burgan, Robert E. (1997) Using GIS to assess forest fire hazard in the Mediterranean region of the U.S. In: 17th Annual ESRI Users Conference, San Diego, CA, 8-11 July, 1997.

Klaver, R.W. et al. (2003) Global Forest Fire Watch: Wildfire Potential, Detection, Monitoring and Assessment, [Online]. U.S. Geological Survey, EROS Data Center, Sioux Falls, SD. Available at: <http://www.na.unep.net/globalfire/indofire/firepaper.html> (accessed 5 March, 2007).

Knight, J.F., R.L. Lunetta, J. Ediriwickrema, and S. Khorram (2006) Regional Scale Land-Cover Characterization using MODIS-NDVI 250 m Multi-Temporal Imagery: A Phenology Based Approach. *GIScience and Remote Sensing*, 43 (1) pp. 1-23.

Kobziar, L. N. and J. R. McBride (2006) Wildfire burn patterns and riparian vegetation response along two northern Sierra Nevada streams. *Forest Ecology and Management*, 222, pp. 254-265.

Koutsias, N., Karteris, M., Fernandez-Palacios, A., Navarro, C., Jurado, J., Navarro, R. & Lobo, A. (1999) Burnt land mapping at local scale. *Remote Sensing of Large Wildfires in the European Mediterranean Basin*, pp. 157-187.

Leeuwen van, W. J. D., Huete, A. R., Didan, K., and Laing, T. (1997) Modeling bidirectional reflectance factors for different land cover types and surface components to standardize vegetation indices, In: Proceedings of the 7th Int.

Symposium on Physical Measurements and Signatures in Remote Sensing, Courcheval, France, 7 – 11 April, 1997, pp. 373-380.

Lentile, Leigh B.; Holden, Zachary A.; Smith, Alistair M. S.; Falkowski, Michael J.; Hudak, Andrew T.; Morgan, Penelope; Lewis, Sarah A.; Gessler, Paul E.; Benson, Nate C. (2006) Remote sensing techniques to assess active fire characteristics and post-fire effects. *International Journal of Wildland Fire*, 15 (3) pp. 319-345.

Lopez-Garcia, M. J. & Caselles, V (1991) Mapping burns and natural reforestation using Thematic Mapper data. *Geocarto International*, 6, pp. 31-37.

Lovich, Jeffrey (2000) Tamarix ramosissima/Tamarix chinensis/Tamarix gallica/Tamarix parviflora. *Invasive plants of California's wildlands*, pp. 312-317.

Lovich, J.E., T.B. Egan, R.C. de Gouvenain (1994) Tamarisk control on public lands in the desert of Southern California: two case studies. *Proc. California Weed Conf. California Weed Sci Soc.*, 46, pp. 166-177.

Lunetta, R.S. Knight, J.F. Ediriwickrema, J. G. Lyon, and L. D. Worthy (2006). Land-Cover Change Detection Using Multi-temporal MODIS NDVI Data. *Remote Sensing of Environment*, 105, pp. 142-154.

Lutes, C.D., Duncan C. Lutes, R. E. Keane, J. F. Caratti, C. H. Key, N. C. Benson, S. Sutherland, and L. J. Gangi (2003) FIREMON: Fire Effects Monitoring and Inventory System. [Online] Available at: http://ams.confex.com/ams/FIRE2003/techprogram/paper_65637.htm (accessed 24 September, 2007). AMS, Boston, MA.

M, J. M., and O, W. C. (1989) A simple method for estimating fire intensity after a burn in California chaparral. *Acta Oecologica-Oecologia Plantarum*, 10, pp. 57–68.

Marchetti, M., Ricotta, C., and Volpe, F. (1995) A qualitative approach to the mapping of post-fire regrowth in Mediterranean vegetation with Landsat TM Data. *International Journal of Remote Sensing*, 16, 2487-2494.

Markvart, T. and Castalzer, L. (2003) Practical Handbook of Photovoltaics: Fundamentals and Applications. *Elsevier*.

Martin, M.P., Flasse, S., Ceccato, P. Y Downey, I. (1999) Fire detection and fire growth monitoring using satellite data. *Remote sensing of large wildfires in the European Mediterranean Basin*, Springer-Verlag, Berlin, pp. 101-122.

McDaniel, K. and Taylor, J.P. (2003) Aerial Spraying and Mechanical Saltcedar Control. In: Proceedings, Saltcedar and Water Resources in the West Symposium. San Angelo, TX: Texas Agricultural Experiment Station and Cooperative Extension, pp. 113-123.

McDaniel, K. and Taylor, J.P. (2003) Saltcedar Recovery After Herbicide-Burn and Mechanical Clearing Practices. *Journal of Range Management*, 56, pp. 439-445.

McDaniel, K.C., J.M. DiTomaso, and C.A. Duncan (2000) Invasive Plants of Range and Wildlands and Their Environmental Economic and Societal Impacts. USDA, pp. 198-222.

Miller, J.D., Yool, S.R. (2002) Mapping forest post-fire canopy consumption in several overstorey types using multi-temporal LANDSAT TM and ETM data. *Remote Sensing & Environment*, 82, pp. 481-496.

Milne, A.K. (1986) The use of remote sensing in mapping and monitoring vegetational change associated with bushfire events in eastern Australia. *Geocarto International*, pp. 25-32.

Miura, T., Didan, K., Huete, A. R., and Rodriguez, E. P. (2001) A performance evaluation of the MODIS vegetation index compositing algorithm. Proceedings of IGARSS 2001 Symposium, 9-13 July 2001, Sydney, Australia.

MODIS. (1999) MODIS Vegetation Index (MOD 13): Algorithm Theoretical Basis Document, 3, pp. 26-29.

Morse, A and R.G. Allen (2001) Application of the SEBAL Methodology for Estimating ET and Consumptive Water-Use Through Remote Sensing; presented for the Raytheon Company, Upper Marlboro, MD.

National Weather Service (NWS) Southern Region Headquarters, National Oceanic & Atmospheric Administration (NOAA). Albuquerque, New Mexico 2006 Weather Highlights. [Online] Available at: http://www.srh.weather.gov/abq/climate/Monthlyreports/Annual/2006/summary_2006.php (accessed 7 July 2007). NWS, Albuquerque, N.M.

National Weather Service, National Oceanic and Atmospheric Administration (NOAA) 2006 Weather Highlights for the Albuquerque Region. [Online] Available at: http://www.srh.weather.gov/abq/climate/Monthlyreports/Annual/2006/summary_2006.php (accessed 1 July 2007). National Weather Service, Albuquerque, N.M.

New Mexico State Forestry et al. (2006) Socorro County Community Wildfire Protection Plan. NM State Forestry, BLM, Socorro County Commission, New Mexico Association of Counties, Socorro, NM.

Orr, B.J.; Bautista, S.; Alloza, J.A.; van Leeuwen, W.J.D.; Cassady, G.M.; Davison, J.E.; Wittenburg, L.; Malkinson, D.; Carmel, Y.; Neary, D.G. (2007) Satellite-derived vegetation dynamics applied to post-fire vulnerability assessment in eastern Spain. Proceedings of the 4th International Wildland Fire Conference, 13-17 May, 2007, Seville, Spain.

P, X., and S-S, L. (1994) A simple radiometric correction model to improve automatic mapping of vegetation from multispectral satellite data. *Remote Sensing of Environment*, 48, pp.191-204.

P, B., and M, J. M. (1998) Methods for quantifying fire severity in shrubland-fires. *Plant Ecology*, 139, pp. 91-101.

Parametrix, Inc (2006) Marcial Fire Burned Area Rehabilitation Plan. Albuquerque, NM.

Parker, D. L., M. Renz, A. Fletcher, F. Miller, and J. Gosz. (2005) Strategy for Long-Term Management of Exotic Trees in Riparian Areas for New Mexico's Five River Systems, 2005-2014. USDA, 29 pp.

Patterson, M.W. & Yool, S.R. (1998) Mapping fire induced vegetation mortality using LANDSAT TM data: A comparison of Linear transformation techniques. *Remote Sensing of Environment*. 65, pp.132-142.

Pelgrum, H., Bastiaanssen, W.B.M. (1996) An intercomparison of techniques to determine the area-averaged latent heat flux from individual in situ observations: a remote sensing approach using the European Field Experiment in a Desertification-Threatened Area data. *Water Resour. Res.*, 32, pp. 2775-2786.

Pereira, JMC. (1992) Burned area mapping with conventional and selective principal component analysis. *Finisterra*, 27, pp. 61-76.

Racher, Brent J.; Mitchell, Robert B.; Schmidt, Charles; Bryan, Justin (2001) Prescribed burning prescriptions for saltcedar in New Mexico. Research highlights--2001: Range, wildlife, and fisheries management. Texas Tech University, Department of Range, Wildlife, and Fisheries Management, 32 (25).

Riano, D.E. Chuvieco, S. Ustin, R. Zomer, P. Dennison, D. Roberts, J. Salas (2002) Assessment of Vegetation Regeneration After Fire Through Multitemporal Analysis of AVIRIS Images in the Santa Monica Mountains. *Remote Sensing of the Environment*, 79, pp. 60-71.

Robert T.G., R.L. Sheley and R.D. Carlstrom (2006) Saltcedar (Tamarisk). [Online] Available at: <http://www.montana.edu/wwwpb/pubs/mt9710.html> (accessed 26 September 2007). MSU, Bozeman, MT.

Roberts, D.A., Adams, J.B., and Smith, M.O. (1993) Discriminating Green Vegetation, Non-Photosynthetic Vegetation and Soils in AVIRIS Data, *Rem. Sens. Environ.*, 44 (2) pp. 255-270.

Robinson, J.M. (1991) Fire from space: Global evaluation using infrared remote sensing, *Int. J. Remote Sens.*, 12, pp. 3-24.

Roerink, G.J., Bastiaanssen, W.G.M., Chambouleyron, J., Menenti, M. (1997) Relating crop water consumption to irrigation water supply by remote sensing. *Water Resour. Manage.*, 11, pp. 445-465.

Rogan, J. & Yool, S. R. (2001) Mapping fire-induced vegetation depletion in the Peloncillo Mountains Arizona and New Mexico. *International Journal of Remote Sensing*, 22, pp. 3101-3121.

Rogan, J., Franklin, J., and D.A. Roberts (2002) A comparison of methods for monitoring multitemporal vegetation change using Thematic Mapper imagery. *Remote Sensing of Environment*, 80, pp. 143-156.

Roy, D.P., Boschetti, L., Trigg, S. (2006) Remote Sensing of Fire Severity: Assessing the performance of the Normalized Burn Ratio, *IEEE Geoscience and Remote Sensing Letters*, 3, pp.112-116.

Sala, Q., Smith, S.D., Devitt, D.A. (1996) Water use by *Tamarix* spp. *ramosissima* and associated phreatophytes in a Mojave desert floodplain. *Ecol. Applications*, 6(3) pp. 888-898.

Seastedt, T. R. and Briggs, J. M. (1991) Long-term ecological questions and considerations for taking long-term measurements: Lessons from the LTER and FIFE programs on tallgrass prairie. *Long Term Ecological Research: An International Perspective*, pp.152-172.

Shafroth, P.B., Stromberg, J.C., and Patten, D.T. (2000) Woody riparian vegetation response to different alluvial water table regimes. *Western North American Naturalist*, 60, pp. 66-76.

Shuttleworth, W.J., Gurney, R.J., Hsu, A.Y., Ormsby, J.P. (1989) The variation in energy partition at surface flux sites. In: *Proceedings of the IAHS Thrid International Assembly*, Baltimore, MD, 186, pp. 67-74.

Smith, L. M., M. D. Sprenger, and J. P. Taylor (2002) Effects of discing saltcedar seedlings during riparian restoration efforts. *Southwest. Nat.*, 47, pp. 598-642.

Smith, S.D., Devitt, D.A., Sala, A., Cleverly, J.R., and Busch, D.E. (1998) Water relations of riparian plants from warm desert regions. *Wetlands*, 18(4) pp. 687-696.

Socorro Soil Water Conservation District. Lower Rio Grande Salt Cedar Control Project. [Online] Available at: http://www.socorrosxcd.com/index_files/page0001.htm (accessed 1 May 2007). Socorro Soil Water Conservation District, Socorro, N.M.

Sunar, F. and Özkan, C. (2001) Forest fire analysis with remote sensing data. *International Journal of Remote Sensing* 22 (12) pp. 2265-2277.

Tasumi, M., Allen, R.G. (2000) Application of the SEBAL methodology for estimating consumptive use of water and stream flow depletion in the Bear River Basin of Idaho through remote sensing. Appendix A: The theoretical basis of SEBAL. Final report submitted to the Raytheon Systems Company, Earth Observation System Data and Information System Project.

Tasumi, M., R.G. Allen, R. Trezza, and J.L. Wright (2005) Satellite-based energy balance to assess within-population variance of Crop Coefficient curves. *Journal of Irrigation and Drainage Engineering*, 131 (1) pp. 94-109.

Taylor, J.P. 1996. Saltcedar management and riparian restoration. Presentation at the Saltcedar Management and Riparian Restoration Conference, Las Vegas, NV.

Taylor, John P. and McDaniel, Kirk C. (2004) Revegetation strategies after saltcedar (*Tamarix* spp.) control in headwater, transitional, and depositional watershed areas. *Weed Technology*, 18, pp. 1278-1282.

Teillet, P. M., Staenz, K., and Williams, D. J. (1997) Effects of Spectral, Spatial, and Radiometric Characteristics on Remote Sensing Vegetation Indices of Forested Regions. *Remote Sensing of Environment*, 61, pp. 139-149.

The US Geological Survey (2007) Landsat: A Global Land-Observing Program. [Online] Available at: <http://erg.usgs.gov/isb/pubs/factsheets/fs02303.html> (accessed 1 October 2007). USGS, Washington, D.C.

Thomas, P. A.; Wein, Ross W. (1985) The influence of shelter and the hypothetical effect of fire severity on the postfire establishment of conifers from seed. *Canadian Journal of Forest Research*, 15, pp. 148-155.

Troxel-Stowe et. al. (2007) Request for Proposal for Lower Rio Grande Salt Cedar Control Project. Socorro Soil Water Conservation District (SSWCD), Socorro, NM, 31 pp.

Troxel-Stowe, Nyleen. Interview with Nyleen Troxel Stowe. SSWCD, Socorro, 7 March 2008.

Twele, André and Barbosa, Paulo (2004) Monitoring vegetation regeneration after Forest Fires using satellite imagery. In: Proceedings of the 24th Symposium of the European Association of Remote Sensing Laboratories, Dubrovnik, Croatia, 25-27 May, 2004.

U.S. Bureau of Reclamation. Dams, Projects, and Power Plants, San Acacia Diversion Dam. [Online] Available at: http://www.usbr.gov/dataweb/dams/san_acacia_diversion.html (accessed 4 May 2007). U.S. Bureau of Reclamation, Washington, D.C.

U.S. Census Bureau. New Mexico county population estimates: April 1, 2005 to July 1, 2006-Table CO-EST2006-01-35, [Online] Available at: <http://www.census.gov> (accessed 15 June 2007) U.S. Census Bureau, Washington, D.C.

Ustin, S.I., D.A. Roberts, J.A. Gamon, G.P. Asner, and R.O. Green (2004) Using Imaging Spectroscopy to Study Ecosystem Processes and Properties. *BioScience*, 54, pp. 523-534.

Van de Hurk, B.J.J.M., Bastiaanssen, W.G.M., Pelgrum, H., van Meijgaard, E., (1997) A new methodology for assimilation of initial soil moisture fields in weather prediction models using Meteosat and NOAA data. *J. Appl. Meteor.*, 36, pp. 1271-1283.

Viedma, O., Melia, J., Segarra, D., and Garcia-Haro, J. (1997) Modeling Rates of Ecosystem Recovery after Fires by Using Landsat TM data. *Remote Sensing of Environment*, 61, pp. 383-398.

Waller, Eric (1999) A Comparison of Landsat Multispectral Scanner Imagery and Aerial Photography for Identifying Land Cover Change in Coastal Southern California. MS Thesis. UCSB, Santa Barbara.

Wang, J., T. W. Sammis, C. A. Meier, L. J. Simmons, D. R. Miller, and D. J. Bathke (2005) Remote Sensing Vegetation Recovery after Forest Fires using Energy Balance Algorithm. Presented at the Sixth Symposium on Fire and Forest Meteorology Sponsored by American Meteorological Society, Canmore, AB, Canada, 25-27 October, 2005.

Wang, J., T.W. Sammis, C.A. Meier, L.J. Simmons, D.R. Miller, and Z. Samani. (2005) A modified SEBAL model for spatially estimating pecan consumptive water use for Las Cruces, New Mexico. 15th Conference on Applied Climatology. Hilton Savannah DeSoto, Savannah, Georgia. 20-24 June, 2005.

Weeks, E.P., Weaver, H.L., Campbell, G.S., and Tanner, B.D. (1987) Water use by saltcedar and by replacement vegetation in the Pecos river floodplain between Acme and Artesia, New Mexico. *Studies of Evapotranspiration*, U.S. Geol. Survey Professional Paper 491, 37 pp.

White, J.D., Ryan, K.C., Key, C.C., Running, S.W. (1996) Remote Sensing of forest fire severity & Vegetation Recovery. *International Journal of Wild land Fire*, 6 (3) pp.125-136.

White, L.D., Hays, K.B., and Schmidt, K.M. (2003) Water use by saltcedar and associated vegetation along selected rivers in Texas. *Saltcedar and Water Resources in the West Symposium*. 16-17 July, 2004, San Angelo, Texas, pp. 53-73.

Wiesenborn, W.D. (1996) Saltcedar impacts on salinity, water, fire frequency-
Wilkinson, R.E. (1972) Water stress in saltcedar. *Botanical Gazette*, 133 (1) pp. 73-77.

Wulder, M. (1998) Optical remote-sensing techniques for the assessment of forest inventory and biophysical parameters. *Progress in Physical Geography*, 22, pp. 449-476.

Wulder, M.A., R.J. Hall, C.C. Coops, and S.E. Franklin (2004) High Spatial Resolution Remotely Sensed Data for Ecosystem Characterization. *BioScience*, 54, pp. 511-521.

Zhan, X., Sohlberg, R. A., Townshend, J. R. G., DiMiceli, C., Carroll, M. L., Eastman, J. C., et al. (2002) Detection of land cover changes using MODIS 250 m data. *Remote Sensing of Environment*, 83, pp. 336– 350.

Zouhar, Kris (2003) *Tamarix* spp. In: Fire Effects Information System, U.S. Department of Agriculture, Forest Service, Rocky Mountain Research Station, Fire Sciences Laboratory. [Online] Available at: <http://www.fs.fed.us/database/feis/> (accessed 14 June 2007). Rocky Mountain Research Station, Ft Collins, CO.

APPENDIX A. 9-PIXEL PLOTS

The 9-Pixel Plot data was generated in order to do a comparison between the Summer 2006 Field Campaign data and the SEBAL maps discussed in Section 4.1. The 9-Pixel Plot data provides a pin-pointed, micro- perspective with data from 15 image dates in contrast to a macro-perspective of the SEBAL maps in Section 4.1 from only 4 image dates. The 9-Pixel Plot locations for each fire site are presented in Figures 31-33. Changes in albedo, Daily (ET_{24}) and Instantaneous ET (ET_{Inst}), ground heat flux (G), Leaf Area Index (LAI), Normalized Difference Vegetation Index (NDVI), and Surface Temperature (T_s) were tracked at the 9-Pixel Plots that corresponded to field sampling locations. This was done by extracting data on the above parameters from 3x3 "9-Pixel Plot" SEBAL output which is calculated for each 30x30 meter pixel in a LandsatTM image. Specifically, the data (mean and standard deviation of the parameters) is extracted using the Zonal Statistics tool in ArcGIS. The follow 9-Pixel Plot Figures are plots of mean values of energy balance parameters of interest (y-axis) for each respective 9-Pixel Number (x-axis) for data extracted from 15 SEBAL image dates—one line represents data for one date. The target center coordinate for each of the 9-Pixels was centered on the center coordinate of each macroplot sampled during the summer of 2006 field campaign.

Mitchell Fire

Fire Date: April 9-16, 2005

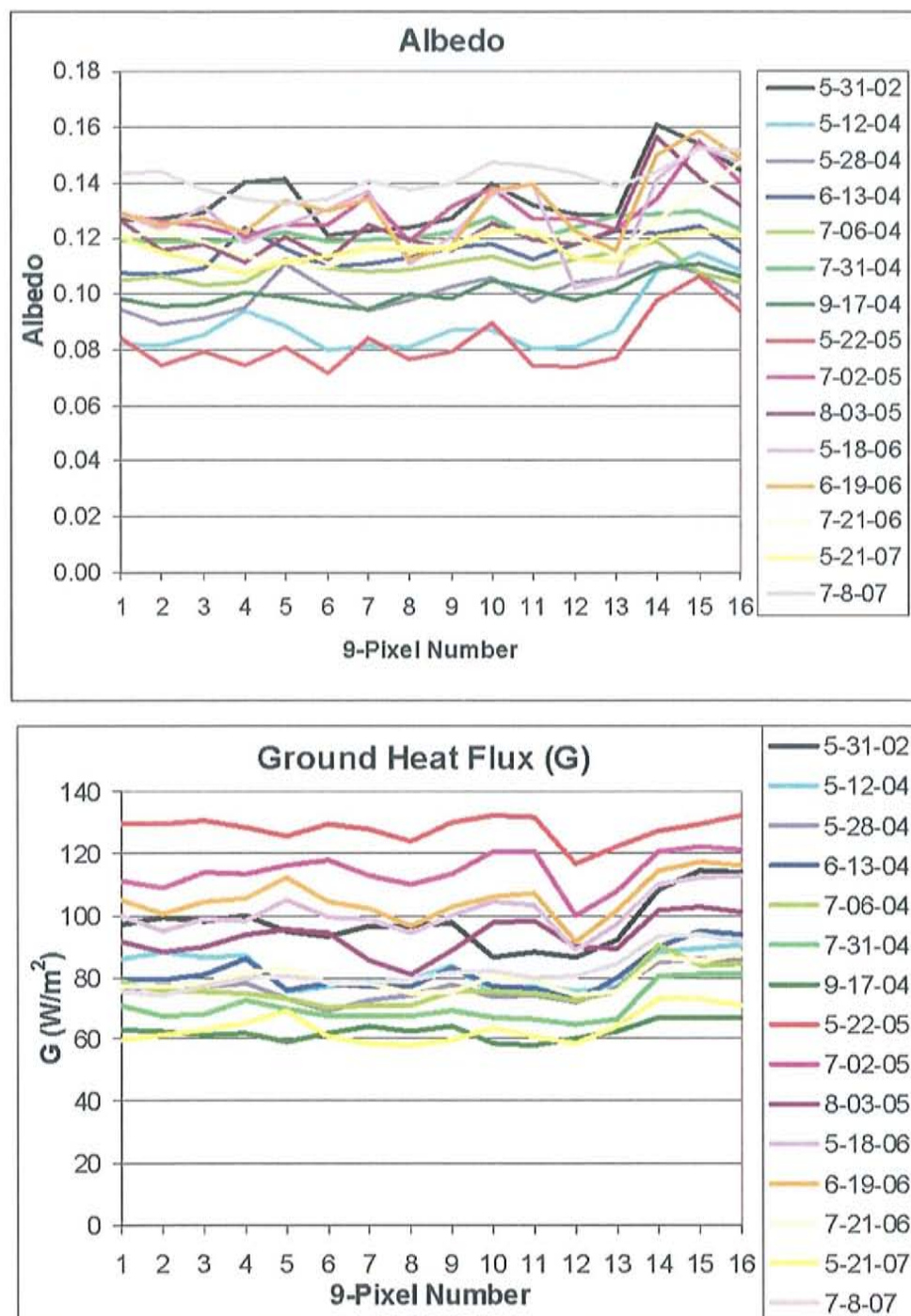


Figure A.1. Plots of Albedo and Ground Heat Flux derived from the SEBAL model and the stated image dates. Each 9-Pixel represents a macroplot sampling location from the Summer 2006 Field Campaign.

Mitchell Fire

Fire Date: April 9-16, 2005

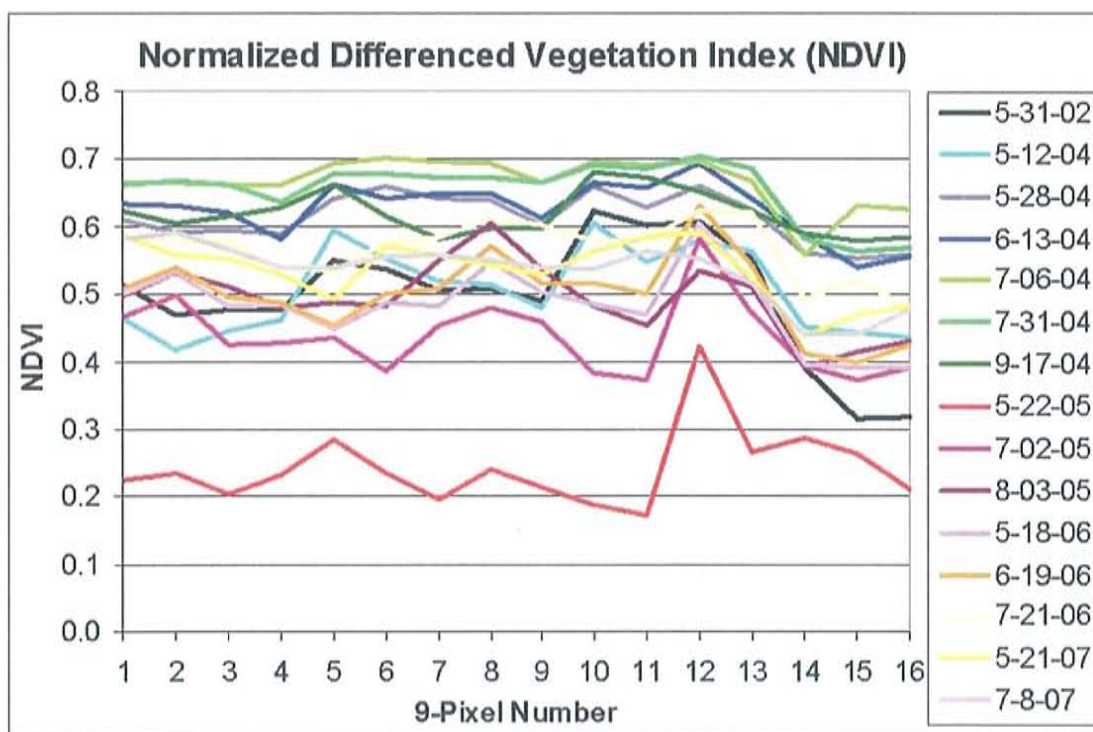
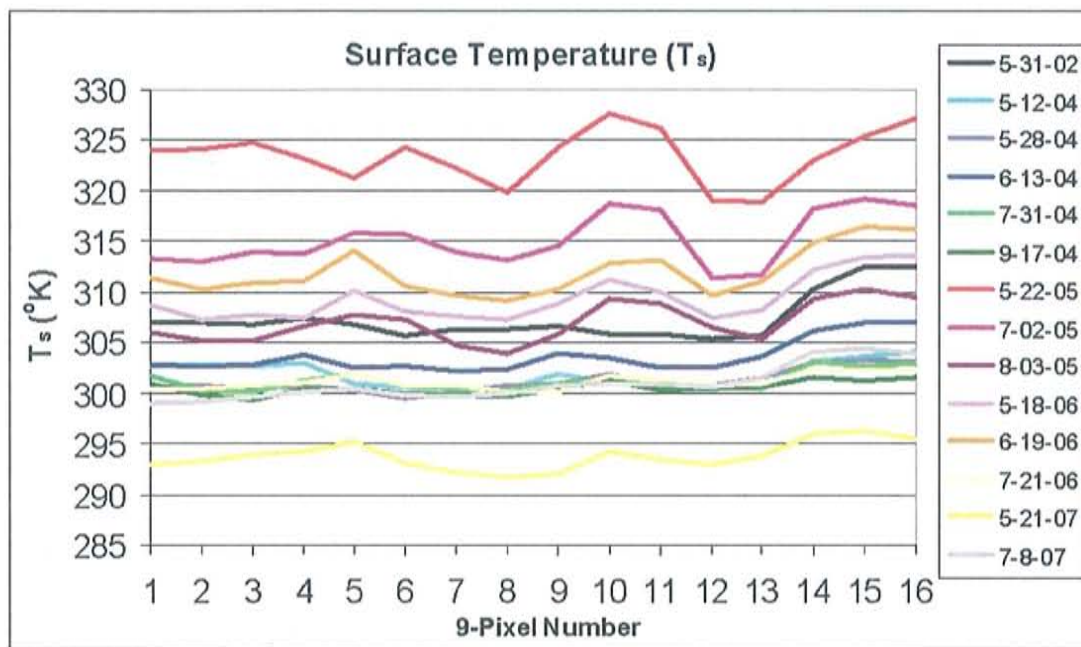


Figure A.2. Plots of Surface Temperature and NDVI derived from the SEBAL model and the stated image dates. Each 9-Pixel represents a macroplot sampling location from the Summer 2006 Field Campaign.

Mitchell Fire

Fire Date: April 9-16, 2005

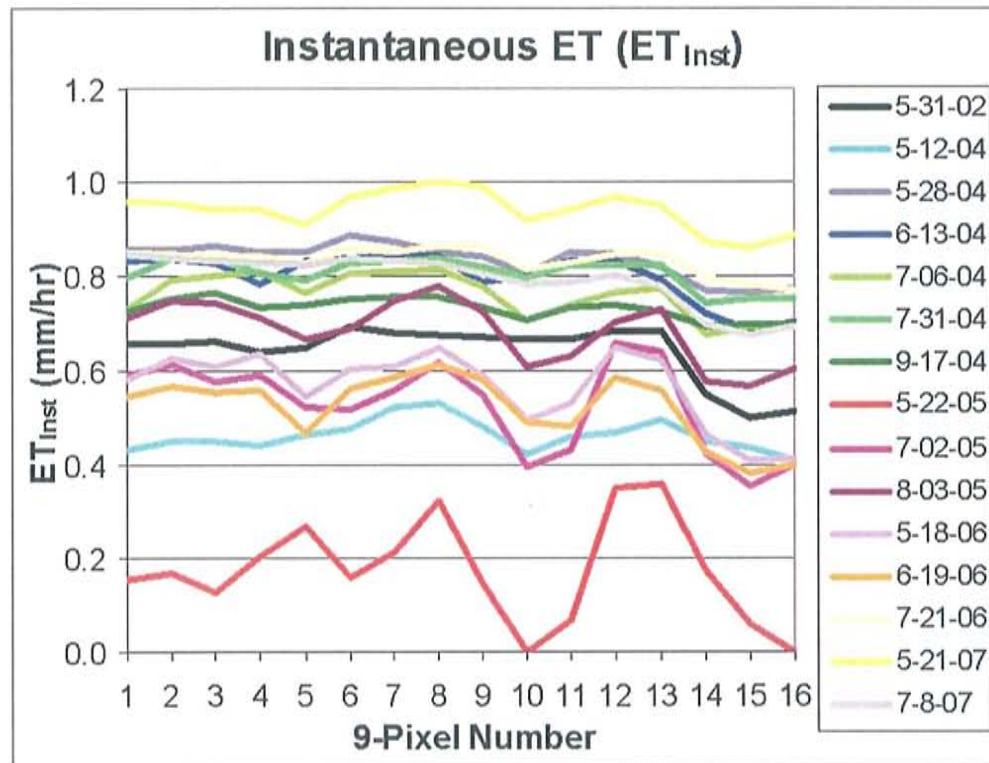
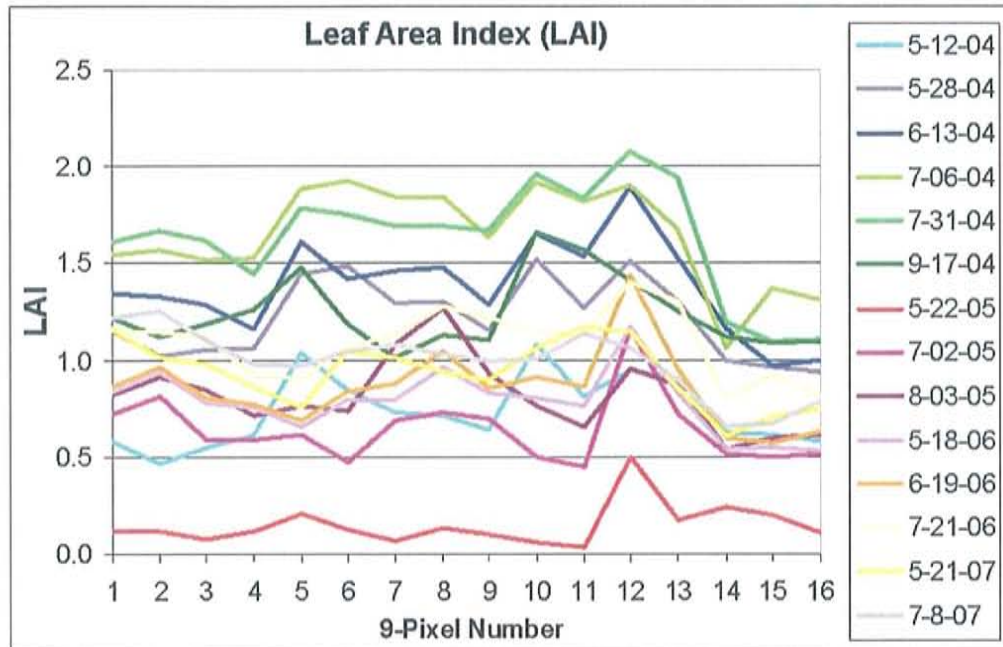


Figure A.3. Plots of LAI and Instantaneous Evapotranspiration derived from the SEBAL model and the stated image dates. Each 9-Pixel represents a macroplot sampling location from the Summer 2006 Field Campaign.

Mitchell Fire

Fire Date: April 9-16, 2005

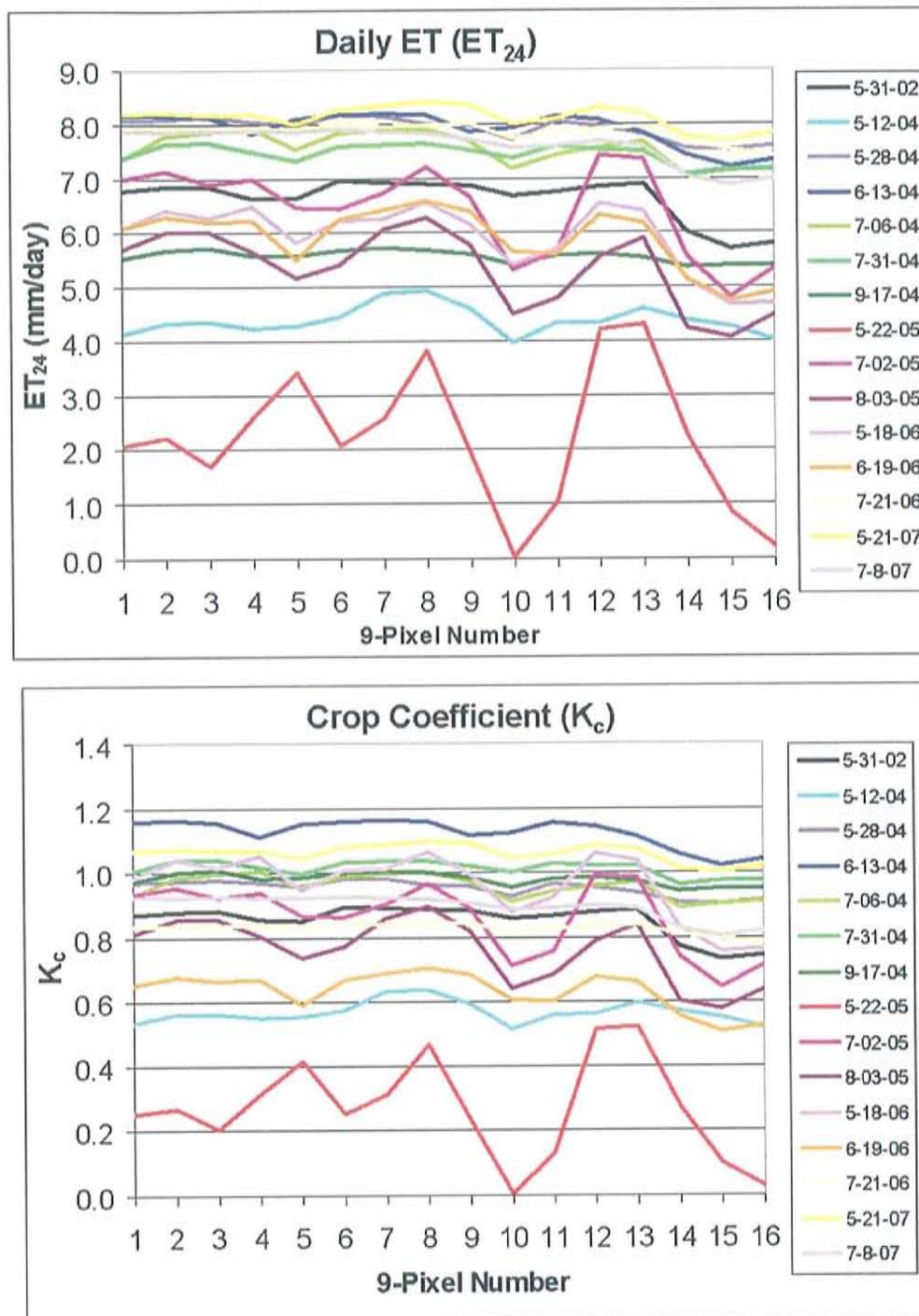


Figure A.4. Plots of Daily Evapotranspiration and the Crop Coefficient derived from the SEBAL model and the stated image dates. Each 9-Pixel represents a macroplot sampling location from the Summer 2006 Field Campaign.

Marcial Fire

Fire Date: May 3-10, 2006

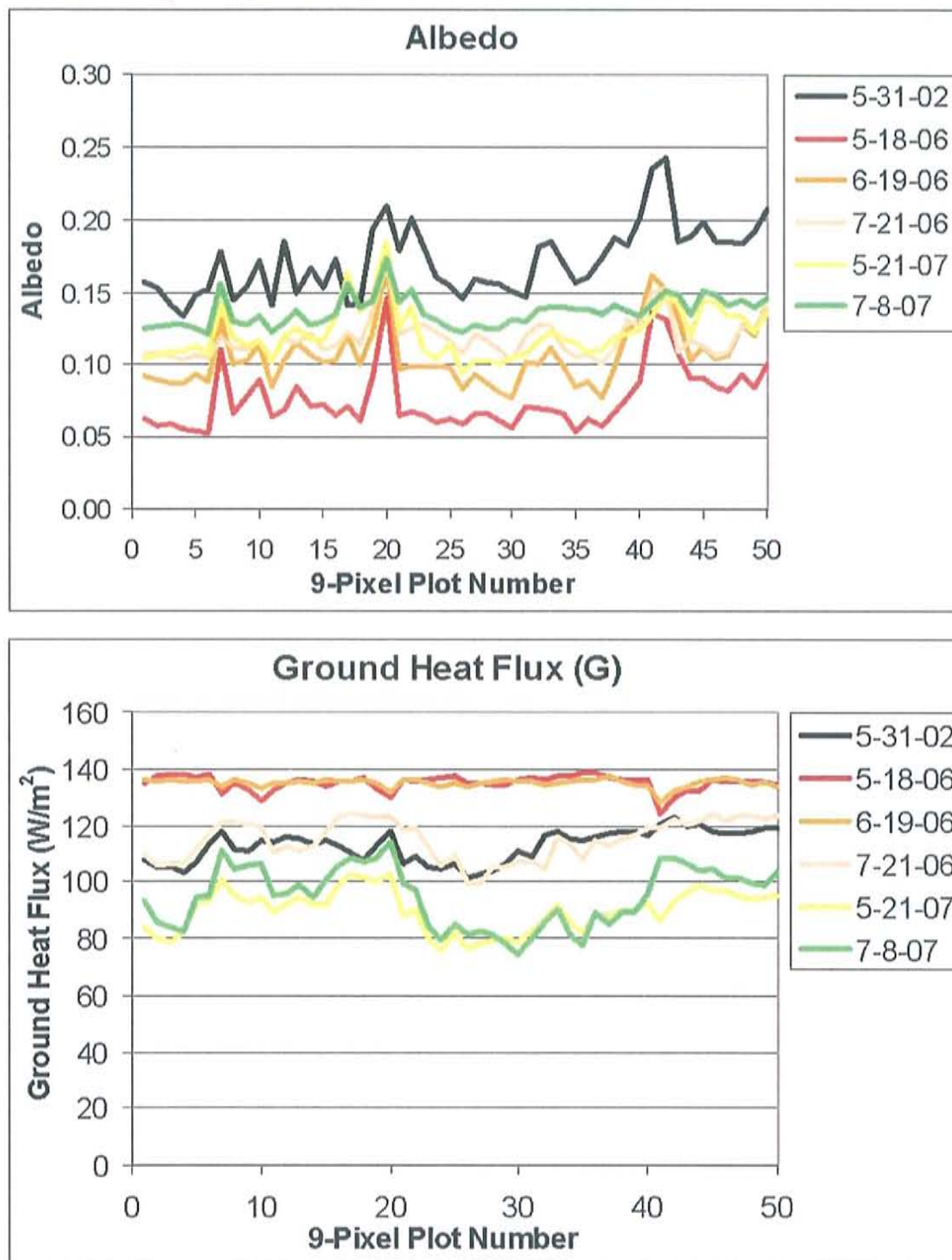


Figure A.5. Plots of Albedo and Ground Heat Flux derived from the SEBAL model and the stated image dates. Each 9-Pixel represents a macroplot sampling location from the Summer 2006 Field Campaign.

Marcial Fire

Fire Date: May 3-10, 2006

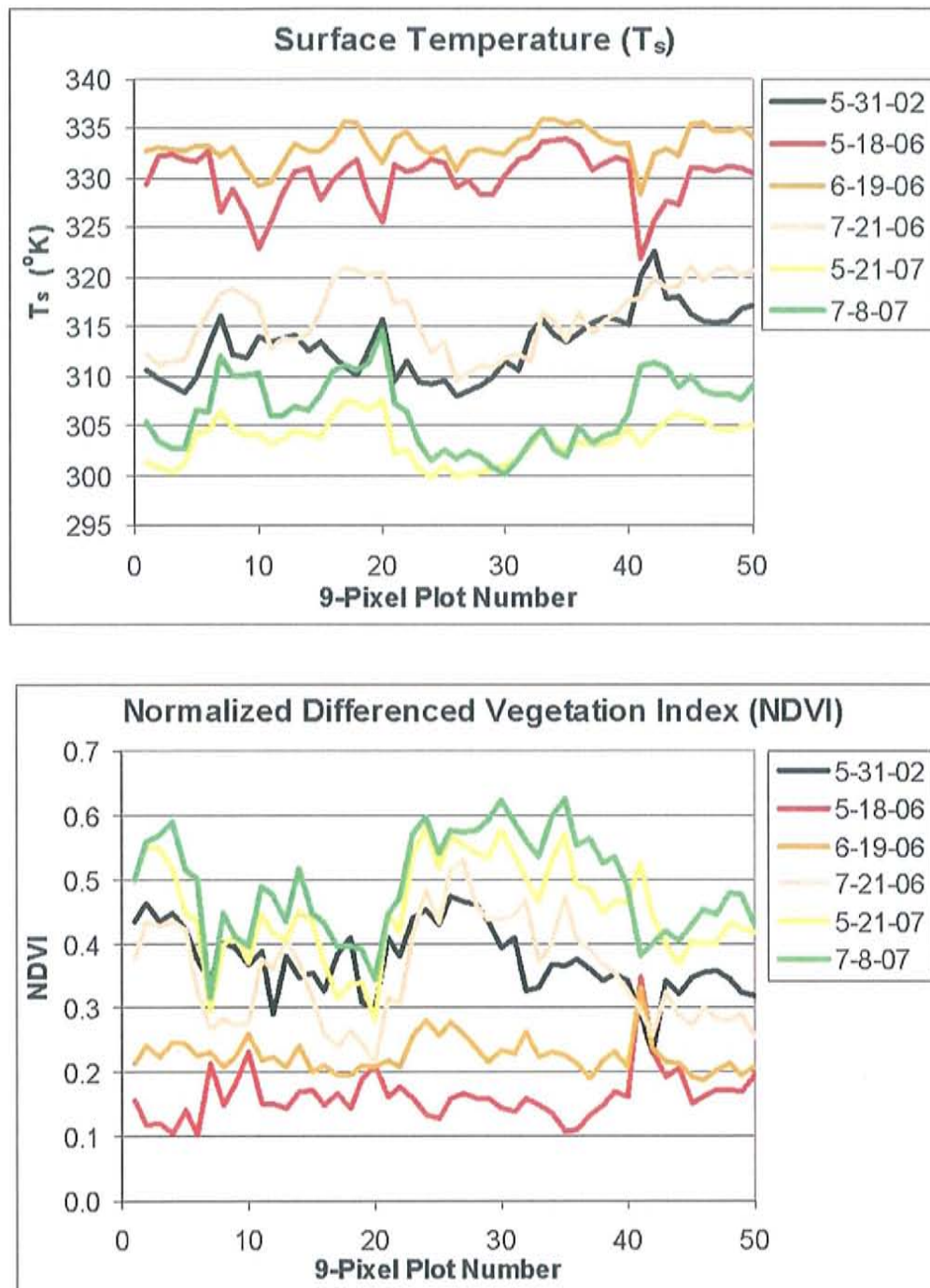


Figure A.6. Plots of Surface Temperature and NDVI derived from the SEBAL model and the stated image dates. Each 9-Pixel represents a macroplot sampling location from the Summer 2006 Field Campaign.

Marcial Fire

Fire Date: May 3-10, 2006

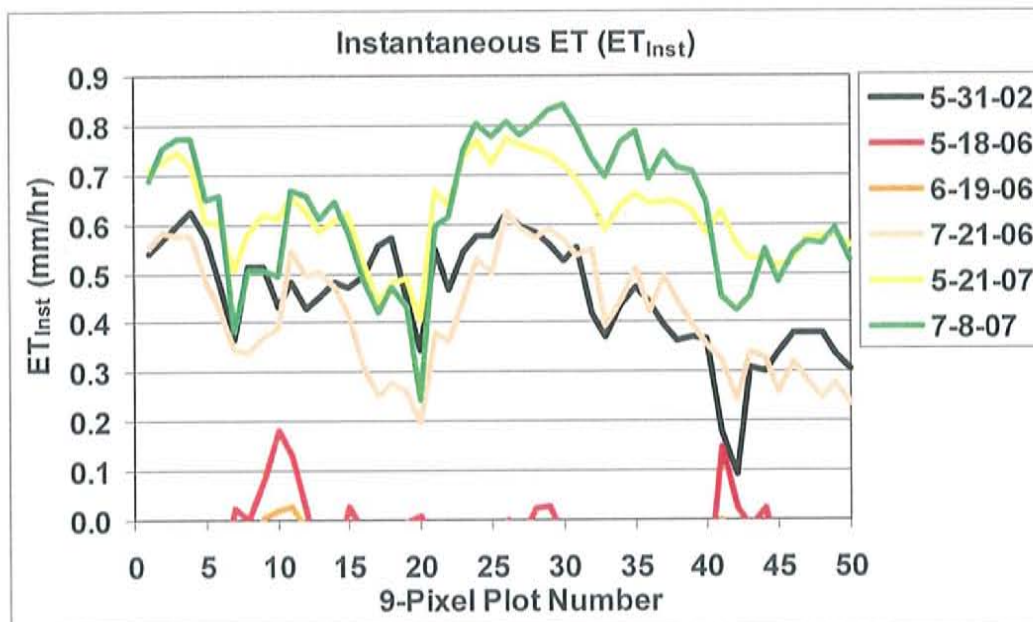
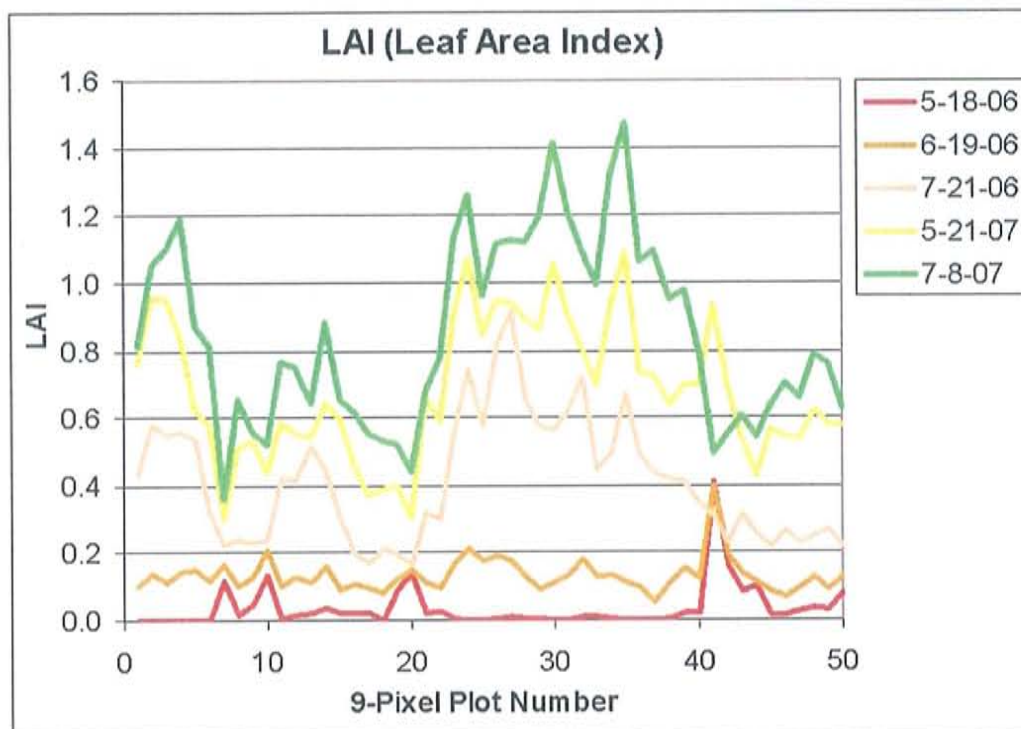


Figure A.7. Plots of Leaf Area Index and Instantaneous Evapotranspiration derived from the SEBAL model and the stated image dates. Each 9-Pixel represents a macroplot sampling location from the Summer 2006 Field Campaign.

Marcial Fire

Fire Date: May 3-10, 2006

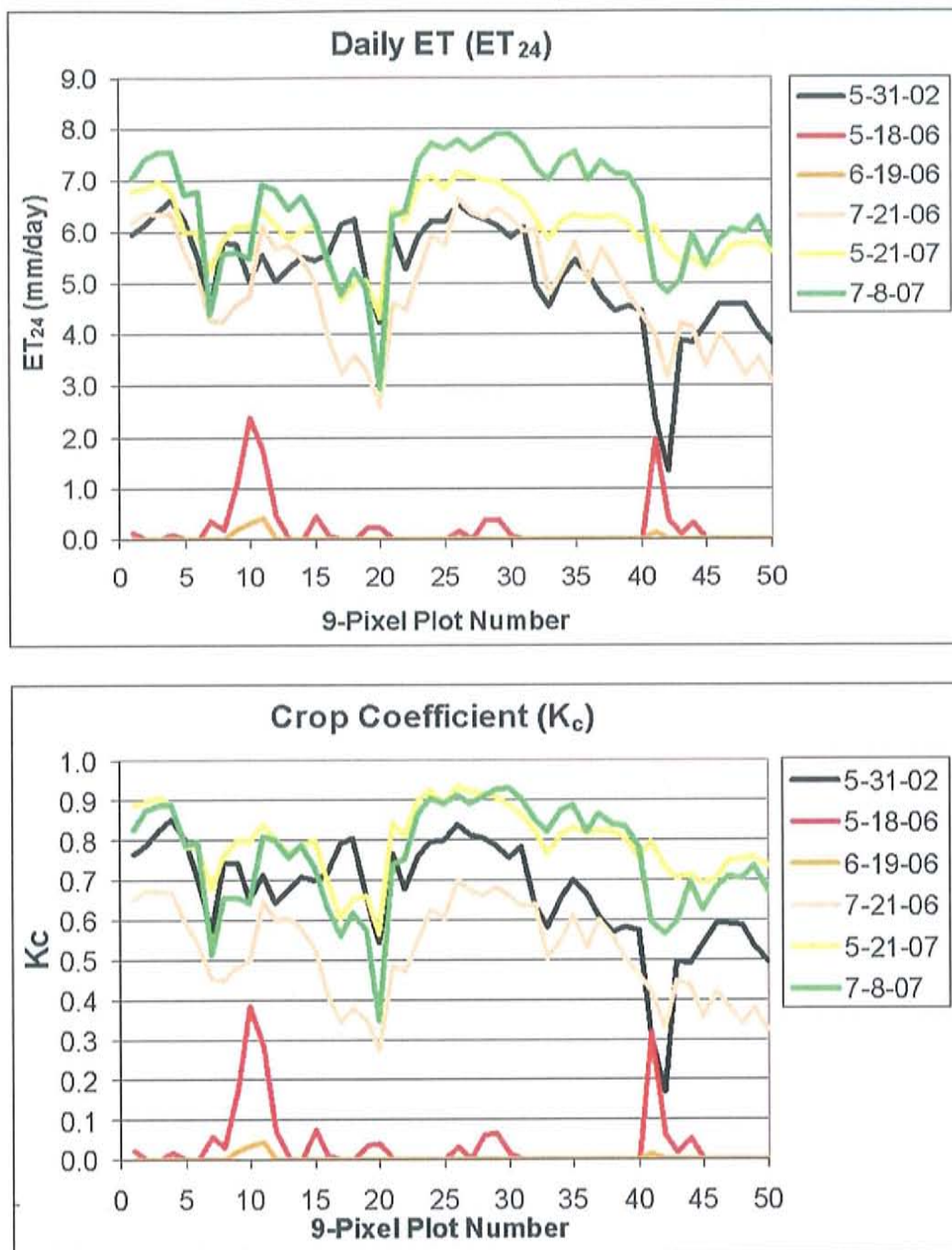


Figure A.8. Plots of Daily Evapotranspiration and Crop Coefficient derived from the SEBAL model and the stated image dates. Each 9-Pixel represents a macroplot sampling location from the Summer 2006 Field Campaign.

Bosquecito Fire

Fire Date: June 6-9, 2006

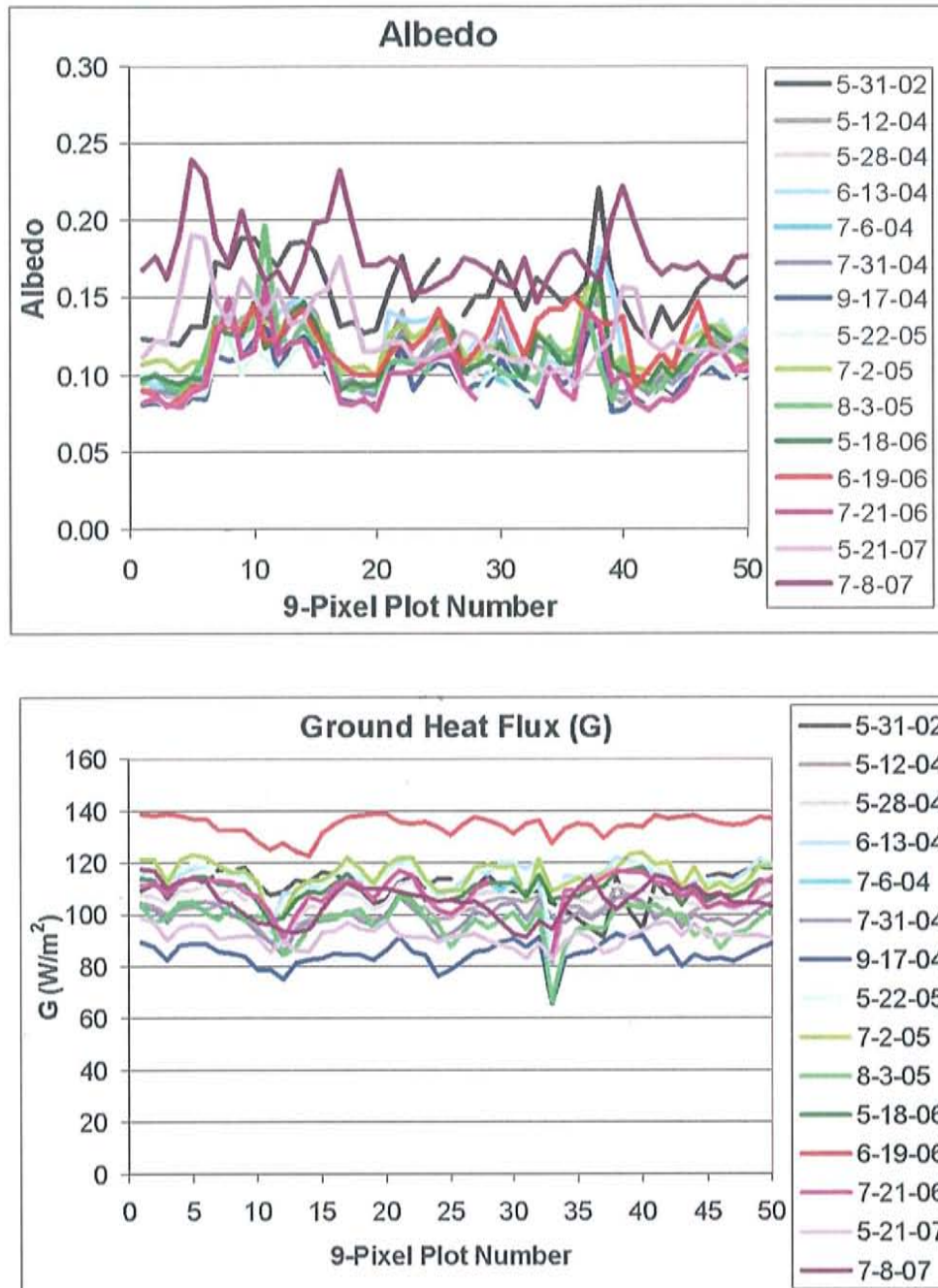


Figure A.9. Plots of Albedo and Ground Heat Flux derived from the SEBAL model and the stated image dates. Each 9-Pixel represents a macroplot sampling location from the Summer 2006 Field Campaign.

Bosquecito Fire

Fire Date: June 6-9, 2006

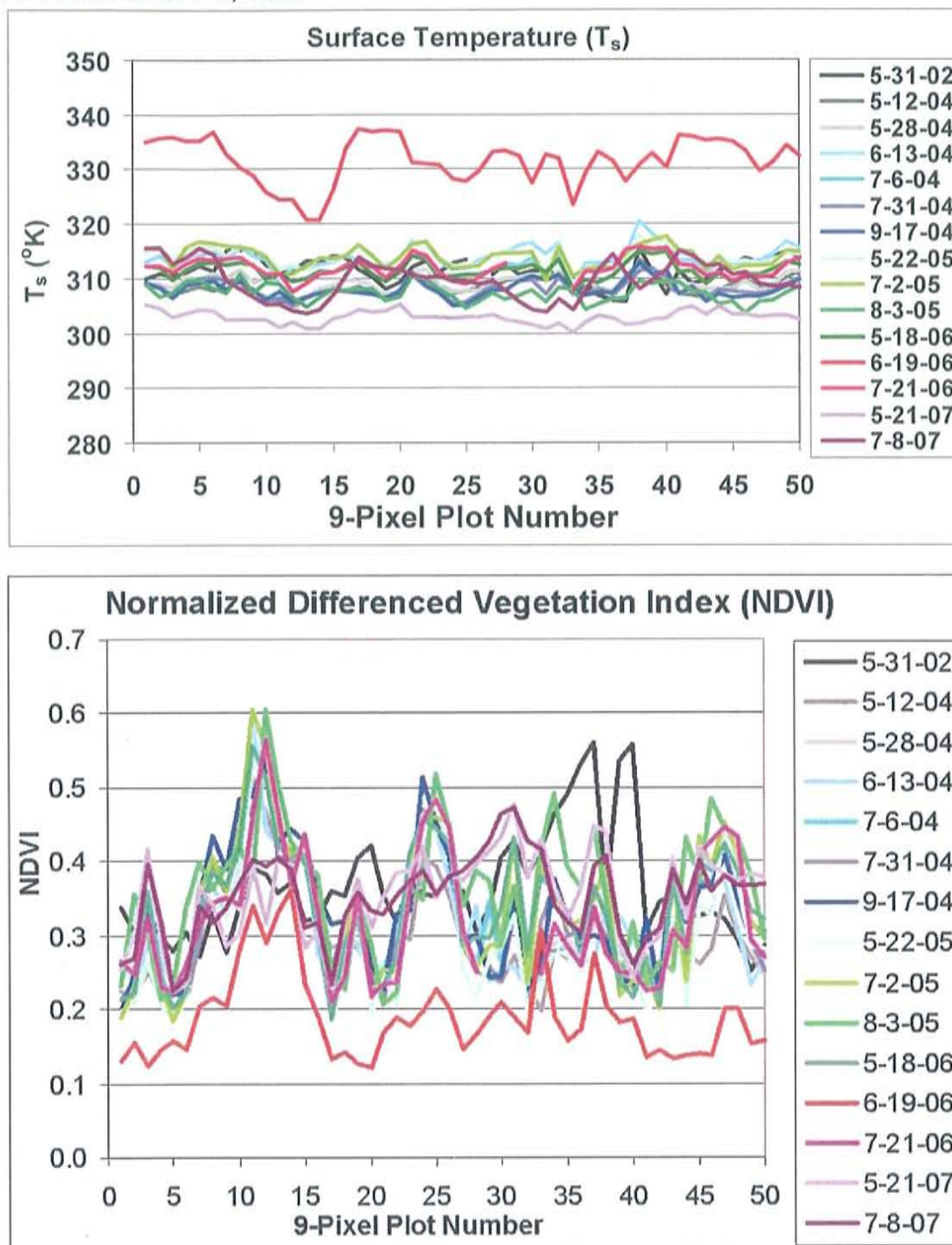


Figure A.10. Plots of Surface Temperature and NDVI derived from the SEBAL model and the stated image dates. Each 9-Pixel represents a macroplot sampling location from the Summer 2006 Field Campaign.

Bosquecito Fire
Fire Date: June 6-9, 2006

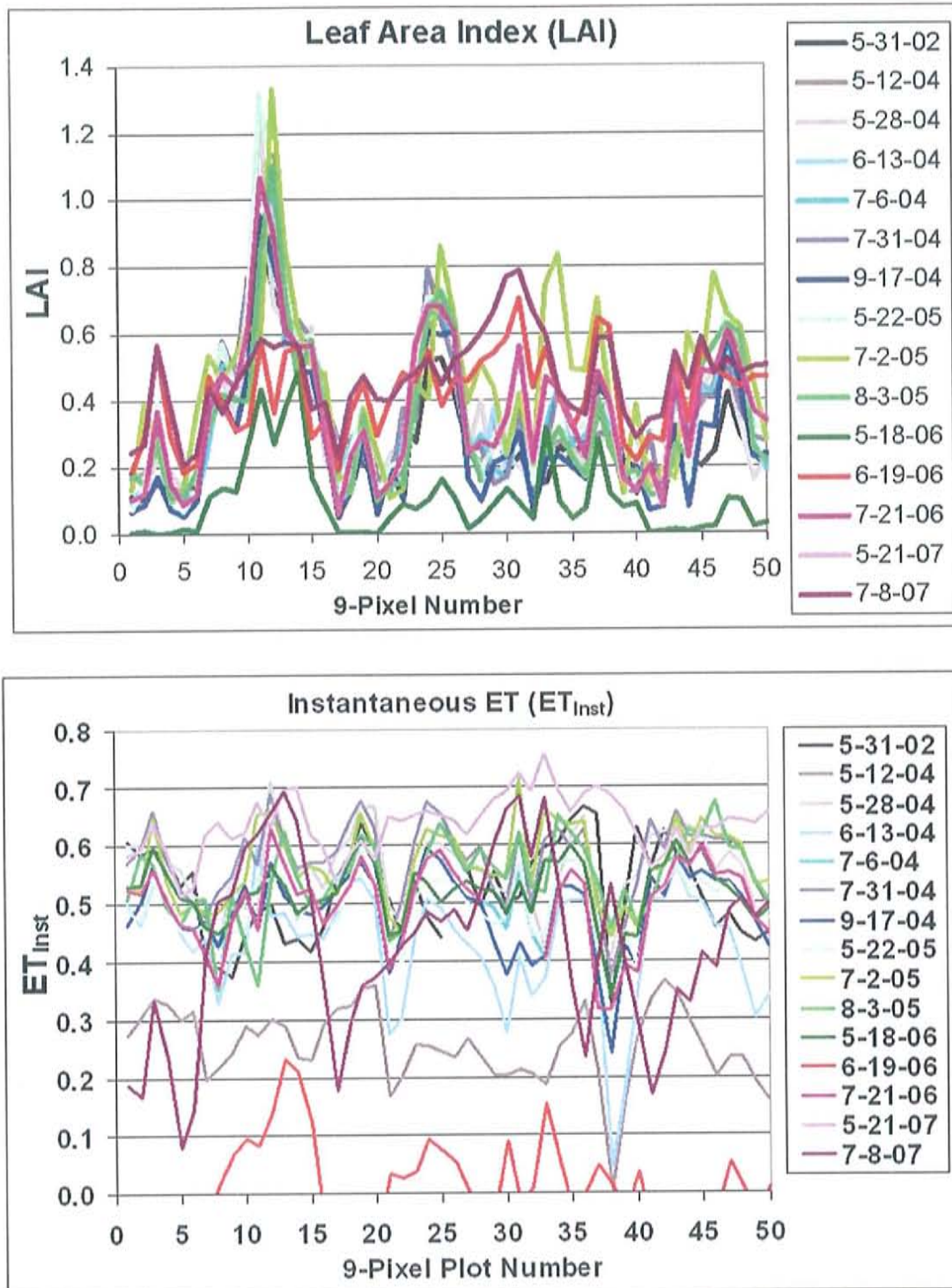


Figure A.11. Plots of LAI and Instantaneous Evapotranspiration derived from the SEBAL model and the stated image dates. Each 9-Pixel represents a macroplot sampling location from the Summer 2006 Field Campaign.

Bosquecito Fire

Fire Date: June 6-9, 2006

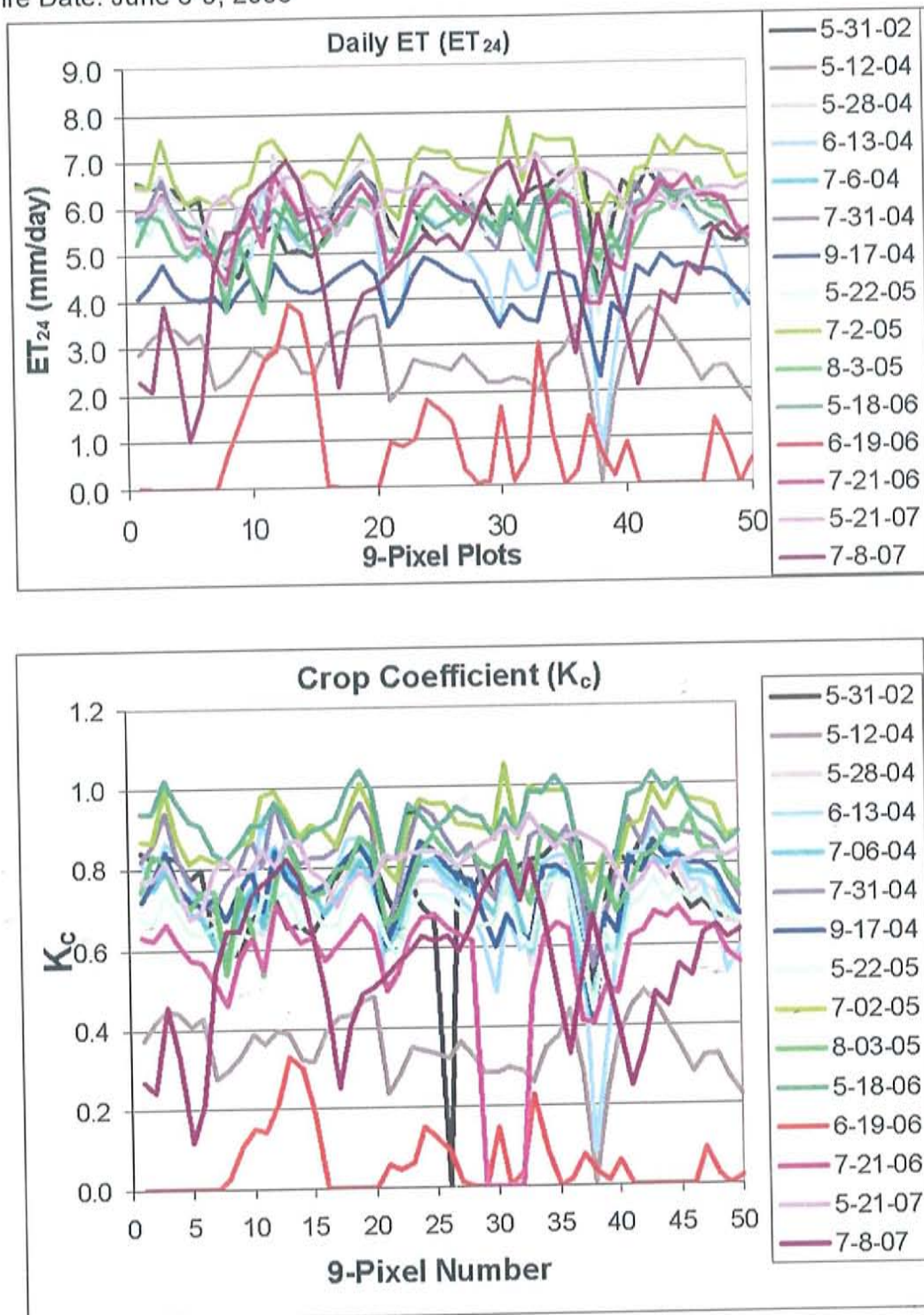


Figure A.12. Plots of Daily Evapotranspiration and the Crop Coefficient derived from the SEBAL model and the stated image dates. Each 9-Pixel represents a macroplot sampling location from the Summer 2006 Field Campaign.

APPENDIX B. SUMMER 2006 FIELD SAMPLING DATA

The following data was recorded from August 7 to October 25, 2007 from ocular measurements of various fire and vegetation parameters to obtain a representation of actual conditions in the field after each of the three fire sites. Data for each parameter was averaged over the four quadrats, resulting in one value per macroplot, and there were up to 10 macroplots per line transect within each fire site. Cover means vegetation cover and is expressed as the percentage of the surface area over which a plant exerts its influence upon other components of the ecosystem.

MITCHELL SUMMER 2006 FIELD SAMPLING DATA

Location	Date	Examiner	Datum	Elev	Trans_ num	Plot_num	Waypt_ num	9_pixel_ num	Plot_Type	Latitude	Longitude	UTM_E	UTM_N
MIT	10/11/2006	NLA	WGS 84	4566	1	1	123	17	M			329982	3755512
MIT	10/11/2006	NLA	WGS 84	4556	1	2	124	18	M			329992	3755399
MIT	10/11/2006	NLA	WGS 84	4560	1	3	125	19	M			330001	3755285
MIT	10/11/2006	NLA	WGS 84	4559	1	4	126	20	M			330013	3755179
MIT	10/11/2006	NLA	WGS 84	4552	1	5	127	21	M			329996	3755082
MIT	10/11/2006	NLA	WGS 84	4570	1	6	129	22	M			329992	3754968
MIT	10/11/2006	NLA	WGS 84	4566	1	7	130	23	M			329980	3754866
MIT	10/11/2006	NLA	WGS 84	4571	1	8	131		M			329978	3754758
MIT	10/11/2006	NLA	WGS 84	4567	1	9	132		M			329963	3754644
MIT	10/11/2006	NLA	WGS 84	4570	1	10	133		M			329973	3754536
MIT	10/23/2006	NLA	WGS 84	4550	2	1	136	1	M	33.92028	-106.8481	329161.4	3754855
MIT	10/23/2006	NLA	WGS 84	4545	2	2	138	2	M	33.9212	-106.8481	329160.5	3754957
MIT	10/23/2006	NLA	WGS 84	4551	2	3	139	3	M	33.92207	-106.848	329174.3	3755053
MIT	10/23/2006	NLA	WGS 84	4539	2	4	140	4	M	33.9228	-106.8484	329138.7	3755135
MIT	10/23/2006	NLA	WGS 84	4534	3	1	142	5	M	33.9202	-106.846	329355.4	3754842
MIT	10/23/2006	NLA	WGS 84	4566	3	2	143	6	M	33.92125	-106.8461	329348.3	3754959
MIT	10/23/2006	NLA	WGS 84	4562	3	3	144	7	M	33.92222	-106.846	329359.5	3755066
MIT	10/23/2006	NLA	WGS 84	4554	3	4	145	8	M	33.92315	-106.8458	329377	3755169
MIT	10/23/2006	NLA	WGS 84	4553	3	5	146	9	M	33.9236	-106.8458	329380.7	3755219
MIT	10/25/2006	NLA	NAD 83	4574	4	1	147	10	M	33.91958	-106.8439	329548.3	3754770
MIT	10/25/2006	NLA	NAD 83	4557	4	2	148	11	M	33.9205	-106.844	329540.9	3754872
MIT	10/25/2006	NLA	NAD 83	4538	4	3	149	12	M	33.9215	-106.844	329542.9	3754983
MIT	10/25/2006	NLA	NAD 83	4561	4	4	150	13	M	33.9225	-106.8443	329517.2	3755095
MIT	10/25/2006	NLA	NAD 83	4554	4	5	151	14	M	33.9236	-106.844	329547.1	3755216
MIT	10/25/2006	NLA	NAD 83	4560	4	6	152	15	M	33.9246	-106.8439	329558.3	3755327
MIT	10/25/2006	NLA	NAD 83	4556	4	7	153	16	M	33.9252	-106.8439	329559.5	3755393

Table B.1. Summary of ocular data collected at the Mitchell Fire Site in October of 2006, 18 months after the fire.

MITCHELL SUMMER 2006 FIELD SAMPLING DATA

Pg. 2

Trans_ num	Plot_num	Total_Tree _Cover	Ttl_Tree_ Percent	Dominant _Species	Stand _ft	Stand_m	Seedling_ Cover	Sapling_ Cover	Shrub_ Cover	Shrub_ percent	Graminoid _Cover	Graminoid _percent	Forb_ Cover
1	1	0.4	40	Graminoid	20	6.096	0	0	0	0	0.6	60	0
1	2	0.4	40	Graminoid	10	3.048	0	0	0.005	0.5	0.6	60	0
1	3	0.1	10	Graminoid	15	4.572	0	0	0.005	0.5	0.9	90	0
1	4	0.3	30	Graminoid	8	2.4384	0	0	0	0	0.6	60	0.005
1	5	0.4	40	Graminoid	18	5.4864	0	0	0.03	3	0.5	50	0.03
1	6	0.2	20	Graminoid	10	3.048	0	0	0.03	3	0.6	60	0.1
1	7	0.03	3	Forb	20	6.096	0	0	0.03	3	0	0	0.9
1	8	0.2	20	Forb	15	4.572	0	0	0.03	3	0	0	0.7
1	9	0.005	0.5	Forb	20	6.096	0	0	0.2	20	0.1	10	0.5
1	10	0	0	Shrub	0	0	0	0	0.4	40	0.03	3	0.005
2	1	0.8	80	Saltcedar	10	3.048	0	0	0	0	0	0	0
2	2	0.9	90	Saltcedar	8	2.4384	0	0	0	0	0	0	0
2	3	0.9	90	Saltcedar	10	3.048	0	0	0	0	0	0	0
2	4	0.98	98	Saltcedar	18	5.4864	0	0	0	0	0	0	0
3	1	0.9	90	Saltcedar	10	3.048	0	0	0	0	0	0	0
3	2	0.8	80	Saltcedar	8	2.4384	0	0	0	0	0.03	3	0
3	3	0.9	90	Saltcedar	8	2.4384	0	0	0	0	0.005	0.5	0
3	4	0.98	98	Saltcedar	15	4.572	0	0	0	0	0	0	0
3	5	0.9	90	Saltcedar	15	4.572	0	0	0	0	0	0	0
4	1	0.9	90	Saltcedar	9	2.7432	0	0	0	0	0	0	0
4	2	0.9	90	Saltcedar	10	3.048	0	0	0	0	0	0	0
4	3	0.9	90	Saltcedar	28	8.5344	0	0	0	0	0	0	0
4	4	0.98	98	Saltcedar	25	7.62	0	0	0	0	0	0	0
4	5	0.6	60	Saltcedar	20	6.096	0	0	0	0	0.4	40	0
4	6	0.7	70	Saltcedar	6	1.8288	0	0	0	0	0.1	10	0
4	7	0.8	80	Saltcedar	8	2.4384	0	0	0	0	0	0	0

Table B.1. Summary of ocular data collected at the Mitchell Fire Site in October of 2006, 18 months after the fire.

MITCHELL SAMPLING DATA

Trans_ num	Plot_num	Forb_percent	Comboveg	Bare_Soil_Cover	Bsoil_Percent	Gravel_Cover	Soil_Texture	Erosion_Type	Erosion_Severity	Fire_Intensity
1	1	0	60	0	0	0	C	Zero	0	3
1	2	0	60.5	0.005	0.5	0	C	Zero	0	3
1	3	0	90.5	0.03	3	0	C	Zero	0	3
1	4	0.5	60.5	0.005	0.5	0	C	Zero	0	3
1	5	3	56	0.005	0.5	0	C	Zero	0	3
1	6	10	73	0.03	3	0	C	Zero	0	3
1	7	90	93	0.03	3	0	C	Zero	0	2
1	8	70	73	0.03	3	0	C	Zero	0	2
1	9	50	80	0.2	20	0	C	Zero	0	2
1	10	0.5	43.5	0.5	50	0	VFS	Gully	2	2
2	1	0	0	0.2	20	0	top 2": C; bottom: SI	Zero	0	2
2	2	0	0	0.1	10	0	top 2": C; bottom: SI	Zero	0	2
2	3	0	0	0.1	10	0	top 2": C; bottom: SI	Zero	0	2
2	4	0	0	0.03	3	0	top 2": C; bottom: SI	Zero	0	2
3	1	0	0	0.1	10	0	top 3": C; bottom: SI	Zero	0	2
3	2	0	3	0.1	10	0	top 3": C; bottom: SI	Zero	0	2
3	3	0	0.5	0.1	10	0	top 3": C; bottom: SI	Zero	0	2
3	4	0	0	0.03	3	0	top 4": C; bottom: SI	Zero	0	2
3	5	0	0	0.1	10	0	top 4": C; bottom: SI	Zero	0	2
4	1	0	0	0.1	10	0	VFS	Gully	1	2
4	2	0	0	0.1	10	0	VFS	Gully	1	2
4	3	0	0	0.1	10	0	3" clay, S bottom	Zero	0	2
4	4	0	0	0.03	3	0	3" clay, S bottom	Zero	0	2
4	5	0	40 ^w	0	0	0	3" clay, S bottom	Zero	0	2
4	6	0	10	0.2	20	0	3" clay, S bottom	Zero	0	2
4	7	0	0	0.2	20	0	3" clay, SIL bottom	Zero	0	2

Table B.1. Summary of ocular data collected at the Mitchell Fire Site in October of 2006, 18 months after the fire.

MITCHELL SUMMER 2006 FIELD DATA

Trans_ num	Plot_num	Crop_Veg _Stage	Crust
1	1	4	not cracked
1	2	4	checked
1	3	4	not cracked
1	4	4	not cracked
1	5	4	not cracked
1	6	4	not cracked
1	7	4	not cracked
1	8	4	not cracked
1	9	4	not cracked
1	10	0	not cracked
2	1	4	not cracked
2	2	4	not cracked
2	3	4	not cracked
2	4	4	not cracked
3	1	4	not cracked
3	2	4	not cracked
3	3	4	not cracked
3	4	4	not cracked
3	5	4	not cracked
4	1	4	not cracked
4	2	4	not cracked
4	3	4	cracked
4	4	4	not cracked
4	5	4	not cracked
4	6	4	not cracked
4	7	4	not cracked

Table B.1. Summary of ocular data collected at the Mitchell Fire Site in October of 2006, 18 months after the fire.

MARCIAL FIRE SUMMER 2006 FIELD SAMPLING DATA

DATE	DATUM	ELEV	TRANS NUM	PLOT NUM	WAYPT NUM	LATITUD E	LONGITUDE
8/7/06	WGS 84	4487	1	1	9	33.69	-106.98
8/7/06	WGS 84	4490	1	2	10	33.69	-106.98
8/7/06	WGS 84	4479	1	3	11	33.69	-106.97
8/7/06	WGS 84	4477	1	4	12	33.69	-106.97
8/8/06	WGS 84	4480	1	5	13	33.69	-106.97
8/8/06	WGS 84	4475	1	6	15	33.69	-106.97
8/8/06	WGS 84	4490	1	7	16	33.69	-106.97
8/8/06	WGS 84	4475	1	8	17	33.69	-106.97
8/8/06	WGS 84	4771	1	9	20	33.69	-106.97
8/8/06	WGS 84	4485	1	10	21	33.69	-106.97
8/9/06	WGS 84	4475	2	1	24	33.69	-106.97
8/9/06	WGS 84	4489	2	2	25	33.69	-106.96
8/9/06	WGS 84	4476	2	3	27	33.69	-106.96
8/9/06	WGS 84	4482	2	4	30	33.69	-106.96
8/9/06	WGS 84	4496	2	5	31	33.69	-106.96
8/10/06	WGS 84	4488	2	6	32	33.69	-106.96
8/10/06	WGS 84	4488	2	7	34	33.69	-106.96
8/10/06	WGS 84	4480	2	8	35	33.69	-106.96
8/10/06	WGS 84	4485	2	9	36	33.69	-106.96
8/10/06	WGS 84	4484	2	10	37	33.69	-106.95
8/10/06	WGS 84	4491	3	1	38	33.69	-106.95
8/10/06	WGS 84	4502	3	2	39	33.69	-106.95
8/10/06	WGS 84	4495	3	3	40	33.69	-106.95
8/10/06	WGS 84	4480	3	4	41	33.69	-106.95
8/10/06	WGS 84	4503	3	5	42	33.69	-106.95
8/10/06	WGS 84	4448	3	6	43	33.70	-106.95
8/17/06	WGS 84	4506	3	7	44	33.70	-106.95
8/17/06	WGS 84	4485	3	8	45	33.70	-106.95
8/17/06	WGS 84	4475	3	9	46	33.70	-106.95
8/17/06	WGS 84	4485	3	10	47	33.70	-106.95
8/17/06	WGS 84	4487	4	1	49	33.70	-106.95
8/17/06	WGS 84	4485	4	2	50	33.70	-106.94
8/17/06	WGS 84	4492	4	3	51	33.70	-106.94
8/17/06	WGS 84	4476	4	4	52	33.70	-106.94
8/17/06	WGS 84	4492	4	5	53	33.70	-106.94
8/17/06	WGS 84	4496	4	6	54	33.70	-106.94
8/17/06	WGS 84	4499	4	7	55	33.70	-106.94
8/17/06	WGS 84	4516	4	8	56	33.70	-106.94
8/17/06	WGS 84	4498	4	9	57	33.70	-106.94
8/17/06	WGS 84	4503	4	10	58	33.70	-106.94

Table B.2. Summary of data collected at the Marcial Fire Site in August of 2006.

MARCIAL FIRE SUMMER 2006 FIELD SAMPLING DATA

DATE	DATUM	ELEV	TRANS NUM	PLOT NUM	WAYPT NUM	LATITUD E	LONGITUDE
8/23/06	WGS 84	4495	5	2	61	33.71	-106.96
8/23/06	WGS 84	4490	5	3	62	33.71	-106.96
8/23/06	WGS 84	4490	5	4	63	33.71	-106.95
8/23/06	WGS 84	4489	5	5	64	33.71	-106.95
8/23/06	WGS 84	4492	5	6	65	33.71	-106.95
8/23/06	WGS 84	4495	5	7	66	33.71	-106.95
8/23/06	WGS 84	4495	5	8	67	33.71	-106.95
8/23/06	WGS 84	4494	5	9	68	33.71	-106.95
8/23/06	WGS 84	4483	5	10	69	33.71	-106.95

Table B.2. Summary of data collected at the Marcial Fire Site in August of 2006.

MARCIAL FIRE SUMMER 2006 FIELD SAMPLING DATA

TRANS NUM	PLOT NUM	UTM E	UTM N	TTL TREE %	DOM SPECIES
1	1	316763.51	3729566.29	30	Tamarisk
1	2	316864.91	3729534.40	70	Tamarisk
1	3	316975.20	3729482.36	50	Tamarisk
1	4	317094.37	3729410.19	60	Tamarisk
1	5	317272.27	3729498.88	90	Tamarisk
1	6	317382.60	3729449.07	40	Tamarisk
1	7	317475.58	3729461.71	10	Tamarisk
1	8	317586.13	3729423.00	20	Tamarisk
1	9	317706.12	3729392.98	20	Tamarisk
1	10	317807.04	3729335.59	0.5	Tamarisk
2	1	317800.17	3729949.20	80	Tamarisk
2	2	317911.45	3729949.30	90	Tamarisk
2	3	318022.65	3729944.97	60	Tamarisk
2	4	318161.47	3729930.13	80	Tamarisk
2	5	318281.76	3729916.75	60	Tamarisk
2	6	318735.88	3729902.59	80	Tamarisk
2	7	318503.72	3729884.80	10	Tamarisk
2	8	318614.77	3729872.71	10	Tamarisk
2	9	318725.80	3729859.51	20	Tamarisk
2	10	318846.28	3729856.12	3	Tamarisk
3	1	319122.79	3729521.41	40	Tamarisk
3	2	319148.06	3729631.87	30	Tamarisk
3	3	319214.90	3729733.78	80	Tamarisk
3	4	319263.28	3729840.47	90	Tamarisk
3	5	319320.73	3729935.90	70	Tamarisk
3	6	319375.61	3730043.58	90	Tamarisk
3	7	319373.92	3730135.69	90	Tamarisk
3	8	319419.35	3730247.99	80	Tamarisk
3	9	319476.89	3730348.97	80	Tamarisk
3	10	319516.12	3730462.49	90	Tamarisk
4	1	319731.75	3730095.66	90	Tamarisk
4	2	319780.34	3730213.45	80	Tamarisk
4	3	319828.92	3730331.24	80	Tamarisk
4	4	319877.31	3730439.04	80	Tamarisk
4	5	319925.64	3730543.52	80	Tamarisk
4	6	320001.82	3730649.70	70	Tamarisk
4	7	320013.13	3730758.20	70	Tamarisk
4	8	320043.09	3730871.91	70	Tamarisk
4	9	320082.23	3730981.00	60	Tamarisk
4	10	320112.12	3731091.37	50	Tamarisk

Table B.2. Summary of data collected at the Marcial Fire Site in August of 2006.

MARCIAL FIRE SUMMER 2006 FIELD SAMPLING DATA

TRANS NUM	PLOT NUM	UTM E	UTM N	TTL TREE %	DOM SPECIES
5	2	318658.68	3731210.89	3	Tamarisk
5	3	318779.45	3731223.03	20	Tamarisk
5	4	318900.08	3731228.51	30	Tamarisk
5	5	319013.34	3731333.97	20	Tamarisk
5	6	319123.31	3731265.33	10	Tamarisk
5	7	319234.86	3731280.97	20	Tamarisk
5	8	319346.61	3731306.59	20	Tamarisk
5	9	319467.67	3731334.26	30	Tamarisk
5	10	319579.16	3731346.58	20	Tamarisk

Table B.2. Summary of data collected at the Marcial Fire Site in August of 2006.

MARCIAL FIRE SUMMER 2006 FIELD SAMPLING DATA

TRANS NUM	PLOT NUM	STAND (FT)	STAND (M)	SEEDLING %	SAPLING %	SHRUB %
1	1	8.0	2.4	0.0	0	0
1	2	6.0	1.8	0.0	0	0
1	3	6.0	1.8	0.0	0	0
1	4	6.0	1.8	0.0	0	0
1	5	6.0	1.8	0.0	0	0
1	6	6.0	1.8	0.0	0	0
1	7	6.0	1.8	0.0	0	50
1	8	5.0	1.5	0.0	0	0
1	9	7.0	2.1	0.0	0	50
1	10	5.0	1.5	0.0	0	10
2	1	5.0	1.5	0.0	0	0.5
2	2	5.0	1.5	0.0	0	0
2	3	6.0	1.8	0.0	0	0
2	4	5.0	1.5	0.0	0	0
2	5	5.5	1.7	0.0	0	0
2	6	5.0	1.5	0.0	0	0
2	7	3.0	0.9	0.0	0	0
2	8	4.0	1.2	0.0	0	0
2	9	5.0	1.5	0.0	0	0
2	10	3.0	0.9	0.0	0	3
3	1	6.0	1.8	0.0	0	0
3	2	7.0	2.1	0.0	0	0
3	3	8.0	2.4	0.0	0	0
3	4	6.0	1.8	0.0	0	0
3	5	7.5	2.3	0.0	0	0
3	6	6.0	1.8	0.0	0	0
3	7	7.0	2.1	0.0	0	0
3	8	6.0	1.8	0.0	0	0
3	9	6.0	1.8	0.0	0	0
3	10	6.5	2.0	0.0	0	0
4	1	5.0	1.5	0.0	0	0
4	2	5.0	1.5	0.0	0	0
4	3	6.0	1.8	0.0	0	0
4	4	6.0	1.8	0.0	0	0
4	5	6.0	1.8	0.0	0	0
4	6	7.0	2.1	0.0	0	0
4	7	7.0	2.1	0.0	0	0
4	8	7.0	2.1	0.0	0	0
4	9	7.0	2.1	0.0	0	0
4	10	7.0	2.1	0.0	0	0

Table B.2. Summary of data collected at the Marcial Fire Site in August of 2006.

MARCIAL FIRE SUMMER 2006 FIELD SAMPLING DATA

TRANS NUM	PLOT NUM	STAND FT	STAND M	SEEDLING %	SAPLING %	SHRUB %
5	2	7.0	2.1	0	0	0.5
5	3	7.0	2.1	0	0	0
5	4	8.0	2.4	0	0	0
5	5	8.0	2.4	0	0	0
5	6	5.0	1.5	0	0	0
5	7	8.0	2.4	0	0	0
5	8	6.0	1.8	0	0	0
5	9	6.0	1.8	0	0	0
5	10	6.0	1.8	0	0	0

Table B.2. Summary of data collected at the Marcial Fire Site in August of 2006.

MARCIAL FIRE SUMMER 2006 FIELD SAMPLING DATA

TRANS NUM	PLOT NUM	GRAMINOID %	FORB %	COMBO VEG %	BARE SOIL %	GRAVEL %	SOIL TEXTURE
1	1	0	0	0	70	0	SL
1	2	0	0	0	30	0	SL
1	3	0	0	0	50	0	SL
1	4	0	0	0	50	0	SL
1	5	0	0	0	10	0	SL
1	6	0	0.5	0.5	60	0	SL
1	7	0	0.5	0.5	90	0	SL
1	8	0	0.5	0.5	80	0	SL
1	9	0	0	50	80	0	SL
1	10	0	10	20	70	0	SL
2	1	0	0	0.5	20	0	SL
2	2	0	0	0	10	0	SL
2	3	0	0.5	0.5	40	0	SL
2	4	0	0	0	20	0	SL
2	5	0	0.5	0.5	40	0	SL
2	6	0	0	0	0	0	SL
2	7	0	0	0	90	0	SL
2	8	0	0	0	90	0	SL
2	9	0	0	0	80	0	SL
2	10	0	0.5	4	90	0	SL
3	1	0	0.5	0.5	90	0	SL
3	2	0	0.5	0.5	70	0	SL
3	3	0	0.5	0.5	20	0	SL
3	4	0	0.5	0.5	10	0	SL
3	5	0	0.5	0.5	40	0	SL
3	6	0	0	0	10	0	SL
3	7	0	0.5	0.5	10	0	SL
3	8	0	10	10	10	0	SL
3	9	0	0.5	0.5	20	0	SL
3	10	0	0	0	0	10	SL
4	1	0	0.5	0.5	10	0	FS
4	2	0	0.5	0.5	20	0	FS
4	3	0	0	0	30	0	FS
4	4	0	0.5	0.5	20	0	FS
4	5	0	0	0	20	0	FS
4	6	0	0	0	30	0	FS
4	7	0	0	0	30	0	FS
4	8	0	0.5	0.5	30	0	FS
4	9	0	3	3	40	0	FS
4	10	0	0.5	0.5	50	0	FS

Table B.2. Summary of data collected at the Marcial Fire Site in August of 2006.

MARCIAL FIRE SUMMER 2006 FIELD SAMPLING DATA

TRANS NUM	PLOT NUM	GRAMINOID %	FORB %	COMBO VEG %	BARE SOIL %	GRAVEL %	SOIL TEXTURE
5	2	0	60	0.5	20	0	SL
5	3	0	20	20	80	0	SL
5	4	0	30	30	10	0	SL
5	5	0	0	0	80	0	SL
5	6	0	0.5	0.5	80	0	SL
5	7	0	0.5	0.5	70	0	SL
5	8	0	0.5	0.5	70	0	SL
5	9	0	0.5	0.5	70	0	SL
5	10	0	20	20	60	0	SL

Table B.2. Summary of data collected at the Marcial Fire Site in August of 2006

MARCIAL FIRE SUMMER 2006 FIELD SAMPLING DATA

TRANS NUM	PLOT NUM	EROSION TYPE	EROSION SEVERITY	CRUST
1	1	S	0	Cracked
1	2	S	0	Cracked
1	3	S	0	Cracked
1	4	S	0	Cracked
1	5	S	0	Cracked
1	6	S	0	Checked
1	7	S	0	Checked
1	8	S	0	Checked
1	9	S	0	Checked
1	10	S	0	Checked
2	1	S	0	Checked
2	2	S	0	Checked
2	3	S	0	Checked
2	4	S	0	Checked
2	5	S	0	Checked
2	6	S	0	Checked
2	7	S	0	Checked
2	8	S	0	Checked
2	9	S	0	Checked
2	10	S	0	Checked
3	1	S	0	Checked
3	2	S	0	Checked
3	3	S	0	Checked
3	4	S	0	Checked
3	5	S	0	Checked
3	6	S	0	Checked
3	7	S	0	Cracked
3	8	S	0	Cracked
3	9	S	0	Cracked
3	10	S	0	Cracked
4	1	G	1	Not cracked, no clay
4	2	G	0	cracked
4	3	G	0	Slightly cracked
4	4	G	0	cracked
4	5	G	0	Checked
4	6	G	0	Checked
4	7	G	0	Checked
4	8	G	0	Slightly cracked
4	9	G	0	cracked
4	10	G	0	cracked

Table B.2. Summary of data collected at the Marcial Fire Site in August of 2006.

MARCIAL FIRE SUMMER 2006 FIELD SAMPLING DATA

TRANS NUM	PLOT NUM	EROSION TYPE	EROSION SEVERITY	CRUST
5	2	Zero	0	cracked
5	3	Zero	0	checked
5	4	Zero	0	checked
5	5	Zero	0	Not cracked
5	6	Zero	0	Lightly cracked
5	7	Zero	0	Not cracked
5	8	Zero	0	Not cracked
5	9	Zero	0	Not cracked
5	10	Zero	0	Not cracked

Table B.2. Summary of data collected at the Marcial Fire Site in August of 2006.

BOSQUECITO FIRE SUMMER 2006 FIELD SAMPLING DATA

Date	Datum	Elev (m)	Trans Num	Plot Num	Waypt Num	9 Pixel Num
9/1/2006	WGS 84	4580	1	0	71	
9/1/2006	WGS 84	4565	1	1	72	1
9/1/2006	WGS 84	4580	1	2	73	2
9/1/2006	WGS 84	4582	1	3	74	3
9/1/2006	WGS 84	4572	1	4	75	4
9/1/2006	WGS 84	4566	1	5	76	5
9/1/2006	WGS 84	4566	1	6	77	6
9/1/2006	WGS 84	4567	1	7	78	7
9/1/2006	WGS 84	4565	1	8	79	8
9/1/2006	WGS 84	4577	1	9	80	9
9/1/2006	WGS 84	4563	1	10	81	10
9/11/2006	WGS 84	4555	2	1	82	11
9/11/2006	WGS 84	4513	2	2	83	12
9/25/2006	WGS 84	4560	2	3	104	13
9/25/2006	WGS 84	4591	2	4	105	14
9/25/2006	WGS 84	4581	2	5	106	15
9/25/2006	WGS 84	4564	2	6	107	16
9/25/2006	WGS 84	4578	2	7	108	17
9/25/2006	WGS 84	4576	2	8	109	18
9/25/2006	WGS 84	4578	2	9	110	19
9/25/2006	WGS 84	4568	2	10	111	20
9/13/2006	WGS 84	4581	3	1	84	21
9/13/2006	WGS 84	4457	3	2	85	22
9/13/2006	WGS 84	4576	3	3	86	23
9/13/2006	WGS 84	4567	3	4	87	24
9/13/2006	WGS 84	4592	3	5	88	25
9/13/2006	WGS 84	4592	3	6	89	26
9/13/2006	WGS 84	4581	3	7	90	27
9/13/2006	WGS 84	4578	3	8	91	28
9/13/2006	WGS 84	4570	3	9	92	29
9/13/2006	WGS 84	4582	3	10	93	30
9/15/2006	WGS 84	4576	4	1	95	31
9/15/2006	WGS 84	4566	4	2	95.5	32
9/15/2006	WGS 84	4589	4	3	96	33
9/15/2006	WGS 84	4585	4	4	97	34
9/15/2006	WGS 84	4578	4	5	98	35
9/15/2006	WGS 84	4575	4	6	99	36
9/15/2006	WGS 84	4573	4	7	100	37

Table B.3. Summary of data collected in September of 2006.

BOSQUECITO FIRE SUMMER 2006 FIELD SAMPLING DATA

Date	Datum	Elev (m)	Trans_Num	Trans_Num	Plot_Num	Waypt_Num
9/15/2006	WGS 84	4573	4	8	101	38
9/15/2006	WGS 84	4578	4	9	102	39
9/15/2006	WGS 84	4575	4	10	103	40
9/29/2006	WGS 84	4566	5	1	112	41
9/29/2006	WGS 84	4566	5	2	113	42
9/29/2006	WGS 84	4571	5	3	114	43
9/29/2006	WGS 84	4577	5	4	115	44
9/29/2006	WGS 84	4575	5	5	116	45
9/29/2006	WGS 84	4578	5	6	117	46
9/29/2006	WGS 84	4575	5	7	118	47
9/29/2006	WGS 84	4574	5	8	119	48
9/29/2006	WGS 84	4576	5	9	120	49
9/29/2006	WGS 84	4571	5	10	121	50

Table B.3. Summary of data collected in September of 2006.

BOSQUECITO FIRE SUMMER 2006 FIELD SAMPLING DATA

Trans_ Num	Plot Num	Latitude	Longitude	UTM E	UTM N	Total Tree %	Dom Species	Stand Height (ft)	Stand Height (m)	Seedling %
1	0	33.986367	-106.8544	328708.44	3762194.2	3	Tamarisk	15	4.57	0
1	1	33.9975	-106.8589	328321.28	3763436.3	0	Tamarisk	2.5	0.76	0.5
1	2	33.996483	-106.8584	328359.27	3763322.8	0	Tamarisk	5	1.52	0.5
1	3	33.995617	-106.8581	328392.93	3763226.1	0	Tamarisk	5	1.52	0.5
1	4	33.994583	-106.8577	328424.73	3763110.9	0	Tamarisk	2	0.61	0.5
1	5	33.99345	-106.8572	328470.17	3762984.3	0	Tamarisk	0	0	0
1	6	33.9926	-106.8568	328505.41	3762889.4	0	Tamarisk	3	0.91	0.5
1	7	33.991617	-106.8563	328548.09	3762779.5	0	Tamarisk	0	0	0.5
1	8	33.990617	-106.8558	328592.27	3762667.8	0	Tamarisk	3	0.91	0.5
1	9	33.989617	-106.8554	328628.74	3762556.2	0	Tamarisk	2	0.61	3
1	10	33.988683	-106.8549	328673.06	3762451.8	3	Cottonwood	50	15.24	0.5
2	1	33.987233	-106.8541	328737.9	3762289.8	20	Cottonwood	40	12.19	0
2	2	33.988033	-106.8549	328673.29	3762379.7	10	Cottonwood	40	12.19	0
2	3	33.988583	-106.8557	328597.42	3762442.1	30	Cottonwood	40	12.19	0
2	4	33.989483	-106.8562	328556.11	3762542.7	0	Tamarisk	2	0.61	3
2	5	33.9905	-106.8564	328538.14	3762655.8	0.5	Tamarisk	2.5	0.76	3
2	6	33.99135	-106.8566	328518.3	3762750.5	0	Tamarisk	2	0.61	0.5
2	7	33.992117	-106.8576	328432.08	3762837.1	0	Tamarisk	2	0.61	0.5
2	8	33.992883	-106.8584	328355.1	3762923.5	0.5	Tamarisk	4	1.22	0
2	9	33.99365	-106.8593	328273.51	3763010.1	0	Tamarisk	5	1.52	0
2	10	33.994433	-106.8602	328195.03	3763098.4	0	Tamarisk	5	1.52	0.5
3	1	34.000633	-106.8585	328359.92	3763783.2	0.5	Forb	2.5	0.76	0.5
3	2	33.999517	-106.8585	328363.83	3763659.3	0	Forb	3	0.91	3
3	3	33.998483	-106.8586	328346.35	3763544.9	0	Tamarisk	4	1.22	0
3	4	33.998617	-106.8598	328238.87	3763561.7	0	Tamarisk	4	1.22	0
3	5	33.998833	-106.8611	328120.76	3763587.9	0	Tamarisk	4	1.22	0
3	6	33.999	-106.8623	328008.72	3763608.4	0	Tamarisk	4	1.22	0
3	7	33.99905	-106.8636	327890.28	3763616.1	0	Tamarisk	4	1.22	0.5
3	8	33.999183	-106.8649	327770.47	3763633.1	0	Tamarisk	3	0.91	3
3	9	33.99935	-106.8663	327639.96	3763653.9	0	Forb	4	1.22	0
3	10	33.99935	-106.8675	327527.58	3763656	0	Tamarisk	5	1.52	0.5
4	1	34.0025	-106.8678	327507.78	3764005.8	0	Tamarisk	3	0.91	10
4	2	34.000417	-106.8671	327565.14	3763773.6	40	Tamarisk	5.5	1.68	0
4	3	34.00405	-106.8662	327660.23	3764175	30	Tamarisk	0	0	0
4	4	34.00415	-106.8649	327778.96	3764183.9	0	Tamarisk	2	0.61	0.5
4	5	34.004283	-106.8636	327894.69	3764196.6	0	Shrub	3	0.91	0.5
4	6	34.004367	-106.8624	328013.38	3764203.7	0	Forb	0	0	0
4	7	34.004433	-106.8612	328119.73	3764209.1	0	Forb	0	0	0

Table B.3. Summary of data collected in September of 2006.

BOSQUECITO FIRE SUMMER 2006 FIELD SAMPLING DATA

9 Pixel Num	Trans _Nu m	Plot Num	Longitude	UTM E	UTM N	Total Tree %	Dom Species	Stand Height (ft)	Stand Height (m)	Seedling %
4	8	34.004517	-106.86	328227.66	3764216.4	0	Graminoid	0	0	0
4	9	34.004583	-106.8588	328338.63	3764221.8	0	Graminoid	0	0	0
4	10	34.0042	-106.8577	328445.6	3764177.3	0	Shrub	0	0	0
5	1	33.99427	-106.8581	328387.15	3763076.8	0	Tamarisk	2.5	0.76	3
5	2	33.995033	-106.8589	328314.79	3763162.8	0	Tamarisk	2	0.61	0.5
5	3	33.99578	-106.8597	328245.47	3763246.9	0	Tamarisk	5	1.52	0
5	4	33.99662	-106.8604	328180.96	3763341.2	0	Tamarisk	5	1.52	0
5	5	33.99735	-106.8611	328116.24	3763423.4	0	Tamarisk	4	1.22	0
5	6	33.99808	-106.8618	328049.96	3763505.6	0	Tamarisk	5	1.52	0
5	7	33.99888	-106.8624	327994.62	3763595.3	0	Tamarisk	3	0.91	3
5	8	33.99968	-106.8631	327934.66	3763685.2	0	Tamarisk	4	1.22	0
5	9	34.000417	-106.8638	327871.49	3763768.1	0	Tamarisk	3	0.91	3
5	10	34.001183	-106.8646	327800.68	3763854.4	0	Tamarisk	4	1.22	0

Table B.3. Summary of data collected in September of 2006.

BOSQUECITO FIRE SUMMER 2006 FIELD SAMPLING DATA

Trans Num	Plot Num	Sapling %	Shrub %	Graminoid %	Forb %	Comboveg %	Bare Soil %	Gravel %
1	0	0	3	0	0	3	90	3
1	1	0	0	0	0	0	98	0
1	2	10	0	0	0	0	90	0
1	3	10	0	0	0	0	90	0
1	4	0	0	0	0	0	98	0
1	5	0	0	0	0	0	100	0
1	6	0	0	0	0	0	98	0
1	7	0	0	0	3	3	90	0
1	8	0	0	0.5	0.5	1	90	0
1	9	0	0	0	0	0	90	0
1	10	0	0	0	0	0	90	0
2	1	3	0	0	0	0	80	0
2	2	3	0	0	0	0	90	0
2	3	0.5	20	0	0	20	70	0
2	4	0	3	0	3	6	90	0
2	5	0	0	0	0	0	90	0
2	6	0	0	0	0	0	98	0
2	7	0	0	0	0	0	98	0
2	8	40	0	0	0	0	60	0
2	9	10	0	0	0	0	0	0
2	10	0.5	0	0	0	0	10	0
3	1	0	0	0	70	70	30	0
3	2	0	0	0	90	90	10	0
3	3	10	0	0	10	10	80	0
3	4	20	0	0	10	10	70	0
3	5	10	0	0	0	0	90	0
3	6	10	0	0	0	0	90	0
3	7	3	0	0	0	0	98	0
3	8	0	0	0	0.5	0.5	90	0
3	9	0.5	0	0.5	40	0.5	50	0
3	10	10	0.5	0.5	0	1	80	0
4	1	0	10	3	0	13	60	0
4	2	0	0	0.5	0	0.5	50	0
4	3	0	0	10	0	10	60	0
4	4	0	0	0.5	0	0.5	90	0
4	5	0	10	0.5	0	0.5	80	0
4	6	0	0	0	20	20	80	0
4	7	0	0	0.5	20	20.5	80	0

Table B.3. Summary of data collected in September of 2006.

BOSQUECITO FIRE SUMMER 2006 FIELD SAMPLING DATA

Trans Num	Plot Num	Sapling %	Shrub %	Graminoid %	Forb %	Comboveg %	Bare Soil %	Gravel %
4	8	0	0	70	0.5	70.5	20	0
4	9	0	0	0.5	0	0.5	98	0
4	10	0	0.5	0	0	0.5	90	10
5	1	0	0	0	0	0	98	0
5	2	0	0	0	0	0	98	0
5	3	10	0	0	0	0	90	0
5	4	3	0	0	0	0	90	0
5	5	3	0	0	0	0	90	0
5	6	3	0	0	0	0	90	0
5	7	0	0	0	0	0	90	0
5	8	10	0	0	10	10	80	0
5	9	0	0	0	3	3	90	0
5	10	3	0	0	3	3	90	0

Table B.3. Summary of data collected in September of 2006.

BOSQUECITO FIRE SUMMER 2006 FIELD SAMPLING DATA

Trans Num	Plot Num	Erosion Type	Erosion Severity	Fire Intensity	Veg Stage	Crust	Soil Texture
1	0	G	1		4	Non existant	VFS
1	1	0	0		1	Charred	SC
1	2	0	0		2	lightly checked, charred 30%	SC
1	3	0	0		2	lightly checked, charred 30%	SC
1	4	0	0		1	lightly charred	SC
1	5	0	0		0	lightly checked	SC
1	6	0	0		0	lightly checked	SC
1	7	G	1		1	Cracked	FS
1	8	S	0		1	Checked, curled	SC
1	9	0	0		1	Checked, curled	SC/S
1	10	0	0		1	Checked, curled	SC
2	1	G	1				SC
2	2	G	1		1	not cracked	CL & SI
2	3	0	0	3	1	cracked	top 3/4": C; bottom SI
2	4	0	0	1	1	cracked	top 3/4": C; bottom SI
2	5	0	0	3	1	not cracked	C
2	6	0	0	3	1	cracked, furled	top 1/8": C; bottom SI
2	7	0	0	3	1	cracked, furled	top 1/8": C; bottom SI
2	8	0	0	3	2	Cracked	top 1/8": C; bottom SI
2	9	0	0	3	2	cracked, small furling	top 1/12": C; bottom SI
2	10	0	0	3	1, 4	not cracked	SIL
3	1	0	0		2	cracked	SC
3	2	0	0		4	cracked	SC
3	3	0	0		4	not cracked	SC
3	4	0	0		0	not cracked	sc
3	5	0	0		1	some cracked areas	top 1/8": C; bottom SI
3	6	0	0		1	some cracked areas	top 1/8": C; bottom SI
3	7	0	0		2 (majority),	cracked	SC
3	8	0	0		4	cracked	SC
3	9	0	0		4	cracked	SI
3	10	0	0				SI
4	1	0	0		4	slightly cracked	SI
4	2	0	0		4	cracked	SIL
4	3	0	0		4	checked	SIL
4	4	0	0		4	cracked	SIL
4	5	0	0		4	cracked, furled	SIL
4	6	0	0		0	cracked	SIL
4	7	0	0		0	cracked	top 1/8": C; bottom SI

Table B.3. Summary of data collected in September of 2006.

BOSQUECITO FIRE SUMMER 2006 FIELD SAMPLING DATA

Trans Num	Plot Num	Erosion Type	Erosion Severity	Fire Intensity	Veg Stage	Crust	Soil Texture
4	8	0	0		0	not cracked	SIL
4	9	0	0		0		SI
4	10	R	2		0	eroded by gully and rill	VFS w/ gravel
5	1	0	0		1	cracked, furled	top 1/8": C; bottom SI
5	2	0	0		1	cracked, furled	top 1/8": C; bottom SI
5	3	0	0	3	1	cracked	SIL
5	4	0	0	3	2	cracked, some furled	top 1/8": C; bottom SI
5	5	0	0	3	4	not cracked	SIL
5	6	0	0	3	4	not cracked	SI
5	7	0	0	3	2	cracked	SI
5	8	0	0	3	4	cracked	SI
5	9	0	0	3	4	cracked	SIL
5	10	0	0	3	4	cracked	SIL

Table B.3. Summary of data collected in September of 2006.

Appendix C. Summer 2006 Field Sampling Maps

The following maps were created from data collected during the Summer 2006 Field Campaign when ocular measurements were taken of various vegetation, soil and fire parameters. Field and location data is presented in tabular form in Appendix A. Site sampling occurred 1 year and 4 months after the Mitchell Fire, and 3 months after the Marical and Bosquecito Fires. The sampling followed the FIREMON protocol and was performed under the guidance of Mr. Jerry Hess. The sampling locations have been matched to 9-Pixel Numbers and such location information can be found in Appendix A. The 9-Pixel Numbers have been labeled on the maps in the figures below in ordered to correlate with the 9-Pixel Bar Graph data presented in Section 4.2.

Mitchell Fire Macroplot Sampling Dominant Vegetation Species October 2006

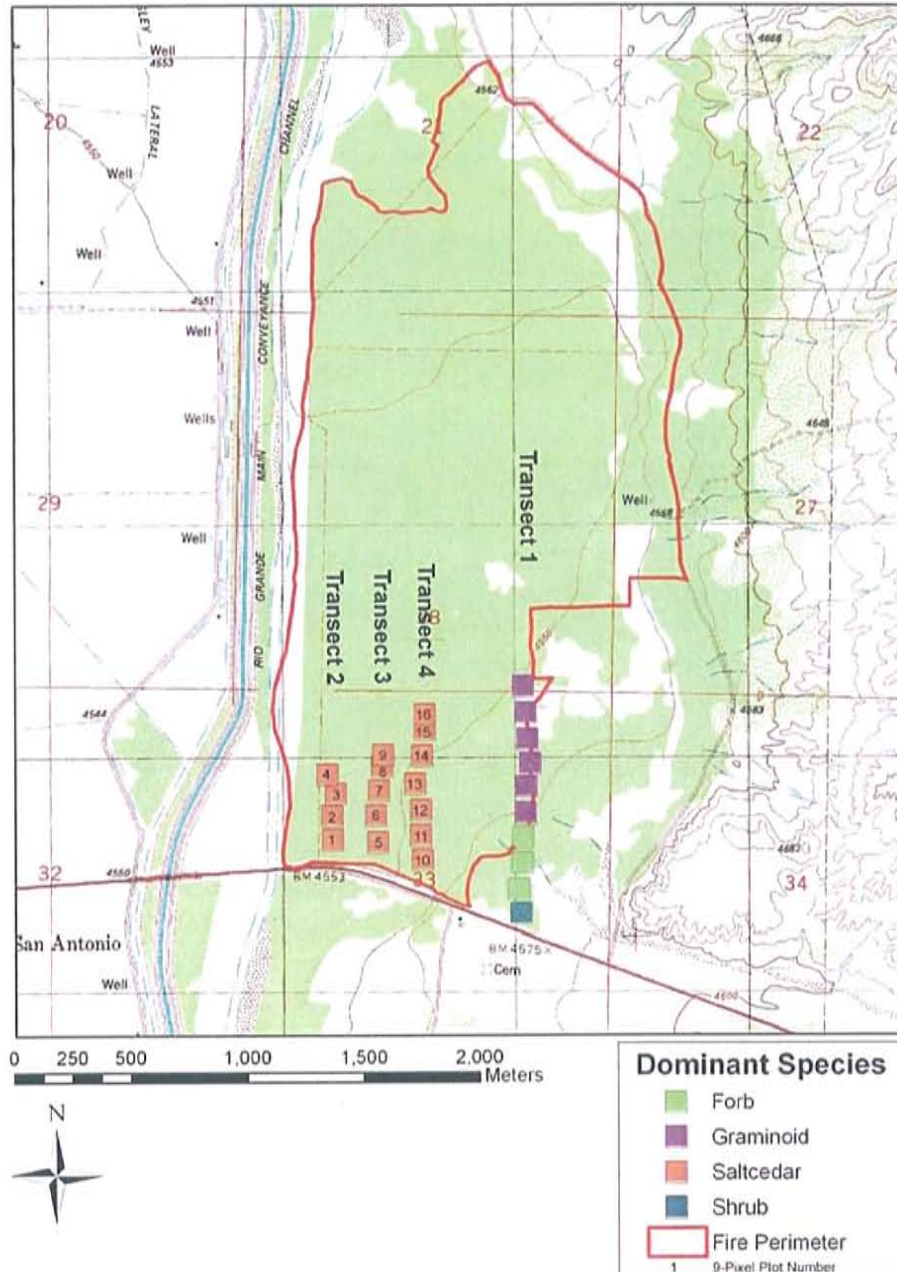


Figure C.1. Ocular measurements of vegetation and environmental parameters from the Summer 2006 Field Campaign.

Mitchell Fire Macroplot Sampling Tamarisk Cover (%) October 2006

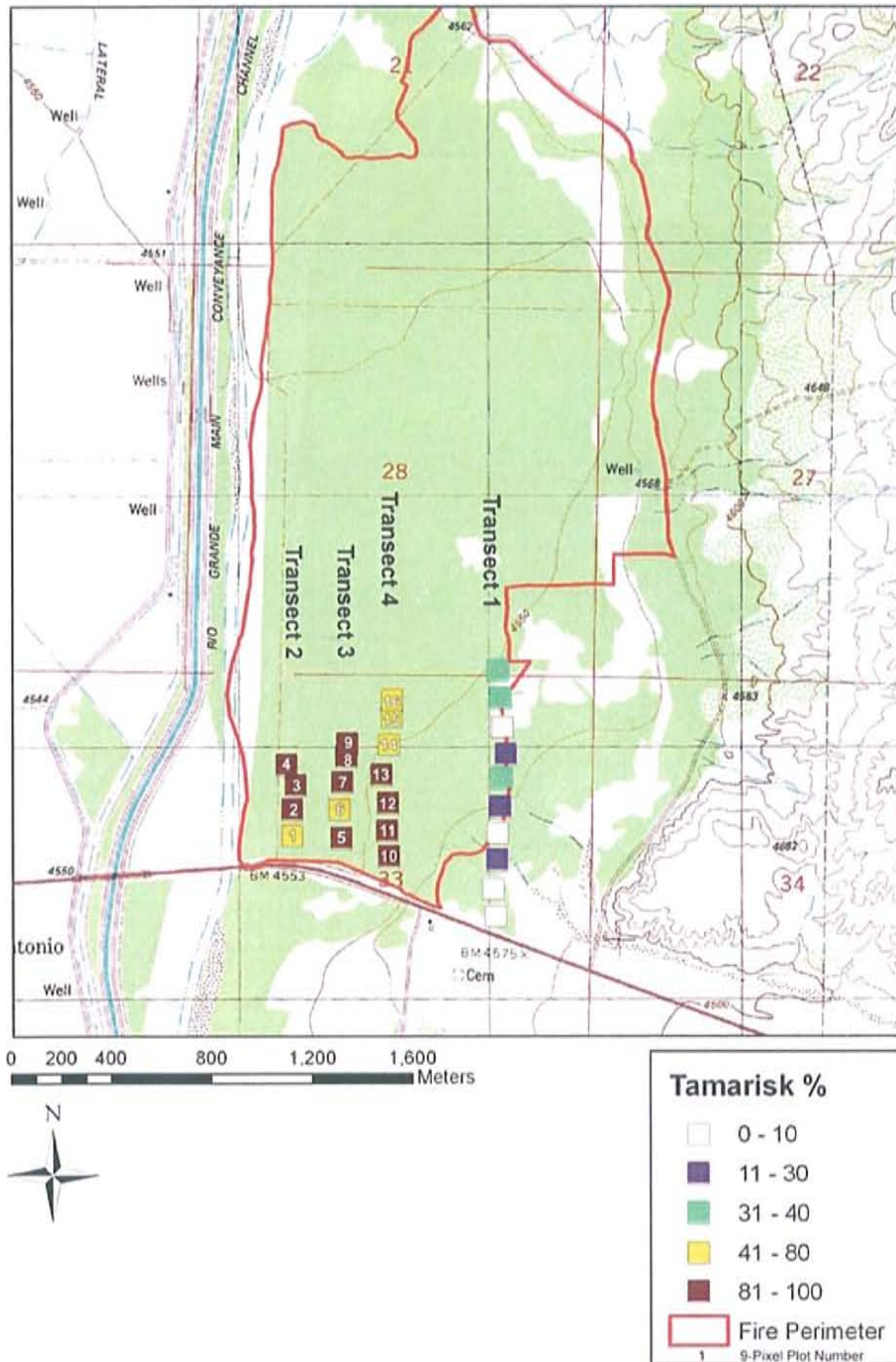


Figure C.2. Ocular measurements of vegetation and environmental parameters from the Summer 2006 Field Campaign.

Mitchell Fire Macroplot Sampling Dominant Vegetation Stand Height (meters) October 2006

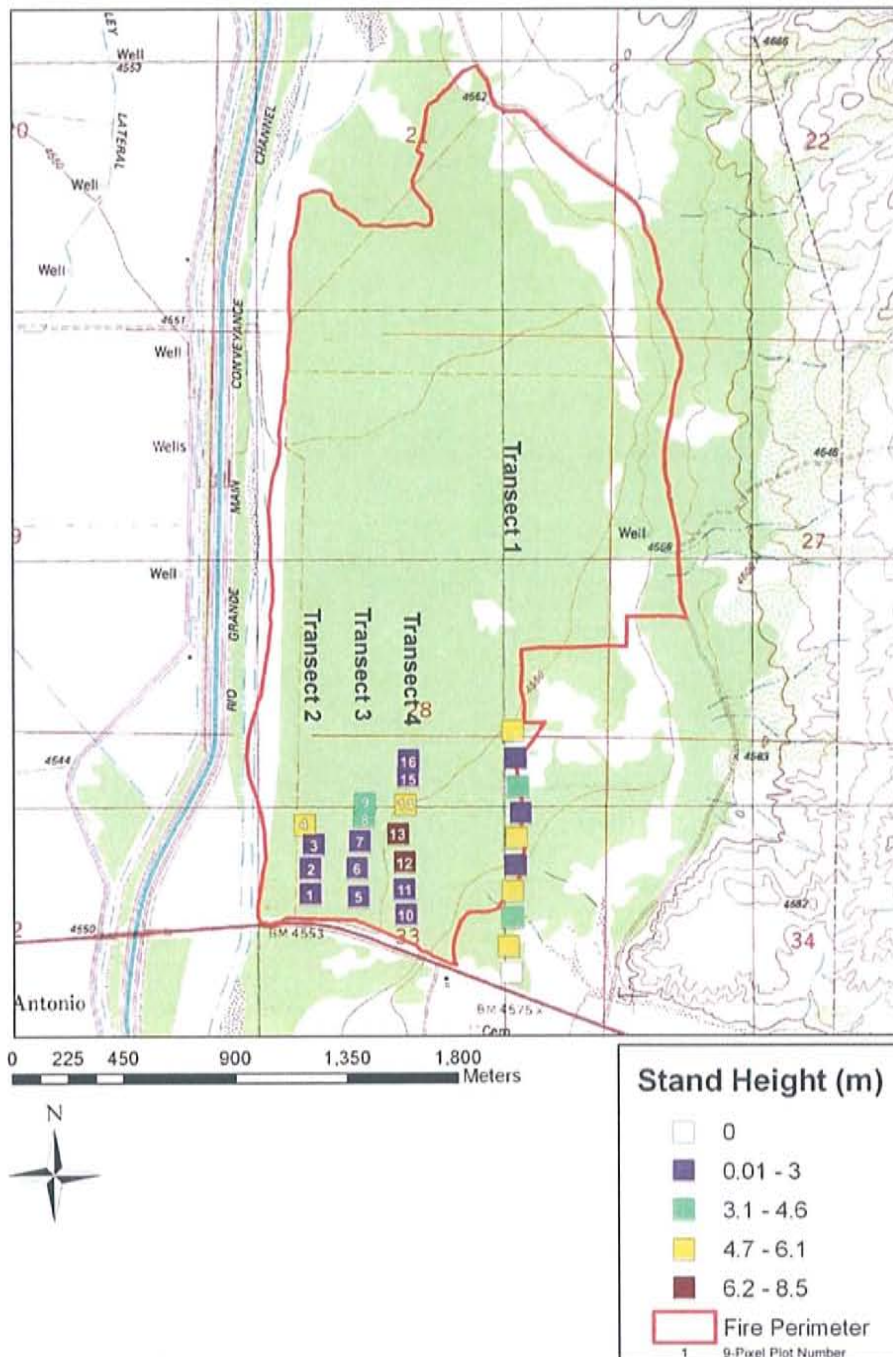


Figure C.3. Ocular measurements of vegetation and environmental parameters from the Summer 2006 Field Campaign.

Mitchell Fire Macroplot Sampling Bare Soil (%) October 2006

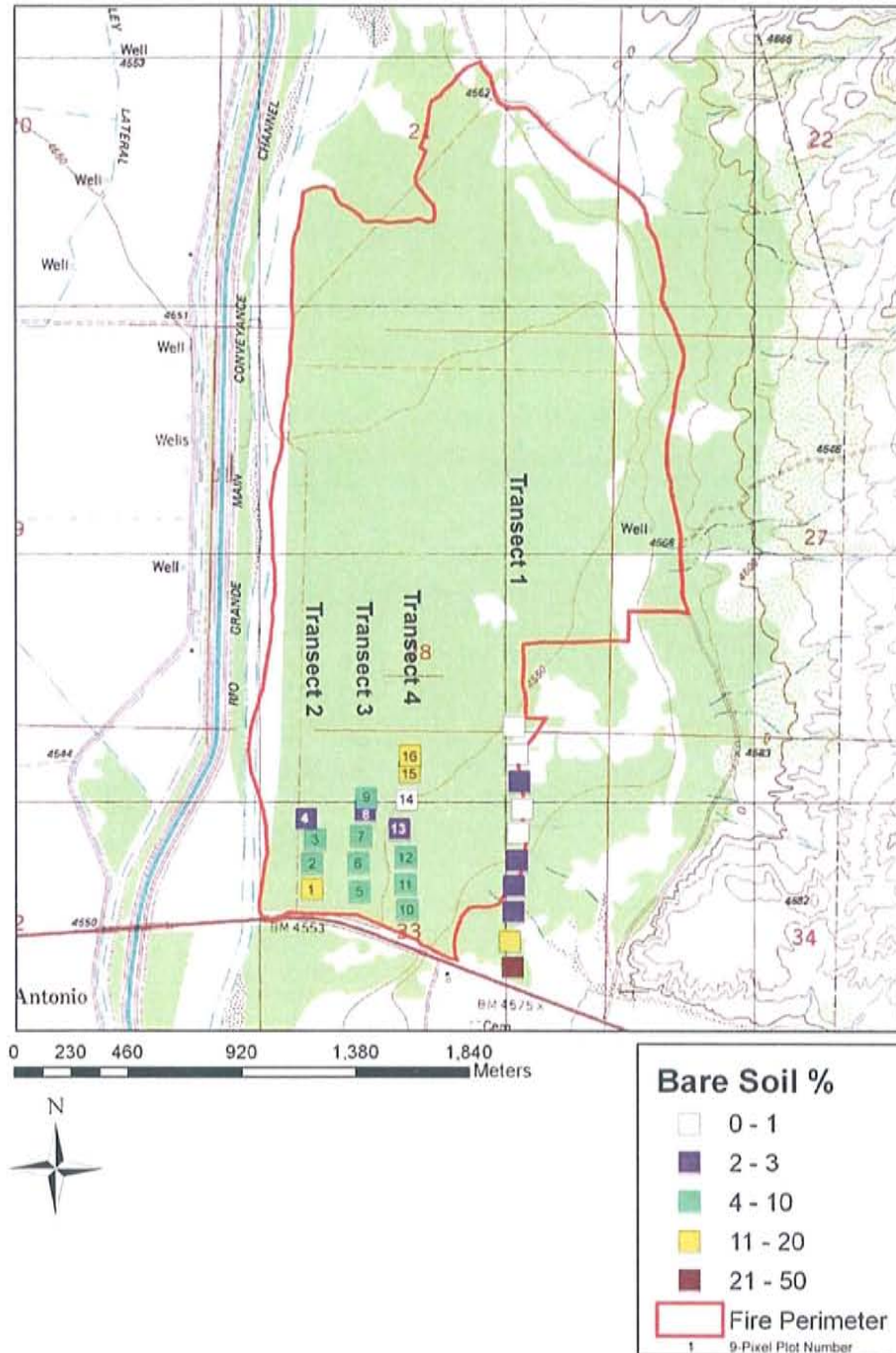


Figure C.4. Ocular measurements of vegetation and environmental parameters from the Summer 2006 Field Campaign.

Mitchell Fire Macroplot Sampling Summation of Shrub, Graminoid and Forb (%) October 2006

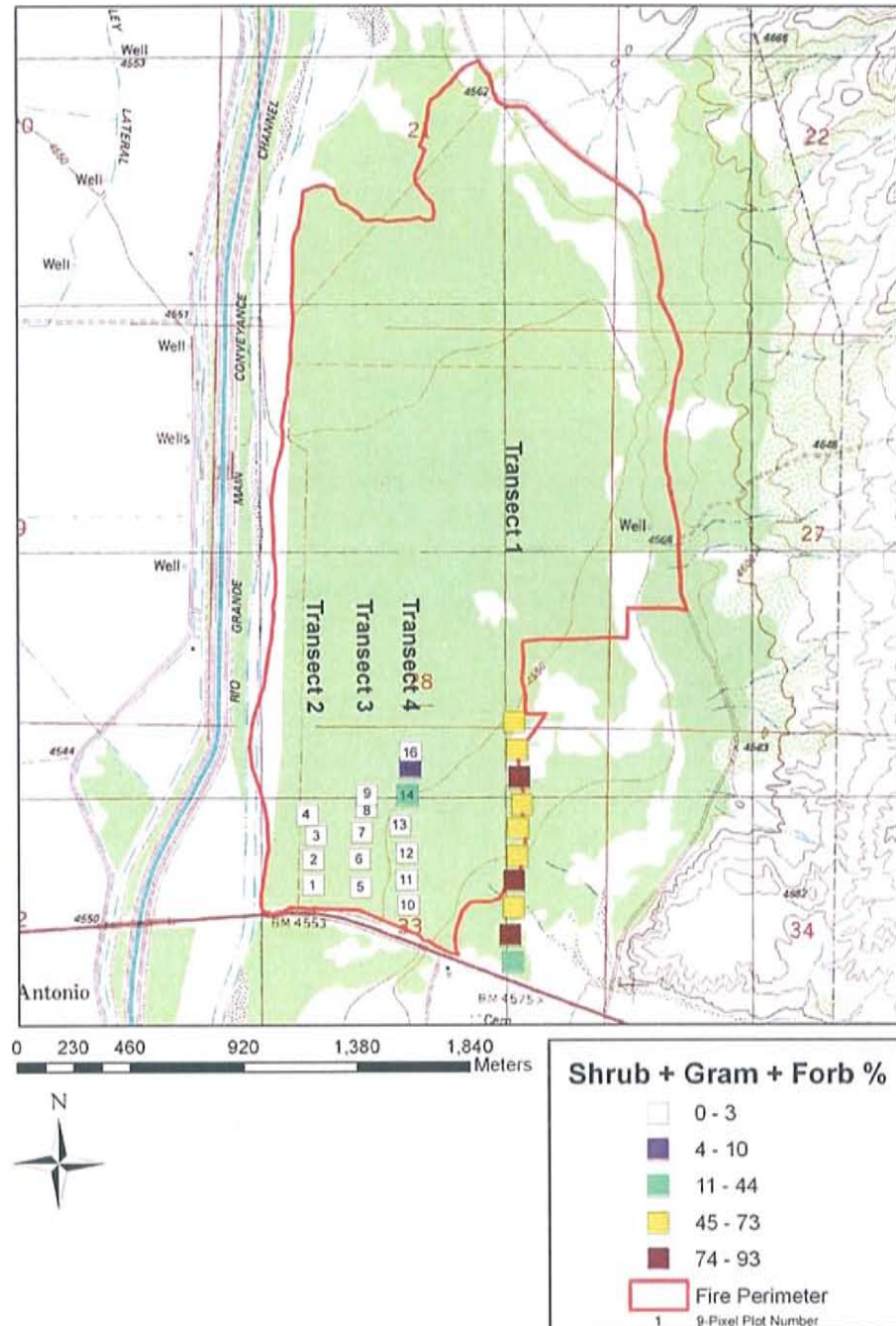


Figure C.5. Ocular measurements of vegetation and environmental parameters from the Summer 2006 Field Campaign.

Map of the Tamarisk Stage (0 - 4) in the Rio Grande area. The map shows a large green area representing the fire perimeter, with various transects (1, 2, 3, 4) and plots (1-16) marked. A scale bar indicates distances up to 1,840 meters. A legend identifies the Tamarisk Stage colors: 0 (white), 1 (purple), 2 (green), 3 (yellow), and 4 (dark red). A red outline indicates the fire perimeter. The map also shows the Rio Grande, a lateral channel, and several wells.

223

Soil Type
October 2006



Figure C.7. Ocular measurements of vegetation and environmental parameters from the Summer 2006 Field Campaign.

Mitchell Fire Macroplot Sampling Fire Intensity October 2006

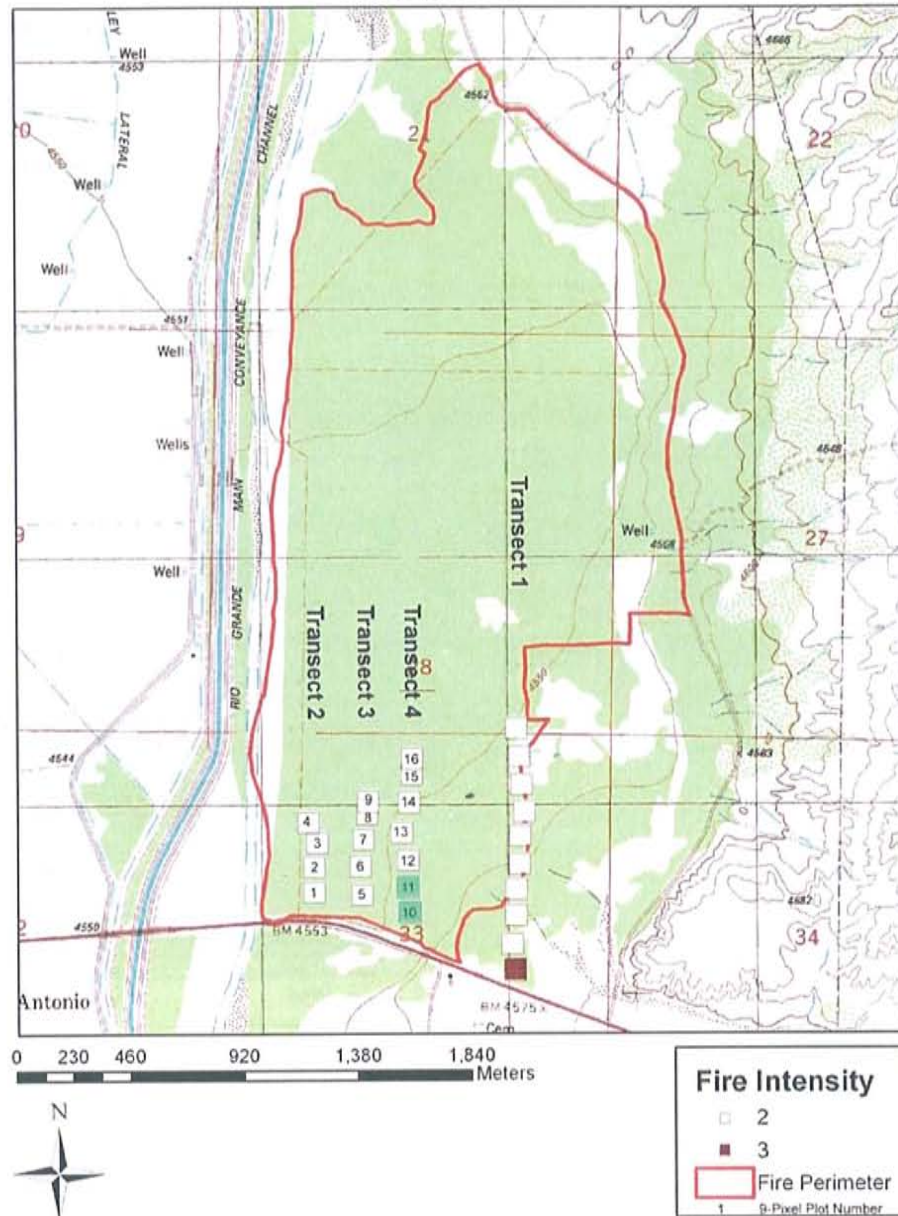


Figure C.8. Ocular measurements of vegetation and environmental parameters from the Summer 2006 Field Campaign.

Marcial Fire
Dominant Vegetation Species Map
Tamarisk Cover (%)
Sampling Performed in August of 2006

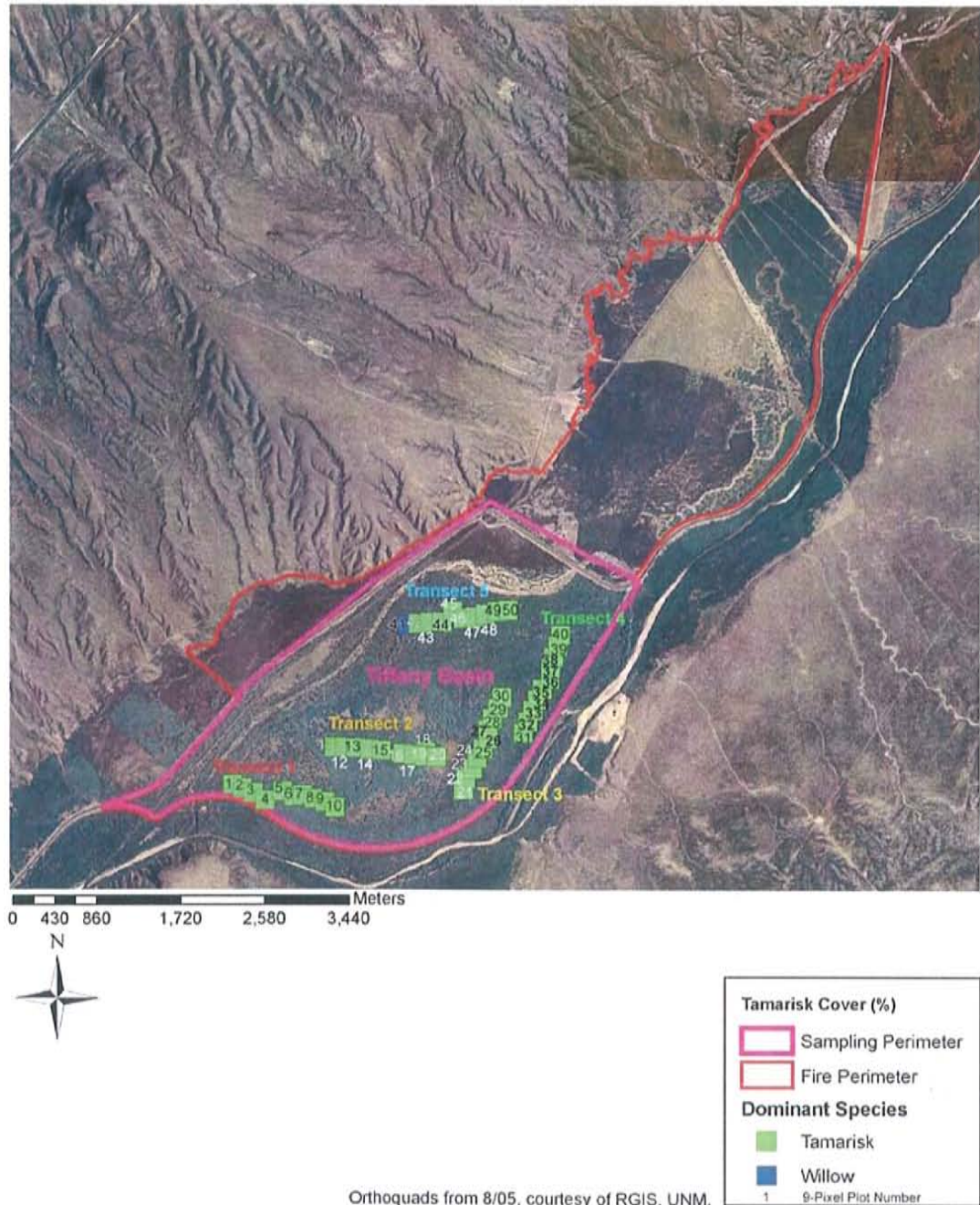
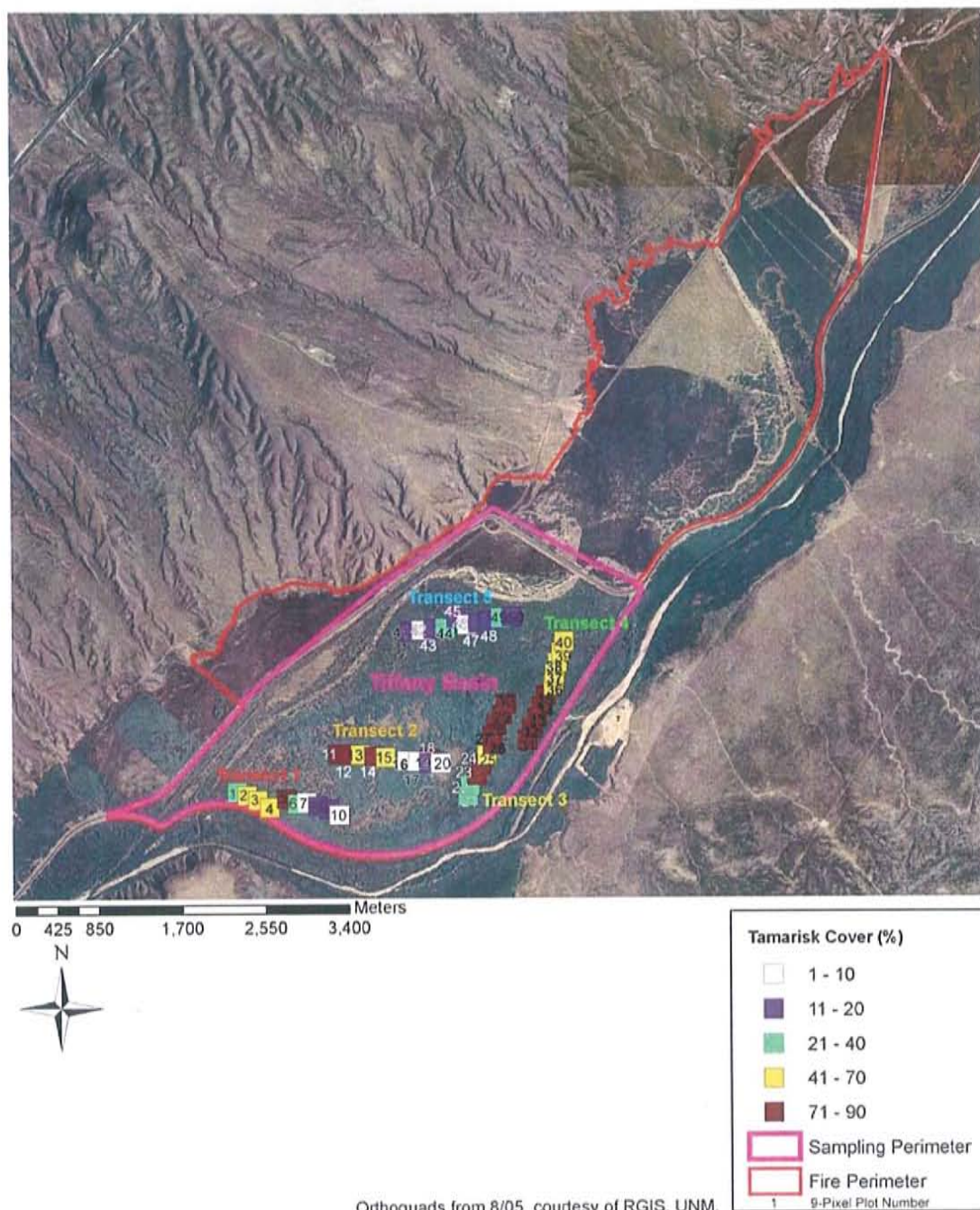


Figure C.9. Ocular measurements of vegetation and environmental parameters from the Summer 2006 Field Campaign.

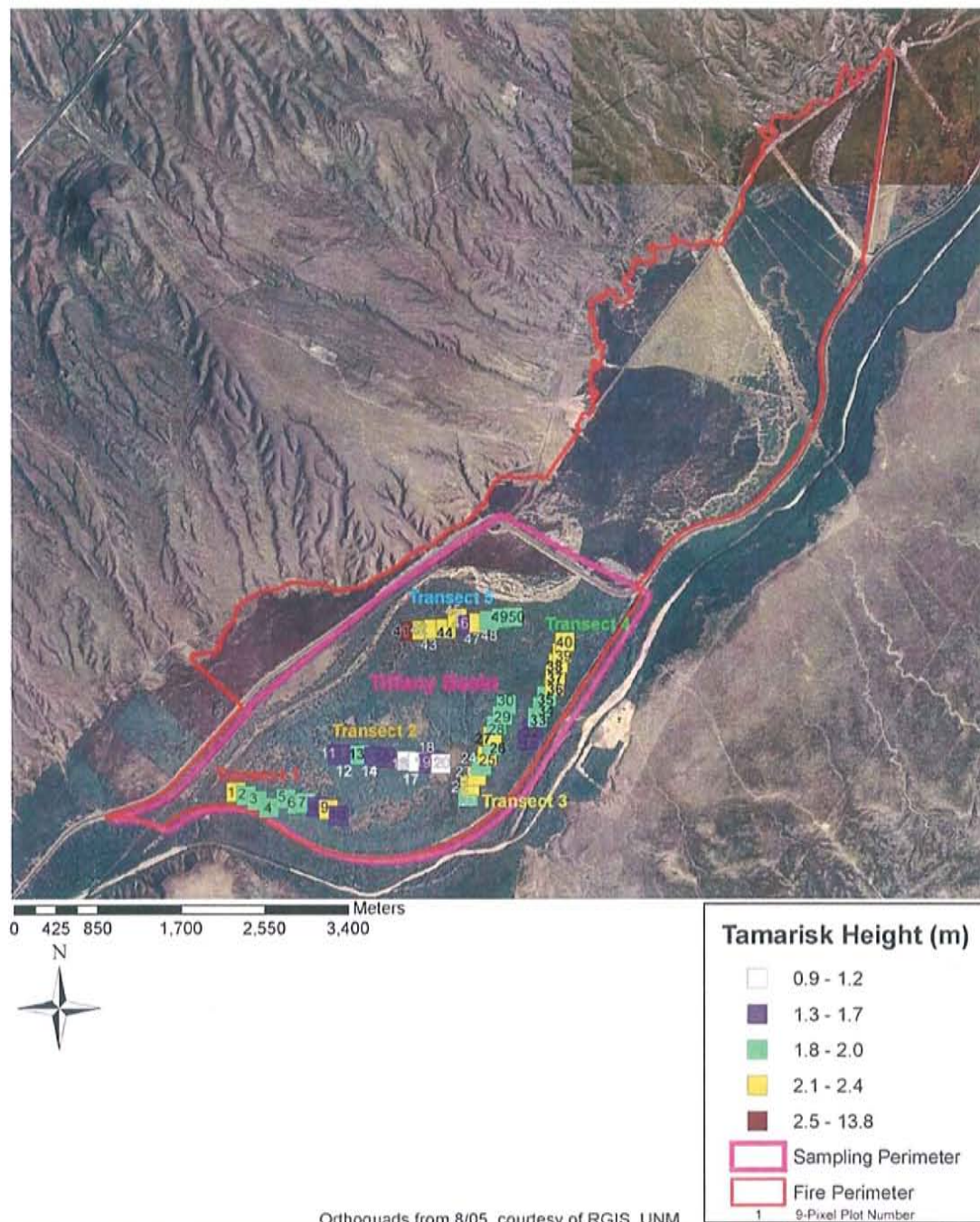
Marcial Fire
Macroplot Sampling Map
Tamarisk Cover (%)
Sampling Performed in August of 2006



Orthoquads from 8/05, courtesy of RGIS, UNM.

Figure C.10. Ocular measurements of vegetation and environmental parameters from the Summer 2006 Field Campaign.

**Marcial Fire
Macroplot Sampling Map
Tamarisk Height (m)
Sampling Performed in August of 2006**



Orthoquads from 8/05, courtesy of RGIS, UNM.

Figure C.11. Ocular measurements of vegetation and environmental parameters from the Summer 2006 Field Campaign.

**Marcial Fire
Macroplot Sampling Map
Bare Soil Cover (%)
Sampling Performed in August of 2006**

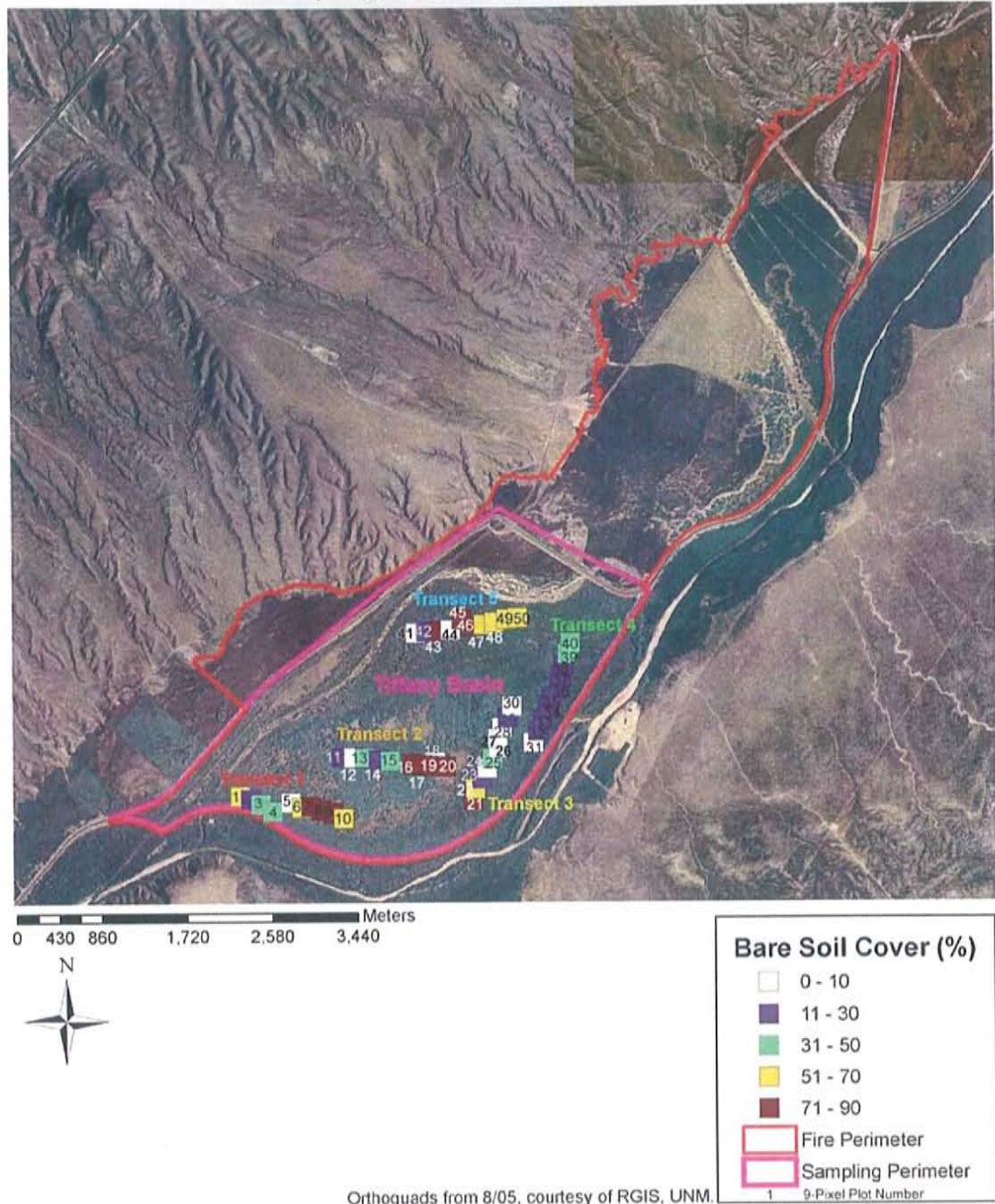


Figure C.12. Ocular measurements of vegetation and environmental parameters from the Summer 2006 Field Campaign.

**Marcial Fire
Macroplot Sampling Map
Soil Type
Sampling Performed in August of 2006**

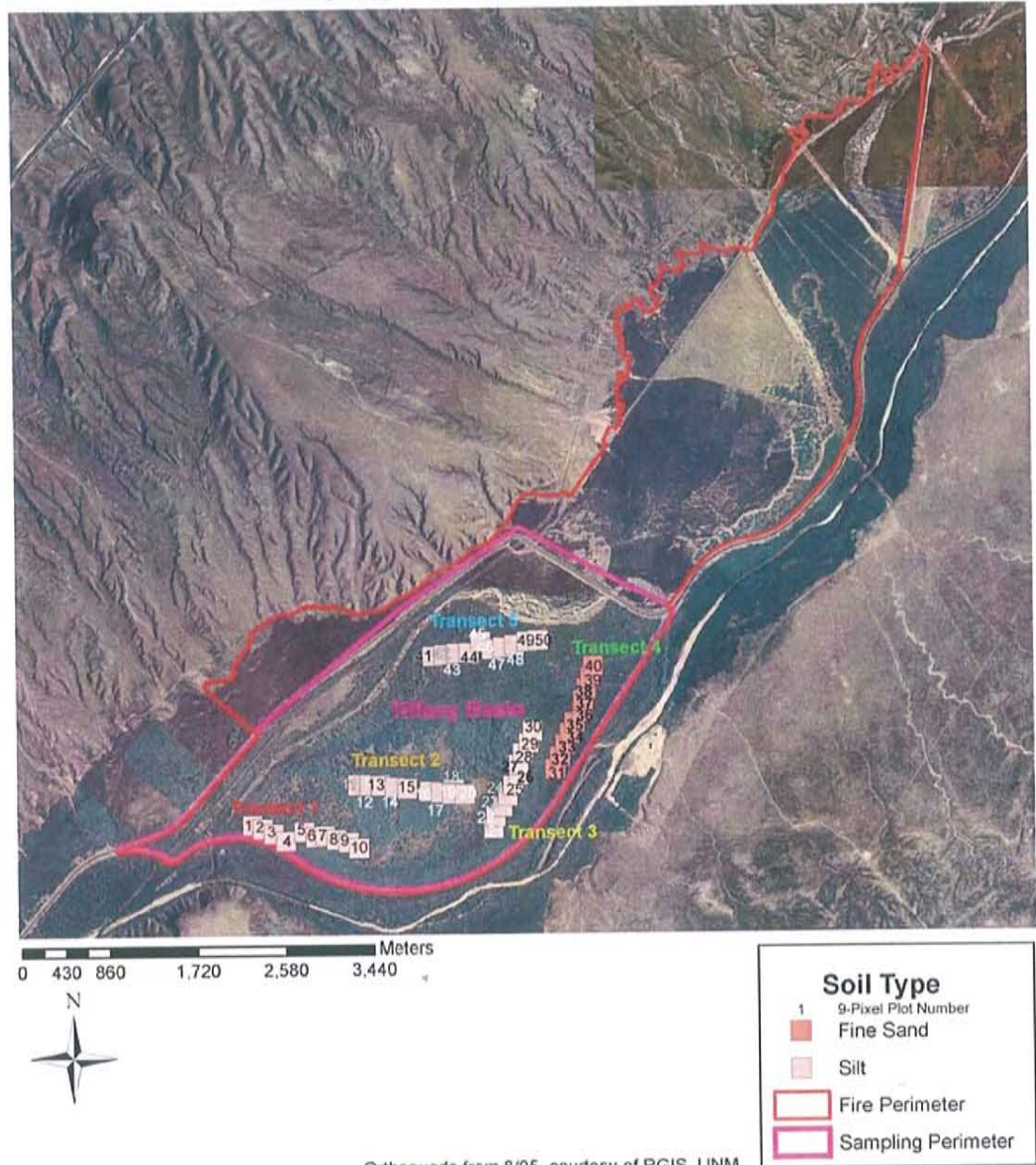
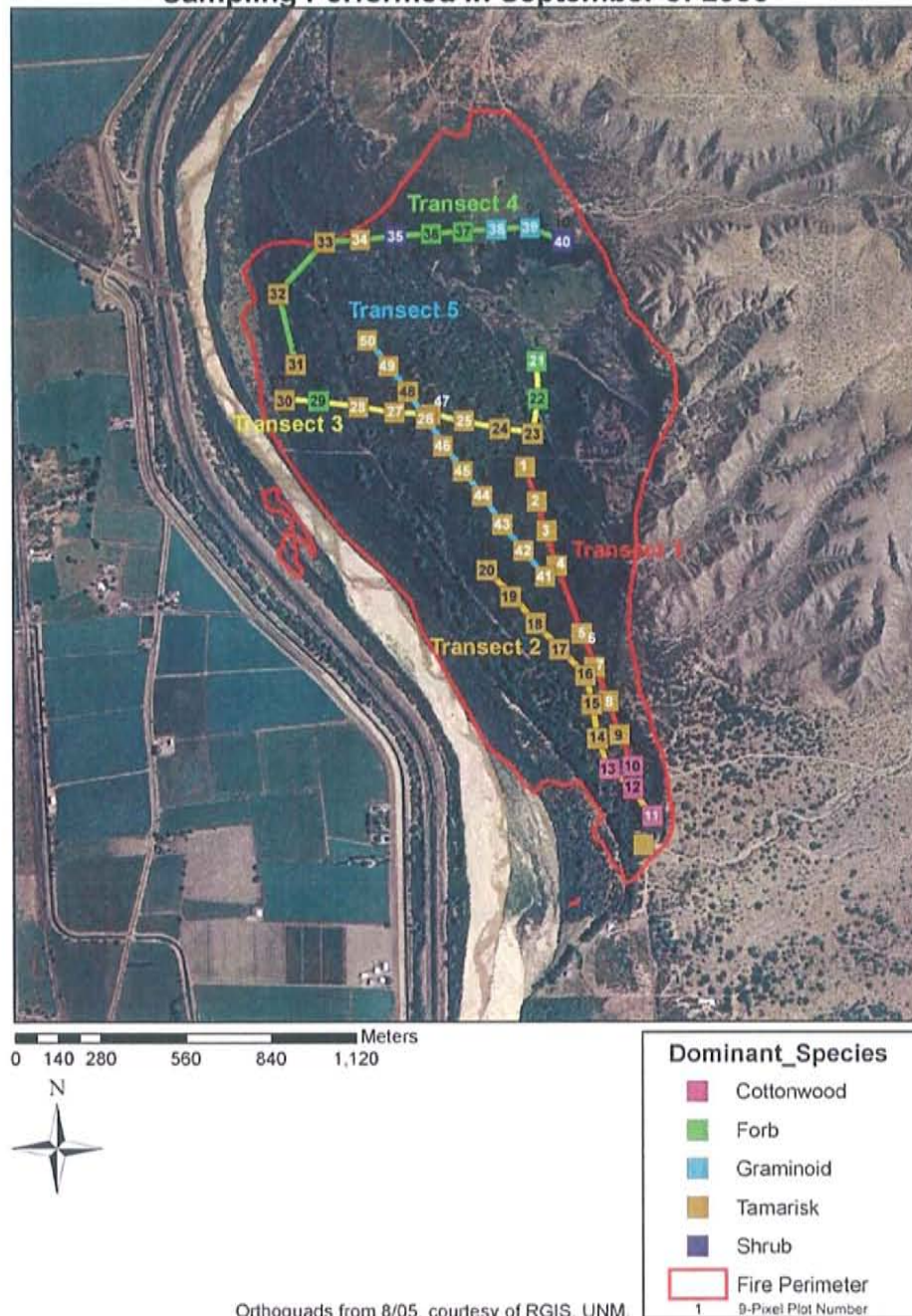


Figure C.13. Ocular measurements of vegetation and environmental parameters from the Summer 2006 Field Campaign.

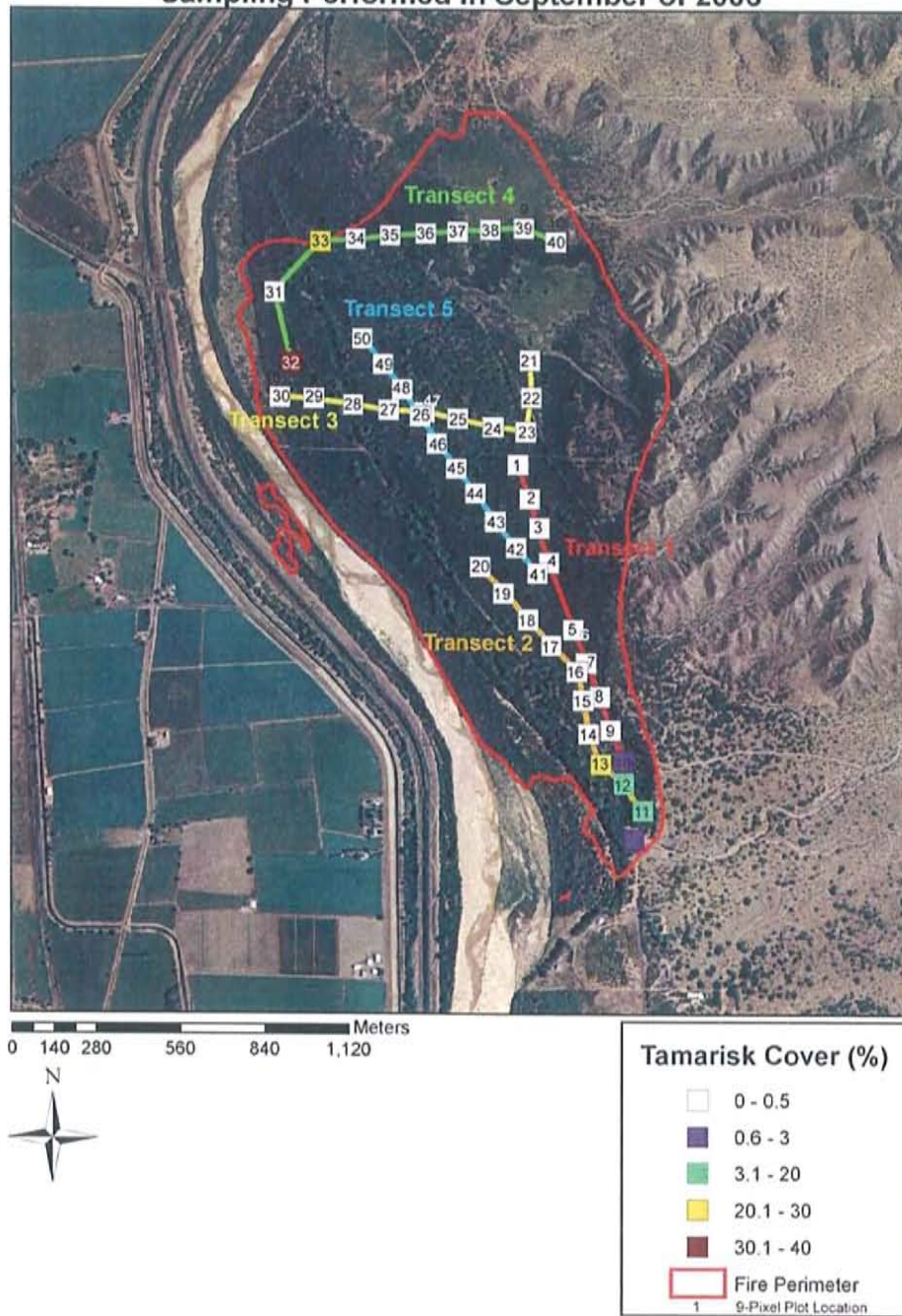
Bosquecito Fire
Macroplot Sampling Map
Dominant Vegetation Species
Sampling Performed in September of 2006



Orthoquads from 8/05, courtesy of RGIS, UNM.

Figure C.14. Ocular measurements of vegetation and environmental parameters from the Summer 2006 Field Campaign.

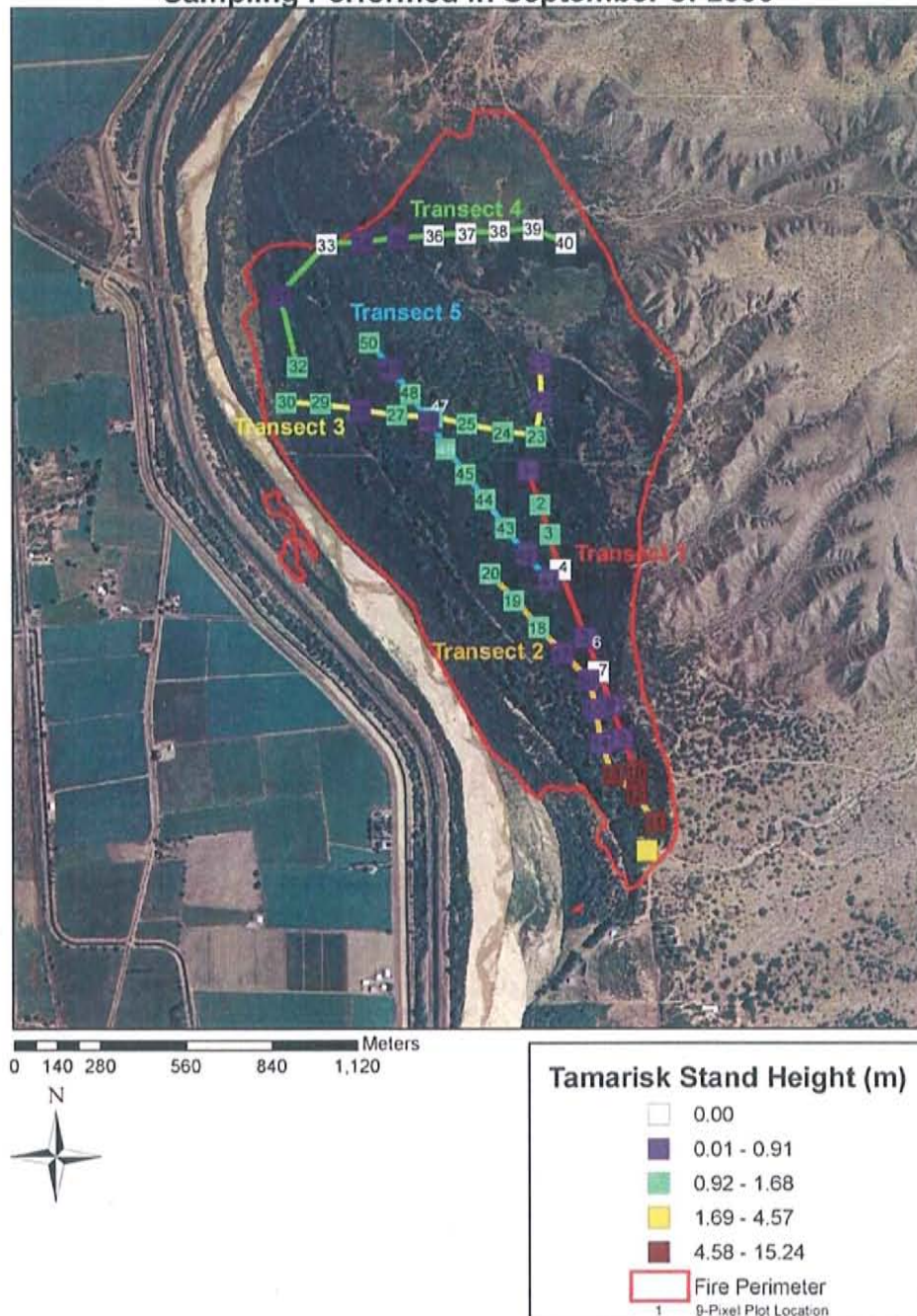
Bosquecito Fire
Macroplot Sampling Map
Tamarisk Cover (%)
Sampling Performed in September of 2006



Orthoquads from 8/05, courtesy of RGIS, UNM.

Figure C.15. Ocular measurements of vegetation and environmental parameters from the Summer 2006 Field Campaign.

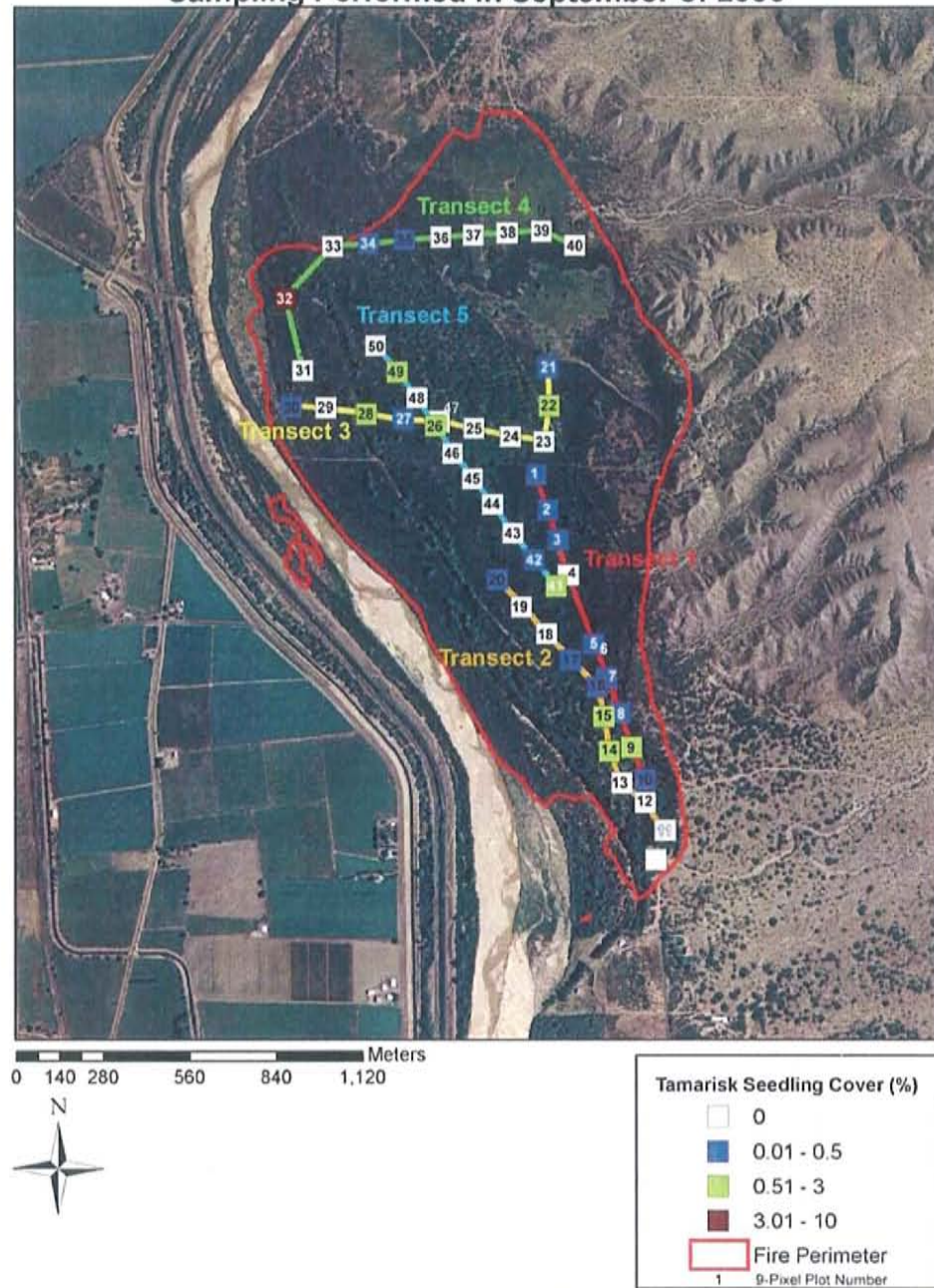
**Bosquecito Fire
Macroplot Sampling Map
Tamarisk Stand Height
Sampling Performed in September of 2006**



Orthoquads from 8/05, courtesy of RGIS, UNM.

Figure C.16. Ocular measurements of vegetation and environmental parameters from the Summer 2006 Field Campaign.

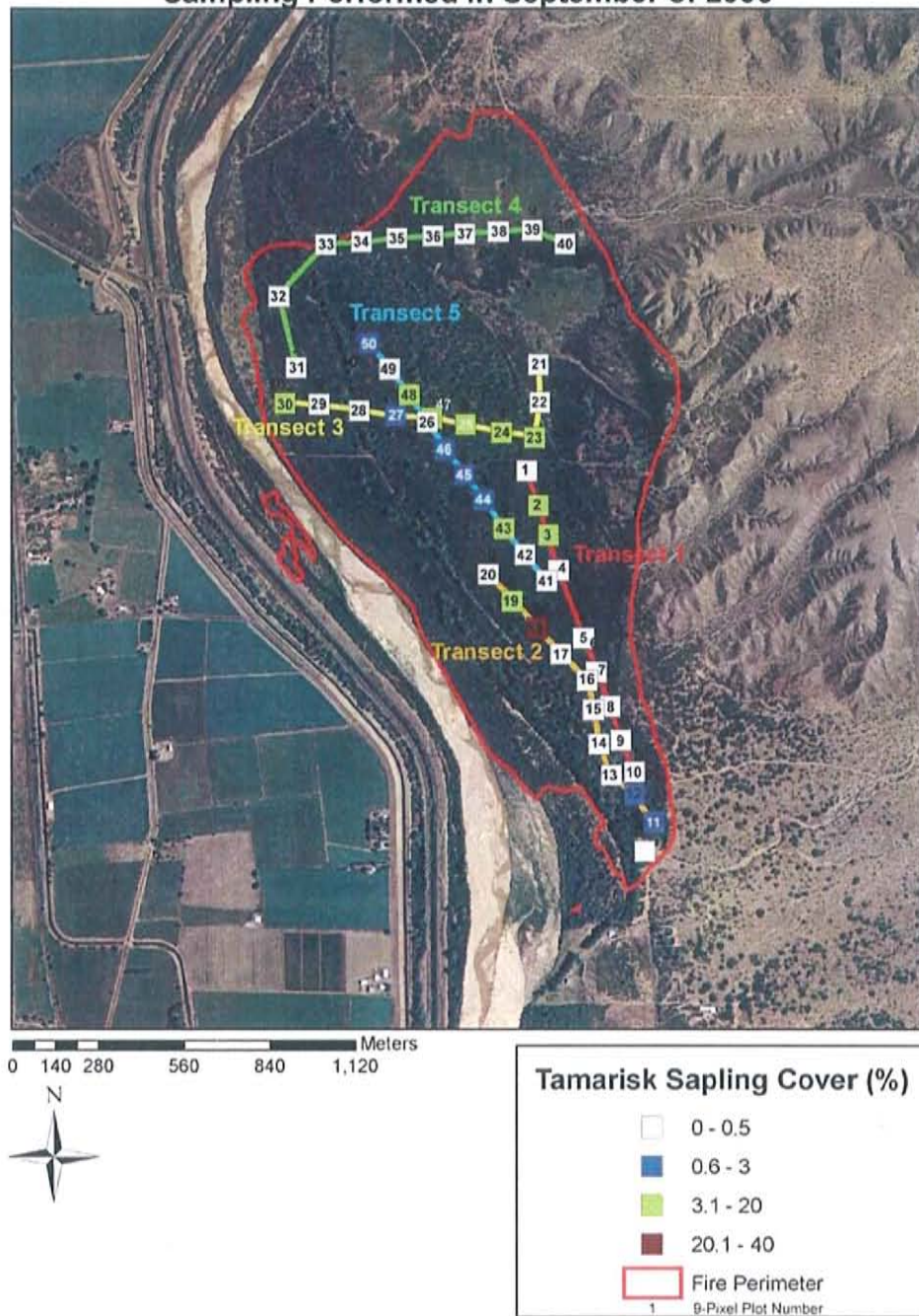
**Bosquecito Fire
Macroplot Sampling Map
Tamarisk Seedling Cover (%)
Sampling Performed in September of 2006**



Orthoquads from 8/05, courtesy of RGIS, UNM.

Figure C.17. Ocular measurements of vegetation and environmental parameters from the Summer 2006 Field Campaign.

Bosquecito Fire
Macroplot Sampling Map
Tamarisk Sapling Cover (%)
Sampling Performed in September of 2006



Orthoquads from 8/05, courtesy of RGIS, UNM.

Figure C.18. Ocular measurements of vegetation and environmental parameters from the Summer 2006 Field Campaign.

Bosquecito Fire
Macroplot Sampling Map
Bare Soil Cover (%)
Sampling Performed in September of 2006

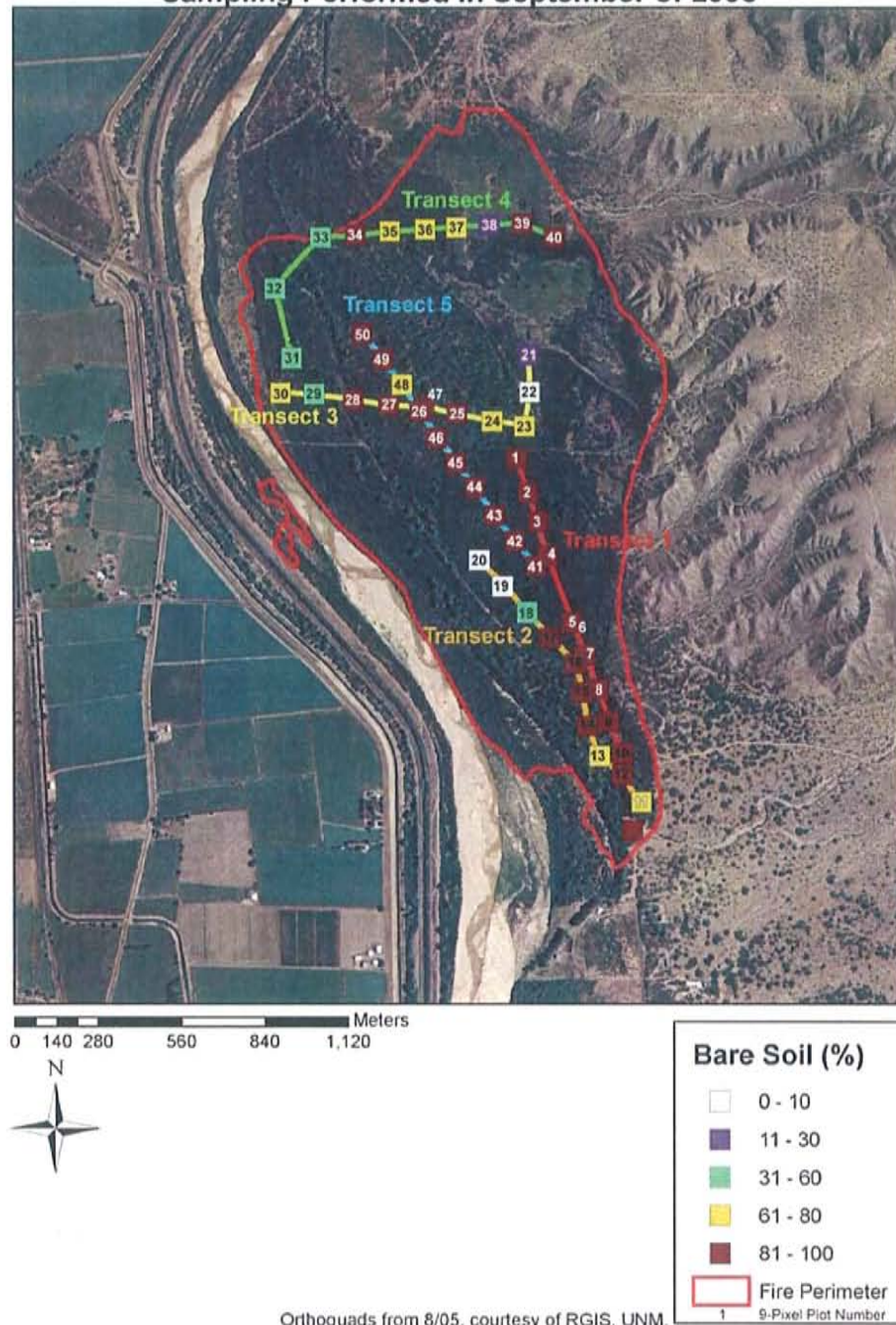
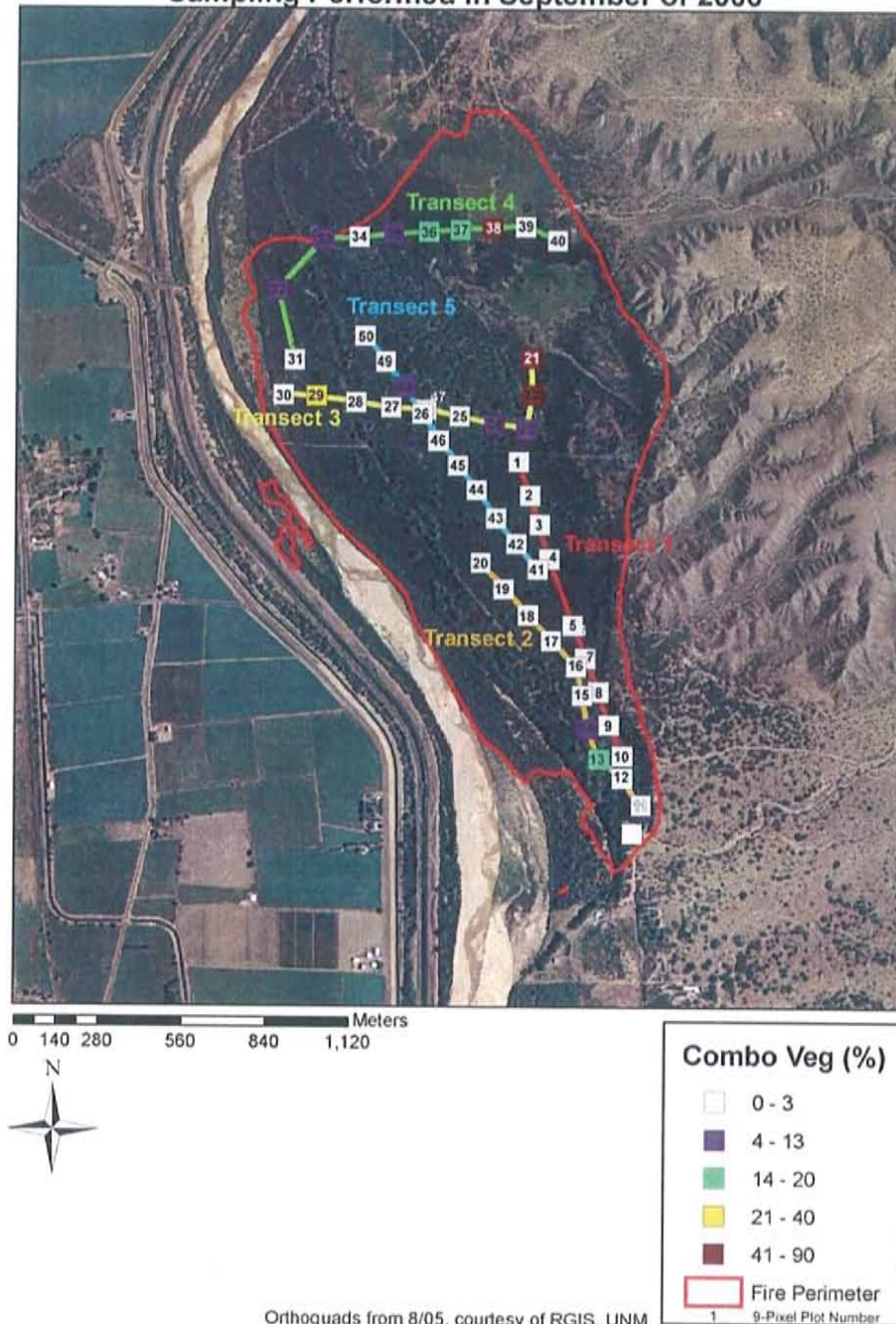


Figure C.19. Ocular measurements of vegetation and environmental parameters from the Summer 2006 Field Campaign.

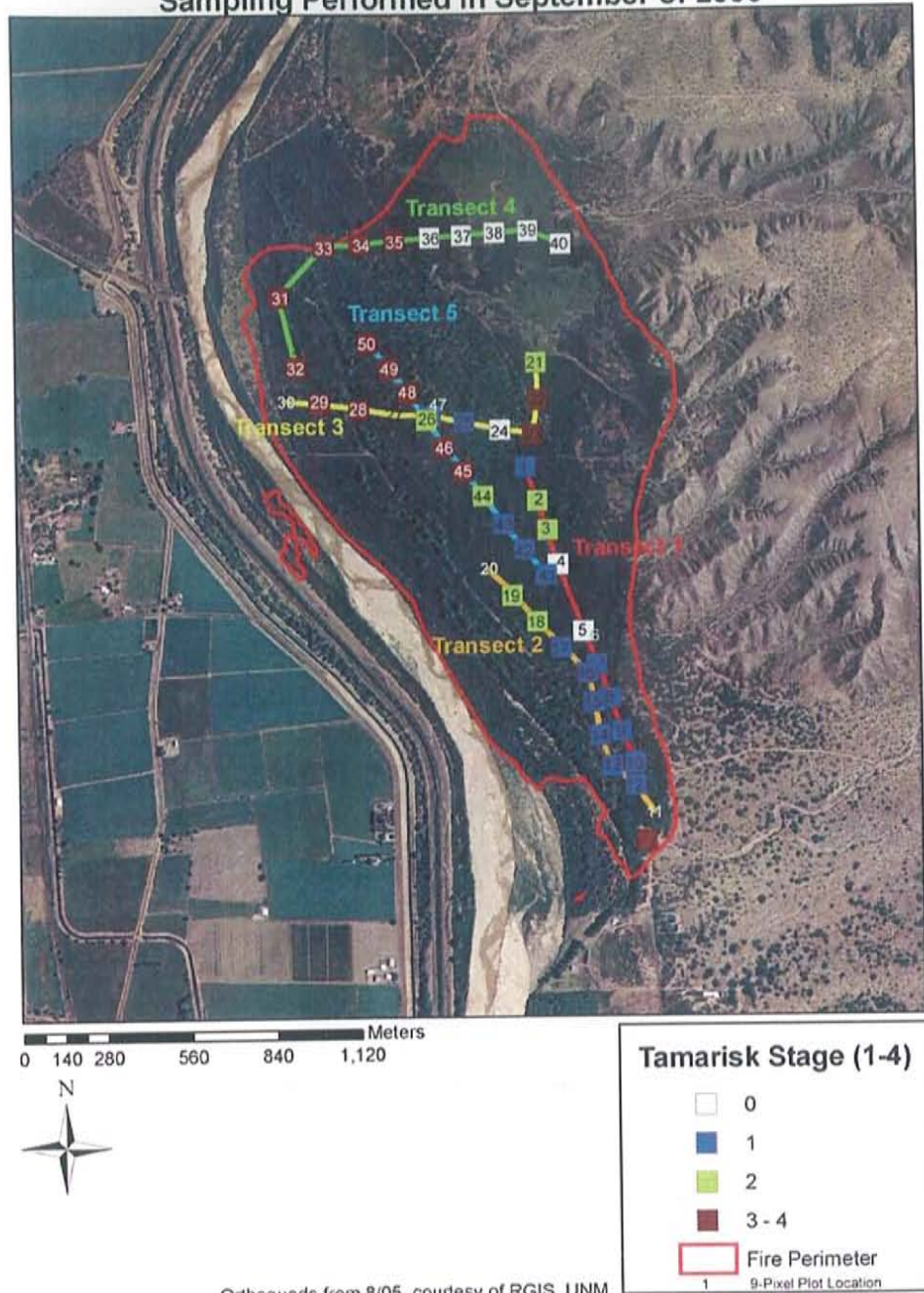
**Bosquecito Fire
Macroplot Sampling Map
Combination of Shrub, Forb and Graminoid (Combo Veg) (%)
Sampling Performed in September of 2006**



Orthoquads from 8/05, courtesy of RGIS, UNM.

Figure C.20. Ocular measurements of vegetation and environmental parameters from the Summer 2006 Field Campaign.

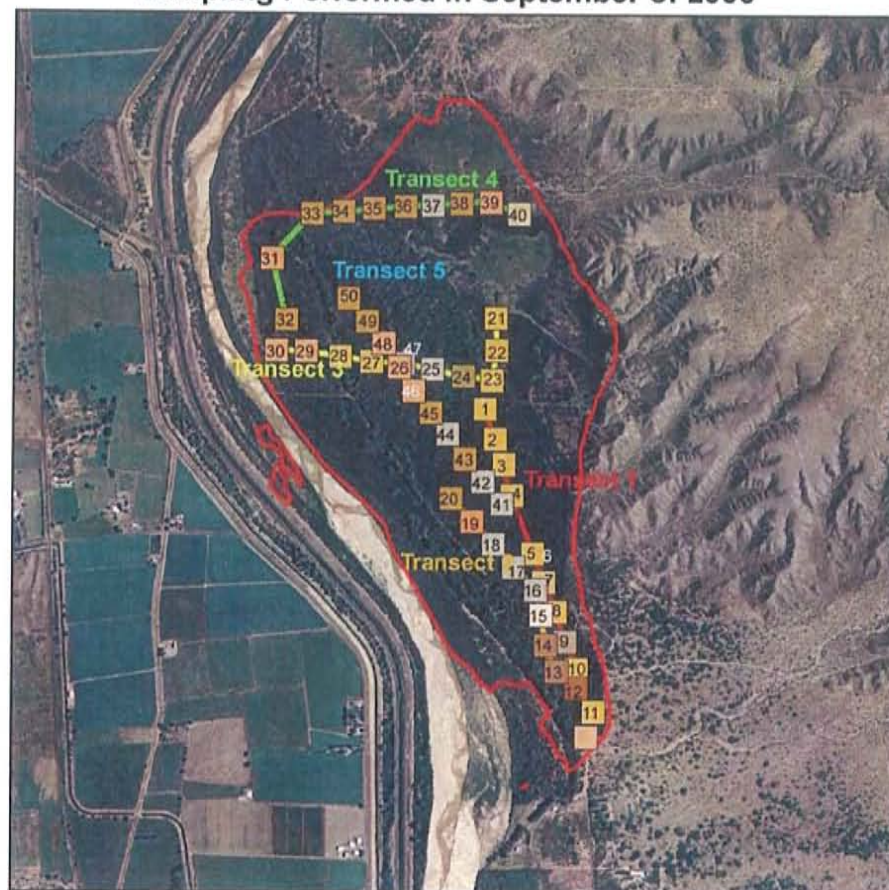
**Bosquecito Fire
Macroplot Sampling Map
Tamarisk Stage (1-4)
Sampling Performed in September of 2006**



Orthoquads from 8/05, courtesy of RGIS, UNM.

Figure C.21. Ocular measurements of vegetation and environmental parameters from the Summer 2006 Field Campaign.

Bosquecito Fire
Macroplot Sampling Map
Soil Type
Sampling Performed in September of 2006



0 175 350 700 1,050 1,400 Meters



Soil Type

- Clay
- Clay & Silt
- Fine Sand
- Sandy Clay
- Sandy Clay/Sand
- Silt
- Silty Sand
- Very Fine Sand
- Very Fine Sand with Gravel

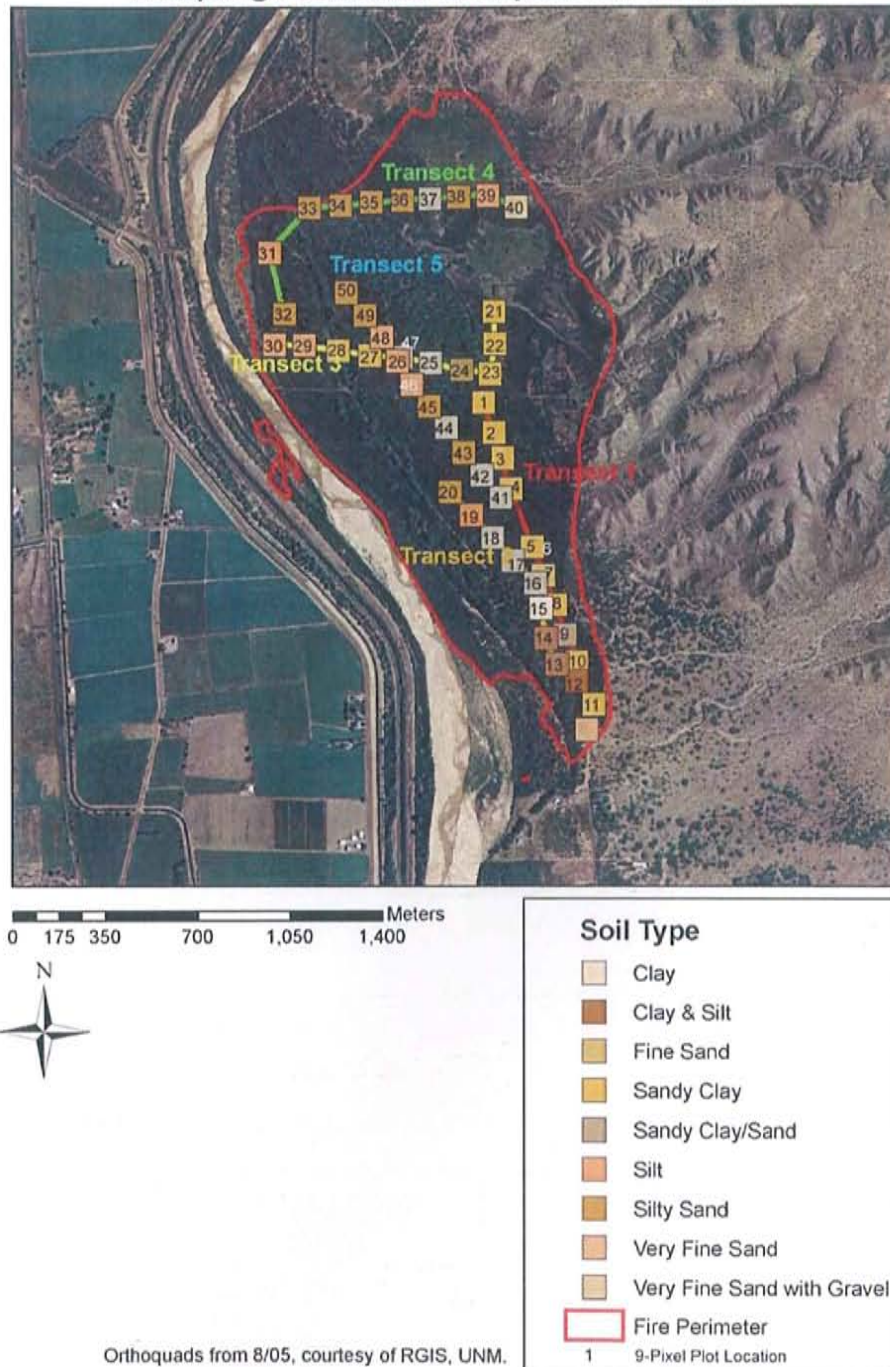
Fire Perimeter

1 9-Pixel Plot Location

Orthoquads from 8/05, courtesy of RGIS, UNM.

Figure C.22. Ocular measurements of vegetation and environmental parameters from the Summer 2006 Field Campaign.

**Bosquecito Fire
Macroplot Sampling Map
Soil Type
Sampling Performed in September of 2006**



Orthoquads from 8/05, courtesy of RGIS, UNM.

Figure C.22. Ocular measurements of vegetation and environmental parameters from the Summer 2006 Field Campaign.